The geochemistry of the grØnnedal- ĭka alkaline complex, South Greenland

R. C. O. Gill

THE GEOCHEMISTRY OF THE GRØNNEDAL-ÍKA ALKALINE COMPLEX, SOUTH GREENLAND.

R.C.O. Gill, B.Sc. (Manchester)

Thesis submitted for the Degree of
Doctor of Philosophy,
University of Durham.

Department of Geology,
February 1972.

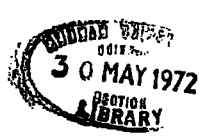

ABSTRACT

Analyses are given of 137 foyaites and related syenites from the Grønnedal-Íka alkaline complex, South Greenland. The distribution of the felsic normative components in the Lower Laminated Series (Emeleus 1964) is interpreted partly in terms of the early settling of nepheline followed by nepheline and feldspar together. The laminated feldspathic syenites identified at the top of the Lower Series are described and their significance is discussed. The Upper Series shows no pronounced differentiation of felsic components.

The problem of describing systematically the complicated chemical variation among the cumulus rocks of the complex is to some extent overcome by the application of R-mode factor analysis, the principles of which are explained.

The chemical characteristics of the various minor syenite units distinguished by Emeleus (1964) are described. Chemical comparisons between all of the syenite units leads to the postulation of three broad "magma associations" contributing to the complex.

Analyses are also given of 50 alkaline dykes belonging to later magmatic episodes. From relationships in the system Na_2O-K_2O-Al_2O_3-SiO_2, it is argued that the members of the peralkaline phonolite suite are related principally by the fractionation of feldspar approximating to $Ab_{55}Or_{40}An_5$ in composition. The bearing of these rocks on phase equilibria in the analogous natural system is discussed, and consideration is given to the possible origins of the initial peralkaline phonolite magma. The chemistry of a number of severely altered dykes of the same type is considered, and an account is given of the chemical and mineralogical changes occurring during alteration.

The geochemistry of suites of lamprophyric and trachyte dykes is examined and possible relationships between them are discussed.

Finally, the magma types thought to be represented in the complex are reviewed, and the significance of their distribution in time is considered together with possible modes of origin.

ACKNOWLEDGEMENTS

This study has been supervised jointly by Dr. C.H. Emeleus and Dr. D.M. Hirst, and I thank them for their readiness to advise, comment and encourage throughout. I am particularly indebted to Dr. Emeleus, who provided the material for the study and who has continually given advice on many subjects. I have benefited greatly from his intimate knowledge of the complex and of the Gardar province generally.

I have learned much from successive generations of research students at Durham. Godfrey Fitton and Dave Stephenson are thanked particularly for many useful discussions. Kevan Ashworth, Brian Curran, George Gale, Malcolm Reeves and Doug Robinson have also been of assistance on numerous occasions. Dick Cayzer, Andy Chambers, Les Knight and Bryan Leach kindly tolerated my unofficial occupation of their office while writing up.

I am grateful to Dr. B.G.J. Upton for providing the standards used in this work. Dr. Andrew Peckett gave valuable assistance during my use of the electron microprobe, and Messrs. Ron Hardy and Alan Carr are thanked for helping with X-ray diffraction. I am especially indebted to Dr. B.A.O. Randall for arranging for several Al_2O_3 determinations to be carried out at short notice at the University of Newcastle-upon-Tyne. I am grateful to Mrs. Lucy Mines for typing the text accurately and efficiently.

The opportunity to embark on this project I owe to Prof. K.C. Dunham, and I am indebted to Profs. G.M. Brown and M.H.P. Bott for extending my contract long enough to make completion possible. I thank the Director of the Greenland Geological Survey for making the rocks available through Dr. Emeleus

Finally, I owe a considerable debt to my wife, Mary, who has sustained me in many ways during the long period I have had to devote to this work. She has also given unstinting help in the tedious final stages. Without her contribution the work would never have been completed.

TABLE OF CONTENTS

LIST OF TABLES

LIST OF FIGURES

*See overleaf

* Figures identified with an asterisk consist of two or more diagrams in which variation in the systems (i) SiO_2-Al_2O_3-(Na_2O+K_2O) and (ii) SiO_2-$NaAlSiO_4$-$KAlSiO_4$ is shown respectively.

LIST OF PLATES

The Plates appear at the end of the thesis. Plates 1 and 2 will be found in the envelope inside the back cover.

1. Geological map of the Grønnedal-Íka complex, South Greenland. (after Emeleus 1964, reproduced by permission).

2. A reconstruction of the Grønnedal-Íka complex (after Emeleus 1964, reproduced by permission).

3. A Lower Series syenite of Group 1 (27118) showing textures suggestive of nepheline accumulation.

4. Coarse-Grained Brown Syenite (31896) with very abundant gieseckite pseudomorphs after nepheline, enclosed in feldspar.

5. Laminated feldspathic syenite of the Lower Series Group IV (27136).

6. Nepheline rich GS-1 Granular Syenite (27095) showing early euhedral nepheline poikilitically enclosed by massive perthitic feldspar.

7. A Coarse-Grained Syenite (126721) showing textural evidence of the early formation of nepheline relative to feldspar.

8. A Porphyritic Microsyenite dyke rock (27200) of Group 1, showing phenocrysts of feldspar (with dust zone) and nepheline.

9. A Porphyritic Microsyenite dyke (39770) of Group 5 cutting the Upper Series, Phenocryst of nepheline and a microphenocryst of biotite.

PART 1

THE NEPHELINE SYENITES

CHAPTER 1

INTRODUCTION

1.1 History and Scope of Investigation

The Grønnedal-Ïka complex, situated roughly eight kilometres E.N.E. of Ivigtût, is among the smallest of the alkaline plutons of the Gardar province of South Greenland. It was intruded at an early stage in the Gardar period, and consequently the complex has been subjected to much of the faulting which occurred during Gardar times, having first suffered intense brecciation in places during the emplacement of a carbonatite plug. At various times throughout the Gardar the complex has been intruded by dyke swarms of varying intensity and composition. It is hardly surprising, therefore, that the complex is the most disturbed and altered of the major alkaline plutons of the area, and this fact, combined with the indifferent exposure, has been and still is a major obstacle to the interpretation of its structure and development.

Although the existence of nepheline syenites in the Ivigtût area was recognised in the middle of the last century, no systematic mapping of the complex is recorded prior to the work of Ussing and Bøggild in the first years of the present century. The complex was studied in more detail by Callisen (1943), but by far the most complete investigation is that of Emeleus (1964). From the detailed reconstruction of the pre-faulting, pre-dyke configuration of the intrusion, Emeleus distinguishes two series of laminated nepheline syenites separated by a gneiss raft. The structure has been intruded by a strongly xenolith-charged body of porphyritic nepheline syenite, which was in turn disrupted by the injection of a carbonatite plug through the centre of the

nepheline syenite mass. Several phases of nepheline syenite dykes are recognised in and around the complex, including a ring-dyke-like body exposed at the north-west margin.

The investigation reported in this volume is concerned with the chemistry and petrology of the syenitic rocks of the complex. The study stems from the work of Emeleus (1964) and is based on the specimens collected by him. Accounts are given of the major nepheline syenite units distinguished by Emeleus, and of later groups of phonolite (see Gill in press), trachyte and lamprophyric dykes cutting the complex.

The various dolerite and basalt dykes found in the area are not considered. They form part of a regional pattern of basic dykes, and as such are the subject of research being undertaken by other workers (Upton 1970).

The carbonatite has been considered only peripherally in the work reported here. This is not to suggest that its importance is minor or that its effect on the complex has been insignificant. The carbonatite does, however, represent a distinct intrusive episode, and there is no evidence to suggest that there has been any interaction with the silicate magmas prior to its intrusion. The only possible exception to this is the Xenolithic Porphyritic Syenite, which appears to have been intruded in a disruptive manner reminiscent of the carbonatite.

In view of these arguments and the expected difficulties with regard to standards for instrumental analysis, the carbonatite has not been studied specifically. Its significance should not be underrated, however, and the body should be a fruitful subject for a separate investigation. Likewise the detailed mineralogical study

of the complex, to which the present work may be considered a precursor, must be deferred to a later study.

The specimen numbers used throughout this thesis refer to the collections of the Greenland Geological Survey (Grønlands Geologiske Undersøgelse, abbreviated to G.G.U.).

1.2 Regional Environment

The Gardar alkaline province, to which the Grønnedal-Íka complex belongs, comprises the youngest division of the Precambrian of South Greenland. The province consists chiefly of a series of plutonic alkaline intrusions akin to the Grønnedal-Íka complex, which are exposed between Ivigtût, Nunarssuit and Igaliko (Fig.1.1). The rock types represented in these complexes range from gabbro to alkali granite, syenite and nepheline syenite, the salic types being greatly predominant. Igneous layering has been developed in many of the alkaline complexes and this fact, together with the great size of the larger bodies and the development of exotic rock types in some of them, places the Gardar among the most important alkaline provinces in the world.

General accounts of the geology of the area are given by Berthelsen and Noe-Nygaard (1965) and Bridgwater (1965). The character and evolution of the Gardar province is discussed by these authors and by Sørensen (1966), Watt (1966) and Upton (in press). Descriptions of some of the layered intrusions, compiled from the work of individual authors, are also given in the volume by Wager and Brown (1968).

The Gardar period is marked by intense faulting. The dominant group of faults extends widely across southern Greenland,

FIGURE 1.1

General geological map of the Gardar province, after Emeleus and Harry (1970).

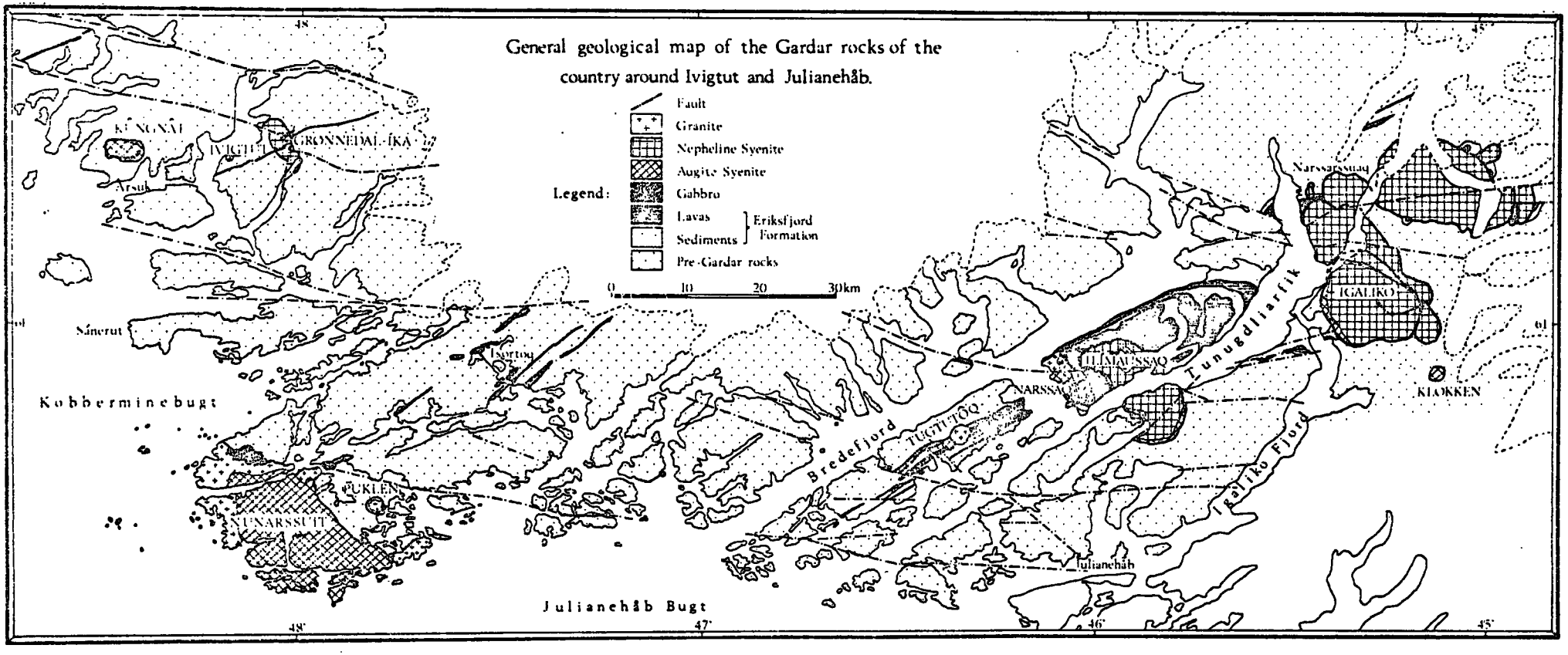
General geological map of the Gardar rocks of the country around Ivigtut and Julianehåb.
Legend:
Fault
Granite
Nepheline Syenite
Augite Syenite
Gabbro
Lavas
Sediments
Eriksfjord Formation
Pre-Gardar rocks
0 10 20 30km
KUNGNAT
IVIGTUT
GRONNEDAL-IKA
Arsuk
Sinerut
Tasiusaq
Kobbermine bugt
PUKLEN
KUNARSSUIT
Julianehåb Bugt
TUGTUTOQ
Bredefjord
NARSSAQ
ILIMAUSSAQ
Tunugdliarfik
Narssarssuaq
IGALIKO
KIAKKEN
Tasiko Fjord
Julianehåb
48°
47°
46°
45°
61°

the faults having a WNW-ESE trend. They are large wrench-faults which emerge in the Gardar area as the bounding faults of two large wrench-fault blocks passing with the same trend through Ivigtût and Nunarssuit (Fig.1.1). Of equal tectonic importance during Gardar times was the prominent set of three dyke-fault zones of ENE-WSW trend passing through the Ivigtût-Grønnedal-Íka area, the Nunarssuit-Isotorq area and the Tugtutôq-Ilímaussaq-Igaliko area respectively (Berthelsen and Noe-Nygaard 1965). Together the two fault systems seem to have had considerable influence on the siting of the plutonic intrusions; nearly all of the major intrusions occur within the dyke-fault zones, frequently at points where they intersect the wrench fault features. The Grønnedal-Íka complex occurs in the first of the dyke/fault zones mentioned above, at its intersection with the Laksenaes fault, a major component of the wrench fault system. Through their continued activity during much of the Gardar, both systems have modified the configuration of the complex considerably (Emeleus 1964, Fig.25).

In addition to the major plutons, Gardar magmatic activity has produced a considerable variety of dyke rocks.They are described in the sections of this thesis dealing with the dykes cutting the Grønnedal-Íka complex.

The Grønnedal-Íka complex includes the most important occurrence of carbonatite in the Gardar province. Minor dykes and plugs of carbonatite are also seen north of Narssarssuaq (Walton 1965; Stewart 1964, 1970).

1.3 Structure and Petrography of the Complex - a Summary

Only a very brief outline of these aspects of Emeleus' (1964) paper is given here, but further observations are made in later parts

of the thesis where relevant. The map of the complex published by Emeleus (1964) is reproduced with permission as Plate 1 of the thesis, together with his reconstruction of the original form of the complex (Plate 2). Fig. 1.2 summarises the historical and intrusive relationships between the units defined in the map, as envisaged by Emeleus. The abbreviated names used in this thesis are also shown in the figure. It is proposed to follow Emeleus' practice of using the word "syenite" to represent "nepheline syenite" throughout, unless the contrary is specified. Similarly the term "feldspar" may be taken to mean alkali feldspar.

From Plate 1 and Fig.1.2 it will be seen that the bulk of the exposed part of the complex consists of two bodies of laminated syenite, referred to here as the Lower and Upper (Laminated) Series. The Lower Series consists of foyaite, in which the degree of feldspar lamination is sometimes marked. Biotite and at least some of the aegirine-augite have grown interstitially, together with variable amounts of cancrinite. In many places the fresh lilac-grey foyaite passes into a brown altered equivalent, and the Lower Series foyaite is mantled on the west and north-west by a similarly altered Coarse-Grained Brown Syenite. The foyaite is interpreted by Emeleus as a bottom accumulation of feldspar and nepheline from a nepheline syenite magma. The lamination of the feldspars is taken to indicate mild convection in the liquid body, but mineral layering is only poorly developed in this part of the complex. The interstitial material is regarded as the product of crystallisation of the trapped liquid.

At the bottom of the Upper Series above the gneiss raft, the picture is very similar, but the foyaite passes upwards across an

FIGURE 1.2

Diagrammatic representation of the subdivision of the Grønnedal-Íka nepheline syenites proposed by Emeleus (1964).

A ⟶ B A cut by B.

A —o→ B Xenoliths of A found in B.

A ----- B A and B possibly represent same liquid.

Continuous gradation between two named units is represented by broken lines dividing the two.

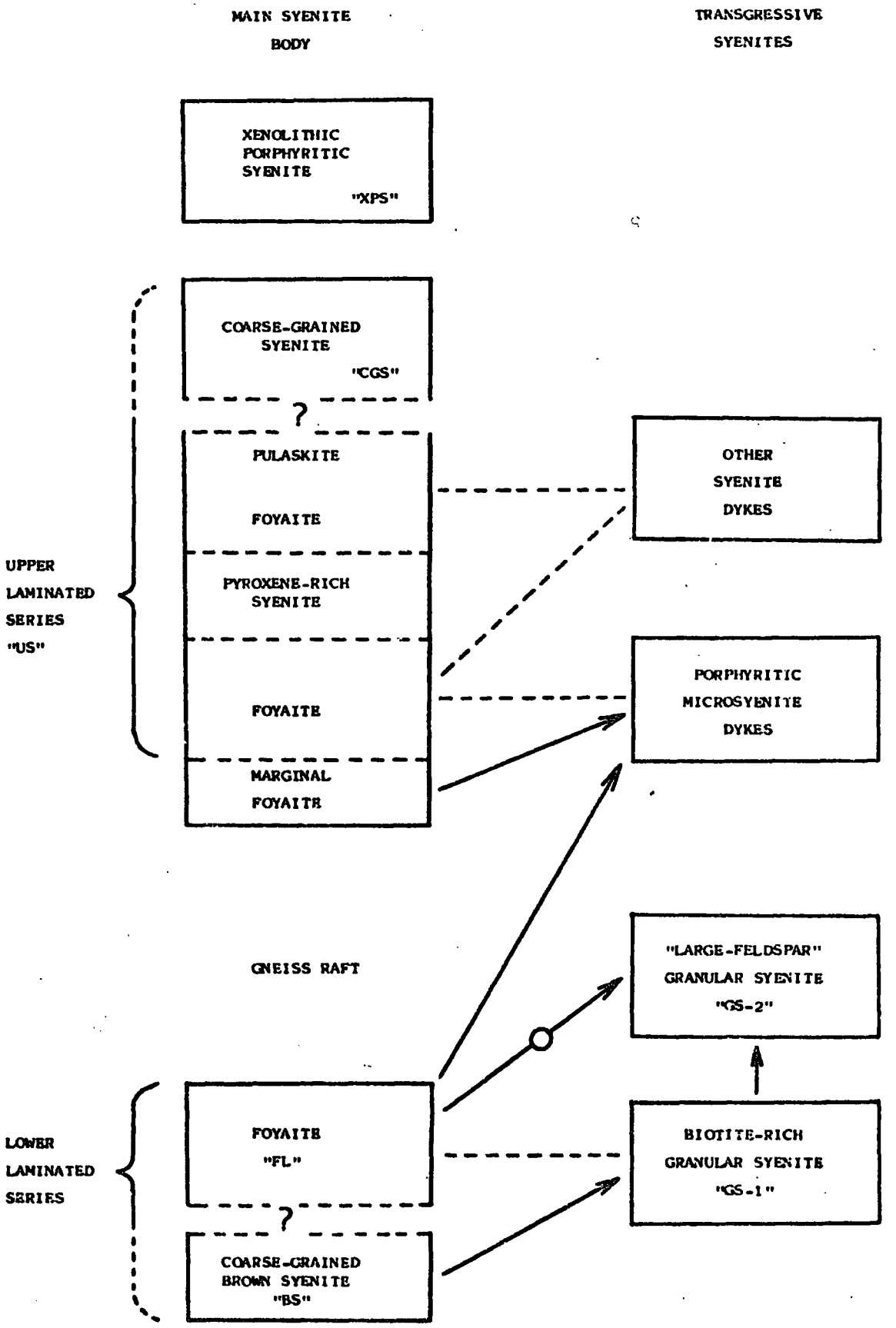
MAIN SYENITE BODY
TRANSGRESSIVE SYENITES
XENOLITHIC PORPHYRITIC SYENITE "XPS"
COARSE-GRAINED SYENITE "CGS"
?
PULASKITE
FOYAITE
PYROXENE-RICH SYENITE
FOYAITE
MARGINAL FOYAITE
UPPER LAMINATED SERIES "US"
OTHER SYENITE DYKES
PORPHYRITIC MICROSYENITE DYKES
GNEISS RAFT
"LARGE-FELDSPAR" GRANULAR SYENITE "GS-2"
BIOTITE-RICH GRANULAR SYENITE "GS-1"
FOYAITE "FL"
?
COARSE-GRAINED BROWN SYENITE "BS"
LOWER LAMINATED SERIES

arbitrary boundary into the "Pyroxene-rich Syenite", in which there is occasionally very pronounced mineral layering. Layers of more or less normal foyaite alternate with bands rich in aegirine-augite and minor apatite. In the more mafic syenites, alkali amphibole becomes a prominent interstitial (poikilitic) mineral.

Above the Pyroxene-rich Syenite, the Upper Series consists of foyaite, sometimes laminated and with occasional sodalite, grading upwards into strongly feldspathic syenite. At the highest levels of the complex there is a "Coarse-Grained Syenite" which may represent the uppermost part of the Laminated Series, but this is not certain since poor exposure conceals the boundary. The "Xenolithic Porphyritic Syenite" is a later intrusion.

Much of the central part of the complex is severely brecciated and impregnated with carbonate as a consequence of the carbonatite emplacement. Carbonate and cancrinite are quite common as secondary minerals in other parts of the intrusion, but cancrinite is also found as a late-stage primary mineral.

The mineralogy of the syenite dykes and the "Granular Syenites" is qualitatively the same as that of the laminated series. The Granular Syenites are of two types. The Biotite-Rich Granular Syenite forms dykes and sills in and around the Coarse-Grained Brown Syenite, and resembles the marginal facies of the Lower Series foyaite. It is referred to in later chapters as GS-1. The Large-Feldspar Granular Syenite (GS-2) forms a large dyke-like body on the north-west fringe of the Brown Syenite.

1.4 Sampling for Chemical Analysis

Alteration is widespread in the undersaturated rocks of the Grønnedal-Íka complex. In the syenites, nepheline commonly shows secondary incursions of fibrous cancrinite and, in more severe cases, of gieseckite (a variable fine-grained micaceous material). It is common for either product to replace nepheline completely. With further alteration the mafic minerals are replaced by chlorite, amphibole and/or epidote, and carbonate may be abundant. This stage of alteration often produces a brown appearance in hand-specimen. Sometimes the coloured minerals are broken down completely into limonite or similar material, such as in the severely altered phonolites described in Section 3.

The chemical changes brought about by such alteration may be severe, and selection of the best preserved rocks for chemical study has been given some priority in the present work.

In many respects the distribution of alteration in the Laminated Series is haphazard, although Emeleus (1964) suggests a tendency for it to be more prevalent in poorly laminated and unlaminated rocks. Two units are however systematically altered throughout, namely the Coarse-Grained Brown Syenite associated with the Lower Series, and the feldspathic syenite found at the top of the Upper Series. Neither of these units was sampled representatively in the field and, for several reasons, systematic chemical study of them has not been possible.

The objective in selecting material for chemical analysis from the remaining units in the Laminated Series has been to obtain a sample which is representative of all exposed parts of the complex but which includes only well preserved specimens. In examining the

TABLE 1.1 The coding by which syenite specimens have been classified according to alteration.

Category	Criteria
Incipient	Cancrinite/gieseckite is marginal or slightly penetrating into nepheline.
Moderate	Nepheline is extensively penetrated, usually by fibrous cancrinite, but overall extinction of nepheline is still clearly seen.
Severe	Gieseckite completely replaces nepheline but other minerals are preserved.
Very Severe	Gieseckite is widely distributed, mafic minerals are broken down into chlorite, epidote, amphibole or opaques. Carbonate and cancrinite are often abundant.

rock collection in thin section, a scale as shown in Table 1.1 has been applied to subdivide the specimens into classes representing their state of alteration. Adequate coverage of the Laminated Series was found to be obtained by combining all appropriate specimens in the "incipient" and "moderate" groups and augmenting them with one or two rocks transitional between "moderate" and "severe". The sample thus obtained was found to be well distributed over the vertical column, with the unavoidable exception of the uppermost part of the Upper Series, which is badly altered (Emeleus 1964, p.17), and to include specimens from all segments of the complex. The incidence of alteration and the distribution of superficial deposits are such, however, that it has not been possible to assemble a series of fresh rocks forming a traverse up the Laminated Series.

Similar standards of preservation apply to the specimens of the syenite dykes, the Granular Syenites and the Xenolithic Porphyritic Syenite selected for analysis. The three samples of Coarse-Grained Brown Syenite selected are however quite severely altered.

CHAPTER 2

CHEMISTRY OF THE NEPHELINE SYENITES

2.1 ANALYTICAL TECHNIQUES

The elements Si, Al, total Fe, Mg, Ca, Na, K, Ti, S and P were determined by X-ray fluorescence spectrometry on powder bricquettes using a Cr target. The method for Mn and Zr was the same except that a W target was used. The analyses were carried out on a Philips PW 1212 automatic spectrometer equipped with a vacuum path. Details of crystals and other conditions used routinely in this department are given by Reeves (1971). A technique (Appendix 4) for overcoming intermittent electronic interference has been applied to all analyses reported on the syenites. Mass-absorption and enhancement differences have largely been eliminated by using standards very similar in composition to the unknowns; such corrections as have been made are described in Appendix 2, in which a list of the standards used is also given.

Fe(II) was determined volumetrically by the method of Wilson (1955) and H_2O and CO_2 by the gravimetric method of Riley (1958).

The instrumental details of the determination of the elements Rb, Ba, Sr, Pb, Zn, La, Y, Th, U and Nb by X-ray fluorescence spectrometry are as given by Reeves (1971). The various corrections applied and the programme 'TRATIO' by which the calculations are carried out are described in Appendix 3.

The analytical data, subdivided according to unit, are tabulated in Appendix 6, together with C.I.P.W. norms.

2.2. THE LAMINATED SYENITES

Chemical Variation in the Lower Series: Classification

Figure 2.1b shows the felsic normative constituents of 31 Lower Series foyaites plotted in the system SiO_2-$NaAlSiO_4$(nepheline)-$KAlSiO_4$(kalsilite), together with relevant liquidus field boundaries and invariant points from the artificial system at 1 kb. P_{H_2O} (Hamilton and MacKenzie 1965) and 5 kb. P_{H_2O} (Morse 1969). From this diagram it is clear that the foyaites extend over a considerable composition range within the system, but nevertheless lie within a narrow linear band. At the lower end of the distribution there is a group of rocks whose compositions fall in the nepheline field of the artificial system at 5 kb. P_{H_2O}. Above them is an ill-defined transitional group lying between the nepheline-feldspar field boundaries at 1 and 5 kb. water vapour pressure respectively. The remaining compositions lie in the feldspar field. Among them two groupings are distinguishable, one lying close to the 1 kb. field boundary, the other falling near the feldspar join.

For convenience of discussion, the groups so defined will be referred to as Groups I, II, III and IV respectively. In Fig. 2.1 and succeeding figures they are distinguished by separate symbols, as defined in the caption to Fig. 2.1. The grouping is nevertheless an arbitrary one, and *a priori* represents no more than a continuous progression of compositions.

Microscopic examination reveals a relationship between the petrographic character of a rock and its position in Fig. 2.1b as represented by the class to which it is assigned. The members of Group I are particularly distinctive: euhedral nepheline crystals

FIGURE 2.1

a. Compositions of the Lower Series foyaites plotted in the silica-undersaturated part of the system (Na_2O+K_2O)-Al_2O_3-SiO_2 expressed in molecular proportions (Bailey and Macdonald 1969; Gill, in press). The point F represents the composition of binary alkali feldspar. PT is the nepheline-feldspar phase boundary, and Q, m and e are the nepheline syenite minima and eutectic in the system SiO_2-$NaAlSiO_4$-$KAlSiO_4$ at 0, 1 and 5 kb P_{H_2O} respectively. The lines A-A' and B-B' are "sodium-loss lines", indicating the loci of compositions from which successively greater amounts of sodium are subtracted (see Chapter 6).

b. Felsic normative minerals of the Lower Series foyaites plotted in part of the system SiO_2-$NaAlSiO_4$-$KAlSiO_4$ (weight proportion). The invariant points and field boundaries of the system at 1 kb (Hamilton and MacKenzie 1965) and 5 kb (Morse 1969) water vapour pressure are also shown (as "1 kb" and "5 kb" respectively).

In both diagrams, square symbols represent well laminated rocks, circles those in which there is poor lamination or none at all. Symbols are filled differently to show the groupings discussed in the text:

○ □	Group I	Nepheline-rich syenites
⊘ ⧅	Group II	Intermediate types
⌀ ⧄	Group III	
⊙ ⊡	Group IV	Feldspathic laminated syenites

Members of the marginal sequence 27126, 27127, 27129 and 27130 are arrowed.

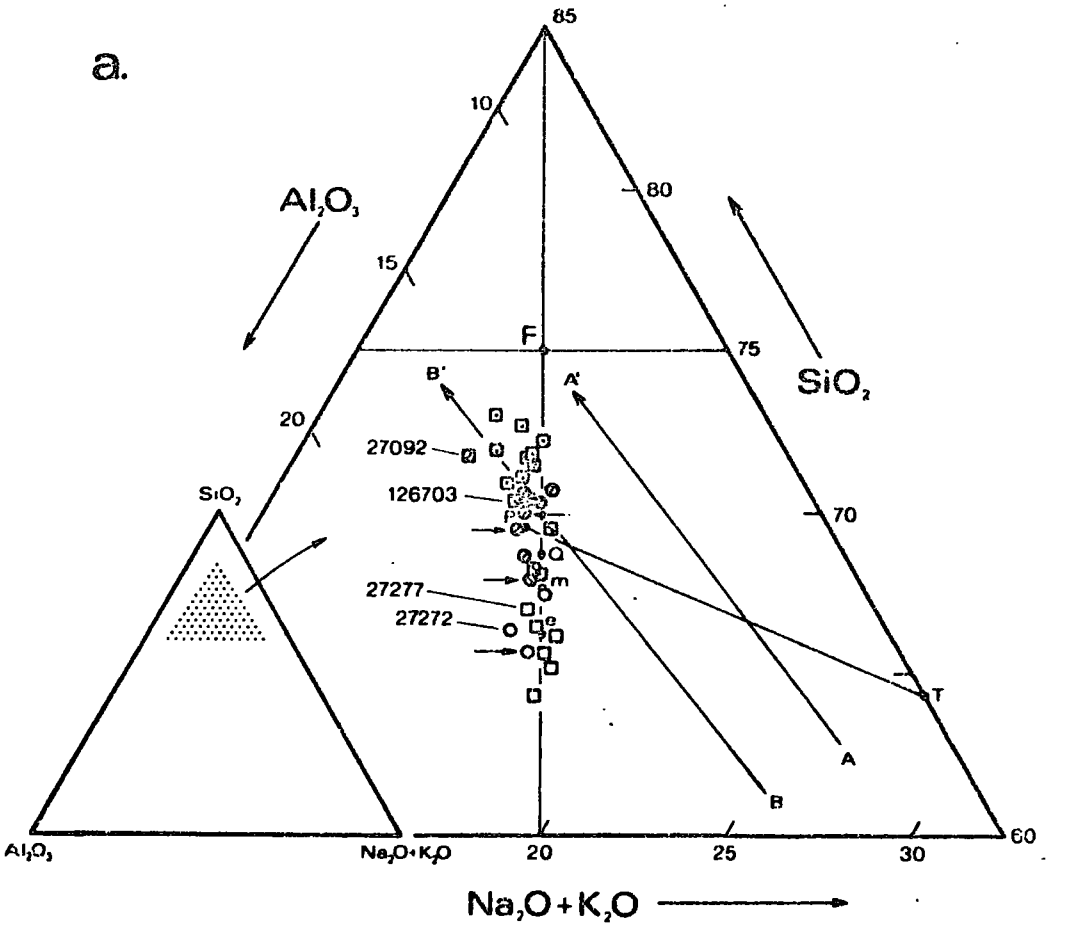
a.
85
10
80
15
F
75
20
70
25
30
60
Al_2O_3
SiO_2
Na_2O+K_2O
B'
A'
27092
126703
27277
27272
m
e
T
A
B

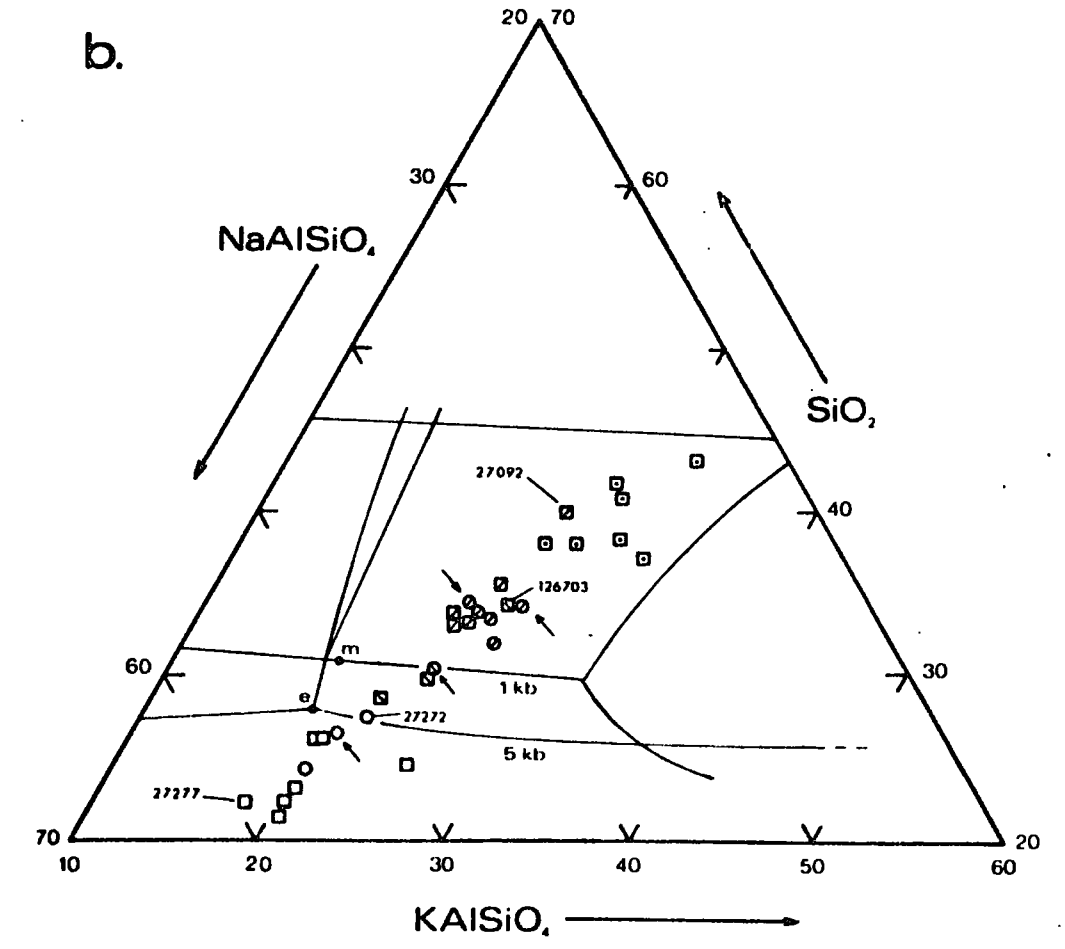
b.
20
70
30
60
40
30
60
70
10
20
30
40
50
60
$NaAlSiO_4$
SiO_2
$KAlSiO_4$
27092
126703
27277
27272
m
e
1 kb
5 kb

of widely varying size are found in great abundance, the smaller ones being often enclosed in perthitic feldspar whose poikilitic habit contrasts with the well-developed lath habit seen in the majority of the foyaites (Plate 3). The interstices of the rock are usually filled with cancrinite, which is optically continuous over large areas, rounding off the corners of the nepheline crystals, and with biotite and aegirine-augite. The content of ferromagnesian phases is often quite large, and there is some evidence that a small amount of pyroxene settling has occurred (for example, the synneusis clusters of pyroxene grains seen in some thin-sections).

In the transitional groups II and III, the large feldspar laths of perthitic feldspar, which are rare in the Group I syenites, assume more normal abundance. Nepheline is still a major mineral, and cancrinite is common interstitially. Biotite and pyroxene occur in variable relative proportions.

In contrast, the members of Group IV are distinctive feldspathic syenites in which pronounced lamination of feldspar has been developed (Plate 5). Nepheline and its alteration products are relatively scarce; alteration to fibrous cancrinite and gieseckite is often well advanced, particularly when nepheline occurs close to areas of biotite. The alteration of the nepheline makes it impossible to establish its place in the order of crystallisation with certainty. Traces of euhedral outline are often discernible, but in view of the strong tendency of nepheline towards idiomorphism this observation may not necessarily indicate an early appearance of the mineral. Biotite is the dominant ferromagnesian mineral, occurring interstitially; it is commonly oxidised and altered to chlorite.

The alteration of nepheline is well advanced in the syenites of

Group IV. All members of the group are corundum-normative, a characteristic which is often attributable to the breakdown of nepheline into micaceous products (see Chapter 6). However, the bulk chemical changes resulting from alteration are regarded as small in view of the low abundance of nepheline and its replacement products in the Group IV rocks, and other factors may contribute to their aluminous character.

More serious changes have to be anticipated when comparable alteration is seen in nepheline-rich rocks. Such is the case in 27092, 27272 and 126703. Reference to Fig. 2.1a shows that these three rocks are among the most aluminous of the Lower Series Syenites. The chemical changes accompanying the formation of gieseckite from nepheline are by and large limited to the loss of sodium (see Chapter 6) and in Fig.2.1a this process is represented by two "sodium-loss paths" AA' and BB'. Reconstruction of possible original compositions for the three rocks mentioned suggests that it may be necessary to adjust the classification based on Fig. 2.1b with respect to these specimens. In thin section 27092 resembles an intermediate-group syenite rather than the feldspathic type with which it appears to be associated in Fig.2.1b, and its position in Fig. 2.1a suggests that it may belong to either Group III or Group IV. Similarly 27272 and 126703 may belong to Groups I and II respectively.

Composition in Relation to Structural Position in the Lower Series

Because of the irregular structure of the Grønnedal-Íka complex, attempts to relate chemical variation in the laminated syenites with structural height or any similar concept of position

(c.f. Wager and Deer 1939, Kempe et al. 1970) produce no systematic trends whatsoever. The failure of this approach, which produces rather scattered plots even when applied to a symmetrical intrusion (Kempe et al. 1970), may be related to the necessity in the Grønnedal-Íka complex of correlating specimens which are widely dispersed along the strike of lamination or layering. It has not been found possible, for the reasons discussed in Chapter 1, to collect specimens systematically on a complete traverse of the Laminated Series.

There is nevertheless a distinct correlation of rock chemistry with position in the Lower Series foyaites, as can be seen from Fig. 2.2, in which specimen localities are shown in terms of the classification evolved in the foregoing paragraphs. For the purposes of Fig. 2.2, 27092 has been assigned to Group III, 126703 to Group II and 27272 to Group I. The symbols used in Fig. 2.2 are those defined in the caption to Fig. 2.1.

Fig. 2.2 shows that the nepheline-rich syenites of Group I are found in the lowest exposed parts of the Lower Series foyaite. (The one exception is 27277, a mafic syenite whose position in Fig. 2.1b may be influenced by the disparity between normative and actual pyroxene compositions. This discrepancy and its consequences are discussed in relation to the mafic syenites of the Upper Series, where the effect is more pronounced). The well laminated feldspathic syenites (Group IV), on the other hand, form a band at the very top of the Lower Series outcrop. The rocks of Groups II and III occupy intermediate positions in the field, and in some cases the two overlap geographically.

FIGURE 2.2

Specimen localities of the analysed specimens of Lower Series foyaite and Coarse-Grained Brown Syenite, showing the geographical distribution of the chemical/petrographic groups distinguished in Fig. 2.1a. Only those parts of the complex relevant to the Lower Series are shown.

⊙ ⊡	Group IV	Feldspathic well-laminated syenites
⊘ ⊠	Group III	Intermediate types
⊘ ⊠	Group II	
○ □	Group I	Nepheline-rich syenites
● ■	Coarse-grained Brown Syenite	

Square symbols represent laminated rocks, circles those which are either poorly laminated or not laminated at all.

Boundaries

————	Established and inferred limits of Lower Series foyaite and Brown Syenite
- - - - - - - -	Boundary between Lower Series foyaites and Brown Syenite
.....	Truncated boundaries
·—·—·—·—·	Laksenaes Fault

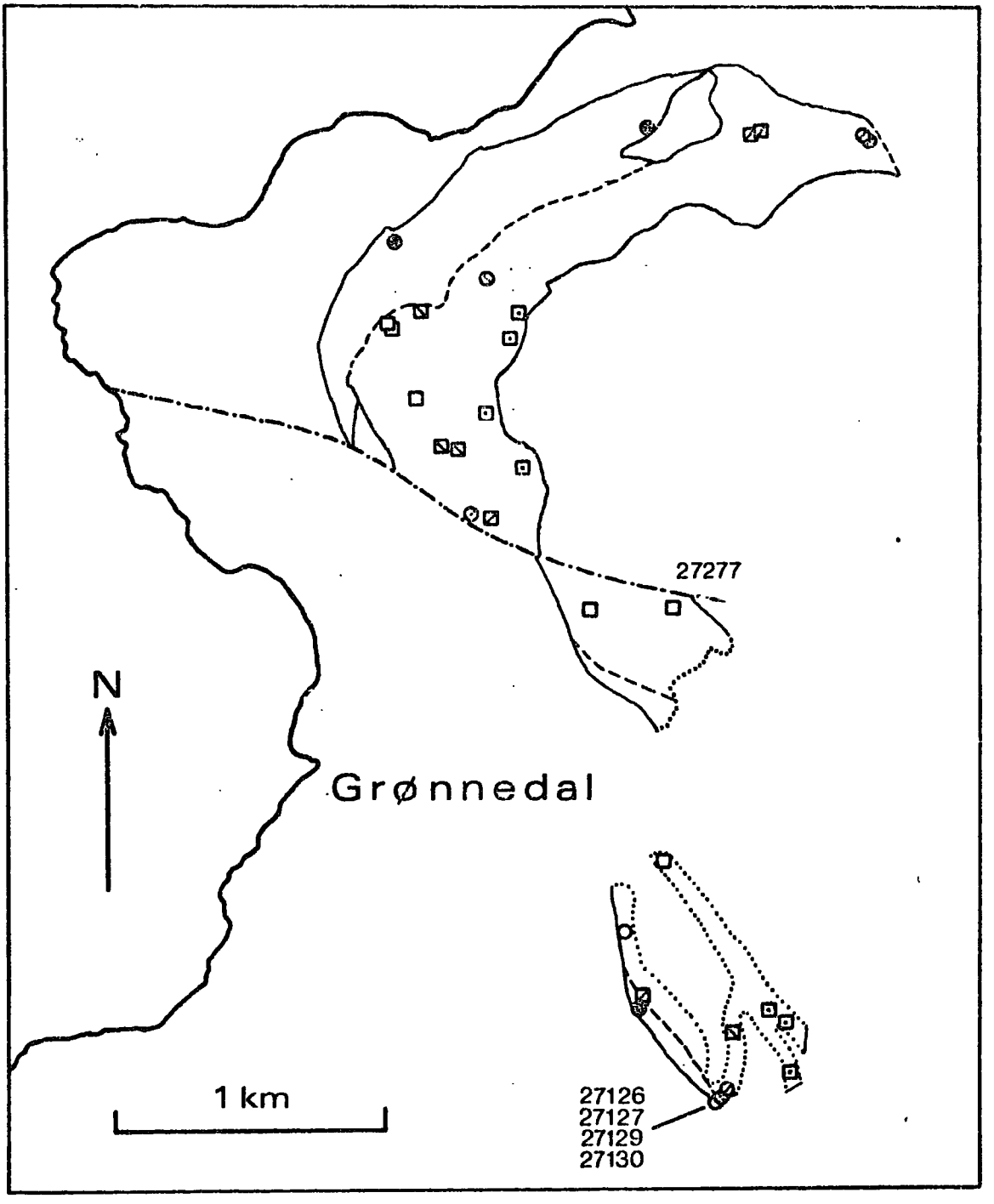
27277
N
Grønnedal
1 km
27126
27127
27129
27130

A similar pattern of mineral differentiation emerges from a series of marginal syenites collected at increasing distances from the gneiss in a stream section in south Grønnedal (see Fig. 2.2); the specimen numbers are, in order of increasing distance from the gneiss, 27130, 27129, 27127 and 27126. Unfortunately no chill representing the composition of the initial Lower Series liquid is preserved. At 13 metres from the gneiss the rock is of the nepheline-rich type, but at successively greater distances into the syenite (up to 30 metres) the composition passes through Group II to Group III. Group IV is not represented here. The marginal series of specimens is regarded as analogous to the Marginal Border Group seen in the Skaergaard Intrusion (Wager and Deer 1939, Wager and Brown 1968).

In Fig. 2.2 the margin between the Lower Series foyaite and the Coarse-Grained Brown Syenite is shown only as a broken line, in recognition of the possible continuity between the two units (Emeleus 1964, p.30). Unfortunately extensive alteration renders the Brown Syenite unfit for chemical comparison with the foyaites, and moreover it has been sampled in the field less systematically than the fresh rocks above it. Petrographic examination of the limited number of rocks available from this unit (for example 27123, 126702 and 31896, the last being shown in Plate 4) reveals textural similarities with the rocks of Group I: very abundant mica/chlorite pseudomorphs after nepheline are set among and often enclosed by massive feldspar crystals in the manner described above in connection with the foyaites of Group I. Available evidence therefore suggests that the pattern seen in the Lower Series foyaites in Fig. 2.2 extends down into the Coarse Grained Brown Syenite beneath, and that

the two units comprise a single series, but there is insufficient sample coverage to justify complete acceptance of this model.

Chemical Variation in the Upper Series

For convenience, the syenites of the Upper Series have been subdivided into "mafic syenites" (Thornton-Tuttle Differentiation Index less than or equal to 70), "less-mafic syenites" (D.I. $\leq$ 80) and "felsic syenites" (D.I. $>$ 80). It must be emphasised that the syenites referred to as "mafic" and "less mafic" may consist simply of a "felsic" syenite matrix together with variable proportions of cumulus pyroxene (and often apatite); no implication of mafic liquids of corresponding composition is intended in the use of such terms. The division between the "felsic syenites" and the rest corresponds broadly but not in detail with Emeleus' (1964) distinction between Foyaite and Pyroxene Syenite, the latter unit including syenites of all three types defined above.

The compositions of the felsic syenites are shown plotted in the system SiO_2-$NaAlSiO_4$-$KAlSiO_4$ in Fig. 2.3b. Comparison with Fig. 2.1b reveals several differences between them and the foyaites of the Lower Series. The great majority of the Upper Series foyaites have compositions lying close to the nepheline-feldspar phase boundary at P_{H_2O} = 1 kb. Only four specimens have compositions falling in the nepheline field at P_{H_2O} = 5 kb; two are sodalite-impregnated (27234, 27235) and, together with a third (27140), are isolated from the major syenite exposures by superficial deposits, and there is consequently some doubt as to their bearing on discussion of the Upper Series in general. Strongly

FIGURE 2.3

a. Compositions of all Upper Series syenites plotted in the silica-undersaturated part of the system (Na_2O+K_2O)-Al_2O_3-SiO_2. Details are given in the caption to Fig. 2.1a.

b. Proportions of the felsic normative minerals of the "felsic syenites" of the Upper Series plotted in part of the system SiO_2-$NaAlSiO_4$-$KAlSiO_4$. The reference points and boundaries shown are described in the caption to Fig. 2.1b.

c. Proportions of the felsic normative minerals of the "mafic syenites" and "less mafic syenites" (see text) of the Upper Series, plotted as in Fig. 2.3b.

The following symbols are used:

● ■ "Mafic syenites" (see text)

◐ ◪ "Less mafic Syenites"

⊘ ◪ "Felsic syenites" with compositions lying in the feldspar field of the system SiO_2-$NaAlSiO_4$-$KAlSiO_4$ at P_{H_2O} = 1 kb.

○ □ "Felsic syenites" lying in the nepheline field at P_{H_2O} = 1 kb.

Square symbols represent laminated rocks, circles those which are either poorly laminated or not laminated at all. Triangles represent feldspathic laminated syenites found in the gneiss raft.

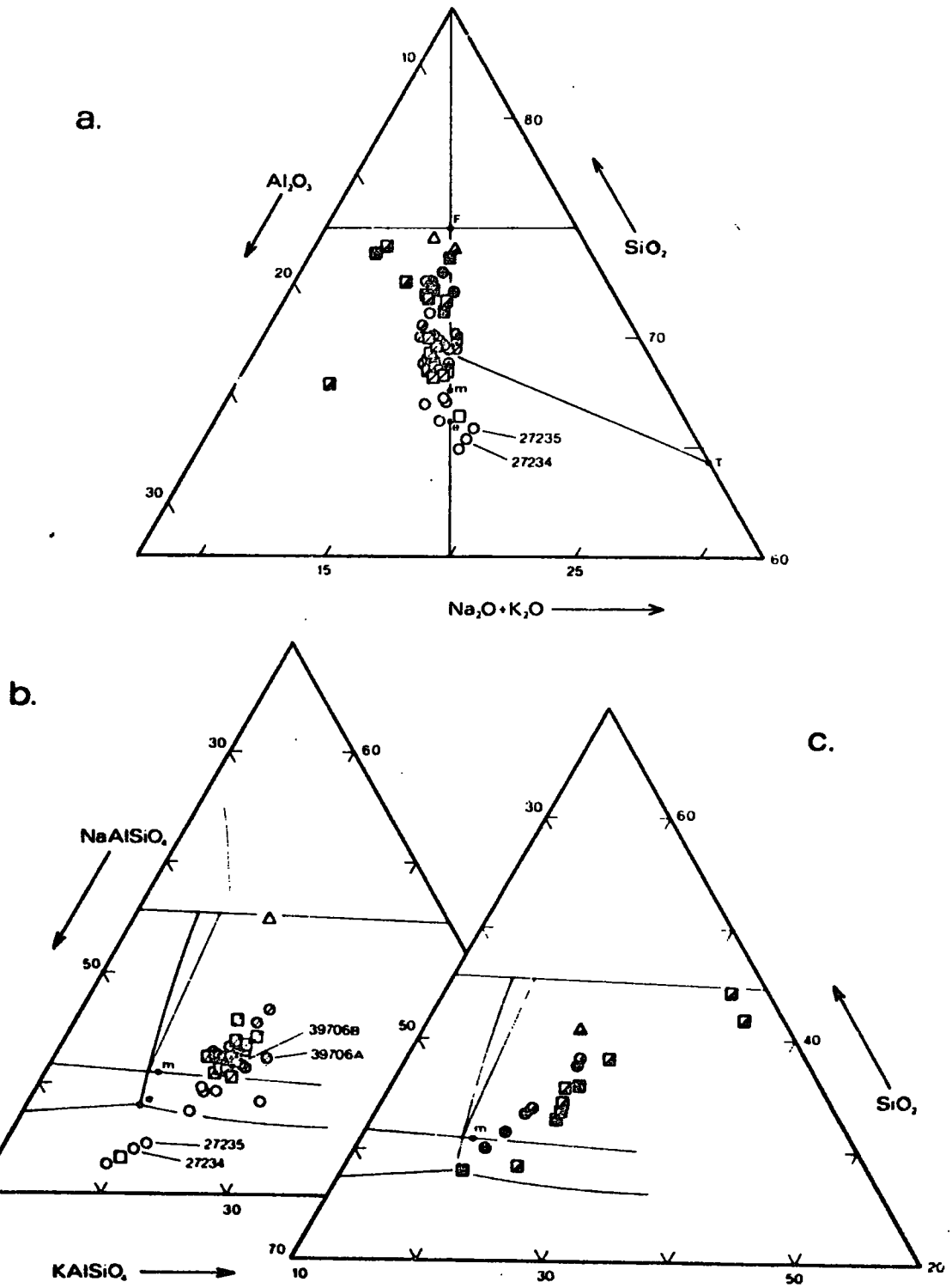
a.
Al_2O_3
SiO_2
Na_2O+K_2O
F
T
m
27235
27234
10
80
20
70
30
60
15
25
b.
$NaAlSiO_4$
$KAlSiO_4$
39706B
39706A
27235
27234
30
60
50
70
10
30
C.
SiO_2
40
20
50

feldspathic syenites akin to Group IV of the Lower Series are not represented in Fig. 2.3b, but it must be remembered that such rocks are found at the top of the Upper Series (Emeleus 1964, p.17); their absence from Fig.2.3b merely reflects their unsuitability for chemical study.

Following the work of Emeleus (1964), the mafic syenites may be regarded as consisting of felsic syenite (itself a cumulus assemblage) to which a variable proportion of cumulus pyroxene and apatite has been added. Depending on the accuracy with which the actual pyroxene composition has been reproduced in the norm, the felsic constituents of such a rock may be plotted in the system SiO_2-$NaAlSiO_4$-$KAlSiO_4$ and compared with the felsic syenite compositions and with relevant experimental equilibria (although the practice would not be acceptable for liquids of the same composition). The mafic and less mafic syenites are presented in this manner in Fig. 2.3c. It should be noted however that acmite appears in the norms of only three of them, whereas petrographic examination shows that the pyroxene in all of these rocks is aegirine-augite. This discrepancy probably accounts for the tendency to more sodic compositions in Fig. 2.3c than are found with the felsic syenites, a tendency which is more marked in the case of the mafic syenites. Otherwise, there is no indication from Fig. 2.3c that the mafic and less mafic syenites differ from the felsic syenites except with reference to the greater proportion of pyroxene and apatite.

While the development of mafic layering is locally very marked, it is clear from Figs. 2.3b and c that there has been

FIGURE 2.4

Specimen localities for the analysed rocks of the Upper Series. Specimens have been subdivided according to normative mineral proportions as described in the caption to Fig. 2.3.

Boundaries

——————— Established and inferred boundaries of the Upper Series (that is, excluding the Coarse-Grained Syenite and the Xenolithic Porphyritic Syenite).

..... Truncated boundaries of the Upper Series.

—·—·—·— Relevant faults.

Stipple Carbonate and carbonate-impregnated rocks.

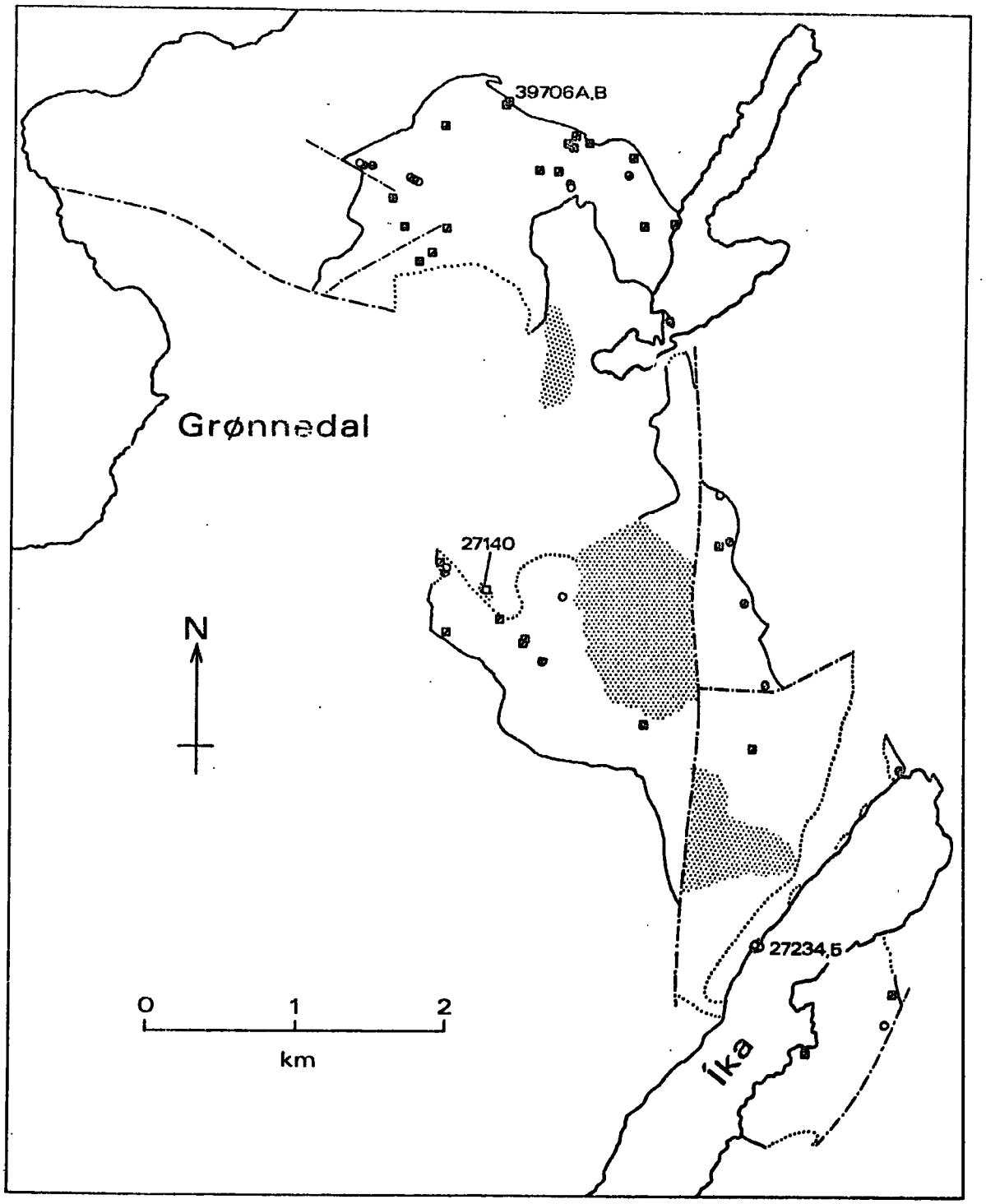
39706A,B
Grønnedal
27140
N
27234,5
0
1
2
km
Íka

little overall differentiation among the felsic components such as to produce in the Upper Series the contrasted assemblage seen in the Lower Series foyaite. A very minor dependence on structural height may be distinguished in that the slightly more feldspathic syenites tend to be found low in the laminated series or close to the margin of the complex.

Application of Factor Analysis to Chemical Variation in the Laminated Series

The Harker variation diagram, though providing a useful means of illustrating chemical variation in volcanic rock series, has little meaning when applied to cumulate rocks. The chemical composition of any such rock consists of at least two components; the cumulus crystal assemblage consisting of one or more mineral species, and a component representing the variable proportion of contemporaneous liquid trapped in the interstices among the crystalline deposit. In addition other influences may operate, such as adcumulus growth or alteration. Chemical variation of this complexity is not of the monotonic type to which the Harker diagram and its later derivatives can usefully be applied. When in addition, as in the present case, it is not feasible to plot data against structural parameters, the petrologist is deprived of simple graphical means of displaying patterns of variation in analytical data.

Variation of similar complexity is often found in the geochemistry of sedimentary rock systems, and notable advances have been made in this field recently through the application of multivariate statistical methods of data reduction, of which the most versatile is factor analysis (Spencer 1966, Spencer et al. 1968,

Reeves and Saadi 1971). It is possible that factor analysis has an equally promising future as a descriptive tool applied to complex igneous systems, and its application to the Laminated Series of the Grønnedal-Íka complex is described in the following pages. The technique has also been used on analyses of a suite of peralkaline phonolites from the same area (see Chapters 5 and 6).

Factor analysis is the systematic numerical analysis of the variance and covariance of a given body of data. Its purpose is to reduce the complex pattern of correlations among a large number of variables to a simpler set of relationships between a handful of compound variables, which are called factors. When a satisfactory solution is obtained, it is usually possible to associate each of the major factors with the operation of a particular physical or chemical control acting on the system. Interpretation of the factor pattern, that is, assigning physical meaning to the associations which emerge from the factor analysis, is achieved by visual examination of the structure of each factor (expressed in terms of the loadings of the elements contributing to it) and of the relative contribution it makes to the composition of each rock (the factor scores). It should be emphasised that factor analysis itself produces no interpretation; its purpose is merely to assemble the data according to the associations found in it, in a form which is the most amenable to geological, physical or chemical interpretation.

The factor analysis calculations reported here have been carried out using a computer programme written in PL-1 (IBM Programming Language 1) by M.J. Reeves. It is described in detail by Reeves

(1971). The various solutions available, the notation used in describing them and the criteria for choosing the most appropriate solution for a given purpose and set of data are outlined in Appendix 5.

Application to the Lower Series

A box diagram representing the Promax solution, with k=3, for the foyaites of the Lower Series is shown in Fig. 2.5. The Group IV feldspathic syenites have been omitted from the factor analysis for the following reason. Care has to be exercised, in using factor analysis, that the population being considered is subject to a single set of controls, and does not include a subset of quite different affinity. The pronounced difference which exists between the feldspathic syenites and the remainder of the Lower Series, considered in the light of the similar densities of feldspar and nepheline, suggests that this condition may not be met if the feldspathic syenites are included. Moreover the feldspathic syenites may be regarded as a monomineralic deposit to a far greater extent than is true of the foyaites in general. Consequently there is a danger that their inclusion will impose on the data as a whole trends which properly apply only to one subset. There is no loss of validity brought about by excluding a particular subset from the factor analysis; indeed the technique improves in resolution as the structure behind the data is made simpler, and it is preferable when in doubt to err in this direction. For similar reasons the mafic syenite 27277 has also been omitted, since the development of mafic layering is not representative of the Series as a whole.

FIGURE 2.5

A box-diagram (see Appendix 5) of the major factors indicated by R-mode factor analysis applied to the Lower Series foyaites omitting rocks of Group IV and the mafic syenite 27277. The figure refers to the Promax oblique solution with k=3; the corresponding numerical data are given in Appendix 5.

Correlations between factors are indicated by linkages between boxes. Those with positive coefficients are shown above the boxes, those with negative coefficients appear below.

An element is entered in a given factor when its loading exceeds 0.3, that is, when the factor accounts for more than 10% of the variance of the element.

Factors accounting for the less than 5% of the total variance are not shown.

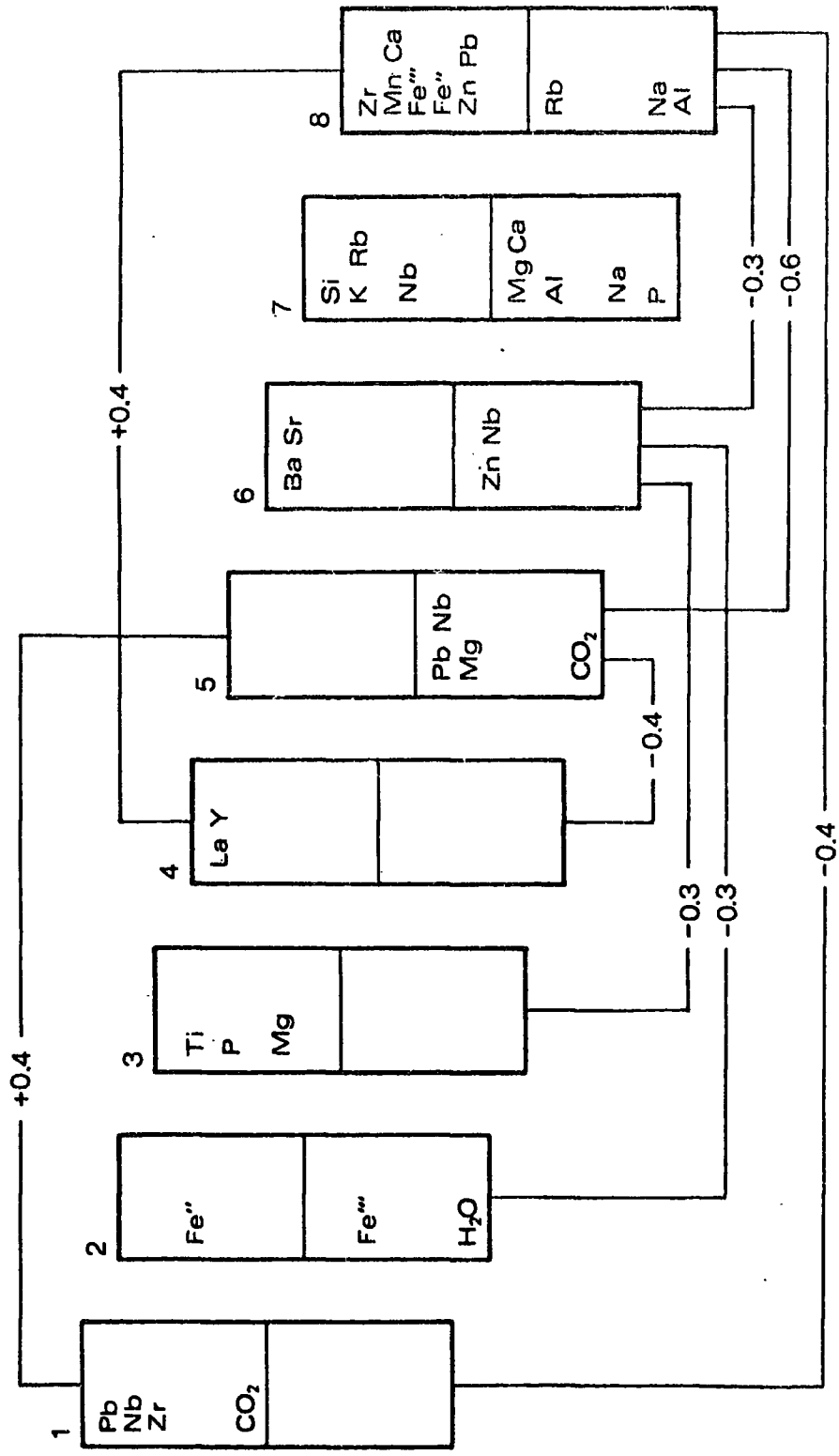
1
Pb Nb Zr
CO_2
2
Fe''
Fe'''
H_2O
3
Ti P Mg
4
La Y
5
Pb Nb Mg
CO_2
6
Ba Sr
Zn Nb
7
Si K Rb Nb
Mg Ca Al Na P
8
Zr Mn Ca Fe''' Fe'' Zn Pb
Rb
Na Al
+0.4
+0.4
-0.4
-0.3
-0.3
-0.3
-0.6
-0.4

The factor pattern shown in Fig. 2.5 contains all factors accounting individually for more than 5% of all the variance in the data. Two factors are found to be dominant, factors 7 and 8. Factor 8, which accounts for 26% of the total variance, is a complex factor consisting chiefly of Zr, Mn, Ca and total Fe opposed to Na and Al. This association of elements appears to represent variation in the proportion of pyroxene. From the positive loadings of Fe^{2+}, Mn and Ca and the negative loading of Na, one concludes that the pyroxene, though alkaline, is not acmite-rich. There is no obvious correlation between factor 8 and the degree of lamination of the rock recorded in the field. This observation suggests that the proportion of trapped liquid is not the only factor determining the amount of pyroxene present (Chapter 1), although the lack of correlation may be due in part to the inherent difficulty in estimating the true degree of lamination.

The prominence of Zr in factor 8 is consistent with occasional reports of high Zr concentrations in pyroxenes separated from alkaline rocks (Kempe and Deer 1970). The igneous geochemistry of Zr is dominated by its inability to substitute for other metals in silicate minerals, and therefore the presence of microscopic inclusionsof zircon appears to be the most likely explanation for such observations. Electron microprobe analyses of alkali pyroxenes in the phonolite dykes (Chapter 4) do not indicate high concentrations of Zr in the lattice (unpublished results).

Factor 7 is nearly equal in importance to factor 8. It is composed principally of Si, K and Rb opposed to Na, Al and P, and clearly reflects variation in the relative proportion of nepheline

and potassic feldspar (c.f. Fig. 2.1). The factor scores (Appendix 5) reproduce the classification into Groups I, II and III, a grouping which has been discussed above (p.13). The strong loading for Rb merely reflects the coherence between Rb and K. The positive loading for Nb and the negative ones for Mg, Ca and P probably represent a correlation of these elements with structural height. It has been established that the nepheline:feldspar ratio varies systematically with structural height (Fig. 2.2), and the loadings in factor 7 suggest that apatite may be concentrated at the bottom of the Lower Series, together with relatively magnesian mafic minerals, while Nb is enriched in the residual liquid fraction which formed the upper part of the Lower Series foyaite.

It may be noted that carbon dioxide does not enter into factor 7, which suggests that the high degree of silica-undersaturation seen in Group I is not brought about by the growth of interstitial cancrinite but does in fact reflect a high abundance of nepheline.

Ba and Sr are opposed to Zn and Nb in factor 6. The affinity which Ba and Sr normally show for K in felsic silicates suggests that factor 6 is broadly related to the proportion of the felsic phases in the rock. This interpretation is supported by the negative correlation with factor 8 (pyroxene and zircon) and factor 3 (biotite, see below), and by the negative loadings for Zn and Nb, both elements being associated with interstitial ferromagnesian phases.

Factor 5 has a strong negative loading on CO_2, with minor associations of Nb, Pb and Mg. The factor accounts for nearly all the observed variance in carbon dioxide, and nearly 10% of the total variance of the population. It indicates that the distribution

of CO_2 is largely independent of other elements, although there is a considerable negative correlation with factor 8. One cannot attach much significance to the minor loadings of Nb, Mg and Pb.

Factor 4 is a homopolar factor in La and Y. The absence of a correlation between this factor and factor 7, which contains a contribution from apatite, implies that the rare earth metals are broadly distributed among the silicate phases as well as apatite, and have not been seriously depleted in the magma by the apparent early fractionation of phosphate. From the positive correlation with factor 8, one concludes that relatively high concentrations may exist in pyroxene and/or zircon.

Factor 3 consists of an unusual association between Ti, P and Mg. The possibility that these elements are associated with early (magnesian) pyroxene, perhaps accompanied, as in the Upper Series, by apatite, seems to be ruled out by the absence of correlation with factors 8 (pyroxene) or 7 (structural height). Particularly with respect to Ti and Mg, there seems to be a tenuous connection between factor 3 and the distribution of biotite among the specimens analysed. Biotite is widespread in most syenite units of the complex, occurring interstitially and sometimes forming large poikilitic crystals. This interpretation of factor 3 is supported by X-ray diffraction experiments, by which small amounts of biotite are readily identified without mechanical separation from the rock. The results of these experiments are given in Fig. 2.6, which shows the correlation between factor scores of factor 3 and the intensity of the 10Å diffractometer peak of biotite for a representative sample

FIGURE 2.6

The relationship between factor 3 score and the intensity of the 10.2Å X-ray diffraction reflection of biotite for ten samples of foyaite from the Lower Series. Smear mounts were prepared from whole-rock powder samples, and the results were obtained using a Philips diffractometer comprising PW 1130 generator, PW 1060 goniometer and PW 4620/4630 electronics panels, run under the following conditions:

Target: Co. Power:60 kV.25mA. Sealed proportional counter EHT. 1.55 kV.
Ratemeter 2×10^2. Time constant 4 secs. Pulse height discrimination used with 3σ channel width.
Scan speed $\frac{1}{2}$ deg. $min.^{-1}$

Statistics

Specimen number	Peak height % f.s.d.	Factor score
27092	7	-0.19
27118A	69	1.62
27126	19	0.80
27127	22	1.25
27129	3.5	-0.92
27159	6	-0.53
27202	17	0.42
27267	15	0.62
39723	10	0.90
126713	52.5	1.76

A correlation coefficient of 0.93 has been calculated for the association between $\log_{10}(I)$ and factor score (factor 3). Reference to tables (Davies 1954 p.276) shows that for ten degrees of freedom this correlation has significance at better than the 0.1% level.

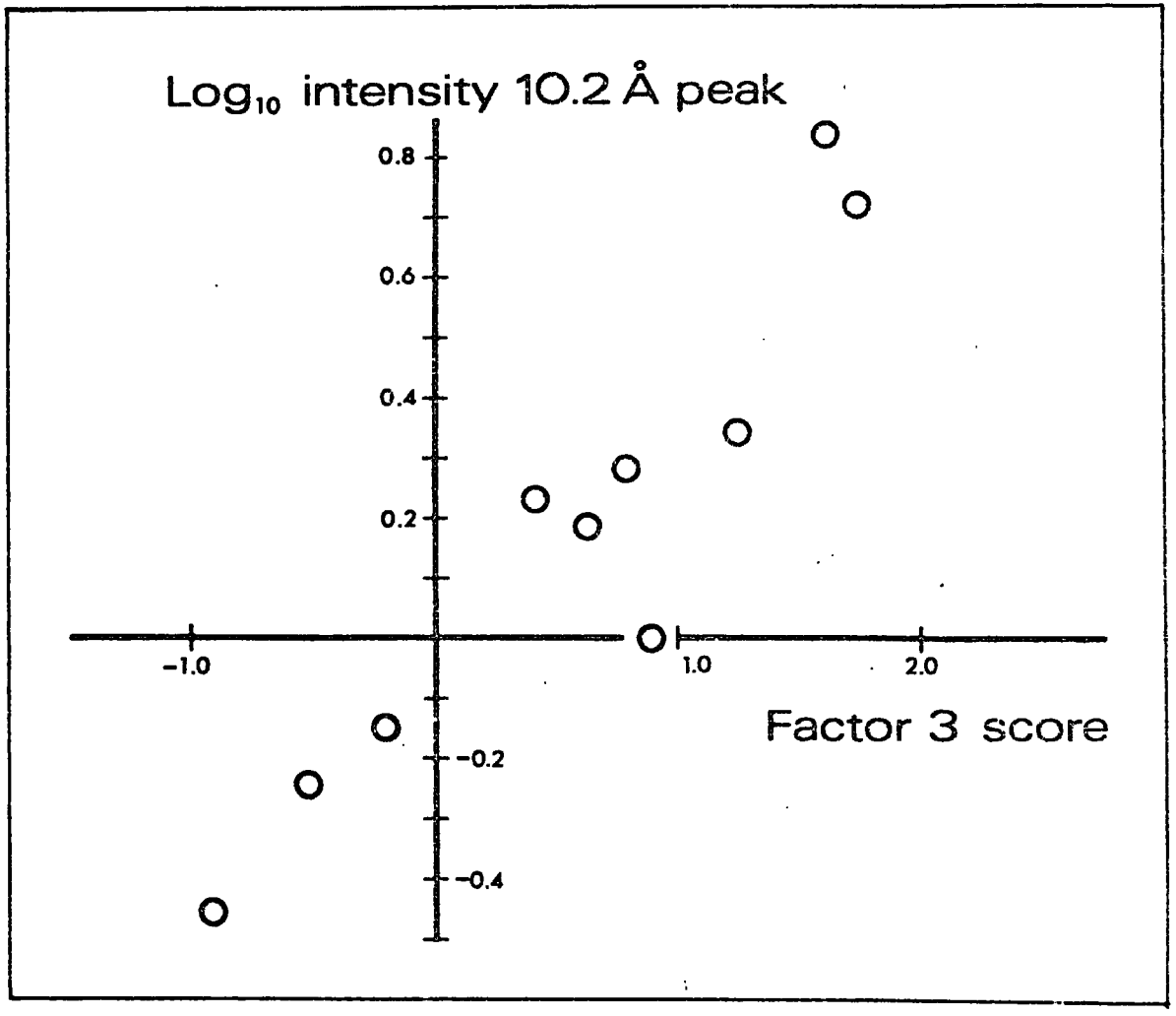
Log10 intensity 10.2 Å peak
0.8
0.6
0.4
0.2
-0.2
-0.4
-1.0
1.0
2.0
Factor 3 score

of ten gieseckite-free* foyaites from the Lower Series. The X-ray diffraction results, though lacking quantitative refinement, provide satisfactory confirmation of the identity of factor 3.

Factor 2 evidently represents oxidation of ferrous iron in a manner related to water content; indeed the factor explains nearly all the common-factor variance of water. The data available does not allow this factor to be identified more precisely.

The identity of factor 1 is not clear. Pb, the dominant component, is present in the syenites at a level close to the analytical detection limit and consequently the error-variance is high. It is therefore reasonable to interpret this minor factor tentatively as representing the error-variance of Pb, but no explanation is then given of the association with Zr (and Nb), which also occurs in the Upper Series factor analysis solution (see below). Nor is the correlation with factors 2 and 8 accounted for. The significance of this factor is not great, however, since it accounts for only 6% of the variance observed in the Lower Series syenites.

---

*The absence of micaceous alteration products is important in this context, since muscovite has a basal spacing more or less indistinguishable from that of biotite. The two minerals can be distinguished on the basis of the 060 reflection (Warshaw and Roy 1961), but the whole rock diffractogram is found to be too complex in the appropriate region to allow positive identification of the peak to be made.

Application of Factor Analysis to the Upper Series

Fig. 2.7 summarises the Promax oblique solution for all the syenites of the Upper Series. The Coarse-Grained Syenite, provisionally regarded as part of the Upper Series, has been excluded. Five factors together account for 93% of the observed variance. The pattern is dominated by factor 5, which alone is responsible for 50% of the total variance. It records the variation in the proportion of the non-felsic cumulus phases, pyroxene and apatite. Strong negative loadings on Si, Al, K and Rb oppose the ferromagnesian components, but Na does not appear at all. This fact, together with the dominance of Fe^{III} among the positive loadings, suggests that, in contrast to that of the Lower Series, the pyroxene is acmite-rich. Moreover, whereas in the Lower Series pyroxene and apatite were found in separate factors, they occur in the same factor in the Upper Series, in agreement with petrographic observation (Emeleus 1964 p.18). There is no evidence as to how the rare-earth metals, which display strong loadings in factor 5, are distributed between the silicate and phosphate phases.

Factor 4 contains an element representing alteration of nepheline to gieseckite, a process in which water and possibly carbon dioxide are gained by the rock at the expense of Na (see Chapter 6). The factor scores correlate broadly with the extent of alteration seen in thin section, although it is not always possible to identify the fine-grained products with confidence. The association of Sr with this process is consistent with the pattern seen in the phonolite dykes described in Chapter 4, but that of Ba is open to no obvious explanation.

FIGURE 2.7

Box diagram representing the major factors of the Promax solution with k=3 for all rocks of the Upper Series syenites excluding the members of the Coarse-Grained Syenite and the sodalite-impregnated syenites 27234 and 27235. The corresponding numerical data may be found in Appendix 5. Other relevant information is given in the caption of Fig. 2.5.

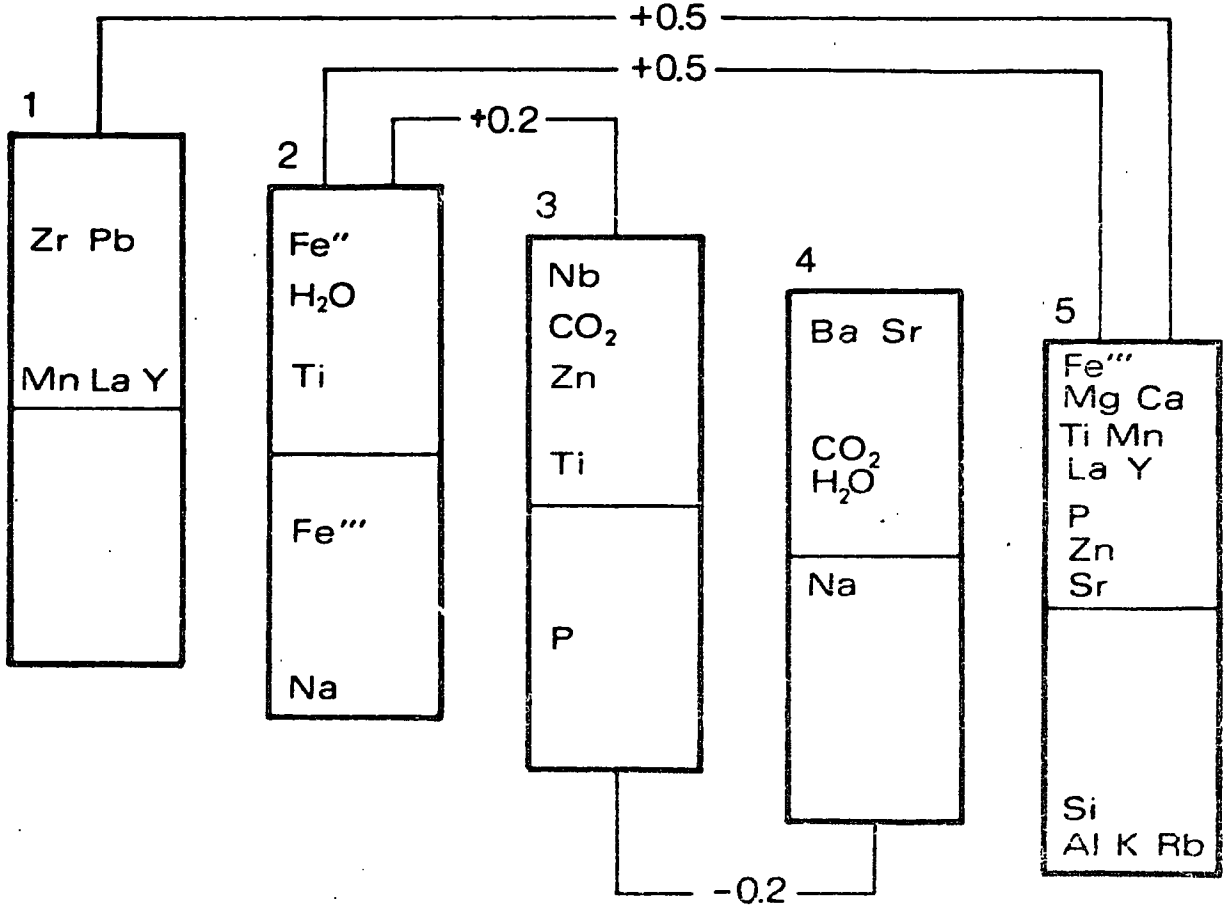
+0.5
+0.5
+0.2
1
2
3
4
5
Zr Pb
Mn La Y
Fe''
H2O
Ti
Fe'''
Na
Nb
CO2
Zn
Ti
P
Ba Sr
CO2
H2O
Na
Fe'''
Mg Ca
Ti Mn
La Y
P
Zn
Sr
Si
Al K Rb
-0.2

The variance of CO_2 is shared nearly equally between factors 4 and 3. In the latter, it is associated with Nb, Zn and Ti and strongly opposed by P. Thus the behaviour of CO_2 is different between the Lower and Upper Series; in the Lower Series it appears to be largely independent of other elements. The significance of the antipathy between CO_2 and P in the Upper Series is not clear.

Factor 2 has a structure which may be associated with variation in the proportion of biotite present, an interpretation which has been confirmed by X-ray diffraction (Fig. 2.8) in the manner described in connection with the Lower Series. Factor 1 is also reminiscent of the Lower Series by virtue of the association between Pb and Zr.

There are several respects in which the Promax solution for the Upper Series as a whole fails to yield to simple petrological interpretation. The lack of definition shown by some of the factors may to some extent be due to the dominance of factor 5, and it is possible that a clearer pattern would emerge if this factor were to be supressed. This may be achieved by defining for factor analysis a sub-set of the Upper Series syenites in which there is little cumulus pyroxene. Accordingly the Promax solution for the "felsic syenites" alone is presented in Fig. 2.9. In spite of the relatively felsic character of the rocks in this sample, the predominant component of the factor pattern still appears to be a pyroxene factor, accounting for 26% of the total variance. The pyroxene is associated with zircon in a manner similar to the Lower Series factor 8, rather than with phosphate. The next factor is of nearly equal importance; it is a biotite factor which is found to

FIGURE 2.8

a. The relationship between the score of factor 2 (Promax solution for all the Upper Series syenites) and the intensity of the 10.2Å X-ray diffraction reflection of biotite for ten samples from the Upper Series.

b. The relationship between the score of factor 6 (Promax solution for the "felsic syenites" alone)and the intensity of the 10Å X-ray diffraction reflection of biotite for nine felsic syenites from the Upper Series (see Fig. 2.9).

In both instances, the method and conditions used for the estimation of biotite are as described in the caption to Fig. 2.6.

Statistics

Specimen number	Peak height % f.s.d.	Factor scores All syenites Factor 2	"Felsic syenites" Factor 6
27002	25	-0.07	1.12
27035	23	-0.44	0.44
27077	29	-0.05	1.02
27143	27	-0.84	-1.01
27154	41.5	0.86	0.54
27158	33	0.03	-0.12
27182	19	0.39	-
27185	8	-1.73	-2.51
27221	11	-0.83	-1.04
39736A	17	-1.44	-1.93

The correlation coefficient between factor 2 and $\log_{10}(I)$ in Fig. 2.8a is 0.77 which, for ten degrees of freedom, indicates that the correlation is significant at about the 0.5% level.

The correlation coefficient between factor 6 and $\log_{10}(I)$ in Fig. 2.8b is 0.76, corresponding to a significance level better than 0.1% (nine degrees of freedom).

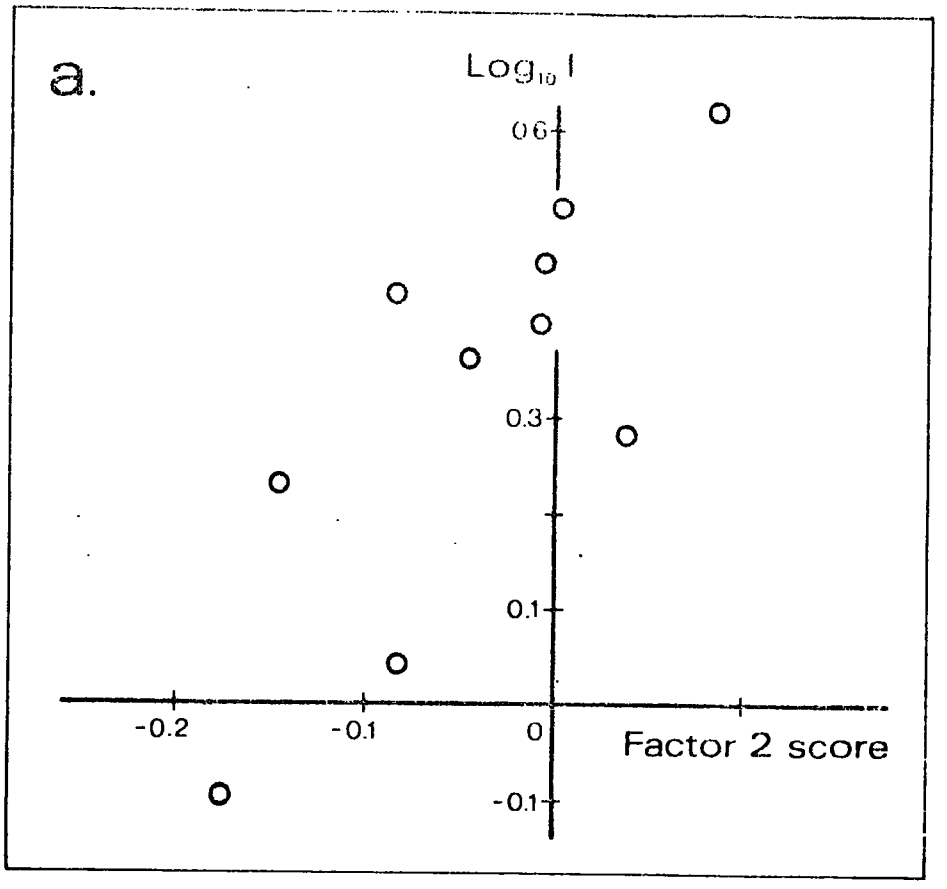
a.
Log10 I
0.6
0.3
0.1
-0.1
-0.2
-0.1
0
Factor 2 score

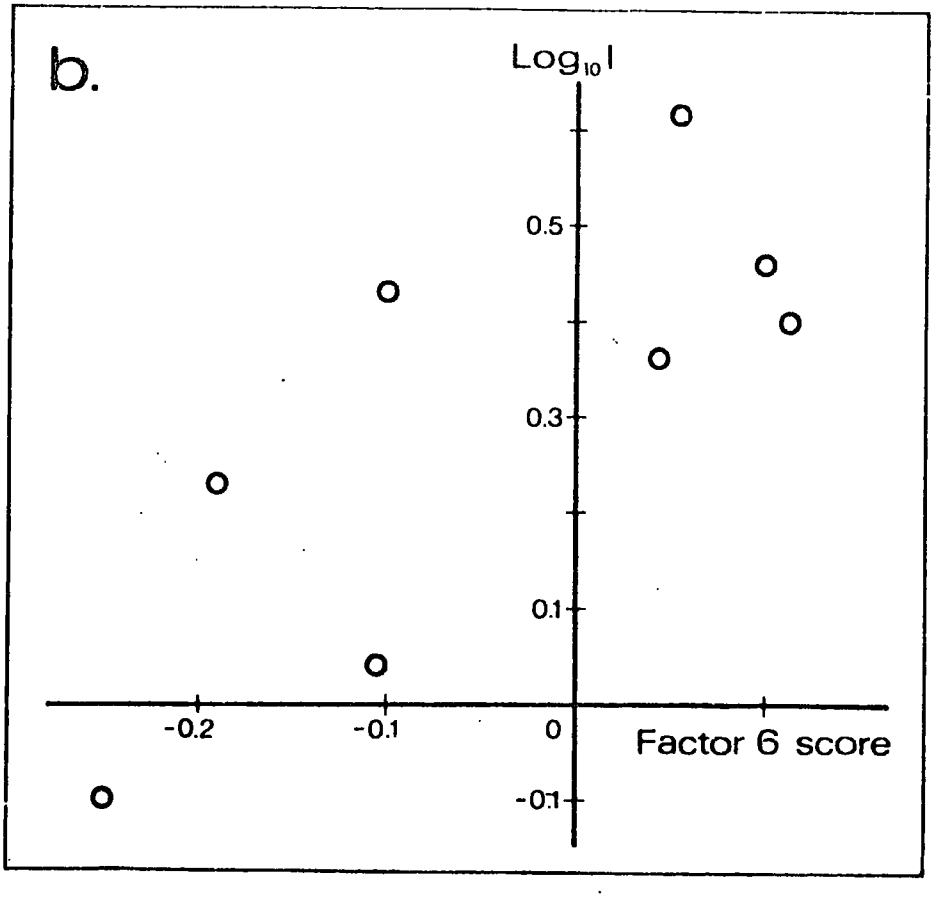
b.
Log10 I
0.5
0.3
0.1
-0.1
-0.2
-0.1
0
Factor 6 score

FIGURE 2.9

Box diagram representing the major factors of the Promax solution with k=3 for the "felsic syenites" of the Upper Series. Corresponding numerical data are given in Appendix 5. Other details are given in the caption to Fig. 2.5.

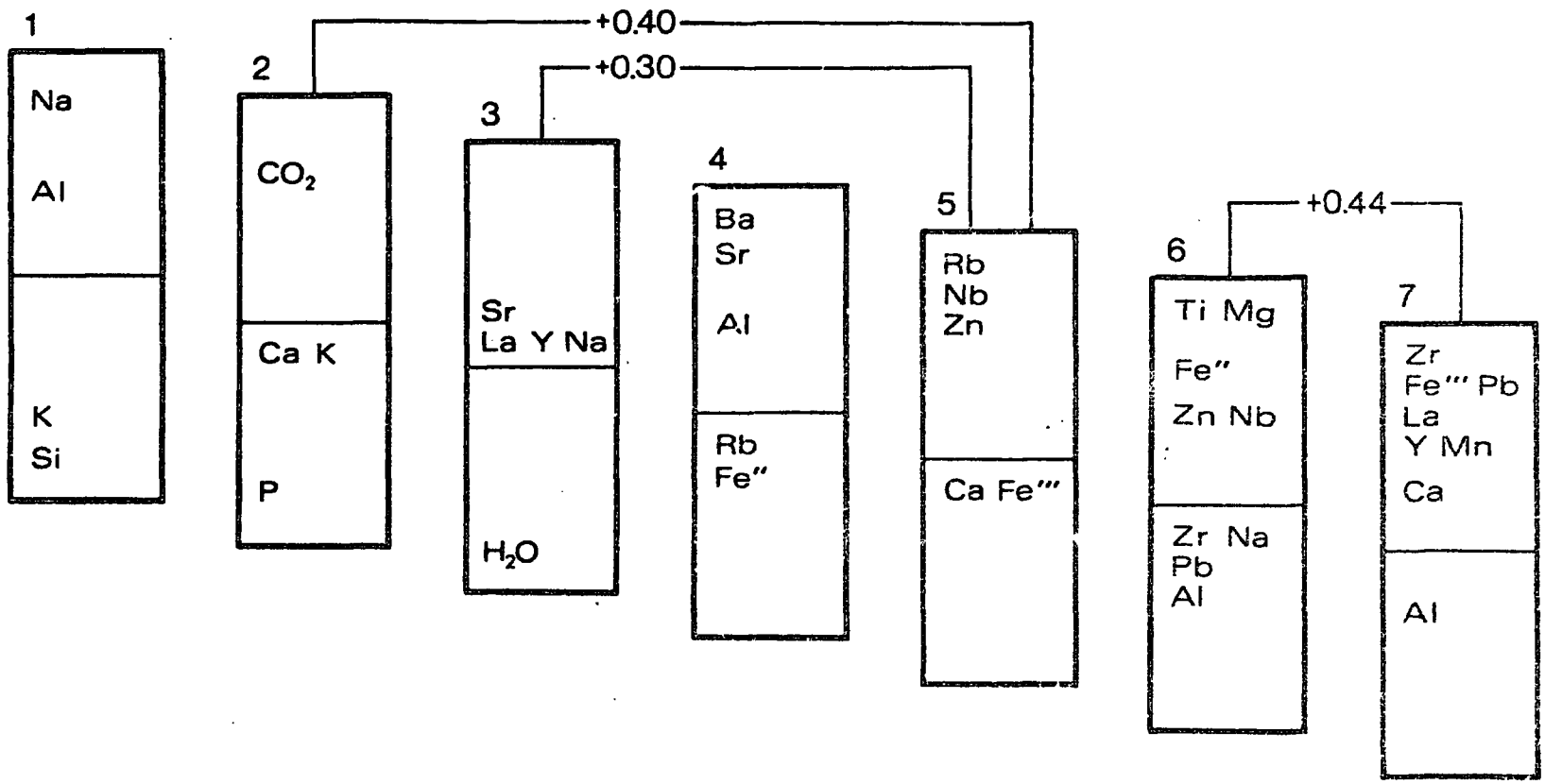
1
Na
Al
K
Si
2
CO2
Ca K
P
3
Sr
La Y Na
H2O
4
Ba
Sr
Al
Rb
Fe"
5
Rb
Nb
Zn
Ca Fe'''
+0.40
+0.30
6
Ti Mg
Fe"
Zn Nb
Zr Na
Pb
Al
7
Zr
Fe''' Pb
La
Y Mn
Ca
Al
+0.44

correlate well with X-ray diffraction estimates of biotite in the whole-rock powders (Fig. 2.8b). A strong positive correlation exists between factors 6 and 7.

Factor 3 in the factor analysis pattern obtained from the Upper Series as a whole is resolved into two correlated factors (2 & 5) when the felsic syenites are considered alone. Factor 5 may perhaps represent the oxidation of ferromagnesian minerals; in thin section pyroxene and particularly biotite are commonly seen to be oxidised along the cleavages and sometimes more extensively. Unfortunately petrographic confirmation of this model is hindered by the sporadic distribution of biotite and pyroxene in thin sections of the felsic syenites.

Factor 4 is similar to factor 6 for the Lower Series foyaites and by analogy probably represents the proportion of felsic components in the rock, although there is no direct evidence for such an interpretation in the present case. Factor 3, like factor 4 for the Upper Series as a whole, correlates well with the degree of alteration of nepheline seen in thin section. The antipathy between CO_2 and P mentioned above recurs in factor 2.

Factor 1 reflects the relative proportion of nepheline and potassium-rich feldspar. In contrast to factor 7 of the Lower Series, which is the second most important factor in the Lower Series solution, accounting for 20% of the total variance, factor 1 is the least of the significant factors obtained from the felsic syenites of the Upper Series and accounts for a mere 7% of the variance. This conclusion provides quantitative support for the earlier observation that nepheline-feldspar differentiation

is of little consequence in the Upper Series.

Factor Analysis: Summary of Conclusions

The application of R-mode factor analysis to three sets of analyses, representing respectively the Lower Series foyaites, the Upper Series as a whole and the felsic syenites of the Upper Series, has led to the following conclusions:

1. A factor representing the proportion of pyroxene, cumulus or otherwise, is the dominant entity in all three solutions. In the Lower Series and the felsic syenites of the Upper Series, there is an association with Zr, thought to be present as inclusions of zircon. When all Upper Series syenites are considered, apatite and the rare earth elements appear as important components.
2. A variable factor representing interstitial biotite is present in all three patterns, accounting for most of the variance of Ti and Mg.
3. In the Lower Series, there is a factor reflecting the relative abundance of nepheline and potassic alkali feldspar (c.f. Fig. 2.1), but the influence of this factor is insignificant in the Upper Series. In the Lower Series, the factor also appears to reflect the variation of Nb, Mg, Ca and P with respect to structural height.
4. Ba and Sr are not closely tied to any other element or specific group of elements. Much of their variance is confined to one factor in each solution. It is possible that this factor is representative of the felsic (K-bearing) components of the

system. Parallel loadings of K or Na do not occur, possibly because these elements also occur in the mafic minerals (biotite and alkali pyroxene respectively).

5. The rare-earth elements are associated with the pyroxene factor in every solution, either occurring within it or as a separate factor strongly correlated with the pyroxene factor.
6. Deuteric and metasomatic phenomena appear to be represented in several forms. In the Lower Series, much of the water variance is associated with oxidation of Fe^{II}, whereas the contribution to the alteration of nepheline is more important in the Upper Series. CO_2 forms a nearly unique factor in the Lower Series, whereas there is a conspicuous antipathy between CO_2 and P in the Upper Series.
7. Two unusual geochemical associations appear persistently: Pb+Zr(+Nb) and Nb+Zn. The former is reminiscent of the incipient alteration factor seen in the factor analysis solution for the well preserved phonolites (Chapter 5).

2.3 THE GRANULAR SYENITES

Emeleus (1964) distinguishes two varieties of Granular Syenite; they are a biotite-rich variety and a second type which is marked by the thick platy character of the alkali feldspars. For convenience these types are referred to here as GS-1 and GS-2 respectively. The former is found in sheets cutting the Brown Syenite and gneiss on the N.W. margin of the complex, and in many respects resembles foyaites in the lower part of the Lower Series. The GS-2 syenite forms the dyke-like body which extends from Eqaluit and the Kontaktelv to the northern side of the Laksenaes fault. In this

rock nepheline is subordinate to feldspar, there is little biotite and the pyroxene is often strongly zoned, although the rocks are not particularly fine-grained.

The Granular Syenite specimens analysed are shown in the systems SiO_2-Al_2O_3-(Na_2O+K_2O) and SiO_2-$NaAlSiO_4$-$KAlSiO_4$ in Fig. 2.10. Examination of the former reveals that several of the rocks in this group are peralkaline. The use of the normative Qz-Ne-Kp plot for peralkaline rocks has been criticised by Bailey and Macdonald (1969) on the grounds that the true proportion of sodium is misrepresented. The reasons are discussed more fully in Chapter 4 of this thesis in connection with the peralkaline phonolite dykes. In the present case the development of the peralkaline condition is sporadic, and the simplest way to allow for its effects in Fig. 2.10b is to show normative and projected non-normative compositions side-by-side. The projection of the non-normative composition point in the system SiO_2-Al_2O_3-Na_2O-K_2O into the SiO_2-$NaAlSiO_4$-$KAlSiO_4$ join may be visualised as shown in Fig. 2.11. The non-normative projected composition point for each peralkaline rock is represented in Fig. 2.10b by an open symbol joined to the corresponding normative composition.

It will be seen immediately for Fig. 2.10 that the syenites of GS-1 type encompass a considerable range of compositions, although the majority of specimens lie in the region of the nepheline-feldspar phase boundaries at 1 kb and 5 kb P_{H_2O}. 27095 is exceptional in being peralkaline and more sodic and undersaturated than its fellows. The cause of the distribution of the GS-1 syenites in Figs. 2.10a and 2.10b is not entirely clear. It is possible that

FIGURE 2.10

a. Compositions of the Granular Syenites plotted in the silica-undersaturated part of the system SiO_2-Al_2O_3-(Na_2O+K_2O), expressed in molecular proportions. The datum points F, P, T, Q, m and e are described in the caption to Fig. 2.1.

b. Felsic normative constituents (closed symbols) of the Granular Syenites plotted in the system SiO_2-$NaAlSiO_4$-$KAlSiO_4$ (weight proportions). For peralkaline specimens, the projections of the composition points in the system SiO_2-Al_2O_3-Na_2O-K_2O on to the SiO_2-$NaAlSiO_4$-$KAlSiO_4$ plane are also shown, as open symbols joined to the corresponding normative compositions.

Key

	Fresh	Nepheline altered	Projected non-normative composition
GS-1	●	⊙	○
GS-2	■		□

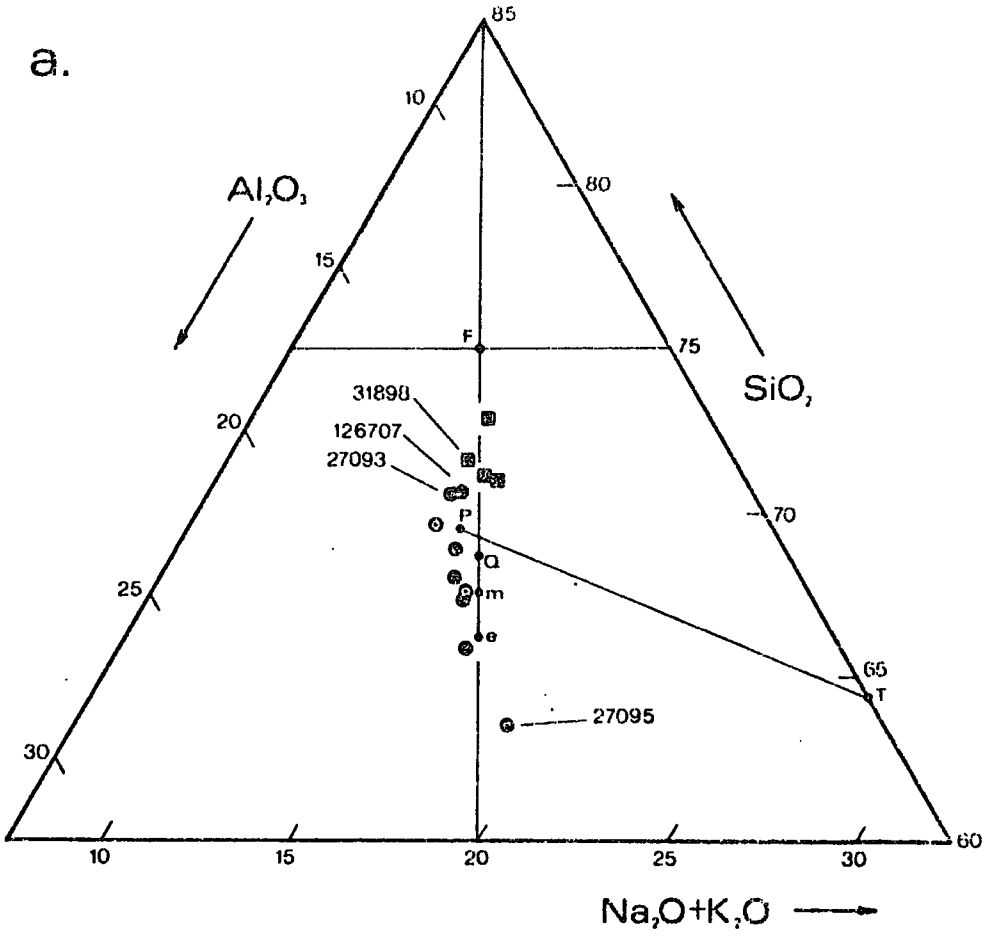
a.
85
10
80
Al_2O_3
15
F
75
SiO_2
31898
126707
27093
20
P
70
Q
25
m
e
65
T
27095
30
60
10
15
20
25
30
Na_2O+K_2O

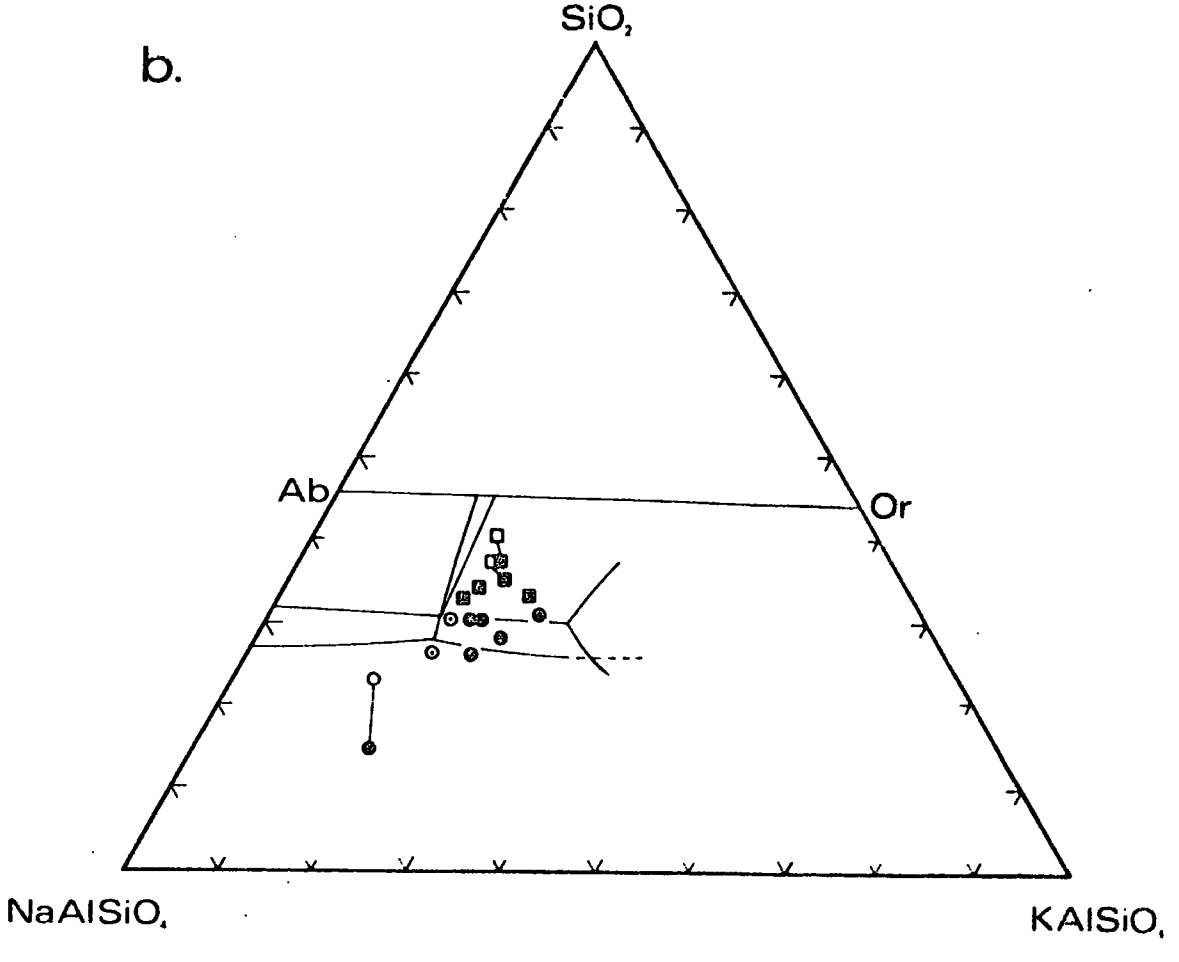
b.
SiO_2
Ab
Or
$NaAlSiO_4$
$KAlSiO_4$

FIGURE 2.11

Schematic representation of the non-normative projection of a peralkaline composition X in SiO_2-Al_2O_3-Na_2O-K_2O into the join SiO_2-$NaAlSiO_4$-$KAlSiO_4$, as X'. The lines XX'Y and Z-Al_2O_3 are parallel. The projection is the point at which the line joining the quaternary composition to the point on the Al_2O_3-SiO_2 edge with equal SiO_2 proportion intersects the Q-Ne-Kp join. By projecting in this manner the SiO_2: (Na_2O+K_2O+Al_2O_3) and Na_2O:K_2O ratios of the rock are preserved.

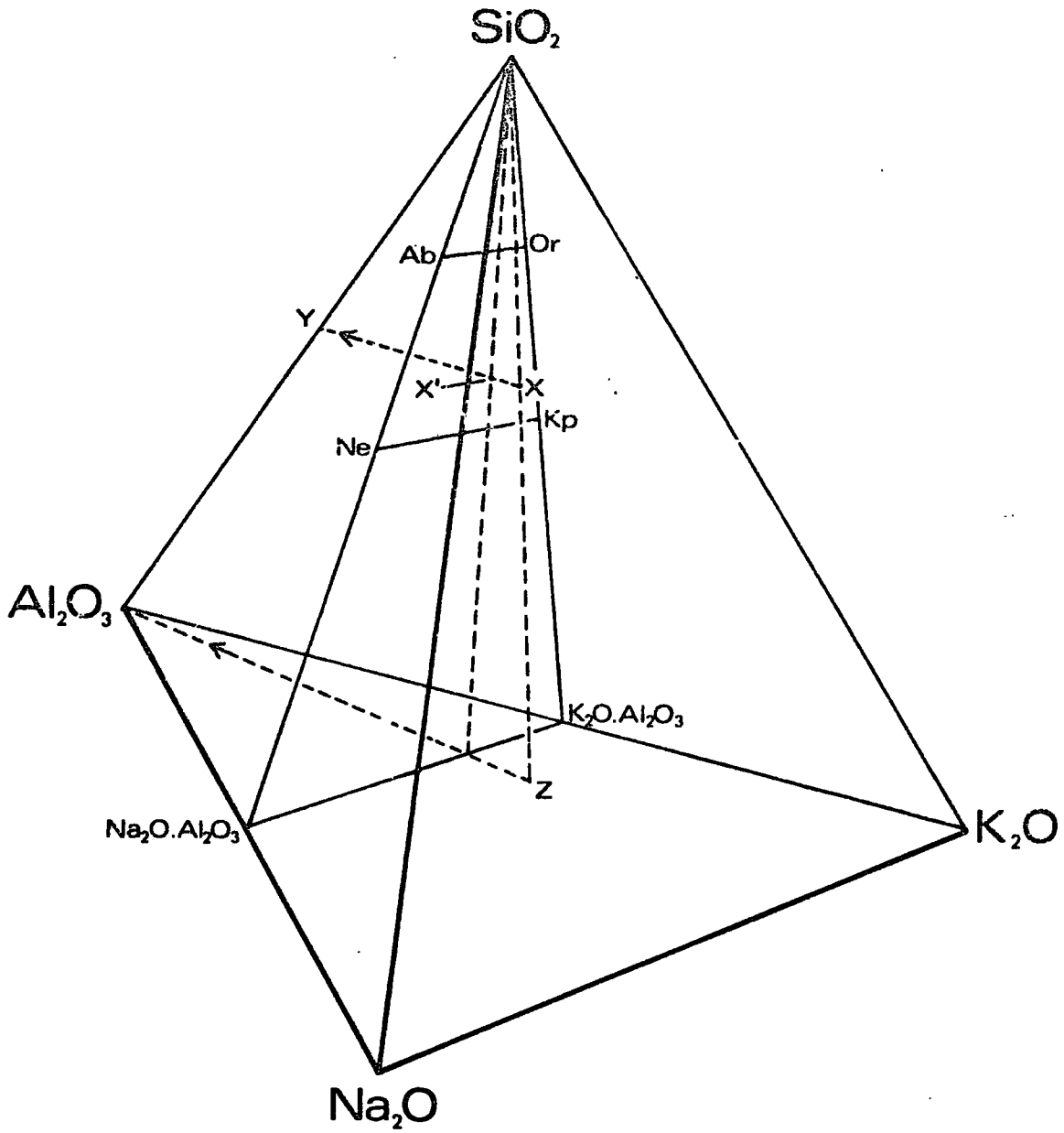
SiO2
Ab
Or
Y
X'
X
Kp
Ne
Al2O3
K2O.Al2O3
Z
Na2O.Al2O3
K2O
Na2O

the alteration of nepheline in 27271 and 39725 (dotted open symbols) and the late-stage formation of cancrinite in 27095 and 39725 have both contributed to the compositional range observed in these rocks. In spite of the superficial resemblance, to the trend seen with the later phonolite dykes (Chapter 4), it is not probable that feldspar fractionation has been a major factor in determining the distribution in Fig. 2.10, because nearly all compositions lie close to the nepheline-feldspar phase boundary. Indeed in some rocks, notably 27095 (Plate 6), there is petrographic evidence for the accumulation of nepheline, in the form of cumulus textures such as are seen in the nepheline-rich foyaites of the Lower Series.

All of the GS-2 syenite compositions fall well within the experimentally determined feldspar stability field in the system SiO_2-$NaAlSiO_4$-$KAlSiO_4$. Several are slightly peralkaline, but in the group as a whole the alkali metals and aluminium appear to be balanced. The iron content is somewhat greater than in GS-1 and the oxidation ratio is considerably higher, but the MgO and CaO contents are of the same order. The contents of a wide range of trace and minor elements are distinctly greater in GS-2 than in GS-1 (see Fig. 2.15). Many of these elements appear to be concentrated in the peralkaline members of GS-2, which suggests that 31898 may have been misidentified; the rock resembles GS-1 syenites in some respects in thin section, and it is relatively mafic and nepheline rich.

If 31898 is removed from GS-2, the group becomes a more integrated entity consisting of peralkaline, relatively feldspathic

syenites with a high trace-element content which is quite distinct from the other Granular Syenites.

2.4 THE COARSE-GRAINED SYENITE

The analyses of seven members of the Coarse-Grained Syenite are shown plotted in the systems SiO_2-Al_2O_3-(Na_2O+K_2O) and SiO_2-$NaAlSiO_4$-$KAlSiO_4$ in Fig. 2.12. The majority of the rocks in this group are peralkaline, and non-normative projected composition points are shown in Fig. 2.12b side by side with the normative data-points, in the manner described above. The Coarse-Grained Syenite covers a range of composition comparable with that of the biotite-rich variety of Granular Syenite, and likewise it extends well into the nepheline field in the Residua system. The most strongly undersaturated rock, 27285, is also exceptionally sodic. In spite of the great dispersion of data-points in Fig. 2.12, petrographic examination shows all members of the group to be very nepheline-rich (Plate 7), with textures reminiscent of the Group I foyaites of the Lower Series. Thus it appears that much of the dispersion in the figure is due to variation in the proportion of ferromagnesian minerals, in which the Al:Si ratio is lower. Pyroxene and biotite are particularly abundant in 27065, 27280 and 126721.

The high average content of CO_2 of the Coarse-Grained Syenite is attributable largely to the very great abundance of cancrinite, which usually forms extensive semi-poikilitic areas enclosing rounded-off grains of nepheline (see for example 27285, 27287). Carbonate is also abundant in some thin sections. While the latter may be a secondary product introduced during later carbonatite

FIGURE 2.12

a. Compositions of the Coarse-Grained Syenites plotted in the silica-undersaturated part of the system SiO_2-Al_2O_3-(Na_2O+K_2O), expressed in molecular proportions.

b. Felsic mornative constituents (closed symbols) of the Coarse-Grained Syenite specimens plotted in the system SiO_2-$NaAlSiO_4$-$KAlSiO_4$ (weight proportions). For peralkaline specimens the non-normative composition point projected from the system SiO_2-Al_2O_4-Na_2O-K_2O, as described in the captions to Figs. 2.10 and 2.11, is also shown (open symbols).

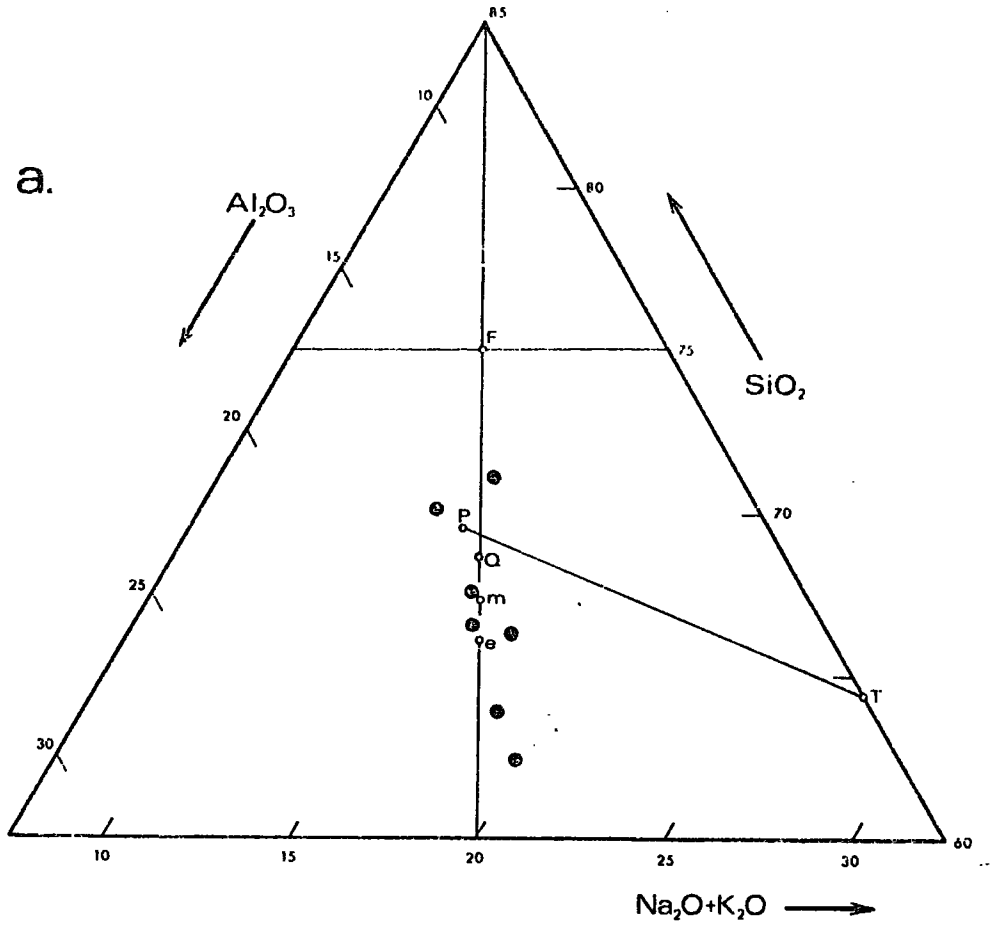
a.
Al_2O_3
SiO_2
Na_2O+K_2O
F
P
Q
m
e
T
85
10
80
15
75
20
70
25
30
60
10
15
20
25
30

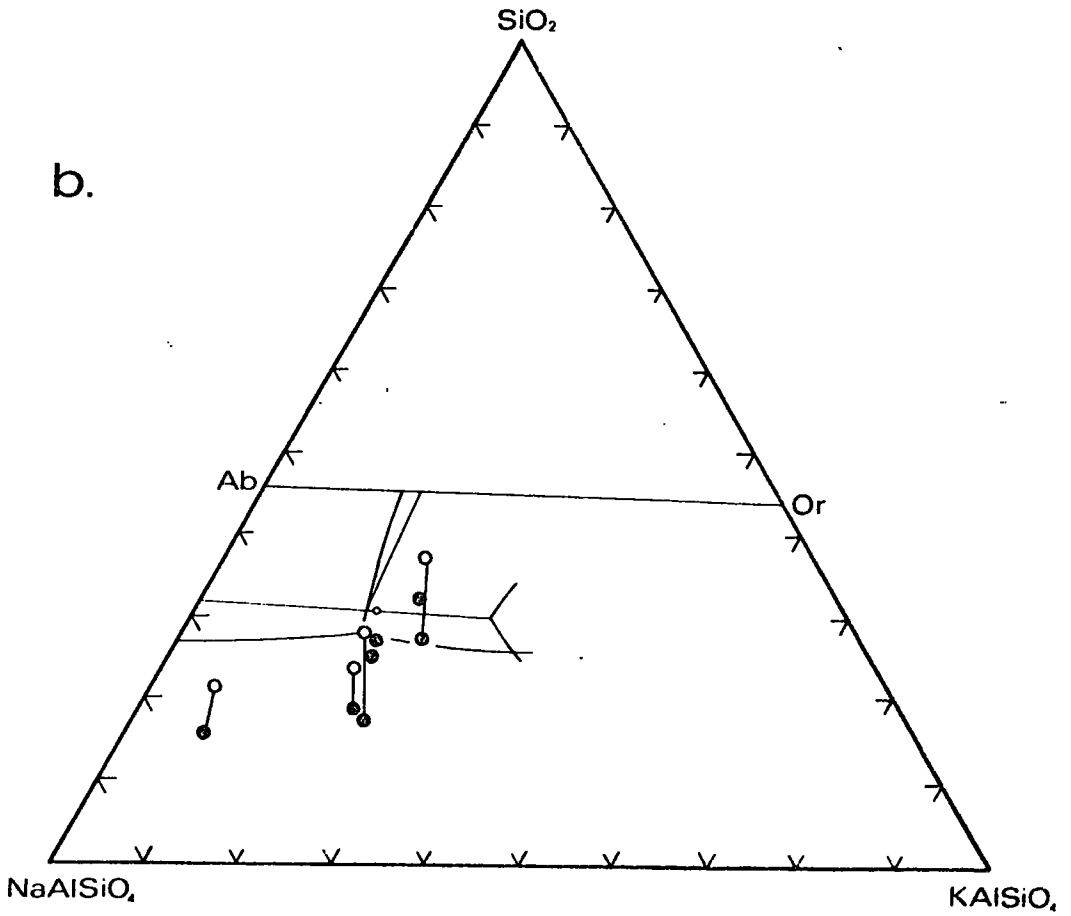
b.
SiO_2
Ab
Or
$NaAlSiO_4$
$KAlSiO_4$

emplacement, the abundance of apparently primary cancrinite seems to indicate either that carbonatite activity took place whilst the Coarse-Grained Syenite was still in a hyper-solidus condition, or that the liquid from which the syenite formed was highly charged with primary carbonate. Certainly carbonate veins are common in the rock. Sodalite is often present, sometimes in association with the carbonate veins (Emeleus 1964 p.18).

2.5 THE XENOLITHIC PORPHYRITIC SYENITE

The felsic components of the members of the Xenolithic Porphyritic Syenite selected for analysis are plotted in Fig. 2.13. From these diagrams it is apparent that with respect to these components the Syenite is relatively constant in composition, in contrast to the biotite-rich variety of Granular Syenite and the Coarse-Grained Syenite. The uniformity extends to other major elements. The alteration of nepheline, which is prevalent in this unit, appears to be a dominant source of variance. This is demonstrated in Fig. 2.13 by the use of symbols reflecting the state of alteration seen in thin section. When the alteration of nepheline to gieseckite is taken into account, the Xenolithic Porphyritic Syenite is seen as a uniform unit whose composition is peralkaline and lies close to the "dry" nepheline syenite minimum in the system SiO_2-$NaAlSiO_4$-$KAlSiO_4$. The variation in the proportion of mafic components is not great (Table A.9a).

The average CO_2 content of the XPS is comparable to that of the Coarse-Grained Syenite, and the remarks made in that context have equal validity.

FIGURE 2.13

a. Compositions of the Xenolithic Porphyritic Syenites plotted in the silica-undersaturated part of the system SiO_2-Al_2O_3-(Na_2O+K_2O), expressed in molecular proportions.

b. Felsic normative constituents (closed symbols) of the xenolithic Porphyritic Syenite specimens plotted in part of the system SiO_2-$NaAlSiO_4$-$KAlSiO_4$ (weight proportions). For peralkaline specimens the non-normative composition point projected from the system SiO_2-Al_2O_3-Na_2O-K_2O, as described in the captions to Figs. 2.10 and 2.11, is also shown (open symbols).

Key

- ● Fresh rock
- ◉ Slightly altered nepheline
- ⊙ More altered nepheline
- ○ Non-normative projection into plane SiO_2-$NaAlSiO_4$-$KAlSiO_4$, as described above.

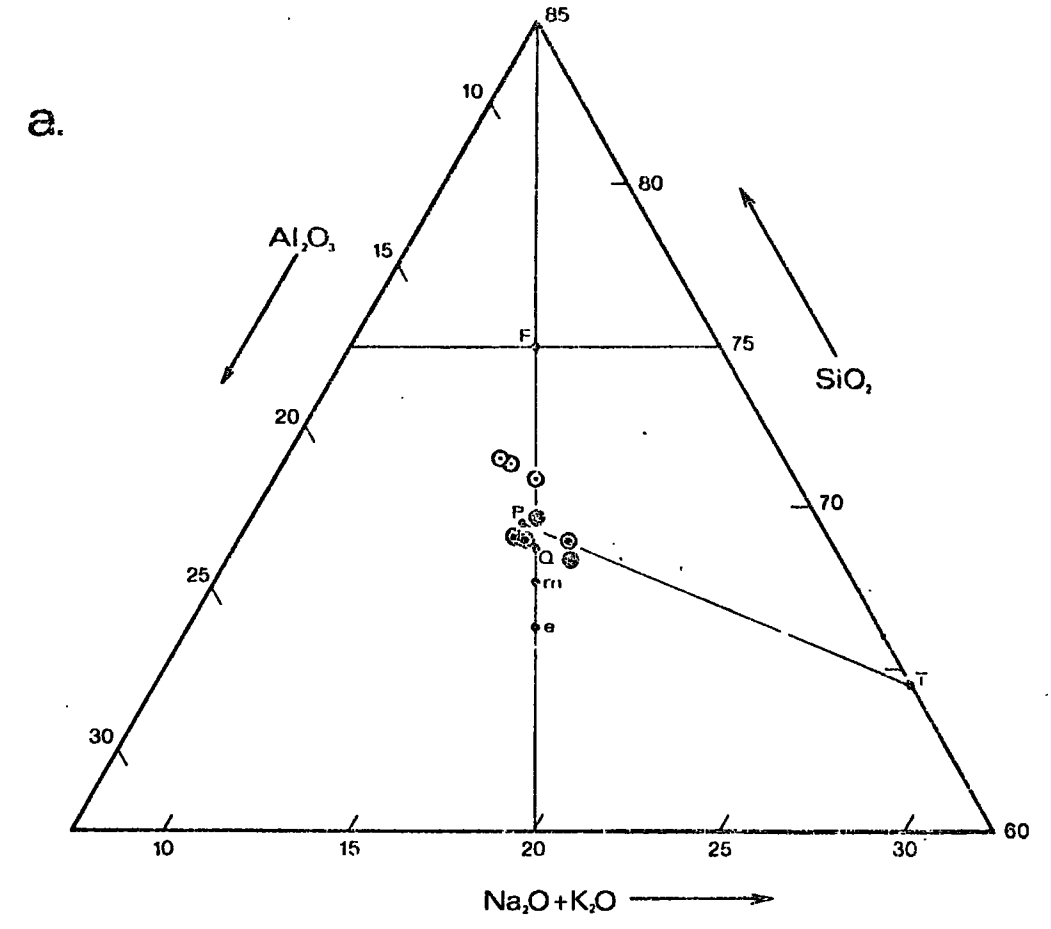
a.
85
10
80
Al_2O_3
15
F
75
SiO_2
20
70
P
Q
m
e
T
25
30
10
15
20
25
30
60
Na_2O+K_2O

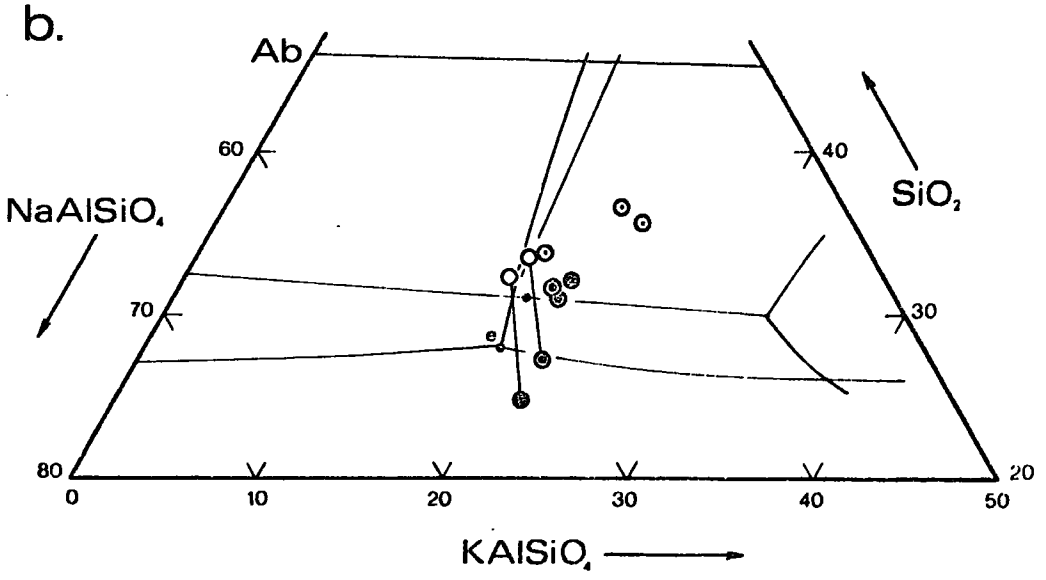
b.
Ab
60
40
$NaAlSiO_4$
SiO_2
70
30
e
80
0
10
20
30
40
50
20
$KAlSiO_4$

2.6 THE SYENITE AND MICROSYENITE DYKES

Dykes of nepheline syenite and nepheline microsyenite are quite common and from their appearance in thin section seem to vary somewhat in type. One may attach some importance to these rocks since they may indicate the range of liquid compositions developed during the emplacement of the main syenite units. Field evidence is at least consistent with view that these dykes are in many cases transgressive equivalents on the liquids from which the laminated units were formed and that the dykes and laminated syenites belong to the same episode of intrusion (Emeleus 1964). In this respect the dykes are to be distinguished from the abundant fine-grained phonolite dykes which appear by their intersections with dolerite dykes to be much later; these phonolite dykes are described in detail in Part 2 (also Gill, in press).

In spite of the petrographic variety seen in the syenite dykes as a whole, there appears to be no simple way in which they may be subdivided. The dykes include two petrographically distinctive groups of microsyenites. Together, however, they account for fewer than half of the specimens collected, and, because the remaining dykes are in no way distinctive, a petrographic classification would not be universally applicable. Attempts to distinguish sub-groups in the analytical data by means of Q-mode factor analysis (see Appendix 5) have been unsuccessful, and the application of R-mode factor analysis produced equally disappointing results. To provide a framework for discussion, the syenite dykes have therefore been subdivided with reference to both age and petrographic type, as shown in Table 2.1.

Table 2.1 Subdivision of the syenite and microsyenite dykes

Age	Petrographic affinity	Characteristics	Group No.
Cutting Lower Series	Porphyritic microsyenite ("27200-type")	Strongly feldspar- and nepheline-phyric	1
	Other Syenite dykes	Coarser-grained	2
Cutting Upper Series	Microsyenite ("31803-type")	Rare elongate feldspar phenocrysts Biotite common	3
	Other syenite dykes	Coarser-grained	4
	Porphyritic microsyenite	As Group 1	5

FIGURE 2.14

a. Compositions of the syenite and microsyenite dykes plotted in the silica-undersaturated part of the system SiO_2-Al_2O_3-(Na_2O+K_2O) expressed in molecular percent.

b. Felsic normative constituents of the syenite dykes plotted in part of the system SiO_2-$NaAlSiO_4$-$KAlSiO_4$ (weight proportions). For peralkaline specimens, non-normative projections are shown as described previously.

Key

▲ Group 1

△ Group 2

● Group 3

○ Group 4

▼ Group 5

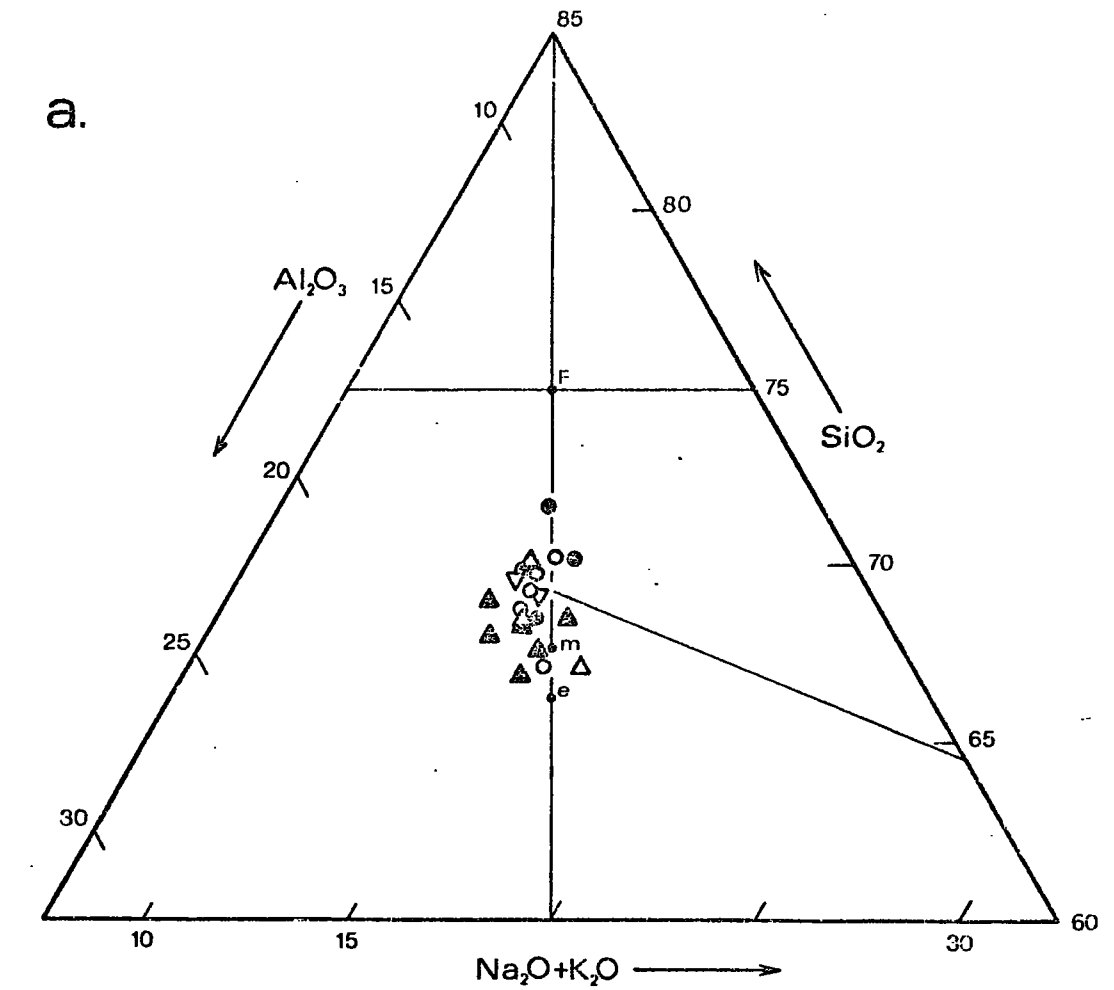
a.
85
10
80
Al_2O_3
15
F
75
SiO_2
20
70
25
m
e
65
30
60
10
15
30
Na_2O+K_2O

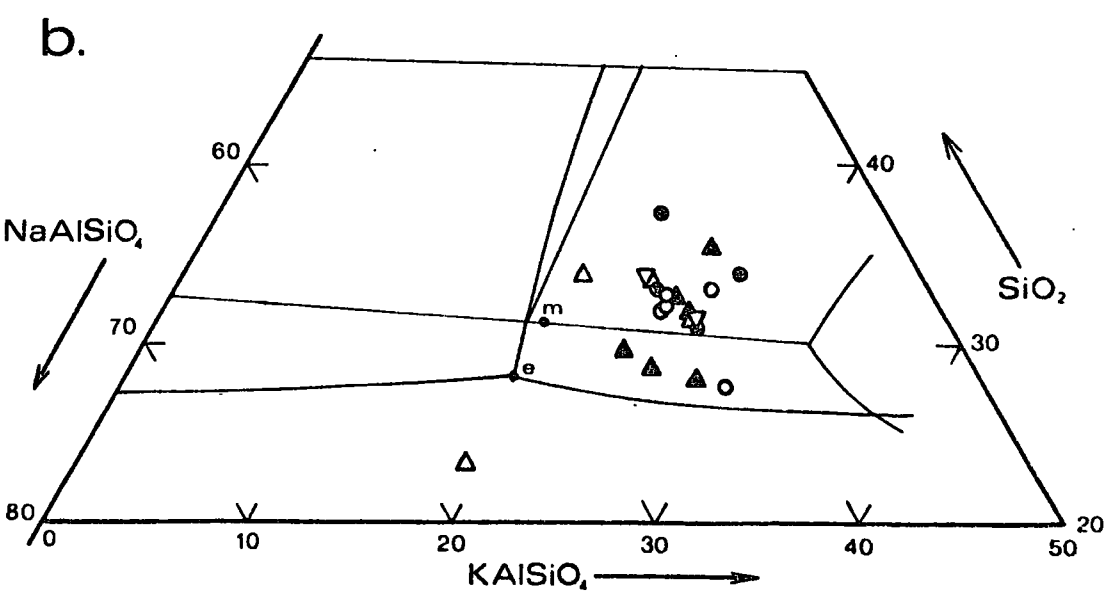
b.
60
40
$NaAlSiO_4$
SiO_2
70
m
30
e
80
20
0
10
20
30
40
50
$KAlSiO_4$

The groupings which emerge from this subdivision are not distinguishable in the relative proportions of the felsic constituents alone (Fig. 2.14). Examination of the analyses of a wider range of elements (Appendix 6, Tables A.6 and A.7) reveals a more consistent pattern, however. Groups 1, 2 and 5 are found to be very similar chemically. The major element chemistry of Group 4 is broadly comparable, but there are distinct differences in the contents of CaO, CO_3 and associated trace elements. More extensive chemical comparisons between units are discussed in the following section.

The microsyenite dykes comprising Group 3 are of a type referred to by Emeleus (1964 p.57) as being similar to the "Scott's Diabase" (tinguaite) group of the Ivigtut area. They form the least undersaturated group of those defined in Table 2.1 and are distinguished by high rare earth, niobium and zinc contents and low concentrations of barium and strontium.

2.7 THE VARIATION BETWEEN THE SYENITE UNITS

In the preceeding sections, the chemical variation observed within the units described by Emeleus (1964) has been discussed. The differences between the units will now be examined, and for this purpose the mean compositions of the various syenites are plotted in the form of a variation diagram in Fig. 2.15. Clearly the averages which have been calculated (Appendix 6, Tables A.6 and A.7) must be viewed with the greatest caution on account of the necessarily haphazard sampling described in Chapter 1. Nevertheless for comparative purposes the means may in most cases be regarded as representative.

FIGURE 2.15

A composite variation diagram illustrating the chemical differences between the units defined in Fig. 1.2 and the text. The mean composition of each unit is indicated by an open symbol, and the chemical variation in the unit is indicated by an error bar, which represents the standard deviation about the mean; the length of the bar is two times the standard deviation. In instances where the standard deviation is too small to depict in this manner, a square symbol is used to represent the mean; in other cases it is indicated by a round symbol. For the Upper Series, the composition of the chill is indicated by a filled circle.

The abbreviated names for the main syenite units are as given in Fig. 1.2. The syenite and microsyenite dykes are represented as D1, D2, ...etc., where the number refers to the groups defined in Table 2.1. The Lower Series foyaite is represented by the means of Groups I to III together and the mean of Group IV alone. A vertical line, intersecting the broken line linking adjacent means indicates the mean composition of the Lower Series as a whole.

Graduations:

Si - CO_2 : wt.% oxide.

Rb - Nb : p.p.m. (weight) metal.

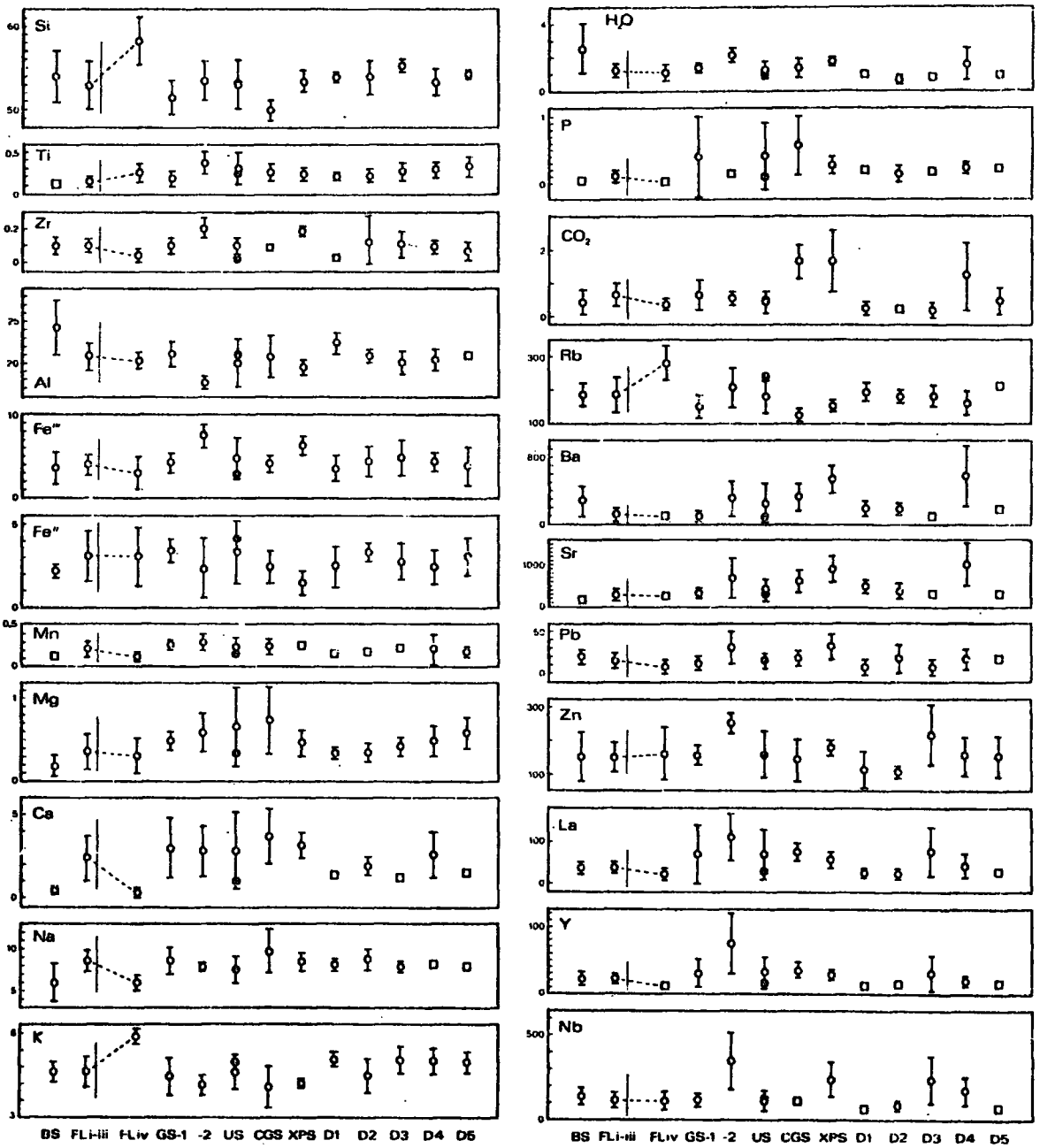
Si
Ti
Zr
Al
Fe"
Fe"
Mn
Mg
Ca
Na
K
H2O
P
CO2
Rb
Ba
Sr
Pb
Zn
La
Y
Nb
BS FLi-iii FLiv GS-1 -2 US CGS XPS D1 D2 D3 D4 D5
BS FLi-iii FLiv GS-1 -2 US CGS XPS D1 D2 D3 D4 D5

The Coarse-Grained Brown Syenite (BS) is exceptional in several ways, largely as a result of its altered state. Al_2O_3 and H_2O^+ are notably higher than in any other unit, Ba is somewhat higher in relation to Sr, whereas Na_2O is depleted to some extent relative to SiO_2, Al_2O_3 and K_2O.

The high concentration of the rest-elements Zr, Ti, Rb, Pb, Zn, La, Y and Nb in GS-2 is remarkable, as are the high content of Fe_2O_3 and the low level of Al_2O_3. In many respects this syenite is similar to the Xenolithic Porphyritic Syenite, perhaps representing a more differentiated fraction of the same magma. If 31898 is omitted (see Section 2.3), the character of GS-2 is still more striking.

There is an emphatic rise in CO_2 in passing to the Coarse-Grained Syenite and the Xenolithic Porphyritic Syenite, and this feature is reflected too in the distribution of Ba and Sr. The same points of difference distinguish the dykes of Group 4 from the other dyke types. In contrast, the remaining dykes form a uniform group, with the exception of the "Scott's Diabase" type which has parallels with the Xenolithic Porphyritic Syenite.

A striking similarity exists between the Granular Syenite GS-1 and the Coarse Grained Syenite, except with regard to the elements associated with the high level of carbonatite in the latter.

The differences between the Lower and Upper Series averages are obscured by the variation within each unit and by the considerable sampling uncertainty. Whereas the mean compositions of the minor syenites may in most cases be related approximately to a liquid composition, there is insufficient evidence a priori upon which

to base with confidence a comparable estimate for either of the major syenite bodies. A major factor in this uncertainty is the feldspathic syenite seen in both units, the significance of which is subject to speculation. For this reason the feldspathic syenites of Group IV are omitted from the mean of the Lower Series in Fig. 2.15. The mean of this group is given separately, and the average composition of the Lower Series as a whole (omitting the Brown Syenite) is indicated by the vertical line on each diagram where it intersects the join between the two components.

In the case of the Upper Series, the composition of the chill specimen (39706B; see Fig. 2.4 and Chapter 3) is indicated by a cross. Supposing this to represent the composition of the initial liquid, comparison with the mean shows that the components of pyroxene and apatite (Fe_2O_3, Na_2O, CaO, P_2O_5, La and Y) are significantly higher in the latter, whereas elements characteristic of the felsic components (K_2O, Al_2O_3, Rb) are lower. From this one concludes that the pyroxene-apatite layers in the Upper Series are over-represented in the sample of specimens examined. This conclusion is hardly surprising in view of the virtual absence of specimens from the Foyaite and Pulaskite above the pyroxene-rich syenite, in which the proportion of ferromagnesian constituents is quite low (Emeleus 1964, p.17).

There is a close similarity between the composition of the chill specimen 39706B and the majority of syenite dykes (excluding Group 3).

CHAPTER 3

FORMATION OF THE COMPLEX

3.1 INTRUSIVE AND COOLING HISTORY OF THE LOWER SERIES

Review

In Chapter 2 it was established that the Lower Series foyaite is a differentiated body of rock, the lower part of which, immediately above the Coarse-Grained Brown Syenite, is particularly rich in normative and modal nepheline. At higher levels there appears to be a continuous progression to a foyaite approximating in composition to the nepheline syenite minimum in the system SiO_2-$NaAlSiO_4$-$KAlSiO_4$ at atmospheric pressure. The very top of the Lower Series is however marked by a distinctive laminated pulaskite with a composition near the alkali feldspar join in the system SiO_2-$NaAlSiO_4$-$KAlSiO_4$, but lying well to the potassic side of the temperature minimum on that join. Feldspathic syenites are also found at a few localities in the gneiss raft (Appendix 6, Tables A.7, A.8 and A.9) but the rocks appear to be more sodic in composition, and the clear textural attributes of the Lower Series pulaskite are lacking.

The place of the Coarse-Grained Brown Syenite in this scheme is not altogether clear. The limited evidence available is consistent with the view that it represents a downward continuation of the Group I (nepheline-rich) foyaite. Petrographic evidence is broadly consistent with this interpretation and indeed some specimens of Brown Syenite (e.g. 31896, Plate 4) appear to have been especially nepheline-rich. The greater

extent of alteration in the Coarse-Grained Brown syenite may have been caused by moisture drawn from the wall-rocks into the relatively dry cumulus deposit where it abuts upon the gneiss. Alternatively alteration may have accompanied the later emplacement of the sheets of Granular Syenite, which would provide both the activation energy and the volatile components required for the alteration process to take place.

Crystal Fractionation in the Lower Series

Emeleus (1964) regards both the Lower and Upper Laminated Series as being the products of the gravity accumulation of crystal phases from a liquid undergoing mild convective circulation. The present Lower Series probably represents the cumulus deposit from a larger body of magma, perhaps of the dimensions indicated by the present Upper Series. A body of magma having much the same configuration as the present Lower Series alone is ruled out by the consistent feldspar lamination at high angles of dip. In the following paragraphs the apparent sequence of crystallisation from this magma body is examined.

The chemical variation seen in the lower parts of the Lower Series may reasonably be explained in terms of the intrusion of a magma oversaturated with respect to nepheline. In other words, the first solid phase to appear on cooling would be nepheline, the separation of which would drive the liquid composition toward the nepheline-feldspar phase boundary. When the liquid composition reached this boundary, nepheline and feldspar would crystallise side by side, but by this time a certain amount of nepheline-settling would have occurred to

produce, when superimposed on the subsequent fractionation of feldspar and nepheline in constant proportion, a continuous downward concentration of nepheline in the cumulus deposit. Textural relationships in the nepheline-rich foyaite are in good agreement with the supposed fractionation of nepheline to the bottom of the chamber (Chapter 2 and Plates 3 and 4). The existence of a similar trend in the marginal rocks found in one of the tributaries of the Radioelv (Fig. 2.2) is further evidence for this sequence of events.

The feldspathic syenite (Group IV) at the very top of the Lower Series constitutes an abrupt departure from this pattern. The unit is a persistent one, being found along much of the upper boundary of the Lower Series from the north-west (under the gneiss raft) down to the Radioelv exposures in the south (directly underneath the Upper Series). The pronounced lamination of the feldspar laths, the compositions of the rocks, considerably to the potassium-rich side of the feldspar minimum, and the paucity of nepheline collectively point to an episode of fairly widespread accumulation of feldspar virtually alone, probably from a liquid in convective motion. There are two possible mechanisms: either feldspar has been separated mechanically from a suspension of feldspar and nepheline together in the liquid, or feldspar was precipitated alone during the period of accumulation represented by the feldspathic syenites; the nepheline present in the rocks would then be a relatively late phase to form.

Crystals settling in a magma sink with a velocity largely

determined by their size (Stokes' Law) and shape (McNown and Malaika 1950). It is conceivable that the feldspathic syenites represent a more rapid settling of feldspar laths, perhaps upon the resumption of settling after the steady-state accumulation of feldspar and nepheline in constant proportion had been interrupted, either by cessation of crystallisation or by a convective overturn. The efficiency of such a layering process is hard to assess, but reference to the literature on layered complexes (see Wager and Brown 1968) suggests the layers produced in this way are rather thin, of the order of inches or at the most feet. In basic rocks density separation invariably predominates over size and shape effects, but this is unlikely to be true in the present case*. Thickness data are not available for the feldspathic syenites, since they were not identified as a unit in the field. While it is possible that they merely form a thin layer or layers, in which case this mechanism might apply, it seems very unlikely that alternating feldspathic and average layers would be overlooked in the field, and that sampling would be restricted to the former. Field confirmation of this point would be of value.

An episode of fractionation of feldspar alone is offered as the more probable alternative. The change from the fractionation of feldspar and nepheline side by side may have been brought about by a change in the liquid composition to bring it into the feldspar field, or by the shifting of phase boundaries in response to changing

---

*Since the densities of nepheline and feldspar are very similar (2.56-2.66 and 2.55-2.63 respectively according to Deer et al. 1963), density separation will not be important in the present case.

physical conditions to achieve the same effect. The relative merits of the two alternatives are considered later.

The following sequence of liquidus assemblages is therefore inferred for the Lower Series, supposing it to have formed at the bottom of a magma chamber large in relation to the present (exposed) dimensions of the Lower Series:

3. Feldspar alone
2. Nepheline + feldspar
1. Nepheline alone

In addition, there is field and petrographic evidence of the fractionation of aegirine-augite. Such instances are isolated and minor in the Lower Series, however, and for the time being will be ignored. The provenance of the ferromagnesian minerals in general is considered later. In the following paragraphs consideration is given to the factors responsible for the changing patterns of the major cumulus phases outlined above.

The Initial Condition of the Lower Series Magma

One may suppose from the present distribution of nepheline in the Lower Series rocks that the composition of the parent liquid in the early stages of fractionation would have plotted within the nepheline field in the residua system at the relevant value of P_{H_2O}, and that the liquid was at or not far below its liquidus. In the present state of knowledge there appear to be two ways in which these circumstances may have come about. Firstly the nepheline syenite liquid may have been the residual salic derivative of a highly undersaturated mafic magma such as nephelinite. Phonolites are associated with nephelinite lavas in parts of East Africa (King 1965,

Wright 1965, Saggerson and Williams 1964) and in spite of the frequent absence of compositions intermediate between them it is commonly supposed that the two are members of a common fractionation sequence (see Wright 1971). There is however no evidence for the existence of nephelinite or similar magma types in the Gardar province and such an origin for the undersaturated magmas of the Grønnedal-Ika complex therefore seems improbable. The question is discussed in more detail in Chapter 8.

It seems preferable therefore to regard the nepheline syenite liquids of the Gardar province as the residua of the fractional crystallisation of alkali olivine basalt magma, which is ubiquitous in the area (Upton 1970), or of the partial melting of rocks of similar mafic composition. One would expect a nepheline syenite liquid derived in this way to approximate in composition to the thermal minimum on the nepheline-feldspar phase boundary in the residua system at the value of P_{H_2O} relevant to the source region, or, in the case of a more primitive liquid, to lie in the feldspar field. With reference to the felsic components above, such a liquid would in the source region be in equilibrium with nepheline and feldspar, or feldspar alone (in contrast to a nephelinite derivative which would initially be in equilibrium with nepheline alone).

The fractionation of nepheline alone from such a liquid in the magma chamber of the Lower Series may be possible, given certain changes in physical conditions in passing from the source region to the magma chamber. Recent experimental studies on the silica-undersaturated part of the system SiO_2-$NaAlSiO_4$-$KAlSiO_4$-H_2O have demonstrated that the feldspar field expands at the expense of that

of nepheline as the water vapour pressure increases (Hamilton and MacKenzie 1965, Morse 1969). At the same time the temperature of the nepheline syenite minimum falls, becoming a eutectic above 5 kb (Morse 1969). Thus the composition of a liquid in equilibrium with feldspar and nepheline at a high P_{H_2O} would, if the water pressure were reduced, be enveloped by the nepheline field. Superficially the observation provides a mechanism by which the initial fractionation of nepheline could be brought about, since if the liquid remained on the liquidus during the transition, nepheline would begin to separate alone.

In the context of a water-saturated magma involving only anhydrous phases, however, such an argument breaks down. Experimental work has shown (Morse 1969) that for the liquidus surface in the residua system ($P_{H_2O} \leq 5$ kb), dT/dP is negative. Thus the relief of water pressure causes the liquidus temperature of any composition in this system to rise. If this applies to the analogous natural system a large change in P_{H_2O}, such as that necessary to shift the nepheline-feldspar phase boundary to the extent implied by the model under discussion, would cause the liquid to solidify rapidly without cooling. In such circumstances little settling would occur and no downward concentration of nepheline would be seen, even if nepheline were to precipitate first.

This objection, based on the dT/dP trend observed in the water-saturated residua system, would probably cease to apply either if the system at high pressure were undersaturated with respect to water, or if it were saturated but under conditions in which a hydrous phase (for example, analcime) controlled the shape of the liquidus.

The possible influence of these two factors will be discussed in turn.

The behaviour to be expected of a water-undersaturated nepheline syenite magma under varying physical conditions may be explained with reference to the hypothetical P(total)-T diagram shown in Fig. 3.1. The information upon which this diagram is based is drawn from the sources given in the caption; to the extent which the available data allows, certain aspects of the diagram have been quantified approximately, but the hypothesis is discussed below in qualitative terms only.

Consider the nepheline syenite liquid on its liquidus at point P. The liquid is undersaturated with respect to water at the relevant pressure, and the dT/dP of its liquidus is therefore positive (see Harris et al. 1970). Suppose that the confining pressure P_T on the liquid body is significantly reduced, for example by the release of the liquid to a higher level magma chamber. For simplicity, the change is represented by a vertical line (PQQ') in Fig. 3.1, although in general the temperature of the liquid may rise if the pressure change is rapid and adiabatic (Harris et al. 1970) or fall if the magma is allowed to lose much heat to the wall-rock during a slow passage upwards. If the rise of the liquid is arrested at Q, it will be intruded in a wholly liquid condition, but if it continues rising until Q', then it will have crystals of the liquidus phase(s) suspended in it at the time of intrusion, unless the degree of supercooling is small.

During the movement of the liquidus from P to Q or Q', P_{H_2O} will change in sympathy with P_T. This may be shown as follows. For a

FIGURE 3.1

Postulated P(total)-T relationships applicable to a nepheline syenite liquid undersaturated with respect to water. The water-saturated liquidus and solidus curves are based on the data of Millhollen (1971) for a natural nepheline syenite and Piotrowski and Edgar (1970) for a natural phonolite. Water-undersaturated liquidi have been drawn schematically by analogy with Yoder and Tilley (1962) and Harris et al. (1970). The point P is an arbitrary starting point at which the liquid is in equilibrium with feldspar and nepheline. Q and Q' represent points at which the liquid might come to rest.

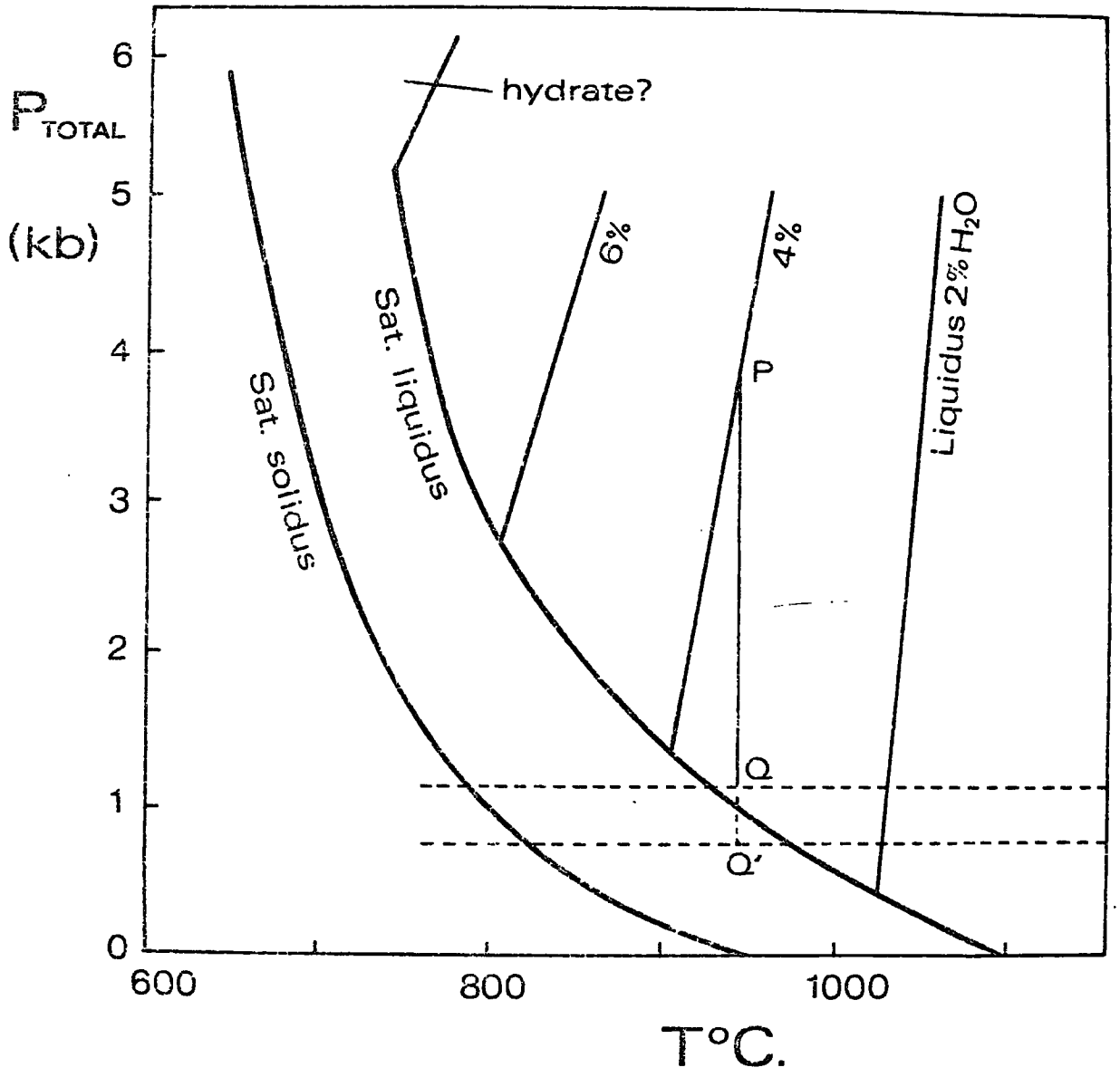
P_{TOTAL}
(kb)
6
5
4
3
2
1
0
600
800
1000
T°C.
hydrate?
Sat. solidus
Sat. liquidus
6%
4%
P
Q
Q'
Liquidus 2% H_2O

63a

liquid which is undersaturated with respect to water, one may write

$$P_{H_2O} = \frac{X_{H_2O} \cdot P_T}{\left(X^{sat}_{H_2O}\right)_{P_T}} \qquad 3.1$$

where X_{H_2O} is the mole fraction of water in the liquid, actual and at saturation. Assuming

$$\left(X^{sat}_{H_2O}\right)_{P_T} \propto \sqrt{P_T} \qquad 3.2$$

(Hamilton et al. 1964), one may derive

$$P_{H_2O} \propto X_{H_2O} \cdot \sqrt{P_T} \qquad 3.3$$

Thus the water vapour pressure in a water-undersaturated liquid will vary directly with the total pressure.

A nepheline syenite liquid following the path PQ(Q') in Fig. 3.1 would therefore undergo a pronounced reduction in P_{H_2O} but would remain above its liquidus for the time taken in passing from P to Q and possibly beyond. Supposing that the position of the feldspar-nepheline phase boundary in the residua system is more sensitive to P_{H_2O} than P_T, therefore, it is possible for a residual liquid in equilibrium with both nepheline and feldspar at depth to be found to lie within the nepheline field at a lesser depth. Whether the magma is intruded in a wholly liquid condition or charged with nepheline crystals would depend upon the water content and the final value of P_T (Fig. 3.1).

It has to be assumed in this argument that P_{H_2O} has greater influence on the position of the phase boundaries in the system

SiO_2-$NaAlSiO_4$-$KAlSiO_4$ than P_T. Unfortunately experimental verification of this supposition is not available, nor has the writer been able to trace end-member (Ab-Ne) P-T data at high dry pressures upon which to base a reasoned prediction.

There is no firm indication that residual liquids necessarily evolve under conditions of water saturation at high pressure, and the residua system at water vapour pressures less than saturation may offer a fruitful area for future experimental studies. In the present situation it is impossible to make an objective assessment of the hypothesis developed above.

For certain compositions at values of P_{H_2O} greater than 5 kb, analcime becomes a liquidus phase in the silica-undersaturated part of the residua system (Morse 1969, Kim and Burley 1971a, Liou 1971). For a liquidus controlled by the melting of a hydrous phase, dT/dP is in some cases positive. By postulating the influence of such a hydrous phase on residual equilibria at depth, therefore, the dT/dP objection facing the high-P_{H_2O} equilibrium hypothesis discussed above for the Lower Series initial liquid may possibly be diminished. Recent studies however show (Kim and Burley 1971a) that dT/dP for the melting of analcime in the system Ab-Ne-H_2O at high pressures is in fact negative, making such a mechanism involving analcime implausible.

Subsequent Development of the Lower Series

On passing upwards through the Lower Series, the nepheline-rich syenites give way to foyaites of more normal composition. These rocks are interpreted as the cumulus products from a liquid whose composition coincided with the nepheline-feldspar phase boundary in the natural residua system.

The apparently sudden change of composition from foyaite to the laminated pulaskite (Group IV syenites) at the top of the Lower Series is thought to indicate a shift in the relative positions of the liquid composition and the feldspar-nepheline phase boundary. Such a change may have been brought about by a fresh pulse of magma relatively depleted in the nepheline component, or may represent the extension of the feldspar field brought about by an increase in P_{H_2O}. It is even conceivable that both mechanisms contributed to the change in circumstances. The arguments in favour of each model are discussed in the following paragraphs, in reverse order.

For the changes in question to have come about through an increase of P_{H_2O}, the water vapour pressure obtaining immediately before the formation of the pulaskites must have been substantially less than that at which the liquid would be saturated with water. If this were not so, the supposed influx of a substantial amount of water would have little influence on crystal-liquid phase relations; in such circumstances its chief effect would be to create, or increase the volume of, a separate water-rich fluid phase.

Direct evidence as to the P_{H_2O} under which the major part of the present Lower Series accumulated is not available. Furthermore, although the volatile constituents are often regarded as playing an important part in the evolution of the continental alkaline suite, quantitative experimental or thermodynamic estimates of P_{H_2O} in relation to P_T for the corresponding magmas do not appear to be available. Whether the Lower Series could have formed under P_{H_2O} conditions well below saturation is therefore not clear. Experimental studies of water solubility in silica-undersaturated melts indicate saturation at water contents of 4-6% at 1 kb and 6-10% at 2 kb (Peters

et al. 1966, Kim and Burley 1971b). One cannot therefore argue with confidence that the Lower Series liquid was significantly undersaturated with respect to water, because water contents of this order of magnitude are not hard to envisage for a nepheline syenite liquid. Moreover at the stage represented by the feldspathic syenites, the water content of the residual magma would already have been reinforced by the deposition of a considerable quantity of anhydrous crystalline material (the present foyaites of Groups I, II and III), making an approach towards water-saturation yet more probable. On balance it seems unlikely that the Lower Series pulaskite is a consequence of a rapid change in P_{H_2O}, but new evidence may require the revision of this conclusion.

The alternative view is that the pulaskite represents an abrupt change in the composition of the liquid. Field evidence opposes the view that much assimilation of wall-rocks has taken place, and one concludes that a fresh batch of liquid may have been introduced, either expelling or contaminating the magma from which the foyaites had been forming. Limiting the discussion to magmas which are now in evidence in the form of intrusive rocks in other parts of the complex, one may distinguish two intrusive episodes which would satisfy chronological requirements in accounting for the feldspathic syenites in this manner. The first alternative is that magma corresponding to GS-2 in composition replaced the original Lower Series magma. The relatively feldspathic character of the GS-2 rocks has been noted (Chapter 2) and it is feasible that the introduction of a liquid of such a

composition would be marked by the precipitation of alkali feldspar alone. The field data are consistent with the possibility that the GS-2 "ring-dyke" was formed at much the same time. It is not envisaged that the Upper Series formed from this magma (see Fig. 2.15 and the discussion in the final section of this Chapter), and one must suppose that it would have been expelled on the emplacement of a distinct Upper Series magma body.

However, field observation is also consistent with the view that the Granular Syenite of GS-2 type was intruded at much the same time as the Xenolithic Porphyritic Syenite, as their chemical similarity might be taken to indicate. This possibility is discussed later in this chapter.

The alternative hypothesis is to suppose that the pulaskites of the Lower Series in fact represent the first cumulus deposit of the Upper Series, the foundering of the gneiss raft (Emeleus 1964) occurring somewhat after the intrusion of the magma rather than during the emplacement. If this is the case, one should be able to find evidence of initial feldspar fractionation in the Upper Series proper. This question is considered fully in the section dealing with the Upper Series. There are however textural differences between the Lower Series, including the feldspathic syenites, and the Upper Series which militate against acceptance of this model. The feldspars in the feldspathic syenites are slender laths of limited size, a form quite foreign to the Upper Series (C.H. Emeleus, pers. comm.).

In the absence of further evidence, the origin of the pulaskites

of the Lower Series remains very uncertain, particularly as no concrete data are available to rule out the influence of changes in volatile pressure.

Distribution of the Ferromagnesian Constituents

Mafic layering of a rather ill-defined sort is developed in the Lower Series foyaite (Emeleus 1964, p.17), and this feature is represented in the analysed suite of rocks by the specimens 27277A (average rock) and 27277M (mafic layer). Even excluding these specimens, factor analysis has shown that the distribution of pyroxene constitutes the largest element in the observed chemical variance. It therefore seems to be an oversimplification to regard feldspar and nepheline as the only liquidus (fractionating) phases. In many thin sections the euhedral habit of pyroxene and the occasional synneusis clusters are good grounds for proposing that pyroxene was among the earliest of the phases to precipitate. The absence of pronounced layering in such circumstances may merely reflect the absence of vigorous convection or of other physical conditions essential to its formation.

In thin section the occurrence of biotite appears to be entirely interstitial. Nevertheless it is by no means uniformly distributed from rock to rock, as factor analysis and X-ray diffraction have demonstrated (Fig. 2.6). The reasons for this sporadic manner of distribution are not clear but it suggests that considerable ionic diffusion took place among the interstices of the rock. The mechanism may have been by exchange with the liquid above the crystal pile (localised heteradcumulus growth), or by a

process of segregation of the pore fluid among the interstices. In either case the solidification of the trapped liquid does not appear on these grounds to have been very rapid, and the data contrast with the supposition by Emeleus (1964, p.26) that the crystallisation of trapped liquid may have kept pace with the accumulation of early formed minerals, thus preserving the potentially unstable high dip of mineral deposition and lamination. If this were the case, one would expect biotite to be more evenly distributed among the rock samples.

The Granular Syenite GS-1

Emeleus (1964) suggests that the biotite-rich Granular Syenite (GS-1) may be contemporaneous with the foyaite of the Lower Series. The chemical work described here is entirely consistent with this view; reference to Fig. 2.15 shows that for every element except Ca, P, La and Y there is close agreement between GS-1 and the average of the Lower Series foyaites. The departure with regard to these elements may be attributed solely to the influence of 27093, which for some reason is anomalously rich in these constituents (Appendix 6, Table A.8c). The remaining members of the GS-1 suite which have been analysed are very similar to the Lower Series foyaite in these respects.

The biotite-rich Granular Syenite is seen cutting Coarse-Grained Brown Syenite and gneiss on the fringe of the Lower Series. No intersections have been observed with the fresher rocks higher up in the Lower Laminated Series. If the Coarse-Grained Brown Syenite is regarded as the downward continuation of the Lower Series

cumulus pile, one may suppose that the minor intrusions of the biotite-rich Granular Syenite represent the fracturing of earlier crystal accumulations, probably as a result of slumping away from the margins of the complex, which would be assisted by the high slope of the cumulus pile reported by Emeleus (1964). Contemporaneous magma would be drawn into these openings, taking with it suspended crystalline material and possibly even mobilising a proportion of the unconsolidated cumulus mush underlying it. This mechanism would account for the considerable concentrations of cumulus nepheline which are observed locally in the Granular Syenite (27095, see Plate 6) and for the textural similarity with the Lower Series foyaite, particularly Group I.

Much of the chemical variation observed in the biotite-rich Granular Syenite is due to the distribution of the ferromagnesian components (Chapter 2). As with the Lower Series, there are instances in which pyroxene fractionation appears to have occurred. This observation too is consistent with a formation from Lower Series magma.

The Granular Syenite of GS-2 type has clear affinities with later intrusive episodes and is discussed later.

3.2 CHEMICAL DEVELOPMENT OF THE UPPER SERIES

Secular Differentiation of the Felsic Components

Plotting the compositions of the analysed Upper Series syenites in appropriate diagrams (Fig. 2.3) reveals a degree of overall differentiation which is slight in relation to the structural pattern of the Lower Series. Largely because of severe local alteration, however, the sample of syenites selected for analysis

is necessarily biased (Chapter 1), and the distribution of analysed compositions in Fig. 2.3 only tells part of the story. In this section an attempt is made to draw together all the available evidence bearing on the distribution of the felsic components in the Upper Series and on the composition of the initial liquid.

Data on the initial composition of the Upper Series liquid is available from a chilled margin specimen from the northern margin of the complex, where the contact with the gneiss is exposed locally (C.H. Emeleus, unpublished field account). Two specimens from this locality have been analysed. They are 39706A, collected at 6 metres from the contact, and 39706B, at 15 cm from the contact (see Fig. 2.4)*. In comparison to the Skaergaard Intrusion, where the marginal chill zone is about 4 m thick (Wager and Brown 1968), one would expect the chill of the Grønnedal-Íka complex, which consists of smaller intrusions, to be relatively thin. The specimen collected at 15 cm from the supposed contact may therefore be taken to rep-

---

*A further specimen (39706C), consisting of gneiss with a small amount of syenite, was collected from the contact itself. It was not found possible to separate sufficient syenite material for analysis from this specimen. It is a microsyenite with microphenocrysts of biotite alone, but similar texturally to the feldspar- and nepheline-phyric porphyritic microsyenites seen cutting the Lower Series, and locally the Upper Series also (39770, 39771). It may therefore be a later dyke intruded along the contact with the gneiss in the same way that porphyritic microsyenite forms a sheet between the Upper and Lower Series further west (Emeleus 1964 p.28).

resent the composition of the initial liquid, but that obtained at 6 m from the contact is more dubious in this respect. Reference to Table A.7E shows that in fact the analyses are very similar, the greatest differences being in the oxidation state of iron and the relative proportions of the alkali metals.

Unfortunately no more extensive marginal suite of specimens is available for the Upper Series. Consequently, in contrast to the Lower Series, there is no means of following changes in the pattern of fractionation in time. A number of specimens collected near to the margins or the base of the Upper Series are somewhat feldspathic (27141, 27143, 27194, 27209 and 39749) but an almost equal number are either average or feldspar-depleted in composition (Fig. 2.3).

Emeleus (1964) records the existence of rocks approaching pulaskite in composition in the highest exposed parts of the Upper Series. These rocks are not represented in the collection available to the writer, and their significance is uncertain. In the field they appear to grade down into, and form part of the Upper Series, and contrast with the strongly undersaturated character of the later Coarse-Grained Syenite which appears above them. There is no evidence of any association with the Lower Series pulaskites, and indeed this is unlikely, since the latter are texturally more similar to the Lower Series than the coarser Upper Series.

Clearly sample coverage of the Upper Series, particularly of the syenites above the Pyroxene-Rich Syenite, is inadequate for working out a detailed cooling history of the Upper Series. The shortcomings are very largely a consequence of the widespread alteration and poor exposure (Chapter 1). In this respect the

Upper Series appears to be the worst represented of the syenite units.

Mafic Layering in the Upper Series

Pronounced mafic layering is developed locally in the Pyroxene-Rich Syenite of the Upper Series. This is not to say that the magma from which the Upper Series was deposited was particularly rich in the mafic components. Reference to Fig. 2.15 demonstrates that no significant difference exists between the Upper Series chill, representing the initial liquid composition, and the mean composition of the Lower Series foyaite (the best available estimate of the liquid from which the Lower Series was deposited). One must suppose that the greater prominence of layering in the Upper Series reflects the existence during deposition of physical conditions more favourable to it. The mafic layers may therefore represent relatively vigorous convective overturns as envisaged for the layering of the Skaergaard Intrusion (Wager and Brown 1968). Sørensen (1969) on the other hand favours an hypothesis of intermittent crystallisation in explaining the layering of the Ilímaussaq kakortokites and the Lovozero differentiated complex; in both instances he suggests that direct evidence for vigorous convective activity is sufficiently rare to suggest that other mechanisms may have operated to produce the layering in these intrusions, and this may be true of the layering in the Grønnedal-Íka complex.

The Coarse-Grained Syenite

Emeleus (1964) considers that the Coarse-Grained Syenite

outcropping in the eastern part of Grønnedal* probably represents the youngest member of the Upper Laminated Series. Chemical analysis shows it to be strongly undersaturated, however, and this is attributable mainly to the great abundance of nepheline and cancrinite. Petrographically the rocks appear to be nepheline-rich and may be nepheline cumulates (Plate 7); there are parallels with the nepheline-rich foyaites of the Lower Series and GS-1.

On this score the Coarse-Grained Syenite has little in common with the Upper Series, in which nepheline-rich rocks are barely if at all represented. It seems unlikely in this case that changes in physical conditions, in particular water fugacity, could have brought about the fractionation of nepheline alone from the Upper Series magma. It has been shown in connection with the Lower Series that relief of water vapour pressure alone would be expected to cause a magma originally on the liquidus to solidify rapidly, and under these conditions the settling of nepheline is unlikely to occur. The syenite may therefore represent a resurgence of the nepheline-rich foyaite magmatism thought to be responsible for the Lower Series. No intrusive contacts supporting this interpretation are exposed, however. One cannot entirely rule out the possibility that the body is an inclusion of Lower Series foyaite brought up from below during emplacement of the Upper Series. The high concentrations of Ca, P, La and Y are consistent with an origin below the lowest Lower Series horizon exposed at present, in view of the

*This unit should not be confused with the coarse-grained syenite found at the head of Urdal (Plate 1), which is thought to be a large inclusion within the Upper Series (Emeleus 1964 p.29). This body has not been examined in the present work.

evidence for the downward concentration of phosphate in the Lower Series (Chapter 2).

3.3 MINOR INTRUSIVE BODIES

The Xenolithic Porphyritic Syenite and Allied Rocks

It has been noted in Chapter 2 that with respect to the felsic components the Xenolithic Porphyritic Syenite forms a relatively uniform body of rock, in which the content of many trace elements is unusually high. The uniform chemical character of the unit is surprising in view of its variable appearance in the field, and may reflect unrepresentative sampling. The results do suggest that little or no xenolithic material has been included in the samples analysed (see Appendix 1), and if sampling has been representative, that little fractionation has occurred in situ.

Many of the characteristics of the Xenolithic Porphyritic Syenite are shared by the Granular Syenite GS-2 and the microsyenite dykes of Group 3 ("31803-type", see Table 2.1 and text Section 2.6). Both of these groups have compositions which are more feldspar-rich than most rocks in the complex. Both types have trace element patterns similar to the Xenolithic Porphyritic Syenite, but this character is less marked in the case of the dykes. Assuming that the rock analyses are representative of magma compositions, the variation between the Xenolithic Porphyritic Syenite, GS-2 and D3 is more in keeping with three distinct magmatic events, but their similarity indicates that the liquids probably had a common derivation and history. Field relationships are consistent with the possibility that they are closely related with regard to time

of intrusion. The Xenolithic Porphyritic Syenite is known to be the latest major syenite intrusion in the complex (Emeleus 1964).

There are several respects in which the Xenolithic Porphyritic Syenite appears to be associated in some way with carbonatite. The highly xenolithic character points to a violent (almost explosive) mode of emplacement similar to that of the carbonatite, and the high contents of the volatiles (particularly CO_2) and the incompatible elements are consistent with the view that this syenite unit has interacted with carbonatite at an early stage, the latter perhaps providing much of the energy for the intrusion of the syenite. If the identity between the XPS and GS-2 is accepted, however, it is necessary to modify this view. Both the high trace element content and the xenolithic character are developed in the latter, but the carbon dioxide level is no greater than average for the complex. Moreover the Coarse-Grained Syenite has a similar average CO_2 concentration to the Xenolithic Porphyritic Syenite, but neither the trace element levels nor the mode of emplacement compare with the latter. Although the participation of carbonatite in the intrusion of the Xenolithic Porphyritic Syenite cannot entirely be ruled out, few of its major attributes appear to be the result of the association.

Other Syenite and Microsyenite Dykes

Five groups of syenite and microsyenite dykes were distinguished in Chapter 2. With the exception of Group 3, which has been discussed in the previous section, all groups were found to be similar in chemical character. Some departure is noticeable in Group 4 with respect to Ca, CO_2, Ba, Sr, La, Y and Nb (Fig. 2.15) but these

anomalies are probably associated with the emplacement of the carbonatite. In all other respects, the syenite dyke averages under discussion (Fig. 2.15) are virtually identical in composition to the Upper Series chill specimen 39706B.

Emeleus (1964) assigned a later date to the Upper Series relative to the Lower Series because porphyritic microsyenite dykes cutting the Lower Series were petrographically very similar to a rock which he interpreted as the chill of the Upper Series magma (39706C). The present work has however revealed that many dykes cutting the Upper Series are indistinguishable chemically from those cutting the Lower Series, and some are indeed of very similar appearance under the microscope (39770, 39771 - compare plates 8 and 9). These observations throw doubt on the argument given by Emeleus, but do not necessarily indicate that his conclusion is incorrect. All that may be stated with confidence is that the Lower and Upper Series represent distinct intrusive events, because the chill specimen 39706B (representing the initial Upper Series liquid) is incompatible with the fractionation history inferred for the Lower Series from the chemical variation seen in it. This conclusion is supported by textural differences between the two series.

3.4 MAGMA ASSOCIATIONS

In the preceding discussion it has been established that the syenites of the Grønnedal-Ika complex are not of a uniform type. They appear to have been formed from several types of magma, each with a distinct chemical identity. Three such "magma associations" are distinguished, on the grounds outlined below. The composition

of the original magma is not now preserved in every case, and the object of the present section is to summarise the character of and identify the differences between the various liquids which have been inferred.

It has been argued that the Lower Series was the first magma body to be emplaced. It is supposed that the present Lower Laminated Series represents the bottom accumulation from a larger body of such magma. Chemical and petrographic evidence suggests that this magma initially fractionated nepheline and perhaps pyroxene, without feldspar. This observation implies that the liquid composition, on intrusion, lay within the nepheline field in the residua system. Similar arguments apply to the biotite-rich Granular Syenite and the Coarse-Grained Syenite which, with the Lower Series, are the representatives of the first magma association. The average compositions of these rocks are plotted in the system SiO_2-$NaAlSiO_4$-$KAlSiO_4$ in Fig. 3.2 as circles; all plot within the nepheline field at P_{H_2O} = 1 kb.

The identity of the magma responsible for the Lower Series and the allied rocks is known only in a qualitative way, as outlined above, since in all three bodies in which it is represented, compositions seem to have been modified to an unknown degree by crystal settling. Quantitative comparison with the other magma types represented in the complex is therefore ruled out.

An indication of the initial Upper Series magma composition is available from the analysis of the chill, but this key rock is exposed in only one locality and therefore only a single analysis is available. Element-by-element comparison shows that the majority

FIGURE 3.2

Inferred variation of magmatic character in the evolution of the Grønnedal-Íka complex. The normative felsic components of the following entities are presented:

D3 - Average analysis of the microsyenite dykes of Group 3 (Table 2.1).

GS-2 - Average analysis of three syenites of GS-2 type (27099, 27100 and 126701).

XPS - Average analysis of five specimens of Xenolithic Porphyritic Syenite (omitting the more altered specimens 27189, 31841 and 58314).

US(AV) - Average analysis of all Upper Series syenite specimens.

US(C) - Analysis of the Upper Series chill specimen (39706B).

DA - Average analysis of all syenite dykes omitting Group 3.

FL - Average analysis of all Lower Series syenite (omitting the feldspathic syenites of Group IV).

GS-1 - Average analysis of all syenite specimens of GS-1 type.

GGS - Average analysis of all specimens of the Coarse-Grained Syenite.

The data points are of three types, representing the three magma groups distinguished in the text.

Because the Coarse-Grained Brown Syenite has been omitted, nepheline-rich rocks may be under-represented in the average analysis of the Lower Series foyaites. This possibility is indicated by an arrow from the FL symbol, showing the direction in which the supposed "true" average would lie.

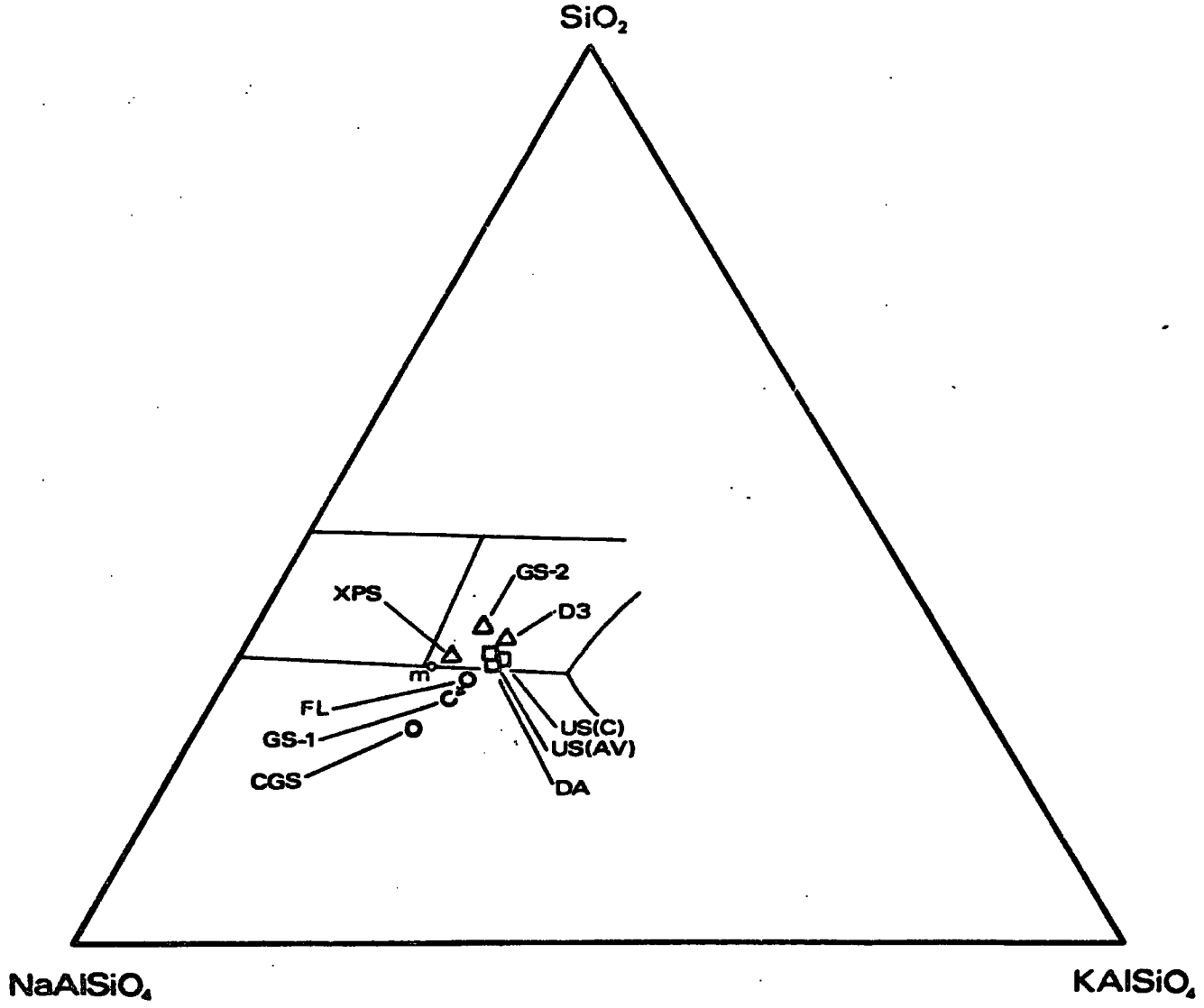
SiO2
NaAlSiO4
KAlSiO4
XPS
GS-2
D3
m
FL
C
O
GS-1
O
CGS
US(C)
US(AV)
DA

of syenite dykes are of very similar composition (Fig. 2.15), but there is no scope for establishing this relationship against accepted statistical criteria. The average analyses of this second magma association plot close to the nepheline-feldspar phase boundary in Fig. 3.2 and the relative uniformity of the Upper Series rocks with respect to their felsic components is consistent with the conclusion that the Upper Series magma composition lay near the feldspar-nepheline phase boundary in the natural phase system.

The trace element chemistry of the second magma association is characterised by low contents of the incompatible elements (Fig. 2.15). These elements tend to be slightly lower in the dykes than in the Upper Series chill, whereas Ba and Sr are marginally higher. If this pattern is significant, it may reflect the presence in the dyke of a small proportion of early-crystallising material derived from the main magma body, a conclusion in keeping with the strongly porphyritic nature of the microsyenites. The distribution of Zr suggests that zircon may be an early phase to crystallise in the Upper Series magma.

One may suppose that, where syenite dykes akin to the Upper Series magma cut the Upper Series, they represent the opening of early cumulus deposits to admit contemporaneous magma, as suggested for the GS-1 dykes cutting the Lower Series.

The third magma association to be distinguished is that represented by the Xenolithic Porphyritic Syenite, the Granular Syenite of GS-2 type and possibly the rare microsyenite dykes of 31803 type (Group 3, see Table 2.1). This association is marked by relatively high contents of the incompatible elements (Zr, Pb,

Zn, La, Y and Nb, Fig. 2.15) and a tendency to peralkaline, somewhat feldspathic compositions (Fig. 3.2). It is not unreasonable to suppose that the various bodies representing this association may have been intruded at much the same moment in the development of the complex, and in a similar manner. The Granular Syenite of GS-2 type is seen to cut and chill against the GS-1 type, and in contrast to the latter it contains numerous xenoliths (Emeleus 1964, p.29), suggesting quite forcible intrusion in much the same manner as the Xenolithic Porphyritic Syenite. No intersections of chronological significance are recorded for the Group 3 microsyenite dykes, except that they are later than the Upper Laminated Series. The chronology of the magma types discussed above cannot be established unambiguously. The simplest interpretation is that shown in Fig. 3.3, which suggests that with the passage of time successive nepheline syenite liquids have moved consistently from nepheline-oversaturation to feldspar-oversaturation, with concomitant changes in $\frac{Na+K}{Al}$ and trace element content. Uncertainty as to the age of GS-2 and the true nature of the CGS puts this hypothesis in some doubt, however.

The possible origins of the magma associations discussed in these pages are considered in Chapter 8. In the intervening chapters the later groups of dyke rocks cutting the complex are described.

FIGURE 3.3

Possible chronology of the Grønnedal-Ika complex, based on the simplest pattern of magmatic trend.

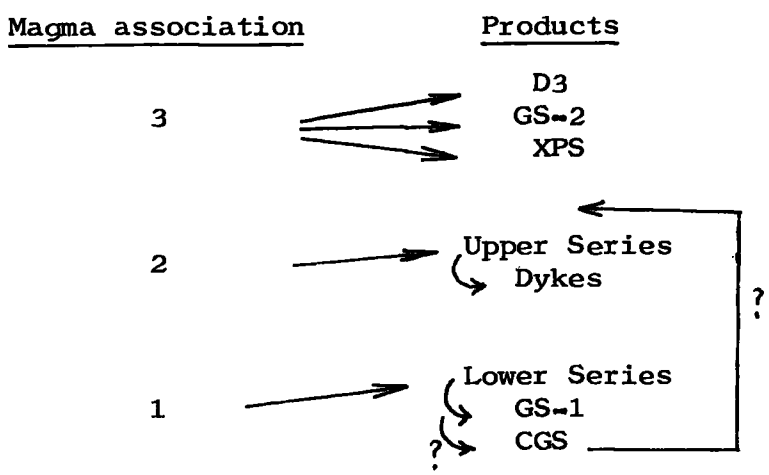

PART 2

THE DYKE ROCKS

Part 2. The Dyke Rocks

CHAPTER 4

THE CHEMISTRY OF THE PERALKALINE PHONOLITE DYKES

4.1 INTRODUCTION

Dyke rocks are found in considerable abundance and variety in the Gardar area, and comprise a volumetrically important part of the magmatic province. Reviews of the dyke activity have been given by Berthelsen and Noe-Nygaard (1965), Sørensen (1966) and Upton (in press). Throughout the province the most abundant type is alkali olivine basalt or olivine dolerite upon which work is currently in progress, on a regional scale (Upton 1970). The salic alkaline dykes are largely restricted to two of the three parallel dyke/fault zones described by Berthelsen and Noe-Nygaard (1965), those passing through the Grønnedal-Íka-Ivigtût area and the Tugtutôq-Ilimaussaq-Igaliko area (Chapter 1). Salic dykes form the youngest group in the dyke sequence, but there are older groups of salic rocks present which both precede and postdate the earlier syenites of the province (Emeleus 1964, Emeleus and Harry 1970).

The Grønnedal-Íka syenites and carbonatite were intruded early in the Gardar period, and there appears to have been a considerable lapse of time between these events and the resurgence of alkaline magmatism represented by the salic dykes in the area. In the period between, igneous activity was mainly of basaltic affinity.

In the alkaline dyke series of Grønnedal-Íka, the phonolites are accompanied by trachytes, basic trachytes and lamprophyres, which are described in succeeding chapters of this thesis. There is also a variety of undersaturated microsyenite dykes, but these

are regarded as belonging to an earlier episode directly associated with the syenite emplacement. The present Chapter deals solely with the later, texturally distinct phonolite suite which forms the most abundant salic syke type in the Grønnedal-Íka area. The specimen numbers used refer to the collection of the Geological Survey of Greenland, Copenhagen.

4.2 PETROGRAPHY

The majority of the phonolite dykes comprise alkali feldspar, nepheline and alkali pyroxene set in a matrix principally composed of analcime. In the more mafic members of the series, small amounts of biotite and amphibole accompany the pyroxene. Opaque minerals are only rarely seen. The rocks are aphyric and fine-grained. The feldspars usually have the largest single dimension of the minerals present (0.1 to 0.5 mm) and characteristically show a pronounced acicular habit. The small grain size of these rocks precludes detailed examination of the minerals present, and does not favour the detection and identification of minor phases.

Slight deuteric alteration of nepheline is apparent in some of the rocks used in this study. The product is either cancrinite or "geiseckite", a fine micaceous aggregate very similar to muscovite. Unpublished work by the author suggests that the effect of these processes on the bulk chemical composition of the rock is small. Rocks showing a greater degree of alteration, in which the interstitial material is affected as well (Chapter 6) have been omitted from the work reported in this chapter.

4.3 CHEMISTRY

For concise presentation, the variation of the major and minor

elements in the phonolite series is shown in composite-diagram form in Fig.4.1. The trace constituents are shown similarly in Fig.4.2. The index of differentiation used in both diagrams is weight percentage normative nepheline. This choice was made because conventional indices show insufficient variation, and there are overriding objections in this instance to using the other indices of feldspar fractionation, namely (Na+K)/Al (used by Nash et al., 1969) and Na/(Na+K).

The numerical data are given in Appendix 5.

Analytical Techniques

The elements Si, Al, total Fe, Mg, Ca, Na, K, Ti and P were determined using X-ray fluorescence spectrometry on powder bricquettes. The instrument used was a Philips PW 1540 (old series) manual spectrometer equipped with a Cr-anode tube and vacuum path. Approximate correction for differences in absorption were made using a procedure similar to that of Holland and Brindle (1966), but these effects were largely eliminated by using as standards a suite of alkaline rocks similar to the unknowns, analysed chemically in the laboratories of the Grønlands Geologiske Undersøgelse (see Borgen, 1967 for procedure). Mn was determined with the same equipment and standards but using a W anode.

Fe(II) was determined volumetrically by the method of Wilson (1955), and H_2O^+ and CO_2 by the gravimetric method of Riley (1958).

X-ray fluorescence spectrometry was also employed in the analysis of the trace elements Ba, Nb, Zr, Y, Sr, Rb, Th, Pb, Zn (W anode) and Cl and La(Cr anode). On this occasion the instrument was a Philips PW 1212 automatic spectrometer. Using the programme 'TRATIO' (see Appendix 3) allowance was made for Kβ interference in the case of Nb, Zr and Y and, for all elements except La, approximate

FIG.4.1

Variation of the major and minor constituents as a function of position in the phonolite series, expressed as weight percent normative nepheline (see text). The figures are graduated in wt.% oxide, except that Cl is in wt.% element.

Solid circles:	fresh specimens
Open circles:	specimens in which nepheline is partially replaced
Solid triangles:	potassium-deficient members (see text).

Fig. 4.1.

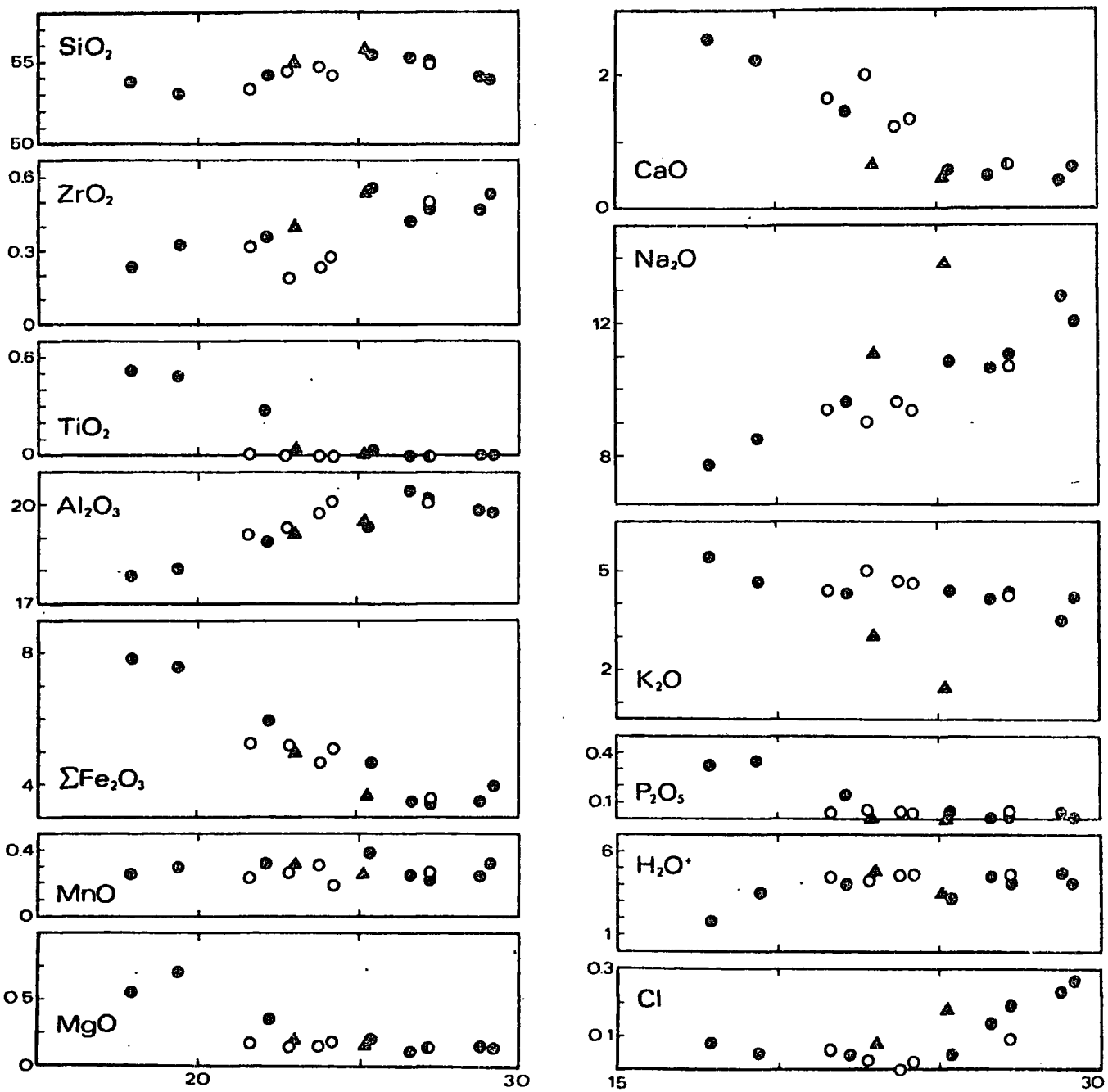
SiO2
55
50
ZrO2
0.6
0.3
0
TiO2
0.6
0
Al2O3
20
17
ΣFe2O3
8
4
MnO
0.4
0
MgO
0.5
0
20
30
CaO
2
0
Na2O
12
8
K2O
5
2
P2O5
0.4
0.1
H2O+
6
1
Cl
0.3
0.1
15
30
Wt. % Normative Nepheline

FIG.4.2

a. Variation of the trace constituents as a function of position in the phonolite series, expressed as weight percent normative nepheline. The figures are graduated in p.p.m. metal.

b. Potassium content (weight percent metal) of the phonolites versus rubidium content. Also shown are a line of constant K:Rb ratio R = 230 (Heier and Adams, 1964) and the best-fit line through the main trend of Shaw (1968), marked "MT".

Symbols are as shown in Fig.4.1.

Fig. 4.2.

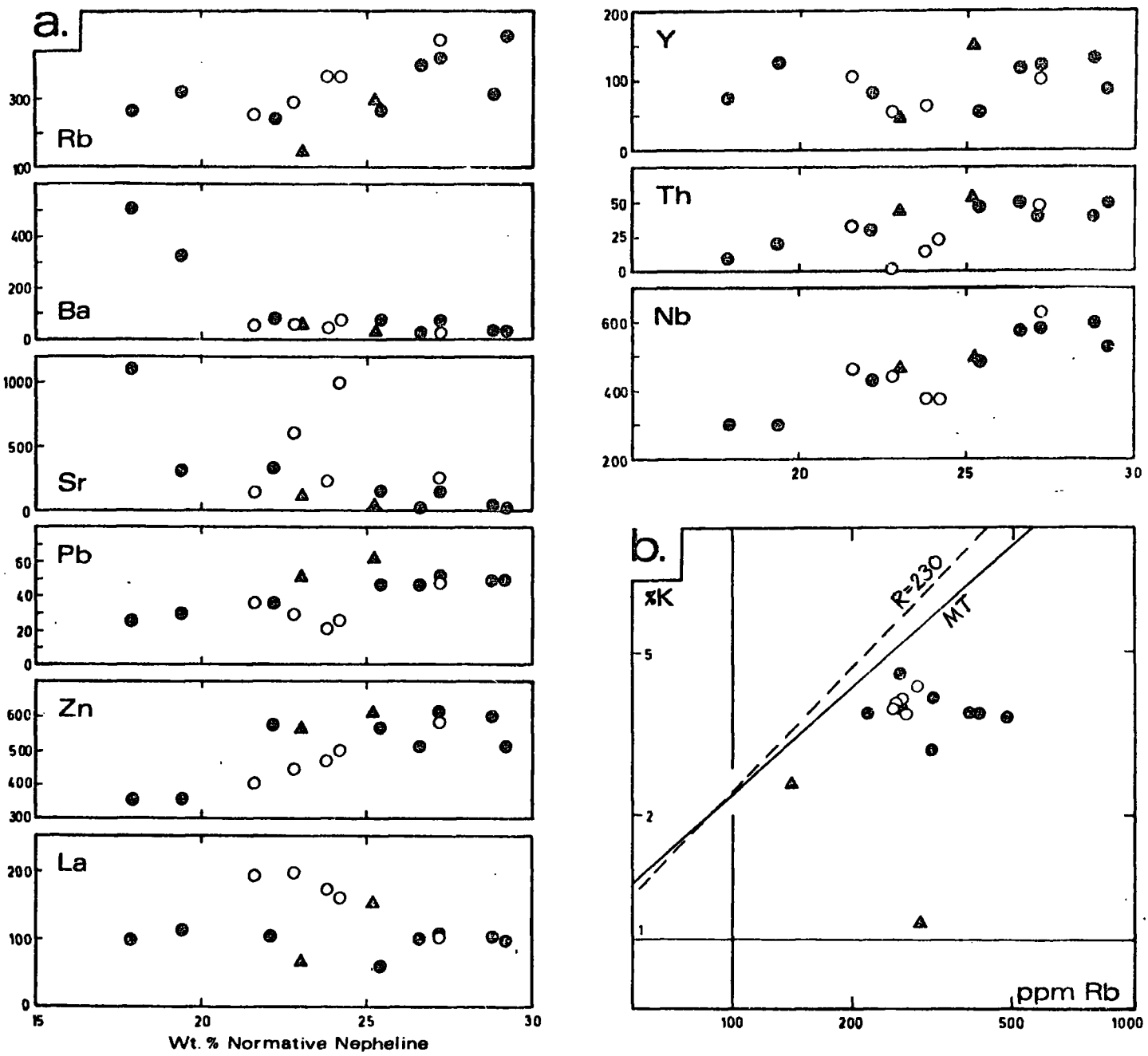
a.
Rb
Ba
Sr
Pb
Zn
La
Wt. % Normative Nepheline
Y
Th
Nb
b.
%K
R=2.30
MT
ppm Rb

correction for absorption differences was made using scattered white radiation as internal standard (Andermann and Kemp, 1958). U.S.G.S. and other international standards and several series of addition standards were employed.

Major Elements

Apart from the complex behaviour of SiO_2, the variation seen in Fig.4.1 is much as would be predicted for a rock series of this kind. Two rocks (27058 and 27151) have exceptionally high sodium:potassium ratios; these specimens are denoted in Fig.4.1 and succeeding figures by filled triangles. There is a notable reciprocity between the patterns of Na_2O and K_2O in Fig.4.1, extending to the disposition of most of the data points about the best-fit lines.

Inspection of Fig.4.1 shows that incipient alteration of the phonolites has brought about small changes in the concentrations of a few elements, notably ZrO_2 and Cl, but that for the rest no distinction can be drawn between fresh and altered specimens. Semi-quantitative determinations of F by emission spectrography on a sample of phonolites indicate concentrations of about 1.0% $\pm$ 0.5%.

Trace Elements

In Fig.4.2 it may be seen that the magmatic evolution of the phonolite series is accompanied by the regular decline of Ba and Sr to very low levels, and the successive concentration of Nb, Zr (see Fig.4.1), Th and Pb. This pattern is typical of highly differentiated magmas, particularly those of alkaline affinity. The incipient alteration described earlier has a perceptible influence on the content of Sr, Pb, Zn and La (but not Y), and to some extent Th.

The behaviour of Rb in relation to K (Fig.4.2b) is much as would be expected of a series of this kind, the pattern of Rb enrichment being characteristic of highly differentiated liquids. The potassium-deficient rock 27151 displays extreme concentration of rubidium relative to potassium. The relationship of the two anomalous rocks 27058 and 27151 to the remainder of the suite is dealt with in a later section of the paper.

The variation in the rare earth elements, represented by La and Y in Fig.4.2, is complex. Ignoring the potassium-deficient member 27151, the subjective eye might fit the distributions to a two-step pattern of successive concentration, the two stages being separated by a phase of impoverishment correlating well with that of phosphorus (Fig.4.1). While it is feasible to suppose that the precipitation of phosphate may have depleted the liquid in the rare earth elements until virtual exhaustion of phosphorus allowed their concentration to rise again, the pattern in Fig.4.2 may yet be spurious.

4.4. EVOLUTION OF THE PHONOLITE MAGMA

Bailey and Macdonald (1969) have illustrated the value of depicting the chemical development of peralkaline salic magmas by plotting rock compositions (and those of coexisting feldspar phenocrysts where present) in appropriate sections of the quaternary system Na_2O-K_2O-Al_2O_3-SiO_2. In doing so, not only does one avoid the systemic distortion inherent in plotting the norms of peralkaline rocks in the system Qz-Ne-Kp (Bailey and Schairer, 1964; Thompson and MacKenzie, 1967), but also the development of silica-oversaturation and peralkalinity (the excess of Na+K over Al in atomic proportions) due to feldspar fractionation can be shown

simultaneously.

Although it has so far been applied only to the oversaturated peralkaline rocks, this approach is equally valid for their undersaturated analogues, and the following paragraphs describe its application to the evolution of the magma from which the Grønnedal-Íka phonolite dykes were formed. It will be shown that the scheme allows an estimate to be made of the phases fractionating, and of their composition, in instances where phenocrysts are absent from the rocks.

The first projection appears in Fig.4.3, which shows part of the plane (Na_2O+K_2O)-Al_2O_3-SiO_2 encompassing the compositions of the phonolites. This diagram can be regarded as the product of condensing the quaternary system Na_2O-K_2O-Al_2O_3-SiO_2 along the direction of the alkali composition axis. Various reference points are also given in Fig.4.3, notably F, the composition of binary alkali feldspar (that of nepheline falls below the lower margin of the diagram), and invariant points P and Q from relevant experimental systems (detailed in the caption).

The distribution of the phonolite compositions in Fig.4.3 can be seen to embrace an essentially linear trend which may be extended back to a point close to the ideal alkali feldspar composition. Superimposed on this linear development, which one may attribute to the fractionation of alkali feldspar, is the record of two other processes. Firstly the slightly altered specimens deviate to a small extent to the Al_2O_3-rich side of the main distribution. This tendency can be linked with the loss of small amounts of sodium from the rock during the breakdown of nepheline (a consequence that is easily understood on comparing the ideal formulae of nepheline and

FIG.4.3.

Part of the system (Na_2O+K_2O)-Al_2O_3-SiO_2 relevant to the undersaturated rocks, showing the compositions of the Grønnedal-Íka phonolites. The portion of the whole system depicted in the main diagram is indicated by the stippled area in the inset figure. All compositions are represented in molecular percent. Symbols are as shown in Fig.4.1.

The point F represents the formula composition of binary alkali feldspar. The three points nearby, labelled "5", "10" and "15", indicate the formula compositions of ternary alkali feldspars incorporating 5, 10 and 15 molecular percent of the anorthite end-member respectively.

The point P is the albite-nepheline-corundum-liquid invariant point in the system Na_2O-Al_2O_3-SiO_2 at atmospheric pressure (Schairer and Bowen, 1956). The line PT represents part of the albite-nepheline field boundary in this system. The point Q is the nepheline syenite minimum in the system SiO_2-$NaAlSiO_4$-$KAlSiO_4$ at 1 atmosphere (Schairer, 1950). The minima at 1 and 5 kb water pressure would be found somewhat lower in the figure (Hamilton and MacKenzie, 1965; Morse, 1969).

The line XY represents the section of the quaternary system depicted in Fig.4.4.

Fig. 4.3.

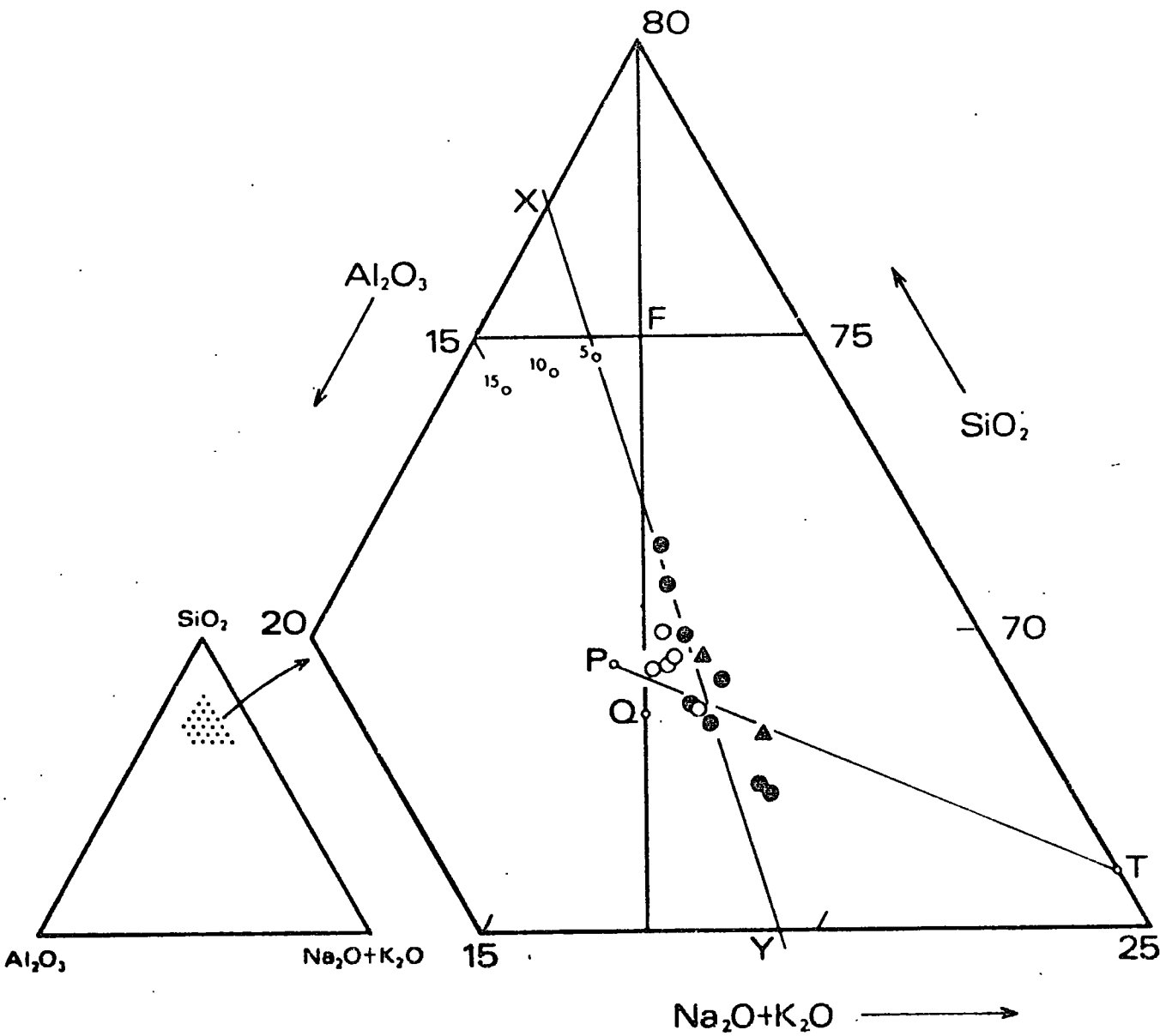
80
X
Al_2O_3
15
F
75
SiO_2
15_o
10_o
5_o
SiO_2
20
70
P
Q
T
Al_2O_3
Na_2O+K_2O
15
Y
25
Na_2O+K_2O

its alteration product, muscovite). One may associate alkali loss in the system (Na_2O+K_2O)-Al_2O_3-SiO_2 with movement of the composition in question directly away from the alkali apex, and the position of the open circles relative to the main trend in Fig.4.3 is consistent with such a process.

Secondly, at the lower end of the phonolite distribution there is a slight shift of successive composition points to the right, which may represent the appearance of nepheline on the liquidus. This interpretation is supported by relationships in analogous synthetic systems: the line PT is the albite-nepheline-liquid cotectic from the system Na_2O-Al_2O_3-SiO_2 (Schairer and Bowen, 1956), and point Q is the nepheline syenite minimum in the system SiO_2-$NaAlSiO_4$-$KAlSiO_4$ at atmospheric pressure. The minima in the same system at 1 and 5 Kb P_{H_2O} would appear below Q in Fig.4.3 (Morse, 1969). The feldspar s.s. - nepheline s.s. field boundary is therefore almost certain to be found at some point in this part of the natural system. At this point the locus of liquid compositions ceases to move directly away from the feldspar composition and instead follows the field boundary as feldspar and nepheline crystallise side by side. By analogy with the system Na_2O-Al_2O_3-SiO_2 the phase boundary probably lies roughly parallel to the line PT in Fig.4.3.

Extrapolation of the undeflected part of the phonolite trend in Fig.4.3 back towards the feldspar composition point suggests that, if the fractionation of feldspar is indeed responsible for the observed evolutionary trend, the feldspar must have a small but distinct molecular excess of Al_2O_3 over Na_2O+K_2O, attributable to a small proportion of the anorthite molecule. The point F (Fig. 4.3) represents the ideal formula composition of binary alkali

feldspar. Three equivalent datum points are also shown representing the compositions of ternary alkali feldspars containing 5, 10 and 15 molecular percent of the anorthite end-member respectively (see caption to Fig.4.3). It can be seen that fractionation of a ternary alkali feldspar containing approximately five mol. percent anorthite would fit the evolutionary trend defined by the phonolite compositions in Fig.4.3. For reasons given later, this figure should be regarded as a minimum for the anorthite content, and in any case only as a rough guide,but a composition of this order is acceptable for a feldspar in equilibrium with undersaturated alkaline liquids (Scharbert, 1966; Nash et al., 1969).

The ideally colinear relationship in Fig.4.3, between the compositions of the phonolites and the hypothetical feldspar fractionate, extends into the quaternary system Na_2O-K_2O-Al_2O_3-SiO_2 as a roughly coplanar set of points distributed about a plane which also contains the locus of feldspar compositions in equilibrium with successive liquids. The plane passes close to the ideal alkali feldspar join, and more or less parallel to it (depending on whether the anorthite content of the feldspar has remained constant throughout the dyke series). Rock compositions can in general be plotted in this planar section, and related to the composition of the feldspar in equilibrium with them, whether this is determined from phenocrysts present or inferred indirectly. Such a diagram is analogous to the second section (in figures 2 and 5) of Bailey and Macdonald (1969) but is of course of quite a different orientation in the quaternary figure.

Fig.4.4a shows the position of this plane (ABC) within the tetrahedron. The simplest construction occurs when the fractionation of binary alkali feldspar is assumed; in this case the plane

FIG.4.4.

a. The SiO_2-rich part of the system Na_2O-K_2O-Al_2O_3-SiO_2 showing the plane ABC, the stippled portion of which is depicted in Fig.4.4b. The plane is represented by the line XY in Fig.4.3. It passes below the alkali feldspar join, the line of intersection with the vertical plane through the join being shown by a dashed line. The stippled portion of the section ABC extends upward to the intersection with the ternary feldspar surface (see points "5", "10" and "15" in Fig.4.3).

b. The compositions of the Gronnedal-Ika phonolites projected into the plane ABC. All compositions are in molecular units. Symbols are as shown in Fig.4.1.

Fig. 4.4.

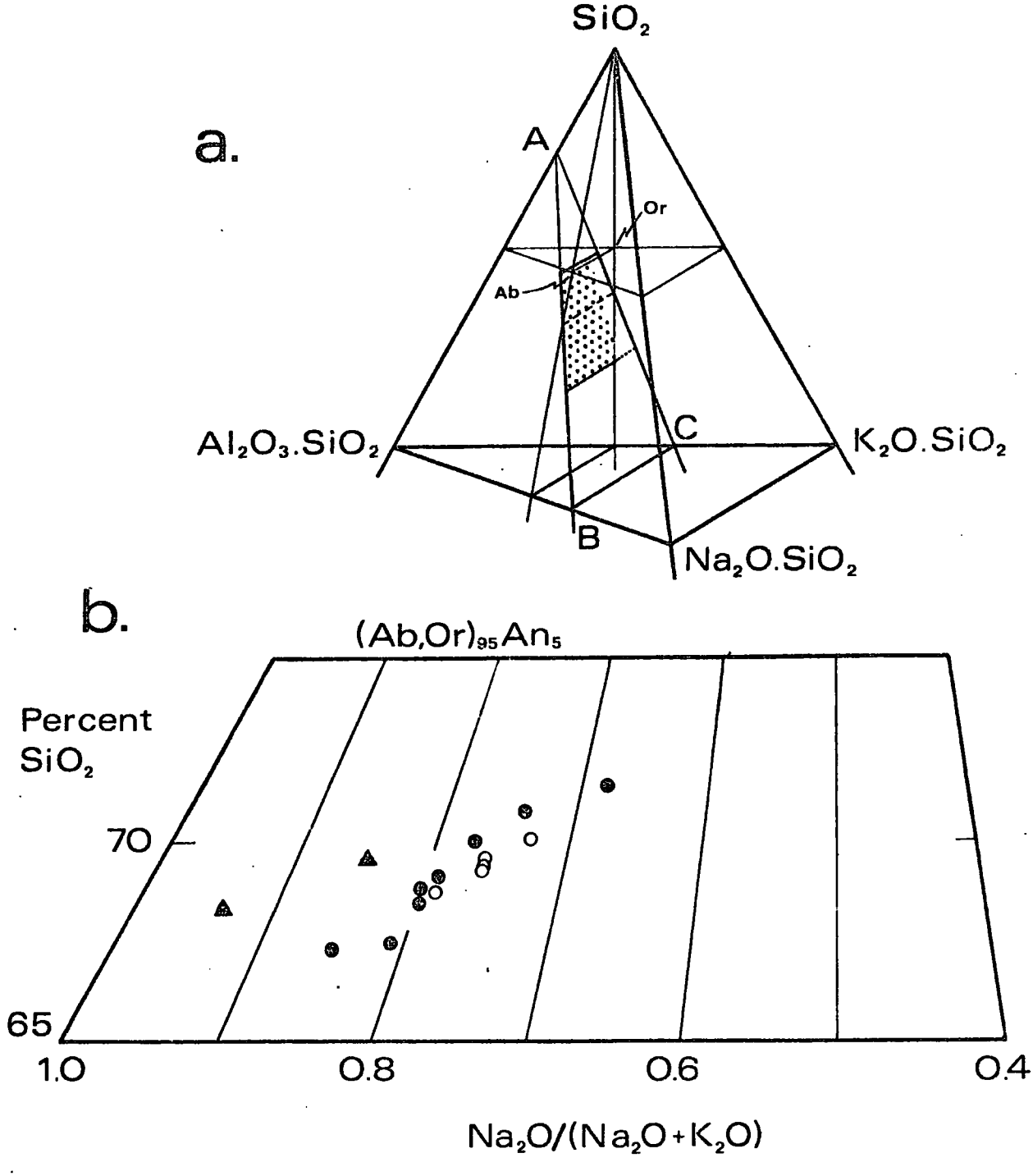
a.
SiO2
A
Or
Ab
Al2O3.SiO2
C
K2O.SiO2
B
Na2O.SiO2
b.
(Ab,Or)95An5
Percent
SiO2
70
65
1.0
0.8
0.6
0.4
Na2O/(Na2O+K2O)

contains the alkali feldspar join Ab-Or. In general, as illustrated in Fig.4.4a, the plane is off-set slightly, intersecting the plane of alkali-alumina parity somewhat below the join.

The phonolite analyses are plotted in such a plane in Fig.4.4b. The section used is defined in the caption, and is represented by the line XY in Fig.4.3. As will be seen from Fig. 4.3, the compositions of the altered rocks may be visualised as lying below the plane of Fig.4.4b in the quaternary system, those of the most highly differentiated members of the suite (found on the extreme left of Fig.4.4b) lying a little above it. With the exception of the two potassium-deficient rocks (see Fig.4.1), all the phonolites conform to a near-linear distribution. The line best fitting the six points lying closest to the plane of the diagram cuts the feldspar line at the top of the diagram in the $Na_2O/(Na_2O+K_2O)$ range 0.55 to 0.60. Examination of Figs. 4.3 and 4.4b together, therefore, points to the fractionation of a feldspar approximating to $Ab_{55}Or_{40}An_5$ (molecular proportions) in composition.

Care should however be exercised in interpreting this hypothetical composition, for two reasons. In the first place it has been derived by linear extrapolation of the trends in Figs. 4.3 and 4.4b, underlying which there is the assumption that the feldspar composition remains substantially constant throughout the series. This is not in general true, particularly with regard to $Na_2O/(Na_2O+K_2O)$, and so the "composition" represents no more than an average about which an unknown degree of variation may have occurred.

Secondly, feldspar fractionation cannot alone account for the entire chemical variation along the phonolite sequence. Fig.4.1 reveals pronounced declines in total iron oxide, MgO, CaO and TiO_2

in addition to the patterns of change attributable to the removal of feldspar. (The CaO content of $(Ab,Or)_{95}An_5$ is about 1.5%, by no means great enough to reduce the calcium content of the liquid).

The most probable explanation of the decline in iron, magnesium and calcium seen in Fig.4.1 is the precipitation of clinopyroxene. In the peralkaline phonolite lavas of Mount Suswa (Nash et al., 1969), pyroxene is the most abundant phenocryst phase after feldspar, and both here and in peralkaline phonolite dykes from the Igaliko complex (Emeleus and Harry, 1970; Emeleus, personal communication) the early pyroxene is found to be soda-poor augite. It is not unreasonable to suppose therefore that the fractionation of augite could have removed iron, calcium and particularly magnesium from the phonolite magma, at the same time having little influence on the percentage of sodium. It may be noted that the MgO content of the Grønnedal-Íka dykes is very low, suggesting that later pyroxenes moved very close to the hedenbergite-acmite boundary of the clinopyroxene field.

It is likely that the precipitation of small amounts of other minerals, most probably fayalitic olivine, titanomagnetite and perhaps biotite, has also contributed to the decline in iron and titanium in the phonolite series. Phenocrysts of olivine and titanomagnetite are quite common in the lavas of Mount Suswa (Nash et al., 1969) and the Igaliko dykes (Emeleus, personal communication).

Because the trend seen in Fig.4.3 is the resultant of vectors from the composition points of all the fractionating phases, the composition attributed to the feldspar in preceding pages requires minor adjustment. After feldspar, the main phenocryst phase appears

to have been pyroxene, whose composition in the system Na_2O-K_2O-Al_2O_3-SiO_2 lies on the SiO_2-Na_2O margin, close to the SiO_2 apex if it is soda-poor. To compensate for the influence of pyroxene, one may suppose the feldspar to have been somewhat more aluminous than the foregoing arguments based on feldspar fractionating alone suggest. Similar reasoning applies to the Or-content.

In summary, the distribution of the compositions in the system Na_2O-K_2O-Al_2O_3-SiO_2 suggests that the fractionation of alkali feldspar was the chief influence on the chemical evolution of the Grønnedal-Íka phonolite magma. The composition of the feldspar appears to have been close to but on the An,Or-rich side of $Ab_{55}Or_{40}An_5$. This conclusion, together with the identification of sodium-poor ferro-augite as the other major phenocryst phase, is in good agreement with phenocryst data from the Mount Sȳswa peralkaline phonolite lavas (Nash et al., 1969), a closely similar suite of rocks. Comparable chemical data for other areas are lacking in the literature.

Origin of the Potassium-deficient Members 27058 and 27151

In two members of the phonolite series (27058 and 27151) the sodium:potassium ratio is anomalously high. Their exceptional character is made clear in Figs. 4.1, 4.3 and 4.4b in which they appear as solid triangles. The relation between these rocks and the main sequence of phonolites is problematical. There is no experimental justification for regarding them as representative of a divergent high-sodium trend, as their position in several diagrams suggests superficially. On the contrary, the analyses of coexisting rocks and phenocrysts given by Nash et al. (1969)

imply that feldspar fractionation operating alone produces a strong convergence of liquid paths into a pronounced thermal trough in the system Na_2O-K_2O-Al_2O_3-SiO_2. The composition of the less extreme rock, 27058, could well lie on a path convergent with the majority trend in Figs. 4.3 and 4.4b, although why it should be the only representative of such a liquid path cannot be explained.

The composition of 27151, however, cannot realistically be thought to lie on a path convergent with the main sequence of phonolites, and its origin is obscure. The high content of the incompatible elements Zr, Nb, La and Th suggests a more extreme character than that of the other phonolites in the suite, but this character is not reflected in much of the major element chemistry. It is possible that the composition of this rock has been modified by the loss of a sodium-rich vapour phase, as envisaged by Macdonald (1969), Macdonald et al. (1970) and Noble (1970). If this were so, the original composition of 27151 would lie to the right of its present position if Figs. 4.1 and 4.2a, and the rock could perhaps be regarded as an extreme member of the main phonolite trend.

4.5 Implied Phase Relations in the System Na_2O-K_2O-Al_2O_3-SiO_2-H_2O

To a large extent, experimental and petrological studies of the peralkaline rocks have been limited to the silica-oversaturated field in the system Na_2O-K_2O-Al_2O_3-SiO_2, the exception being the rocks of Mount Suswa (Nash et al., 1969). Following the formulation of the "orthoclase effect" by Bailey and Schairer (1964), Thompson and MacKenzie (1967) postulated from experimental data that the thermal valley in the SiO_2-$NaAlSi_3O_8$-$KAlSi_3O_8$ section of the quaternary system extends into the peralkaline

volume as a low temperature zone moving relatively closer to the Na_2O-Al_2O_3-SiO_2 boundary as the excess of alkali oxides over alumina increases. In the following paragraphs, the bearing of the Grønnedal-Íka phonolites on the extension of this low temperature zone into the undersaturated volume of Na_2O-K_2O-Al_2O_3-SiO_2 is examined. In this discussion, the system should regarded as the quaternary condensed part of the system Na_2O-K_2O-Al_2O_3-SiO_2-H_2O, to which the work of Thompson and MacKenzie refers.

Fig.4.5 shows the compositions of the main series of Grønnedal-Íka phonolites projected into the plane $Al_2O_3.3SiO_2$-$Na_2O.3SiO_2$-$K_2O.3SiO_2$, which is the horizontal section containing the Ab-Or join in Fig.4.4a. The diagram also shows, as WZ, the line of intersection of the experimentally observed low temperature surface (Thompson and MacKenzie, 1967) with the plane of the section.

While the lack of phenocrysts in the Grønnedal-Íka dykes precludes direct demonstration, it can reasonably be supposed that the phonolite compositions lie close to the axial surface of the low temperature zone extended into the undersaturated volume of the system Na_2O-K_2O-Al_2O_3-SiO_2. The trend in Fig.4.4b intersects the SiO_2-$NaAlSiO_4$-$KAlSiO_4$ section at a point close to but on the $KAlSiO_4$-rich side of the thermal depression joining the alkali feldspar and nepheline syenite minima (Morse, 1969), represented by the point M, Fig.4.5. The phonolite sequence may therefore be regarded as a series of liquids moving into the peralkaline thermal trough from the potassic side. Alternatively the phonolite analyses may lie in a natural low temperature zone found at more potassic compositions than that in the analogous artificial system.

FIG.4.5.

Part of the plane $Al_2O_3.3SiO_2$-$Na_2O.3SiO_2$-$K_2O.3SiO_2$ in the system Na_2O-K_2O-Al_2O_3-SiO_2, showing

(a) the compositions of the Grønnedal-Íka phonolites in molecular proportions projected into the plane by joining their positions in the tetrahedron to the SiO_2 apex,

(b) the intersection of the axial surface of the low temperature zone of Thompson and MacKenzie (1967) with the plane of the section (WZ), and

(c) the trace of the probable phonolite liquid path, in the low temperature zone extended into the undersaturated volume, projected into the plane of the diagram in a similar manner to the data points (MV).

The inset figure shows the portion of the plane shown in the main figure. Thompson and MacKenzie (1967) and Nash et al. (1969) refer to the plane incorrectly as $Al_2O_3.6SiO_2$-$Na_2O.6SiO_2$-$K_2O.6SiO_2$.

Symbols are as in Fig.4.1. The potassium-deficient members are not shown.

Fig. 4.5.

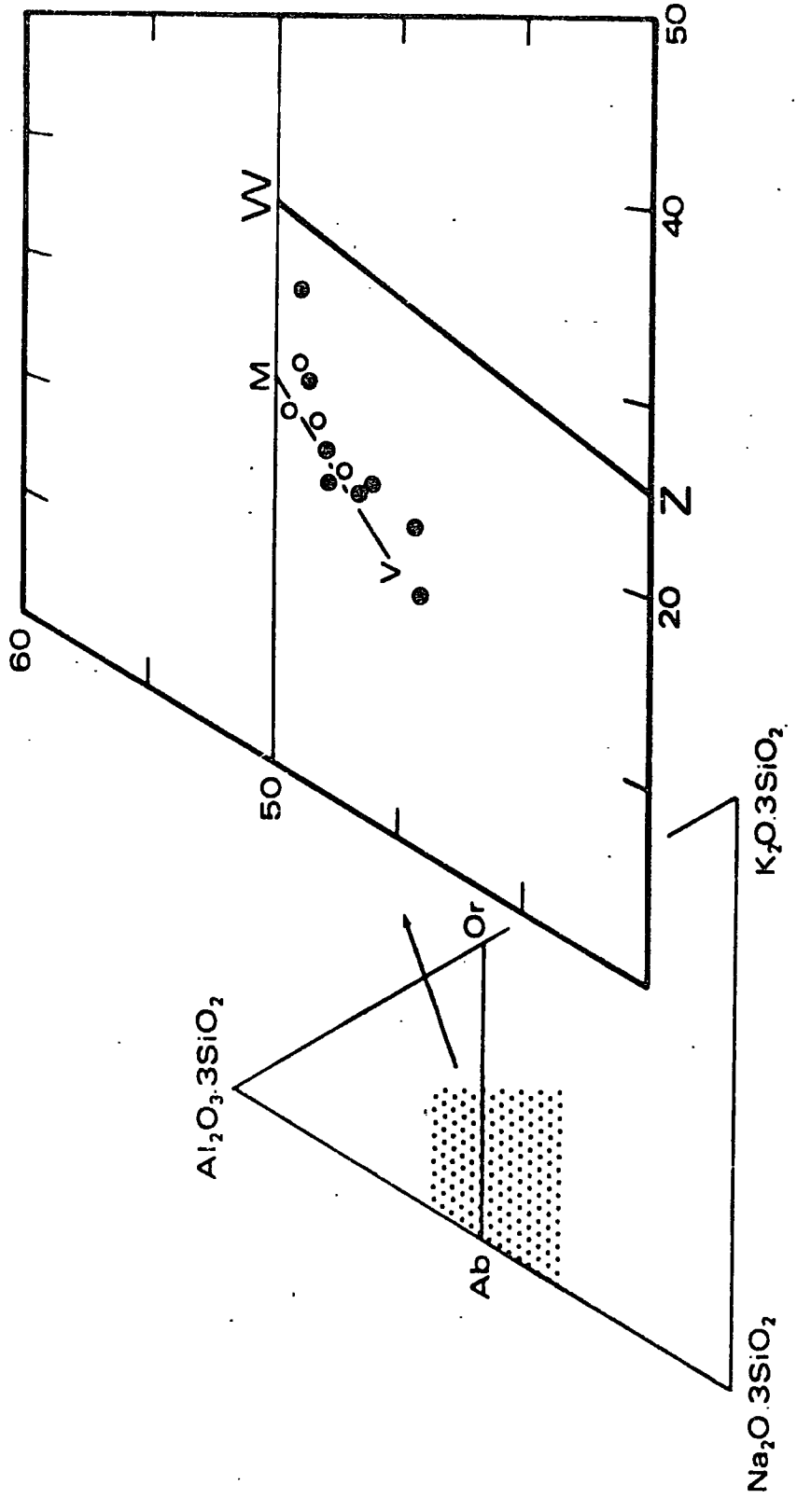

In either case, the results given in this paper indicate that at the degree of undersaturation of the dykes the low temperature surface has moved towards the Na_2O-Al_2O_3-SiO_2 margin relative to the line WZ in Fig.4.5. This situation parallels that in the Petrogeny's Residua system and is consistent with the trend of the axial surface shown by Thompson and MacKenzie (1967) (their figure 7), who makes it clear that the zone is not radial to the SiO_2 apex of the quaternary system.

The lines WZ and MV are divergent in Fig.4.5. This may be attributed to the down-plunging of the phonolite trend (Fig.4.3) in the low temperature zone. To the extent that the present data and those of Thompson and MacKenzie (1967) are definitive, the axial surface in this part of the system may be regarded simply as a planar extension of that shown by Thompson and MacKenzie. There is no hint of the curvature in the axial surface inferred by Nash et al. (1969) from the reversal of feldspar zoning in the Mount Suswa lavas, but features of this subtlety are unlikely to be detected in the variation of bulk rock composition.

4.6 IDENTITY AND PETROGENESIS OF THE PARENT MAGMA

It is commonly supposed that magma of trachyte composition is the immediate parent of both the phonolites and the alkaline rhyolites. The oversaturated and undersaturated end-members are each associated with trachyte in many provinces (see Bailey and Schairer, 1966) and relations in the systems Qz-Ne-Kp (see Morse, 1969) and Na_2O-Al_2O_3-Fe_2O_3-SiO_2 (Bailey and Schairer, 1966) are consistent with the hypothesis. The Grønnedal-Íka phonolite dykes are similarly associated with saturated trachytes in the field, as are the lavas of Mount Suswa. Nash et al. (1969) conclude that the

latter have been derived from a nearly saturated trachyte parent, and such a process may lie behind the pattern of the Grønnedal-Íka dykes seen in Fig.4.3. It is conventional to regard alkali olivine basalt as the progenitor of trachyte (for example, Upton, 1960).

It may be seen from Fig.4.6 however that the Greenland dykes are significantly more undersaturated than their counterparts from Mount Suswa. Moreover, work on the trachytes with which they are associated in the field (Chapter 7) reveals a sizeable compositional gap between the two types. Recent papers (Coombs and Wilkinson, 1969; Wright, 1971) suggest that between the spectrum of basaltic magmas and their salic differentiates there exists a continuum of parallel lineages at differing degrees of silica-undersaturation, several of which may be represented in any one province. The pattern of analyses in Fig.4.3 may thus represent a lineage from a nepheline-poor basanite liquid via a slightly undersaturated trachyte, running alongside that which produced the associated saturated-trachyte activity.

Very little evidence is available as to the mechanism of fractionation, whether fractional crystallisation or partial melting. The absence of phenocrysts from the phonolites (and the associated trachytes) is unusual, but can be interpreted in terms of either model. Superficially the rarity of exposed mafic plutonic rocks in the Gardar province, as elsewhere, points to the dominance of partial melting at depth in the production of the salic magmas (c.f. Bailey, 1964; Bailey and Schairer, 1966; Wright, 1971), but several authors (Upton, 1960; Sørensen, 1966; Berthelsen and Noe-Nygaard, 1965) have suggested that the regional structure is compatible with extensive magma chambers at depth in which the fractional crystallisation of large volumes of mafic magma may

FIG.4.6.

Compositions of the Mount Suswa lavas (Groups 3 and 4) plotted in a portion of the system (Na_2O+K_2O)-Al_2O_3-SiO_2 (in molecular units); Data are from Nash et al.(1969). The area shown is the same as in Fig.4.3; the distribution of the fresh Grønnedalíka phonolites is represented by the stippled area.

Solid triangles:	Rock	) Group 3
Open triangles:	Residual glass	)
Solid circles:	Rock	) Group 4
Open circles:	Residual glass	)

Fig. 4.6.

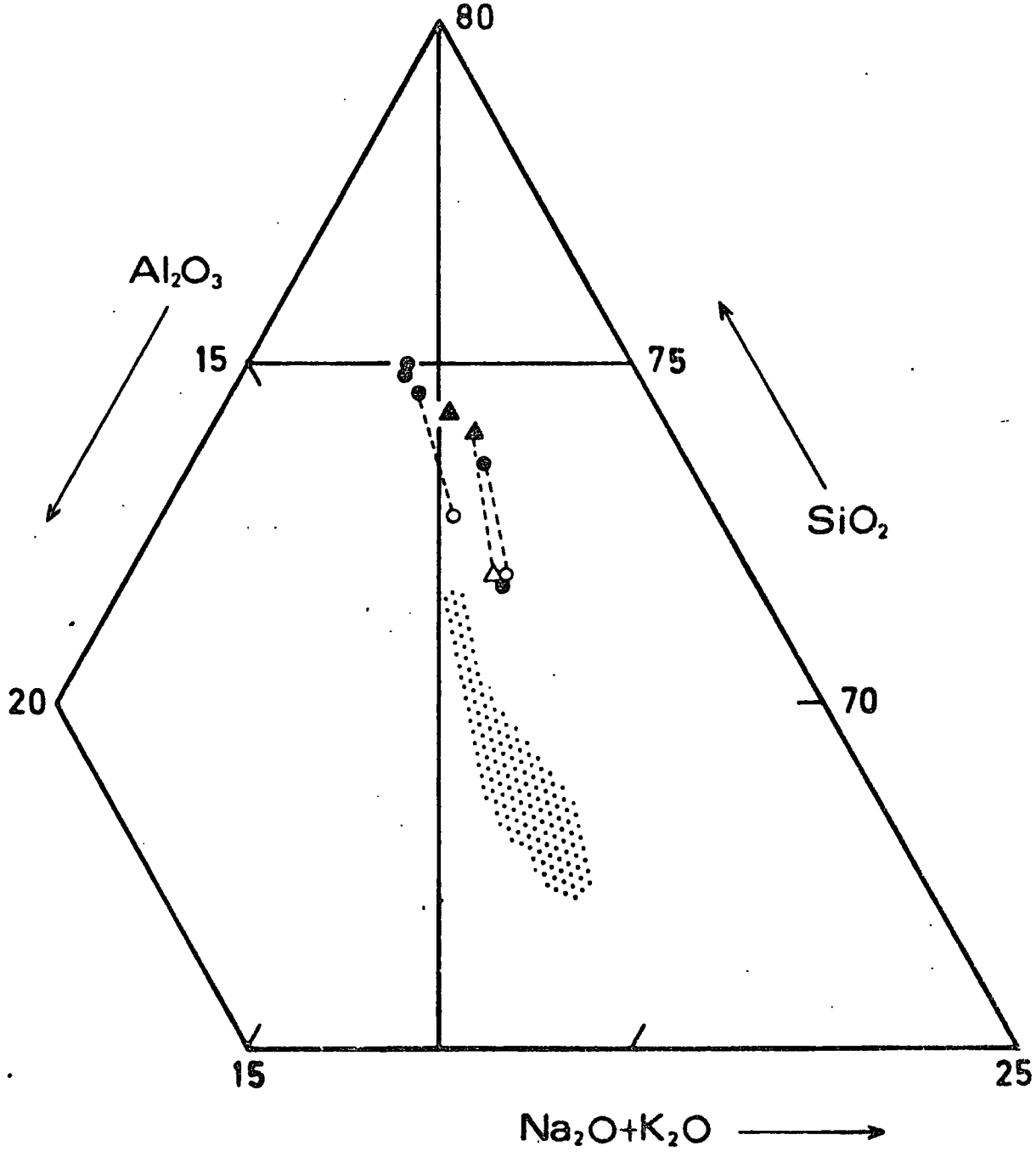

have occurred. The latter alternative is supported by the abundance of anorthosite inclusions present in the basic Gardar dykes (Bridgwater and Harry, 1968). In the absence of definitive chemical criteria, however, it would be inappropriate to embark on further speculation here.

CHAPTER 5

APPLICATION OF R-MODE FACTOR ANALYSIS TO THE PHONOLITE DYKES

The preceding chapter led to the conclusion that chemical variation in the peralkaline phonolite dykes of the Grønnedal-Íka area is attributable to two dominant influences, magmatic evolution resulting chiefly from feldspar fractionation, and alteration of nepheline to gieseckite. R-mode factor analysis, a multivariate statistical technique hitherto little used in igneous petrology, has been applied to the data reported in the previous chapter, with two objectives:

1. To illustrate the applicability of the technique to petrological data in an instance which is simple and well understood from conventional methods of study;
2. To extract from the data any further influences which may be operating, apart from those already defined.

The background to factor analysis has been summarised in Chapter 2, and no further introduction will be given here. Other relevant points are discussed in Appendix 5.

A box diagram representing the pattern matrix of the Promax oblique solution with k=3 for the phonolite data given in Appendix 6 (omitting the potash-poor members 27058 and 27151) is shown in Fig.5.1. Simple structure has been taken as the criterion to determine the most appropriate value of k; in other words, the solution shown has the lowest number of salient loadings (on the dominant two factors).

Factors 6 and 5, accounting for 45% and 17% of the observed variance respectively, correspond well with the controls enumerated

FIGURE 5.1

Box diagram of the Promax oblique solution with k=3 for the peralkaline phonolite dykes of the Grønnedal-Íka area. The potash-poor specimens 27058 and 27151 have been omitted from the sample. The corresponding numerical data for the solution are given in Appendix 5.

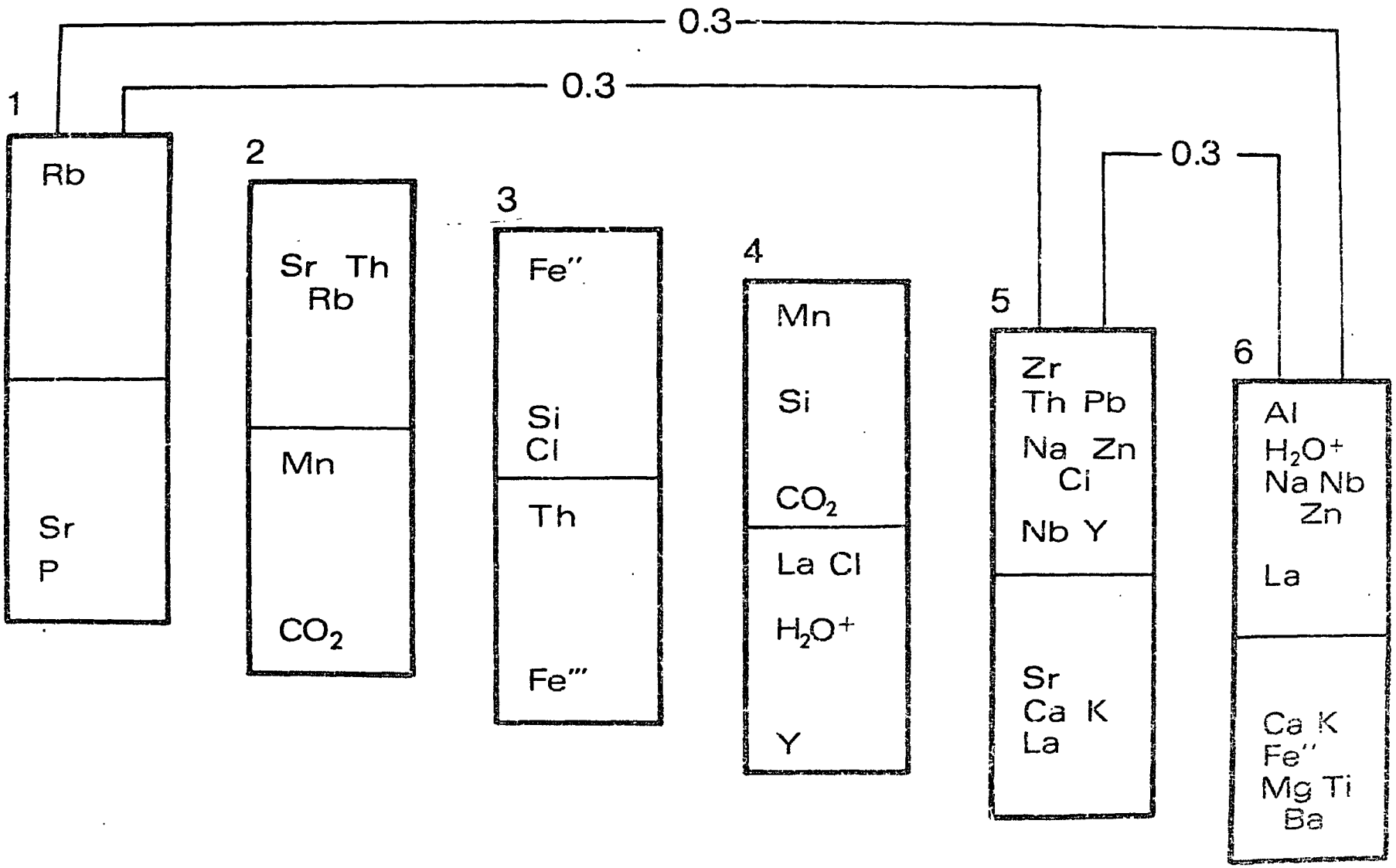
0.3
0.3
0.3
1
Rb
Sr
P
2
Sr Th
Rb
Mn
CO2
3
Fe''
Si
Cl
Th
Fe'''
4
Mn
Si
CO2
La Cl
H2O+
Y
5
Zr
Th Pb
Na Zn
Ci
Nb Y
Sr
Ca K
La
6
Al
H2O+
Na Nb
Zn
La
Ca K
Fe''
Mg Ti
Ba

in the previous chapter. The structure of factor 6 reflects the increase in Al, H_2O, Na, Nb and Zn with progressive magmatic fractionation, and the accompanying decline in Ti, Ba Fe^{II}, Ca and K. The identification of this factor is of course no great achievement, since the variation it represents is obvious from the variation diagrams given in Chapter 4. Of greater significance is the emergence of an "alteration factor", factor 5. It comprises positive loadings on Zr, Th, Pb, Na, Zn, Cl, Nb and Y and negative loadings on Sr, Ca, K and La. The first group nearly coincides with the elements which are depleted in the slightly altered rocks in the suite, presumably as a consequence of the alteration process. Nb and Y were not previously identified as members of this group, but both occur with barely significant loadings in factor 5. The elements appearing in factor 5 with negative loadings are those whose concentrations are found to be enhanced in the altered phonolites relative to the fresher rocks. With the exception of 39779, the specimens identified as "altered" in the foregoing chapter have factor scores on factor 5 which are consistently less than -0.50.

It should be noted that through the application of factor analysis it has proved possible to describe the subtle chemical changes accompanying alteration, by referring only to the chemical variation in the rocks. Using conventional arguments it would be hard to distinguish such changes without reference to a petrographic scale such as that established in Chapter 4.

The phonolites are fine-grained rocks and therefore polycrystalline alteration products cannot be identified with absolute confidence. Thus it is not always possible to distinguish correctly

between micaceous products (gieseckite), whose formation brings about pronounced changes in rock chemistry, and cancrinite, whose effects are comparatively mild. Uncertainty of this kind is behind the appearance of 39779 among the "altered" rocks defined in Chapter 4 whereas its chemistry is well preserved. Conversely the alteration factor score of 27183 indicates a certain degree of alteration, whereas the rock was classified as fresh because in thin section the product appears to be cancrinite.

Factors 5 and 6 have significant positive covariance, attributable largely to the sharing of certain elements (Na, Nb, Zn, Ca and K).

Most elements behave in a simple monotonic manner in progression along the phonolite series, the concentration rising or declining in a smooth linear or logarithmic pattern. There are however several exceptions to this generalisation: these are elements which behave in a more complex manner and appear to have a point of zero slope in their variation as plotted in Figs. 4.1 and 4.2. The behaviour of the rare earth elements in this manner was mentioned in Chapter 4. This tendency to non-linearity is reflected in factor 4: those elements whose trends appear to be upwards-convex in Figs. 4.1 and 4.2 have positive loadings, whereas those with the opposite tendency have negative loadings. There is insufficient data to judge the significance of the pattern represented by factor 4 and the observation may be spurious. There is no obvious physical explanation of factor 4, but it may represent a number of associations which cannot be resolved in the present small volume of data.

Factor 3 evidently represents oxidation and is broadly characteristic of the more altered rocks in the series. Little

significance can be attached to factors 1 and 2, and the associations they represent probably arise from the inadequate volume of data used. Multivariate analysis functions with best results when the body of data to be analysed is large. When this condition is not met, there is always the danger of picking out spurious associations which are present by chance in the data but which are not representative of the population from which the sample has been drawn.

In conclusion, the application of factor analysis to the suite of peralkaline phonolites described in Chapter 4 substantiates in some detail the conclusions drawn from conventional methods of examination. Other associationsof possible significance are identified, but there is insufficient detail to ascribe physical meaning to them.

CHAPTER 6

THE ALTERED PHONOLITE DYKES

6.1 Introduction

Phonolites constitute the most abundant salic dyke type in the Grønnedal-Íka area, and among them severely altered rocks form a volumetrically significant sub-group. The onset of alteration in the phonolites as a whole occurs in two discrete stages, between which intermediate instances are rare. The first stage, in which individual nepheline crystals are replaced, usually by gieseckite, has been discussed in Chapters 4 and 5, and its effect may for most purposes be ignored. In contrast the second stage of alteration brings about much more profound changes. The altered phonolites, considered jointly with the fresher rocks, provide an opportunity for examining the alteration phenomena which are widespread in the Grønnedal-Íka complex, and the study of these processes may shed light on the metasomatic agents which are possibly responsible.

6.2 Petrography of the Altered Phonolites

The petrography of the altered phonolites is uniform and simple. Needles of alkali feldspar and small particles of opaque or limonitic material are set in a ground-mass which appears to consist of gieseckite. The feldspar retains the pronounced acicular habit observed in the well preserved phonolites (Chapter 4), and the general appearance in thin section, apart from the identity of the interstitial material, is reminiscent of the fresher rocks. On these grounds it may reasonably be supposed that the altered dykes of this type have in fact been derived from rocks essentially identical to

or at least comagmatic with the peralkaline phonolites, and the rocks are therefore referred to as "altered phonolites", although no trace of feldspathoid minerals has been preserved.

The points of difference between the fresh and severely altered phonolites may be summarised as follows:

(a) the mafic minerals characteristic of the fresh phonolites, usually aegirine, have been replaced by oxidised alteration products;

(b) whereas the matrix of the well preserved phonolites consists of analcime, the corresponding material in the altered rocks is micaceous.

The coincidence of these two alteration phenomena suggests that, unlike the first stage of alteration discussed previously, the process operating here is not simply a deuteric effect but that external agents play an essential part. The arguments for and against this interpretation are considered below.

6.3 Chemistry

Chemical analyses and CIPW norms of eight altered phonolites are tabulated in Tables A.6, A.7 and A.8 in Appendix 6. Comparison with the corresponding data for the unaltered phonolites indicates several gross differences. Firstly the sodium content is much lower in the altered rocks, whilst silicon and potassium show a slight rise and aluminium stays almost the same. These changes account for the presence of corundum and quartz in the norms of the altered rocks, in contrast to normative acmite and nepheline in the fresh dykes. The water content, though variable, is

noticeably lower in the altered phonolites, being in the region of 1.0-1.5% as opposed to 4.5% in the unaltered rocks. This may be related to the difference in water content between analcime and mica. Among the trace elements, the Ba content rises in passing to the altered rocks, whereas Zn is depleted in them.

6.4 Mineralogical Aspects of Alteration

The chemical changes accompanying the alteration of a phonolite depend on the nature of the minerals which are attacked and on that of the products. The identity of the former is a subject for speculation or assumption, but some limit may be imposed on the chemical effects of alteration if the identity of the products is known. Microscopic examination provides only the broadest indication of the nature of the alteration products, of which cancrinite and gieseckite are the most common. Little is known of the character of the micaceous product in particular, and in view of the profound changes which its formation, supposedly at the expense of nepheline or analcime, brings about, an examination of this material by X-ray diffraction methods has been undertaken.

Specimens of gieseckite have been obtained from several rock types in the Grønnedal-Ĩka complex. The material is so abundant in the altered phonolites that identification of the micaceous product is possible using the whole-rock powder. Altered syenites in which large aggregate-pseudomorphs after nepheline can be identified in the hand-specimen constitute the other source of gieseckite; in such cases the specimen of gieseckite has been drilled from a cut face of the rock by means of a dental drill.

TABLE 6.1 Summary of X-ray diffraction determinations on gieseckite.

Spec Number	Petrographic type	XRD sample	Alteration products identified with little ambiguity	Products inferred from small number of peaks
27107	Syenites	Powder drilled from altered nepheline crystals	Muscovite* Analcime, sodalite	Cancrinite?
27108			Analcime Muscovite*,cancrinite	Sodalite
27101	Microsyenite dyke	Powder from altered phenocrysts	Muscovite*	-
31825	Altered phonolites	Whole rock	Muscovite*	Sodalite
39781			Muscovite*	Quartz or Sodalite

*Muscovite refers to 10Å potassic layer silicate-hydromuscovite and illite may occur.

The results obtained from these samples using photographic and diffractometric methods, are summarised in Table 6.1.

In every case except one, muscovite appears to be the dominant component of gieseckite. The identification is based on the 10Å basal spacing alone, however, and the possibility of confusion with illite must be considered, although the basal peak measured in these experiments was somewhat narrower than that obtained from most illites (Warshaw and Roy 1961). However, the danger of misidentification is of no great significance; the value of the X-ray diffraction experiments has been to establish that a potassic aluminosilicate, whether it is muscovite, hydromuscovite or illite, is the principal component in the samples of gieseckite examined. The potassium layer silicates are easily distinguished from the sodium analogue of muscovite, paragonite, which has a basal spacing of 9.6-9.7Å. Paragonite has not been detected in the experiments reported here.

There is only limited solid solution between paragonite and muscovite even in the region of the experimental solidus, and at the lower temperatures to be expected during metasomatism/alteration there is unlikely to be more than 10% of the paragonite molecule in muscovite (estimate based on the data of Eugster and Yoder 1955). Even allowing for small amounts of discrete paragonite which may not have been detected in the work reported here, and bearing in mind the minor phases associated with the mica (Table 6.1), one may conclude that sodium is very much subordinate to potassium in the gieseckite specimens studied.

In the minerals from which gieseckite is presumed to have been

formed, the situation is the reverse. From the data reported by Miyashiro (1951), Deer et al. (1963) and Heier (1966), it is probable that the nepheline found in the Grønnedal-Íka dykes and syenites will contain no more than 15-25% of the kalsilite molecule. With the exception of rare potassium-bearing phenocrysts from basaltic lavas, analcime is invariably more sodic than nepheline, the maximum K_2O content being less than 1% (Deer et al. 1963). Thus the chief consequence of the decomposition of either material into gieseckite will be the loss of sodium, either to other phases in the rock or more probably away from the rock entirely. Potassium on the other hand will be lost in very small proportions, if at all. Indeed calculation shows that unless the kalsilite content of nepheline involved in such a reaction exceeds 25% there must be a net gain in potassium rather than a loss in order to balance the equation and to satisfy the K_2O content of muscovite. This conclusion applies to all probable analcime compositions. Comparison of the formulae of nepheline, analcime and muscovite indicates that the relative proportions of SiO_2 and Al_2O_3 will undergo only slight changes.

Experimental work in the system nepheline-albite-H_2O indicates a very extensive region of analcime stability at low temperatures (Saha 1961), but even in the sodic system the formation of mica has been recorded, suggesting the loss of Na_2O and possibly Al_2O_3 and SiO_2 as well in the vapour phase. It seems probable that when potassium is admitted to the system the stability field of mica is greatly extended. In the light of experimental work, the decomposition of natural nepheline in the syenites and phonolites

into muscovite and analcime may be regarded as simply a deuteric effect, brought about by slow cooling of nepheline in the presence of water vapour which is a primary component of the rock. If this model is valid, the distribution of nepheline alteration among a suite of rocks such as the fresher phonolites may be related to the amount of water present after solidification and the cooling rate of the rocks. Rapid chilling would presumably impede progress to sub-solidus assemblages which are in equilibrium with excess water.

If the bulk of the gieseckite in the altered phonolite has been formed from analcime rather than nepheline, as seems probable, it is necessary to postulate the introduction of potassium from outside the system, since analcime alone contains too little to account for the proportion of muscovite seen in these rocks.

6.5 Chemical Changes during Alteration

The most important chemical differences between the fresh phonolites and their supposed altered equivalents are shown in Figs. 6.1 and 6.2. In both diagrams the predicted effect of what may be referred to as "model" alteration is shown for comparison with the actual changes. The "model" process referred to is the simplest possible hypothesis of alteration, the bulk loss of sodium from the rock. It is represented by two "sodium-loss" lines in Fig. 6.1 and 6.2. These lines simply indicate the loci of compositions from which progressively larger amounts of sodium are subtracted, the proportions of all other elements being held constant. The arrows indicate the direction of successively smaller Na_2O content.

Examination of Figs. 6.1 and 6.2 indicates that "model"

FIGURE 6.1

Part of the system SiO_2-Al_2O_3-(Na_2O+K_2O), in molecular proportions, showing the compositions of the altered phonolites. The compositional range of the fresh phonolites (Chapter 4) is indicated by the stippled area.

The point F indicates the formula composition of binary alkali feldspar. The two diagonal lines are the loci of compositions from which sodium is subtracted in progressively larger amounts.

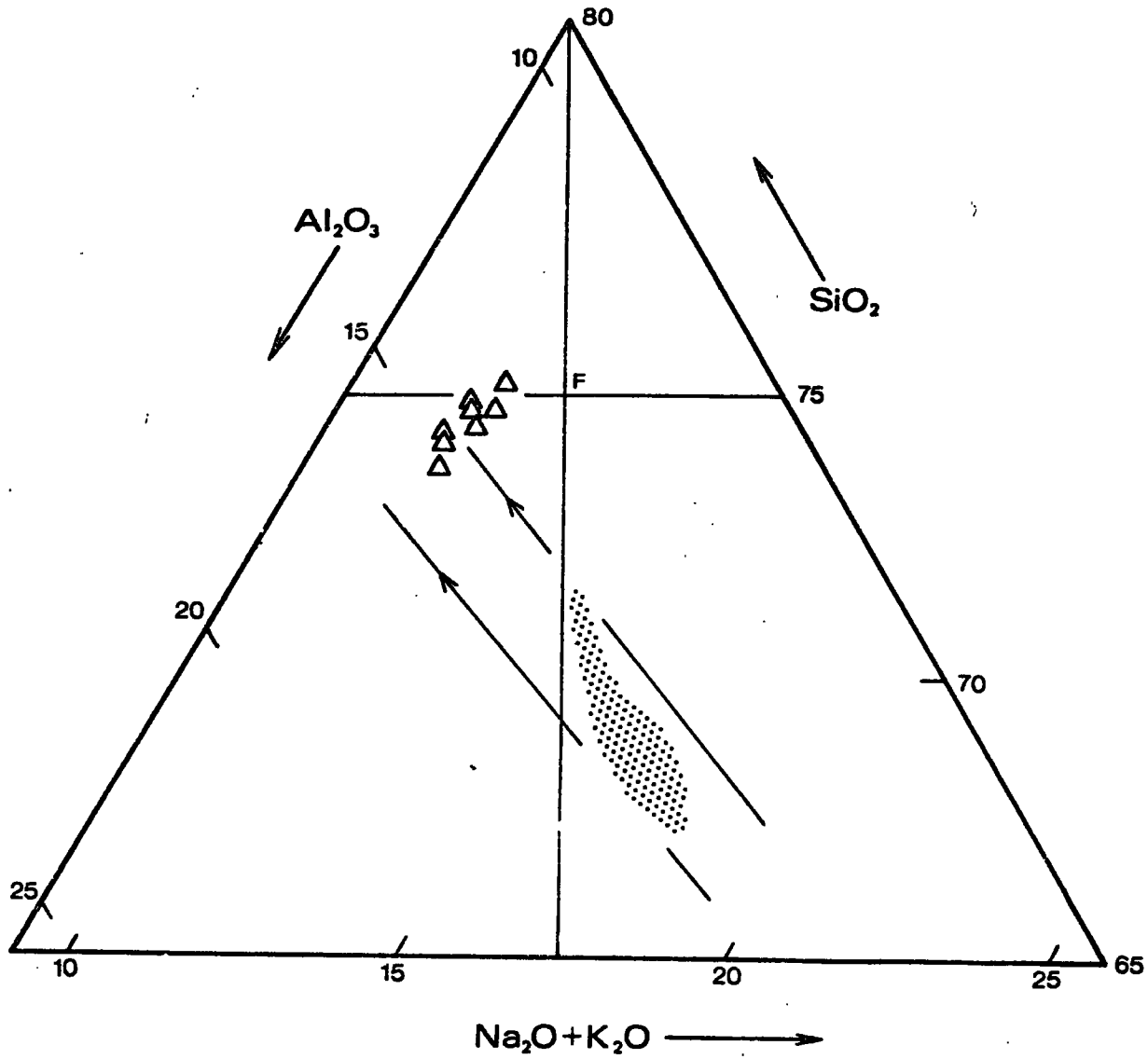
80
10
Al_2O_3
SiO_2
15
F
75
20
70
25
65
10
15
20
25
Na_2O+K_2O

FIGURE 6.2

Plot of Na/(Na+K) versus (Na+K)/Al in cation atomic proportions, showing the compositions of the fresh and altered phonolites. Two sodium-loss lines are shown, having the same qualitative significance as in Fig. 6.1.

Key

○ Fresh and slightly altered phonolites (Chapter 4)

△ Altered phonolites

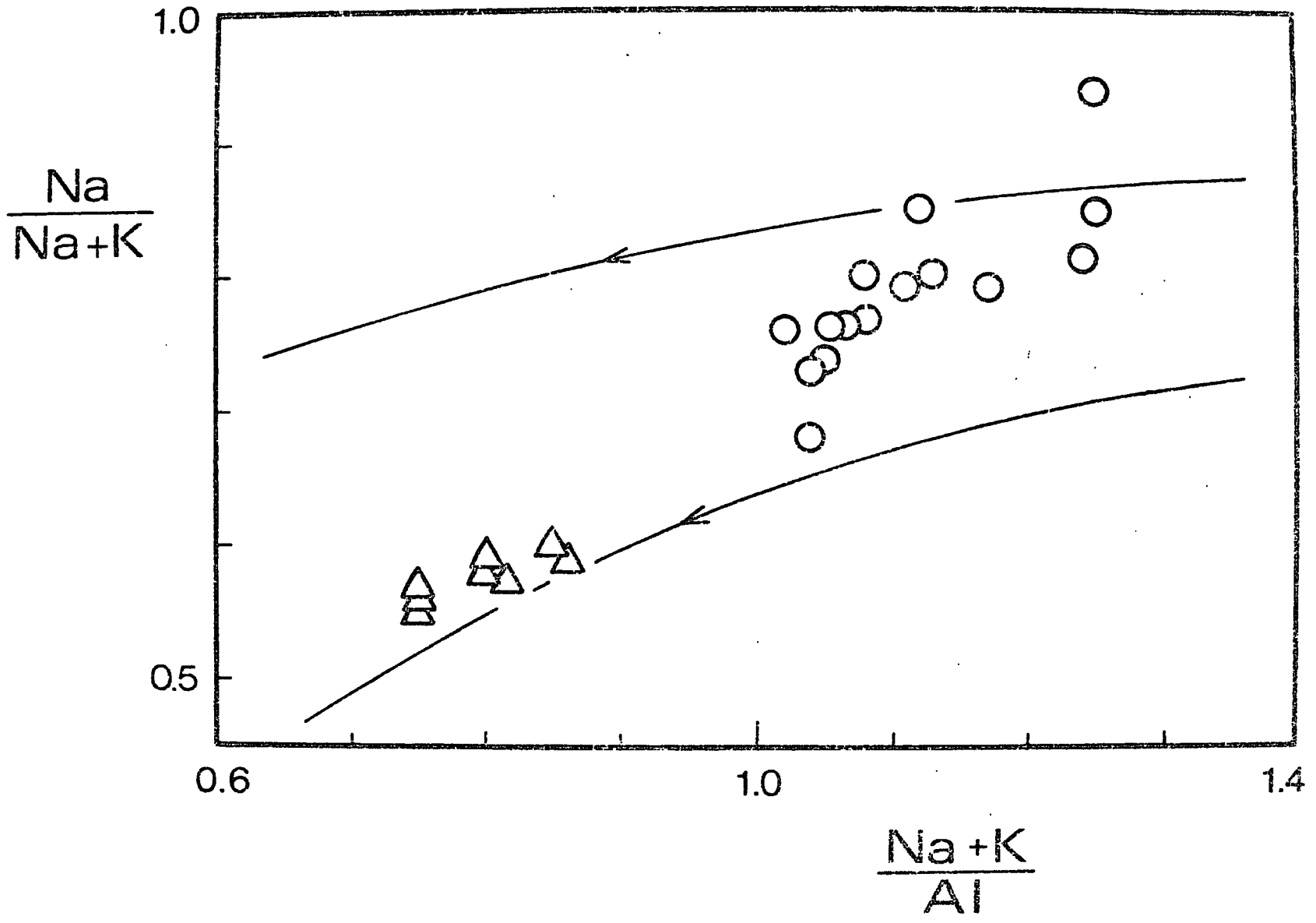
1.0
0.5
Na / Na+K
0.6
1.0
1.4
Na+K / Al

alteration accounts for the observed changes only if the primary composition of the now-altered phonolites corresponded to the least-differentiated of the preserved phonolites, or were more primitive still. If the primary compositions were equivalent to the more advanced members of the phonolite series, it is clear that both the SiO_2:Al_2O_3 and the K_2O:Al_2O_3 must have risen during alteration.

A more comprehensive picture of the alteration process is afforded by applying factor analysis to the fresh and altered phonolites together. The result is shown in Fig. 6.3. The pattern consists of seven factors which together account for 89% of the observed variance. Factor 7, which is responsible for 35% of the total variance, may be taken to represent the alteration process under examination. The strong negative loadings for Na and H_2O^+ agree with the depletion of these elements inferred from direct comparison of the two phonolite groups. They are opposed by high positive loadings for Si, K and Ba, and there are lesser components in the factor which reflect the enhancement of Ti and La and the relative depletion of Zn, Cl, Mn, Pb and perhaps Ca in the altered rocks. Nearly all of these minor loadings indicate variables with respect to which the fresh and altered phonolites are easily distinguished at a statistically significant level. The factor 7 scores provide a distinct demarkation between the two groups.

Factor 6 is very similar to factor 6 in the solution for the well preserved phonolites alone (Fig. 5.1) and must therefore indicate the degree of primary fractionation represented by a given rock. Several minor loadings are lost in passing to the solution

FIGURE 6.3

A box diagram of the Promax oblique solution with k=3 for the phonolite suite including the altered phonolites. The potash-poor specimens 27058 and 27151 and a galena-bearing altered phonolite 31818A have been omitted from the sample. The corresponding numerical data for the solution are tabulated in Appendix 5.

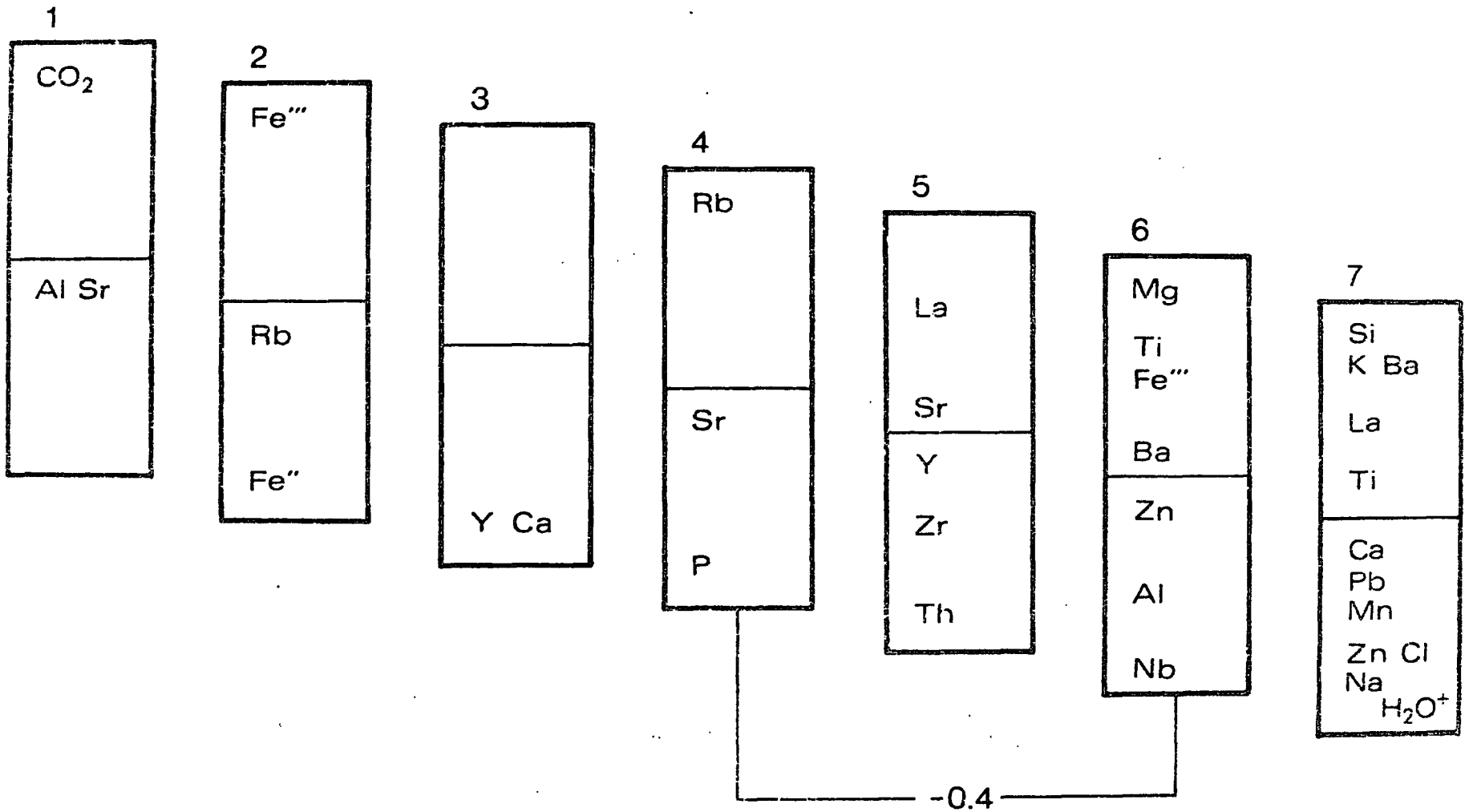
1
CO_2
Al Sr
2
Fe‴
Rb
Fe″
3
Y Ca
4
Rb
Sr
P
5
La
Sr
Y
Zr
Th
6
Mg
Ti
Fe‴
Ba
Zn
Al
Nb
7
Si
K Ba
La
Ti
Ca
Pb
Mn
Zn Cl
Na
H_2O^+
-0.4

now under discussion, but this is because the variance of the elements concerned, La, Na, H_2O^+, Ca and K, is dominated by factor 7. The relatively subtle manner in which these elements participate in factor 6 of the fresh phonolite pattern is therefore not distinguishable in the present case.

The factor scores of factor 6 are of particular relevance. Those of the well preserved specimens vary from +2.5 for the least differentiated member (27183) to -1.2 for the most advanced. The altered specimens however extend over a smaller range of factor scores, from +0.9 to -0.5. It may be concluded with some confidence from this pattern that the altered phonolites were, in their primary state, intermediate members of the phonolite sequence. It seems therefore that the incidence of alteration is unlikely to depend on differences in primary composition, unless the altered dykes originally formed an independent series.

The structure of factor 5 has much in common with the factor representing incipient alteration in the fresher phonolites. As in the case of factor 6, some components present in that factor are missing, since the variance of the elements concerned, Pb, Na, Zn, Cl, Nb, Ca and K, is dominated by factor 7. Nevertheless the variation in factor score between specimens is more or less identical to the pattern representing the fresh phonolites alone. The separate identity of the two alteration factors in the present solution is further evidence that the two classes of alteration differ in type and not merely extent.

With the exception of factor 3, the remaining factors are similar to those obtained in the factor analysis of the unaltered

phonolites, although the order of importance is different. Although one characteristic of the alteration process under discussion is the breakdown of iron-bearing silicates, oxidation does not appear to be important in the process, since the oxidation factor identified in the solution shown in Fig. 5.1 now has less influence. Presumably this fact reflects the high primary oxidation state in the phonolites.

6.6 Origin of the Altered Phonolites

It emerges from the discussion above that the altered phonolite dykes cannot simply be regarded as the product of purely deuteric (closed-system) alteration acting on members of the fresh phonolite series. It remains to consider the alternative ways in which these rocks may have been formed.

The most straightforward model is that this transition has been brought about by metasomatism, which in the context of alkaline magmatism is referred to as "fenitisation". The subject is reviewed by McKie (1966), Heinrich (1966, p.68) and Woolley (1969). Broadly speaking fenitisation involves the introduction of the alkali metals and aluminium into the fenitised rock, often accompanied by the formation of alkali amphibole or pyroxene. In many cases the original K:Na ratio of the rock is little altered. Certain more specialised processes are however included within the scope of fenitisation which are more akin to the changes thought to accompany alteration of the phonolite dykes.

If fenitisation of some kind is responsible for the extensive alteration observed in the phonolite dykes, it must provide a mechanism by which K and Ba are introduced in significant proportions, and which causes aegirine to decompose to iron oxides. It is

reasonable to suppose that the alteration of analcime to gieseckite and the consequent loss of Na could be a spontaneous response to such changes. Woolley (1969) records rare instances of potassium-metasomatism of this kind, which he refers to as "feldspathisation". The process is responsible for the formation of the "feldspathic orthoclasite breccia" (Sutherland 1965) which, when present, forms the innermost silicate mantle around a carbonatite body, and therefore marks the highest grade of carbonatite fenitisation. Other instances of potash-metasomatism in alkaline provinces, which are less restricted in occurrence, are described by Currie (1971) and Heinrich and Moore (1970), but the breakdown of ferromagnesian silicates is not always apparent in these cases. Feldspathic breccias such as described by Woolley are nearly mono-minerallic rocks consisting of orthoclase or sanidine with minor amounts of iron oxides. Wolley however records that associated phenomena, in particular the decomposition of aegirine, may extent into the syenites beyond the zone of feldspathic breccia sensu stricto.

A process of this nature, which broadly agrees with the characteristics of alteration inferred above, may have been partially responsible for the present condition of the altered phonolite dykes, although the effects produced are by no means as extreme as in many of the instances described above. There is however insufficient chemical data on feldspathisation, particularly with regard to trace elements, to allow this argument to be carried further. Moreover the hypothesis is open to objection on chronological grounds; intersections and faulting in the field indicate without reasonable

doubt that the phonolites post-date the emplacement of carbonatite in the Grønnedal-Íka complex. It is therefore necessary to postulate a later episode of carbonatite metasomatic activity, for which there is no independent evidence, if feldspathisation is to be regarded as the agent by which the phonolites have been altered.

An alternative but quite unsupported hypothesis is that the altered phonolites are a relic of a distinct phonolite series, whose petrographic similarity to the group described in Chapter 4 is no more than coincidental. If it is supposed that the magma composition was more potassic than that from which the fresh phonolites were formed, the matrix of the rocks may have consisted of nepheline. The susceptibility of nepheline to form micaceous alteration products under hydrothermal conditions is well established. The experiments by Bailey (1969) indicate that aegirine is stable under such conditions, but the iron oxides seen in the altered phonolites may conceivably be the relics of alkali amphibole, not pyroxene. Amphibole appears to be quite susceptible to oxidation. Upton (1964a) has observed such a reaction in a quartz-porphyry dyke in Tugtutôq, and Ernst (1962) records similar evidence of sub-solidus instability in experimental amphibole system at high fugacities.

6.7 Summary

1. Experiments show that gieseckite usually consists of muscovite with minor amounts of analcite. The latter may become a major component in some cases.
2. In the breakdown of nepheline to gieseckite, the dominant chemical change to be expected is the loss of sodium. In the case of the incipient alteration observed in the "fresh" phonolites, the

effects are small, largely because nepheline is not very abundant. The alteration of nepheline to a similar extent in a nepheline-rich syenite could however cause marked loss of sodium, but smaller changes are to be expected if analcime or cancrinite form a major part of the product.

3. The chemical differences between the fresh and altered phonolites do not conform to a simple sodium-loss model. The discrepancies can be explained in terms of incipient feldspathisation, or the existence of a distinct series of phonolites from which the altered rocks were formed by deuteric alteration. There is however no direct evidence in support of either model.

CHAPTER 7

THE CHEMISTRY OF THE TRACHYTE AND LAMPROPHYRIC DYKES

7.1 Introduction

In addition to the phonolite dykes described in the previous chapter and the ubiquitous basalt/dolerite dykes, there is evidence in the Grønnedal-Ika area of significant amounts of trachyte and lamprophyre magmatism. In the present chapter the chemistry of these minority types is discussed.

Emeleus (1964) described a variety of dykes falling broadly within the lamprophyre field. Several of the types enumerated are poorly represented, each being seen in one or two dykes only. There is one particularly abundant type, however, comprising kersantite and augite kersantite. The mineralogy of this larger group has several parallels with the trachytes in the area, and indeed several were first named as basic trachytes. The possibility exists that the kersantites and trachytes may be directly related, and the two groups therefore merit chemical examination together. In view of their small number and the consequent uncertainty in relating them to other rocks in the province, the minor lamprophyric types described by Emeleus (1964) are not discussed here.

7.2 Petrography

The lamprophyres are largely aphyric (very rare phenocrysts of feldspar and apatite are seen in one or two rocks) and of variable grain size, usually less than 2 mm. The most abundant mineral is feldspar, the plagioclase cores of which are invaded by sericite to a variable extent. Biotite is the chief ferromagnesian mineral, except in the more mafic lamprophyres in which titanaugite has equal status. Pyroxene occurs in about half of the lamprophyres. Opaque oxides are seen in all of them. Chlorite is found in every lamprophyre,

being more abundant in those with no pyroxene. In the mafic specimens two generations of chlorite are distinguishable, one of them occurring interstitially, possibly as a primary phase. Carbonate is found throughout the suite.

Using the nomenclature of Rosenbusch (Hatch et al. 1961), these lamprophyres fall into the kersantite sub-group, some of them being augite kersantites. Though not all of the textural attributes of lamprophyres are seen in every rock, the term lamprophyre seems to be more appropriate than trachydolerite on the grounds of mineralogy.

The trachytes fall into two distinct petrographic sub-groups: firstly there is a relatively fine-grained group in which the characteristic mafic assemblage is biotite-chlorite-opaque with occasional instances of alkali pyroxene; in the second set the mafic minerals are biotite and alkali amphibole, both of which occur interstitially. The types will be referred to as biotite trachyte and biotite-riebeckite trachyte respectively. The biotite, which is invariably strongly pleochroic, differs somewhat in character between the two rock types; in the biotite trachytes it is pleochroic from deep green to yellow, but in the biotite riebeckite trachytes from dark brown to yellow.

The biotite-riebeckite trachytes were referred to as quartz trachytes by Emeleus (1964). Quartz is so rarely seen, however (not in all rocks falling in the group), that the present writer believes the nomenclature defined above to be preferable.

Generally speaking alkali feldspar is the only felsic phase seen in the biotite trachytes. In one rock (39756) occasional interstitial aggregates of micaceous material reminiscent of the alteration product "gieseckite" are found replacing nepheline in the phonolite dykes and nepheline syenites of the Grønnedal-Ika complex (Emeleus

1964, also Chapters 4 and 6). It may be concluded that the rock has developed a silica-undersaturated residuum, a capacity not apparent in the other trachytes.

7.3 Chemistry

The analytical methods used in analysing the lamprophyres and trachytes have been described elsewhere (see Chapter 4 for the trachytes and Chapter 2 for the lamprophyres).

The chemical variation observed is depicted in composite variation diagrams in Figs. 7.1 and 7.2, in which the Differentiation Index of Thornton and Tuttle (1960) has been used as abscissa. The most prominent feature to emerge from this figure is the composition gap lying between Differentiation Index 62 and 75, corresponding to SiO_2 contents of 52 and 56% respectively. The failure of compositions within this interval to be represented in the dyke sample makes any genetic link that might exist between the lamprophyres and trachytes hard to establish with confidence. Nevertheless the gap coincides with the recognised "Daly Gap" (Chayes 1963a, 1963b) seen in many alkaline suites, and cannot be regarded necessarily as evidence against an association between the two groups.

The various petrographic groups defined in Section 7.2 are represented in Figs. 7.1 and 7.2 by distinct symbols, as described in the caption. A distinction is also drawn between the main body of kersantites and two rocks (27049 and 39717) which, though classified as kersantites and therefore falling within the scope of the present work, appear on petrographic and chemical grounds to belong to distinct lines of descent. Their different character is clear from Figs. 7.1 and 7.2.

The chemistry of the lamprophyres is notable for the high contents of magnesium, titanium and, particularly in the intermediate members of

FIGURE 7.1

Variation of major and minor elements in the lamprophyres and trachytes, plotted against Differentiation Index (Thornton and Tuttle 1960).

Key

▲ Kersantites and augite kersantites

▼ Kersantites with abundant chlorite

△ Other kersantite types (see text)

● Biotite trachytes

○ Biotite-riebeckite trachytes

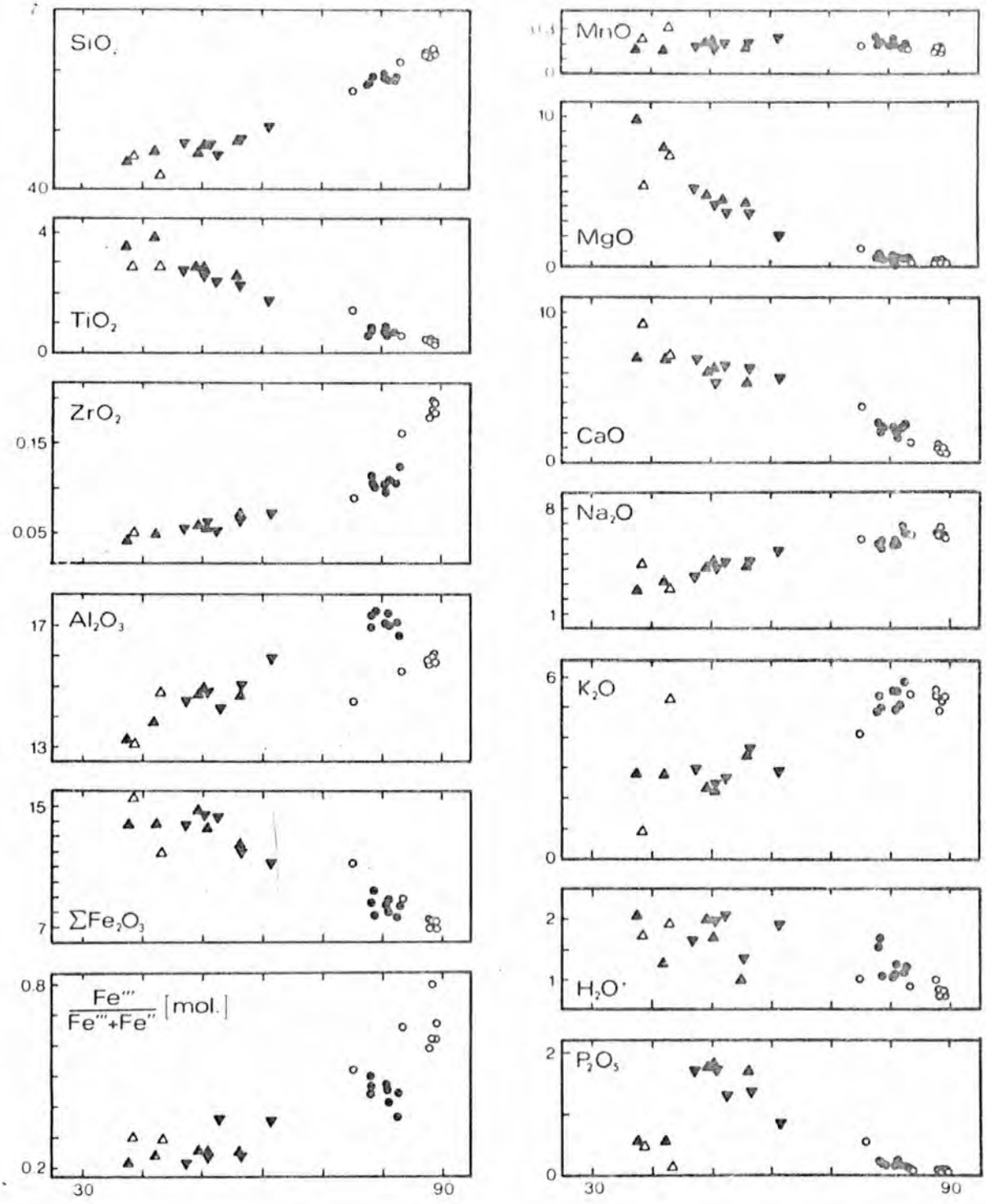
SiO2
40
TiO2
4
0
ZrO2
0.15
0.05
Al2O3
17
13
ΣFe2O3
15
7
Fe'''/Fe'''+Fe'' [mol.]
0.8
0.2
30
90
MnO
MgO
10
0
CaO
10
0
Na2O
8
1
K2O
6
0
H2O+
2
1
P2O5
2
0
30
90

D.I.

FIGURE 7.2

a. Variation of relevant trace elements in the lamprophyres and trachytes, plotted against Differentiation Index. The symbols are as in Fig.7.1.

b. K metal % versus Rb metal p.p.m. for the Grønnedal-Ika lamprophyres and trachytes. The symbols are as shown in Fig.7.1. The following reference lines are shown:

(i) K:Rb = 230, the "normal" ratio for igneous rocks (Taylor 1965).

(ii) The "main trend" of Shaw (1968), identified as "MT".

(iii) K:Rb = 416, the median K:Rb ratio of basic alkaline rocks from the Nandewar Mountains (Abbott 1967).

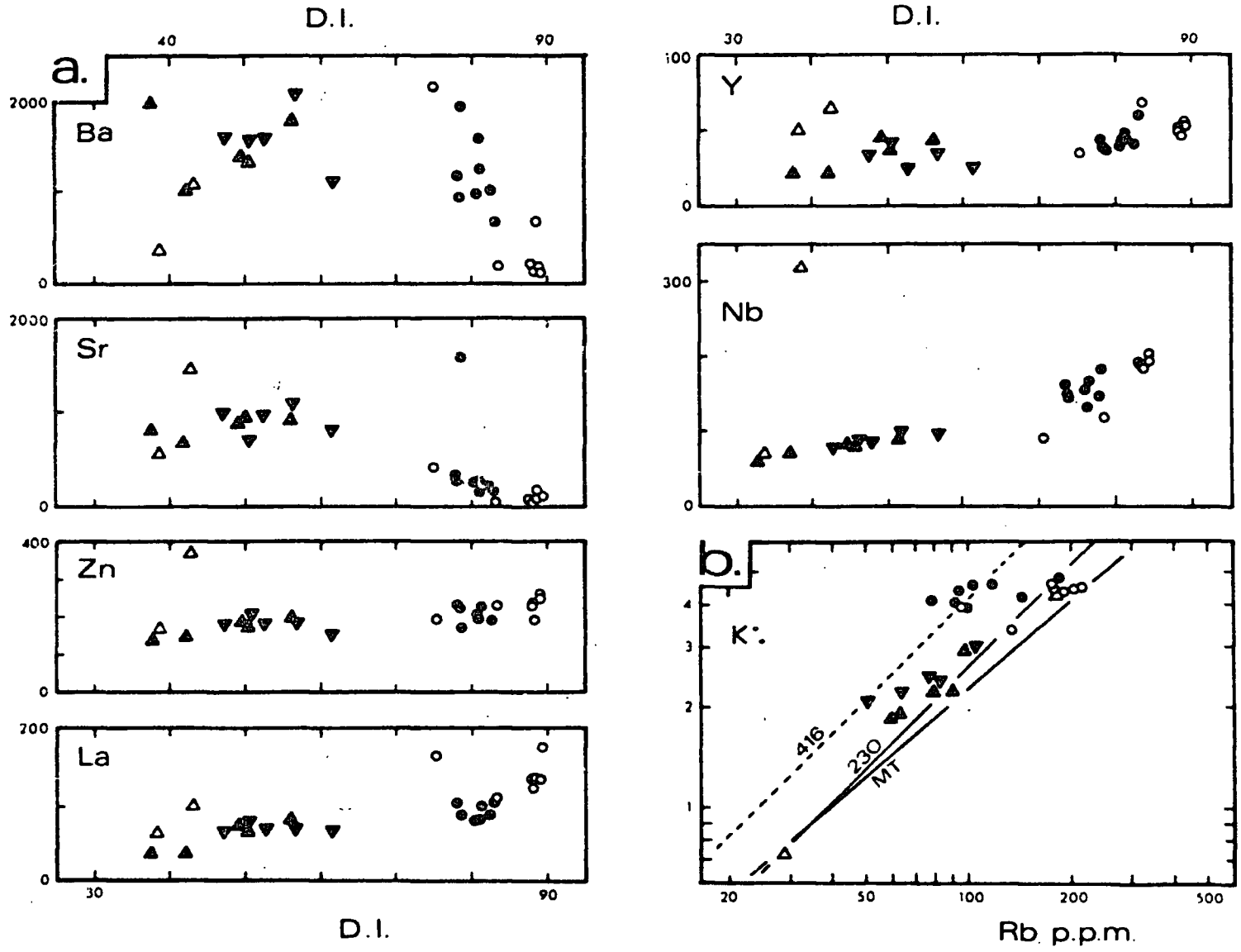
D.I.
a.
Ba
Sr
Zn
La
D.I.
Y
Nb
b.
K
416
230
MT
Rb p.p.m.

the series, phosphorus. Magnesium shows a particularly rapid decline in passing to more advanced lamprophyres. The K:Na ratio is high in the mafic rocks but achieves more normal values in progression along the series (Fig. 7.1). Olivine is present in the norm at about the 10% level, but only trivial amounts of normative nepheline occur. Nepheline assumes significance in the norms of the distinctive lamprophyres 27149 and 39717.

One may divide the lamprophyres into fresh and altered classes based on the abundance of chlorite in each rock. This division is represented in Figs. 7.1 and 7.2 by inversion of the triangular symbol for the more altered rocks, in which chlorite appears in an appreciable quantity. The value of doing this lies in demonstrating that bulk chemical changes accompanying chloritisation are insignificant. This conclusion may usefully be applied to the biotite trachytes, in which chlorite is uniquitous. On the assumption that the chemistry of chlorite-formation is qualitatively the same in trachyte and lamprophyre, one may be reasonably confident that the chemical differences between the biotite trachytes and biotite-riebeckites trachytes, in particular that in Al_2O_3, have not arisen to any significant extent from the formation of chlorite in the former group.

Whereas the lamprophyres are dispersed evenly between Differentiation Index values of 36 and 62%, the two groups of trachytes display little evidence of fractionation internally, most of the variance of the biotite-riebeckite being accounted for by two specimens, 39733 and the more mafic 39790. Except for the latter

rocks, there is no overlap between the two sets of trachytes with respect to Differentiation Index and many other variables.

In several respects, most notably with regard to Al_2O_3, the two trachyte groups appear to lie on distinct trends, but this interpretation should be viewed with caution since it rests largely on the compositions of the isolated biotite-riebeckite trachytes 39733 and 39790, either or both of which may be unrepresentative.

Only trivial amounts of quartz appear in the norms of the biotite trachytes; that is, the group is normatively silica-saturated. The exceptions are 39756, in which there is 6% normative nepheline, in agreement with the nepheline alteration products seen in thin section, and 27081, in which no modal nepheline derivative has been observed.

In contrast the biotite-riebeckite trachytes reveal significant amounts of quartz in the norm, together with small amounts of acmite in a few cases.

The relative variation in K and Rb in the lamprophyres and trachytes is illustrated in Fig.7.2b. The most notable feature is that the biotite trachytes possess a distinctly higher K:Rb ratio than the other rocks. One of the biotite-riebeckite trachytes (31848) has a similar ratio, but this probably results from the alteration of biotite apparent in this section. The nepheline-normative trachytes 27081 and 39756, like the biotite-riebeckite trachytes, possess more normal relative proportions of K and Rb. There is a suggestion of rising K:Rb among the lamprophyres, particularly in those with higher values of the Differentiation Index, but the felsic lamprophyric dyke 27172 does not conform to this pattern.

The cause of the high K:Rb ratios often observed in intermediate

FIGURE 7.3

a. FMA diagram (wt. percent) showing the compositions of the kersantites and trachytes in relation to alkali basalt trends from other provinces.

   A = Gardar olivine basalt - trachydolerite trend (Upton 1965).

   B = Hebridean trend (Tilley and Muir 1964).

   C = Hawaiian trend (Tilley and Muir 1964).

   D = Gough Island (Tilley and Muir 1964).

   The trend passing through the majority of the kersantites and trachytes of the Grønnedal-Íka complex is shown as a broken line.

b. Compositions of the kersantites and trachytes plotted in the plane K_2O-Na_2O-CaO.

The specimen symbols used are the same as in Fig.7.1.

a.

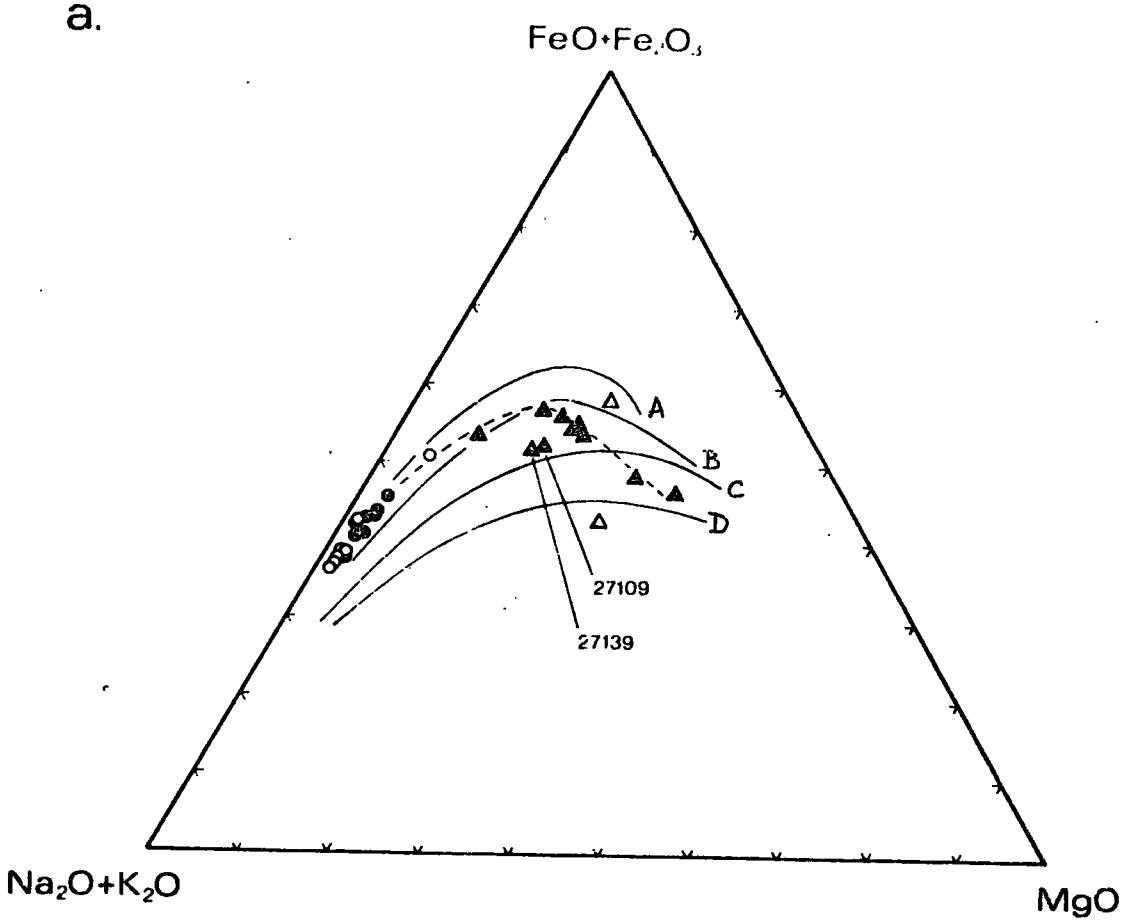
FeO+Fe2O3
A
B
C
D
27109
27139
Na2O+K2O
MgO

b.

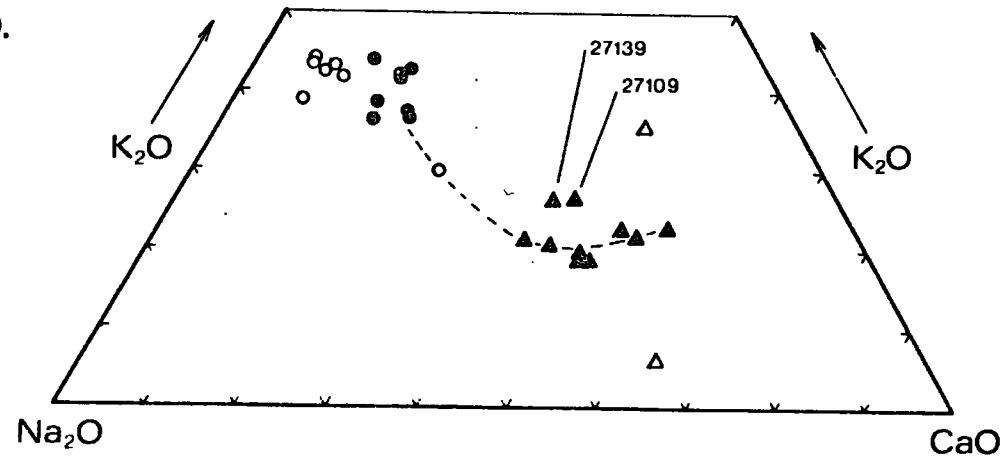
27139
27109
K2O
K2O
Na2O
CaO

alkaline rocks (Abbott 1967) is not readily understood. One factor which may have contributed to the pattern seen in Fig.7.2b is the fractionation of biotite (Shaw 1968) but this hypothesis is refuted by Noble and Hedge (1970).

The distribution of the lamprophyres and trachytes in FMA and K_2O-Na_2O-CaO diagrams is shown in Figs. 7.3a and 7.3b. The diagrams serve to demonstrate the somewhat different character of 27109 and 27139 with respect to the other lamprophyres; they are more potassic and show a lower degree of iron enrichment than the other kersantites, but the differences are slight in comparison to the departure shown by the anomalous lamprophyres 27049 and 39717. In many respects, there appears to be considerable flexibility in the evolutionary paths available, even among the rocks described as kersantite.

7.4 Compositional Affinities and Origin of the Lamprophyre Suite

A number of authors, most recently Upton (1965), have proposed that lamprophyre magmas of camptonite composition may have been derived from olivine basalt magma, by crystal fractionation processes which are largely determined by the development of an unusually high volatile content. Such an origin is consistent with and largely based upon the quite widespread association between the two types of magma. One might suppose that the kersantites of the Grønnedal-Íka area could be related in a similar manner to the alkali basalt magma represented by the abundant olivine dolerite dykes seen in the same area (described by Emeleus 1964). For comparison of the two types, various relevant compositions are presented in Table 7.1. Because differences in water and carbon dioxide contents in these rocks are not necessarily representative of differences between the liquids

Table 7.1. Average analyses* of Grønnedal-Ika kersantites and associated basaltic rocks

A. Mean analysis of two mafic augite kersantites, 27010 and 31878.

B. Mean analysis of seven "intermediate" kersantites: 27015, 27109, 27139, 27148, 31865, 31870 and 39734.

C. Analysis of the felsic lamprophyric dyke 27172.

GIOD. Analysis of Jernhat olivine dolerite, Grønnedal-Íka complex (Emeleus 1864, table 3).

PGB. Mean analyses of four gabbros, approximating to primitive Gardar basalt magma (Upton 1965, Table 3, analysis B).

K. Mean analyses of 95 kersantites (Metais and Chayes 1963).

	A	B	C	GIOD	PGB	K
SiO_2	46.70	49.03	53.21	47.80	45.55	54.23
TiO_2	3.74	2.66	1.76	1.71	2.81	1.38
Al_2O_3	13.79	15.21	16.73	17.51	18.83	15.54
Fe_2O_3	8.52	3.72	4.10	4.06	2.40	3.17
FeO	9.70	9.55	6.73	8.68	11.28	5.57
MnO	0.16	0.20	0.24	0.15	0.24	-
MgO	9.08	4.39	1.99	7.70	6.08	6.59
CaO	7.07	6.26	5.91	7.85	7.95	6.53
Na_2O	2.95	4.24	5.29	2.49	3.56	3.12
K_2O	2.57	2.90	3.02	1.86	0.90	3.85
P_2O_5	0.59	1.71	0.91	0.20	0.44	-

*All analyses have been recalculated to be water- and carbon dioxide-free (see text).

from which the rocks in question were formed, the analyses quoted in Table 7.1 have been recalculated free of water and carbon dioxide. The range of the Grønnedal-Íka kersantites is represented by three analyses: analysis A is the average of the two most mafic rocks in the suite, 27030 and 31878, analysis C is that of 27172, the most salic member, whereas analysis B is the average of the remaining rocks omitting the anomalous kersantites 27049 and 39717.

Relatively little is known at present of the evolution of the basaltic liquids in the Gardar province, and a regional study of this topic is under way (Upton 1970). Consequently little comment will be made on the small but obvious differences between the olivine dolerite from the Grønnedal-Íka complex (GIOD) and the "primitive Gardar basalt" calculated by Upton (PGB). The discrepancy is not large enough to disguise the quite different character of the mean mafic-kersantite analysis, in which Al_2O_3 is strongly depleted relative to the basalts while MgO, (MgO+FeO), K_2O and (Na_2O+K_2O) are significantly higher than in the basaltic rocks. It is hard to envisage a simple process of crystal fractionation which could give rise to this relationship, and one may reasonably conclude that the lamprophyres under discussion, of which the mafic rocks 27030 and 31878 are presumed to represent the parent liquid, are not related in a straightforward manner to either basaltic type represented in Table 7.1. It is worthwhile to note in passing that the composition of the Jernhat olivine dolerite (GIOD) appears to be transitional between the undifferentiated Gardar basalt (PGB) and the lamprophyre suite with respect to the variables identified above, and this conclusion is reinforced by its high contents of H_2O and CO_2, constituents which achieve characteristicallyhigh levels in the lamprophyres.

The kersantites of intermediate composition have much in common with the average lamprophyre analyses given by Métais and Chayes (1963), in which the points of departure from the basalt analyses are yet more pronounced. More detailed comparison is inappropriate, however, in view of the wide spread in the analyses compiled by Métais and Chayes. The average analysis of 95 kersantites given by these authors is shown in Table 7.1 (K).

Turner and Verhoogen (1960) make much of the similarity between the lamprophyres in general and the continental leucite-basalt association, which includes such rocks as the strongly potassic lavas of the Western Rift Valley of East Africa. Relative to the typical Gardar basalts, the compositions of the Grønnedal-Íka lamprophyres err in the direction of the potassic rocks, notably in their high K_2O, MgO, TiO_2, P_2O_5, Ba and Sr contents, but to a lesser extent such that several attributes of the latter group are lacking. In particular the strongly undersaturated character, represented usually by modal leucite and normative nepheline, is only slight in the lamprophyres under discussion; potassium is in all cases subordinate to sodium in the rocks described in this Chapter and the magnesium content, though high, does not equal that of many leucite basalts (Holmes and Harwood 1937).

It is an open question whether the lamprophyre dykes from the Grønnedal-Íka area acted as feeders to surface volcanism related in character to the potassic lavas of East Africa or whether, as may be true of many lamprophyres, they are only minor associates of the plutonic activity in the area. The apparent petrographic and chemical connection with the biotite trachytes suggests perhaps that the former view is more accurate. Turner and Verhoogen (1960) draw

little distinction between the two modes of occurrence and propose that the potassic rocks in general may be formed by the "sweating out" of the lowest temperature phases of micaceous granite by the passage of common alkali basalt magma, into which they are incorporated forming a highly potassic liquid. Such a model does not account for the characteristically low SiO_2 and high MgO contents (together with Ni, Cr, Co and V) shared by the potassic lavas and many lamprophyres, nor is it generally applicable. Other models have to be considered for the relatively potassic lavas of some oceanic provinces (Le Maitre 1962, Baker et al. 1964) and may equally apply to their continental analogues.

There are indications from the present work that magmas of differing degrees of K-Mg enrichment coexisted in the Gardar province, as they are seen to do within quite localised areas in East Africa and elsewhere. The present state of knowledge suggests that the "undifferentiated Gardar basalt" calculated by Upton (1965) accounts for the major part of basalt activity in the Gardar, but this view may be modified as a result of work in progress. Studies in other alkaline provinces (Baker et al. 1964, Cundari and Le Maitre 1970) have pointed to the influence of processes other than high level crystal fractionation in determining initial magma composition (see O'Hara and Yoder 1967) and similar conclusions may perhaps apply to the Gardar, although there is no direct evidence from the present work as to the nature of these processes.

7.5 Petrogenesis of the Trachytes

In many petrographic and chemical respects, there are grounds for supposing that the kersantites and trachytes may belong to a

common fractionation trend. The lamprophyres and biotite trachytes have qualitative mineralogical characteristics in common, and in spite of the compositional gap mentioned in earlier paragraphs there is a pronounced consanguinity of chemical trends between the groups. K-Rb relationships provide a more specific indication of comagmatism, since the kersantites appear to show a progressive rise in the K:Rb ratio from normal values to the unusually high values characteristic of the biotite trachytes.

An attempt has been made to establish a mineralogical link between the kersantites and the biotite trachytes by an electron microprobe study of the zoning found in the mineral species common to both types of rock. It was hoped thus to bridge the gap and to establish a continuity of mineral composition trends from lamprophyre to trachyte. The attempt has proved fruitless because, although the zoning of biotite and feldspar in the kersantites was found to span a significant range, a mineralogical composition gap was still found to exist. In view of the possible differences between the order of crystallisation in the two dyke types, such a test should strictly be based on phenocryst zoning alone, and the aphyric nature of the rocks may lie behind the inconclusive results obtained from this work.

In all the variation diagrams which have been considered, the disposition of analyses is broadly consistent with the supposition that the two trachyte groups are comagmatic. Those discontinuities which do exist, in Al_2O_3 and K_2O-Na_2O-CaO, may be explained in terms of changes in the fractionating phase assemblage, particularly the probable appearance of potash feldspar on the liquidus when the liquid composition attains the two-feldspar boundary in the ternary feldspar system (see Carmichael 1963).

FIGURE 7.4

a. Compositions of the Grønnedal-Ika trachytes represented in part of the plane SiO_2-Al_2O_3-(Na_2O+K_2O). The symbols used are the same as in Fig.7.1

b. Compositions of the Tugtutoq microsyenites plotted in the same system. The following symbols are employed:

△ Hastingsite microsyenites

○ Biotite-rich microsyenites

□ Riebeckite microsyenites

The point F represents the composition of binary alkali feldspar.

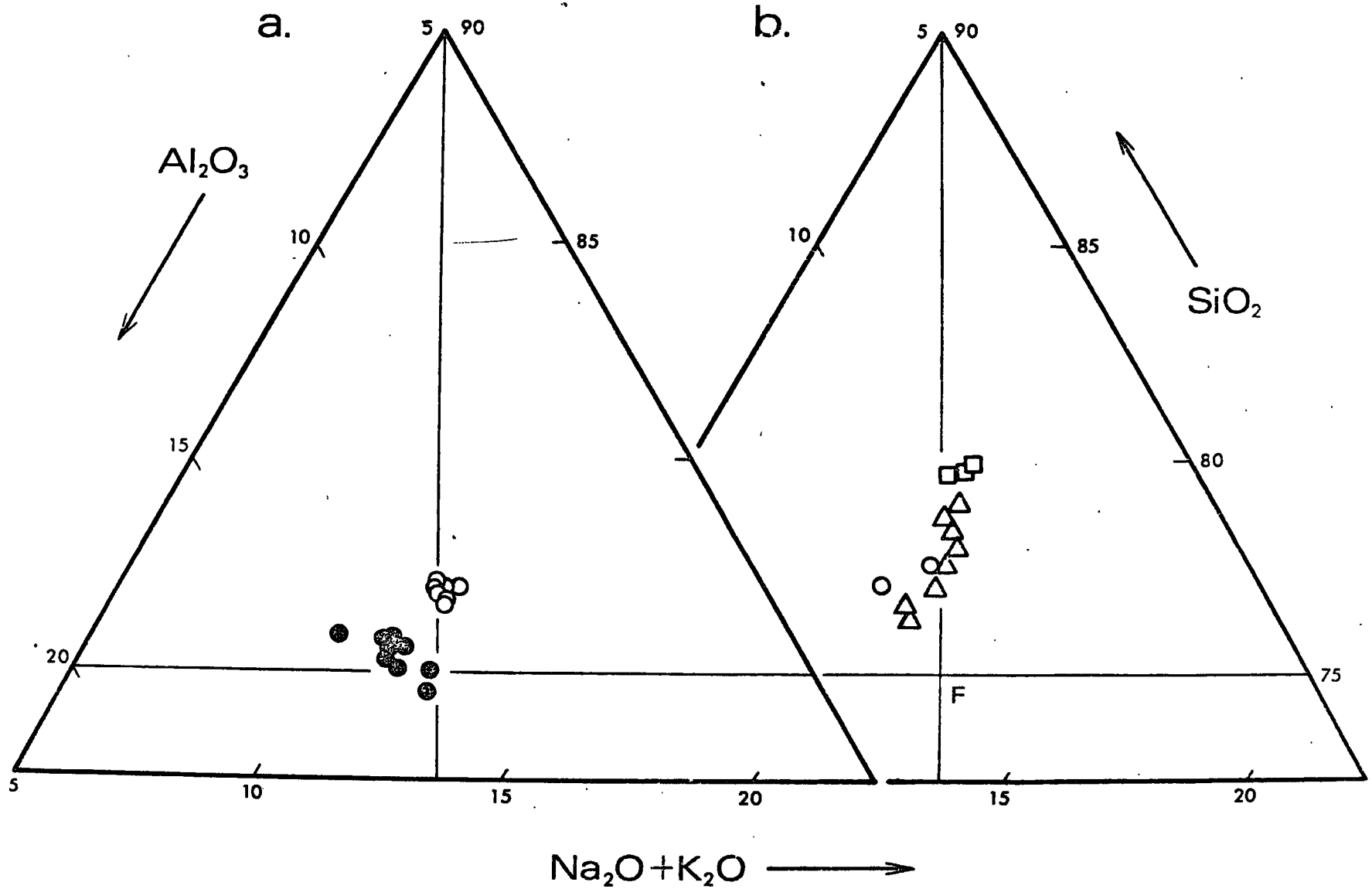
a.
b.
Al_2O_3
SiO_2
Na_2O+K_2O
5
90
10
85
15
20
80
75
F

If this view is correct, the trachytes may be considered to represent a magma series similar to that forming the microsyenite and microgranite dykes of the Tugtutôq Peninsula. These dykes are associated in the field with "trachydolerite" dykes whose petrography is reminiscent of the lamprophyre dykes described in the present study, and the microsyenites are assumed to be derived from these liquids (Macdonald 1969). The comparison with the Grønnedal-Íka dykes is summarised in Fig.7.4, which shows the compositions of both dyke groups plotted in part of the system SiO_2-Al_2O_3-(Na_2O+K_2O). From this diagram and the general chemical compatibility apparent from analytical tables, one may conclude that magmas capable of producing strongly silica-oversaturated residua were present in the Grønnedal-Íka area during Gardar times, although as part of a much later episode than the main syenite/carbonatite emplacement.

The silica-undersaturated biotite trachytes and the mafic biotite-riebeckite trachyte indicate that the situation was in fact of greater complexity than this picture suggests. With so little information, it is impossible to resolve the inter-relationships of these rocks in any greater detail. If in fact the trachytes are residua of lamprophyre fractionation, it is quite possible that the variety of parent (kersantite) liquids suggested by the limited work described here accounts in some degree for the range of trachytic liquids which appear to be present.

PART 3

CONCLUSION

CHAPTER 8

GENESIS OF THE GRØNNEDAL-ÍKA MAGMAS IN THE BROADER CONTEXT OF THE GARDAR PROVINCE

8.1 Introduction

The intrusions described in the foregoing chapters may be divided into two broad episodes:

(i) An older episode of major syenite emplacement (Chapters 1,2,3);

(ii) A younger episode of salic dyke intrusion (Chapters 4,5,6,7).

Little or no evidence is found in the field bearing on the relative duration of each episode, but the two are separated in time by the intrusion of the carbonatite and the major mafic dykes, and by the first group of faults (Emeleus 1964, p.70). The alkaline dykes must therefore be regarded as being a significantly later episode of alkaline magmatism (although they do appear to be found in greatest concentration near the syenite complex).

It can be seen that the overall composition of the alkaline activity changed significantly over this period of time. In Chapters 2 and 3 it has been argued that the Lower and Upper Series and allied bodies were derived from magmas whose compositions corresponded roughly to the nepheline-feldspar phase boundary in the system SiO_2-$NaAlSiO_4$-$KAlSiO_4$. In other words, they were near to minimum-melting compositions in the undersaturated part of the natural residuum system. The Xenolithic Porphyritic Syenite magma association may represent a slight departure from this state of affairs. In contrast, the magmas from which the later alkaline

dykes were formed were phonolitic trachytes and orthotrachytes, and appear to represent magmatism significantly closer in composition to silica-saturation.

In the present chapter the possible origins of such magmas are discussed, and the significance of these changes with time is considered in the broader context of the development of the Gardar province.

8.2 Variation in Magma Type in Continental Alkaline Provinces

The exceptional flexibility in the types of magma involved in volcanism and plutonism in continental alkaline provinces, particularly the East African rift system, has engaged the attention of petrologists for a considerable time. For many years it was felt to be desirable to establish a causal relationship between the structural phenomena of rifting and the characteristic spectrum of magmatism with which, broadly, it is associated. More recently, many workers have come to accept that rift tectonics and volcanism are together the superficial manifestation of more deep-seated phenomena (King and Sutherland 1960, King 1970, Harris 1969, 1970, Baker et al.1970). Several authors have proposed that continental rift valley phenomena are the consequence of a relatively localised thermal disturbance in the Upper Mantle (Elder 1965, 1966, Harris 1969, Gass 1970). This disturbance is regarded as a hot region of mantle which causes the isotherms to rise relative to the surrounding shield areas and thereby depresses the high pressure phase-transformation boundaries.

In this context, Harris (1969) has made a significant contribution

to the understanding of the distribution of mafic magma types in East Africa and the neighbouring areas. His arguments rest on two generalisations:

1. In areas in which magmatism is most intense, the basalt composition tends to become less alkaline, in some cases becoming silica-saturated. At progressively greater distances from such centres, basalts change to undersaturated and strongly undersaturated types.
2. The concentrations of the residual ("incompatible") trace elements tend to be highest in the strongly undersaturated basalts, becoming progressively less abundant on moving towards tholeiitic types. Such concentrations are highest however in carbonatites and in kimberlites and the associated potassic ultramafic lavas.

The concentration of the residual trace elements is taken to indicate the depth in the mantle at which the magma was generated. In passing to the surface the liquid will acquire, by a variety of segregation processes (Harris 1967), a concentration of the residual elements which is proportional to the depth of mantle through which it has passed.

Harris (1969) argues that the depth of derivation, and therefore the type of basalt liquid, is dependent on the geothermal gradient obtaining in the area in question. In an area of high gradient, partial melting temperatures are met at shallow depths in the mantle, so that the dominant magma type is tholeiitic basalt with low trace element concentrations. Where the geothermal gradient is lower, the point at which the geotherm and the first-melting curve intersect retreats to successively greater depths, producing,

in accordance with high-pressure phase studies, magmas which are more alkaline in composition and which have enhanced contents of the residual elements. Carbonatites and kimberlites are regarded as the characteristic form of magmatism in regions with the lowest heat flow of all.

Some interest has been expressed in recent years in the factors which determine whether a given alkali basalt evolves to produce oversaturated or undersaturated residua (Bailey and Schairer 1966, Morse 1969). Recent work suggests however that much of the apparent flexibility in the composition of the salic derivative magmas in alkaline provinces may be directly related to variation in the composition of the mafic rocks with which they are associated (Coombs and Wilkinson 1969, Wright 1971). Thus it is possible that the character of the salic products in an alkaline province and their variation with time and location may also be traced to the depth in the mantle at which the parent (basaltic) liquid was derived. High level crystal fractionation processes may therefore exert little control over the variation between phonolite and rhyolite seen among the salic residua of alkaline provinces.

In the East African context these ideas are represented, for example, by the distinction in the Eastern Rift of two genetic series of volcanic products; they are a strongly undersaturated series comprising ankaratrite-nephelinite-phonolite, and a mildly alkaline series consisting of alkali basalt-trachybasalt-alkali trachyte-soda rhyolite (Saggerson and Williams 1964, Saggerson 1970, King 1970). The distribution of the various salic types therefore imitates quite closely that of the "corresponding" mafic magmas, and it possible to distinguish the tendency for trachyte and

trachytic phonolite lavas to be found in and around the rift graben and near to the thermal and topographic culminations along the rift, whereas the bulk of the phonolite lavas tends to be found marginal to these areas (see, for example, Williams 1969). Similarly in Ethiopia one may distinguish between the nepheline-bearing trachytes of the plateaus on either side of the rift and the peralkaline trachytes and their silicic derivatives found in the rift zone itself (Le Bas and Mohr 1968, Mohr 1971). Peralkaline rhyolites are characteristic of the Gulf of Aden, where basalts are transitional between alkaline and tholeiitic (Red Sea) types (Cox et al. 1970).

In this scheme however "phonolite" must be regarded as the product of a wide range of thermal regimes. This is because it is the minimum-melting derivative of a spectrum of undersaturated mafic magmas from melanephelinite to nepheline-poor basanite (see Chapter 4). Phonolitic trachytes, the residuum of the latter end-member, perhaps may be distinguished as the product of a comparatively high thermal gradient.

8.3 Mechanisms of Salic Magma Production in the Gardar Province

Continental and oceanic alkaline provinces are known to share much the same range of alkaline rock types (Harris 1969), but the distribution and relative abundance of these types is quite different. Of special relevance is the prominence of salic magmas such as trachyte, phonolite and rhyolite in the continental provinces. For example, in the Kenya province such magmas account for half the total volume of lavas represented (Baker et al. 1971), a proportion which is quite unknown in oceanic volcanism. Clearly,

there are processes operating in the continental province which either modify or substitute for the straightforward fractional crystallisation of mafic liquids, which is thought to be dominant in oceanic islands.

Many basic and intermediate dykes in the Gardar province carry abundant anorthosite xenoliths and plagioclase megacrysts. The consistent relationship between the composition, type and abundance of these inclusions and the composition of the host rock has led to the suggestion by Bridgwater (Bridgwater and Harry 1968) that much of the Gardar area is underlain by anorthosite. The distribution of the inclusions in the Gardar dykes has been explained by Bridgwater in terms of an extensive magma chamber in which alkali basalt magma became compositionally stratified in response to the pressure gradient existing between the bottom and the top of the chamber. Thus plagioclase crystals floated upwards until, reaching a layer of liquid of the same density, they became suspended in it. This hypothesis accounts better than any other for the distribution of the various types of inclusion in the host dykes. It is regarded by some as evidence of the operation of liquid-state fractionation as a factor in the evolution of mafic liquids (Upton et al. 1971).

If this liquid-stratification mechanism does operate, it is not hard to understand the prominence of the salic derivatives among the volcanic products seen nearer the surface. The concentration of the refractory mafic components towards the base of the magma column will inevitably cause a rise in the liquidus and solidus temperatures at such levels. If the original alkali basalt was close to its liquidus, as seems likely (Harris et al. 1970),

a point is reached where the deepest parts of the magma column solidify because the solidus temperature has risen above the actual temperature. If the upward migration of the entire column is envisaged (Upton et al. 1971), a progressively larger amount of the mafic component of the liquid is left behind in solid form as migration proceeds, and the magma reaching the shallower parts of the crust is significantly weighted in favour of the salic residual components.

The existence, during the development of the Gardar province, of large columes of differentiated basic magma at depth, as suggested by the feldspathic inclusions, has led to the supposition that liquid and crystal-liquid fractionation are the chief processes responsible for the large volumes of salic magma represented in the Gardar (Bridgwater and Harry 1968). Other processes such as partial melting (Bailey 1964) do not therefore appear to be necessary to explain the relative abundance of syenite and basalt. Further support for this view is given by the widespread occurrence, among the feldspathic dykes, of composite dykes in which microsyenite xenolith-poor margins give way to a later core of olivine basalt or dolerite. The transition may be either continuous or with an abrupt chilled margin. These dykes are thought to represent early intrusion of salic magma from the top of the differentiated magma body, followed by the later intrusion of a basic liquid fractionation from lower in the magma column. The composite feldspathic dykes provide evidence supporting the view that such processes as have been described can produce a syenitic liquid from the alkali basalt found universally in the province.

It is significant however that the syenite members of the composite feldspathic dykes are largely restricted to quartz syenite in composition. Nepheline syenite is represented only in rare cases (Bridgwater and Harry 1968, p.123, D. Bridgwater, pers. comm.), and even then may be of phonolitic trachyte type. If the dykes described in the very thorough account of Bridgwater and Harry are representative, such observed instances of the production of nepheline syenite as the residuum of a basaltic liquid are of minor importance. In view of the abundance of nepheline syenite in the province, the significance of this observation should be considered, since other mechanisms than that outlined above may be feasible.

If the hypothesis put forward by Harris (1969) and applied in the preceding pages to the salic alkaline derivatives is valid, phonolite and foyaite may be regarded as the residual liquids of magmatism in regions of intermediate to low geothermal gradient. In these circumstances, the progressive solidification of a stratified mafic magma body from the bottom upwards may be supposed to operate more efficiently, such that the weighting factor in favour of the salic differentiates at the surface is very much increased in comparison to the products seen in higher heat flow areas. Consequently the more mafic fractions of the magma body in which the feldspathic material analogous to that described above would occur would only very rarely be represented at the surface.

Alternatively there seems to be no reason why nepheline syenite magmas may not be regarded as the products of partial fusion at depth. The partial melting of mantle material to produce salic alkaline liquids directly has been proposed by Wright (1966,1969,1971)

and Presnall (1969), but other authors have suggested that the partial melting of basaltic material at the base of the crust may be a more important mechanism (Bailey 1964, Harris 1970). For salic magmatism in areas of low heat flow, partial melting may become a progressively more probable alternative to fractional crystallisation and allied processes. For example, one may suppose that a relatively high heat flow is necessary to sustain the liquid condition of a basic magma for a sufficient time to allow significant liquid or crystal fractionation to occur, particularly if this occurs at a high level in the crust. In regions where the geothermal gradient is lower, the persistence of liquid magma in this way is generally possible only at progressively greater depths in the crust or mantle, particularly when it is considered that smaller volumes of magma are produced in such areas (Harris 1969) and that magma-bodies will therefore be smaller and their thermal capacities lower. Magma in these regions which is not immediately admitted to the surface as mafic lava may well solidify relatively rapidly at depth. A rise in heat flow, or in local temperatures as a result of the further accumulation of hot basic material, may then cause partial melting of these deep-seated mafic rocks, "sweating off" the initial (low-temperature) phonolitic melts.

These arguments are intended merely to illustrate one feasible partial fusion scheme, and the model given should not be regarded as unique in anyway.

8.4 Evolution of Salic Magma Type as represented in the Grønnedal-Íka Complex

The magmatism represented in the Grønnedal-Íka complex took

place over a range of time, and may include in the dyke rocks elements derived ultimately from other magmatic centres in the area. In these circumstances it would be unwise to pursue too exact an interpretation of the sequence of magma types represented, but a speculative attempt to assess the significance of the sequence in relation to the Gardar province as a whole is perhaps appropriate.

D. Stephenson (personal communication), among others, has emphasised the geographical variation in rock type in the Gardar province. The major undersaturated intrusions, the Grønnedal-Íka, the Ilímaussaq and the Igaliko complexes, fall to the north-east side of a line drawn from Kûngnât to Narssaq (see Fig. 1.1). Saturated and oversaturated intrusions on the other hand fall on or to the south-west side of this line. Stephenson relates this pattern to the possible existence of a structure akin to the East African rift valley, where a similar pattern is observed. This geographical factor may represent one of the controls on the composition of magmas appearing in the Grønnedal-Íka complex.

The Lower Series magma, the first to be intruded, is regarded as having been oversaturated with respect to nepheline. No unmodified representative of this liquid is available, however (Chapter 3), and thus its composition is not known quantitatively. It was followed by the emplacement of the Upper Series magma which, from qualitative arguments based on the fractionation history seen in the cumulus rocks and from comparison of its chill with relevant phase equilibria, is regarded as approximating in composition to a low-pressure nepheline-feldspar phase boundary.

The character of both liquids is consistent with their

derivation either by partial melting or fractional crystallisation. If a basaltic parent is involved, rather than direct derivation of the syenite liquid from the mantle (Wright 1971), its possible identity ranges considerably, from melanephelinite to nepheline-poor basanite (see section 8.2). Phonolites are associated with melanephelinite magmatism in East Africa (King 1965), for example, but they are also commonly viewed as the residual products of liquids of alkali basalt type (Bailey and Schairer 1966). It has been argued in Chapter 3 that an association with highly under-saturated mafic magmas of nephelinite affinity is improbable because only rare occurrences of rocks of this type have been reported from the Gardar province (see, for example Stewart 1970). The mechanisms discussed in an earlier part of this Chapter, whereby basic rocks may be strongly under-represented, might tend to modify this view but intuitively it seems very unlikely that such rocks would go entirely unrepresented (or undetected) if they contributed signif-icantly to the magmatism of the province. Large volumes of nephelinite lavas (and ijolite intrusives) are seen in East Africa in association with phonolite lavas. On the other hand, the Grønnedal-Ika complex appears to predate all major dyke episodes, suggesting that unmodified parental material may have been very sparsely represented, if at all, at the surface.

There seem to be good grounds for regarding the Xenolithic Porphyritic Syenite magma-type in a different light. In relation to the main body of nepheline syenites, it has high concentrations of the residual trace elements, and its mode of emplacement and its present composition suggest that it was highly charged with

volatiles, a feature which is not in evidence in the other syenites. There is a tendency to show a relatively feldspathic and peralkaline nature. In these respects it bears comparison with the later phonolitic trachytes of the Grønnedal-Íka complex (Chapter 4), with the nepheline syenite member of the Hviddal giant dyke (Upton 1964b) and possibly with the parent magma of the Ilímaussaq intrusion. In all these instances there is evidence of peralkaline volatile-rich residua in which high concentrations of the incompatible elements may be achieved. The rocks do not compare quantitatively with the reknowned agpaitic layered rocks of the Ilímaussaq and Lovozero massifs, and none of the type-minerals of such rocks are reported in the Grønnedal-Íka complex, but in many respects this character is seen in its incipient stage in the Xenolithic Porphyritic Syenite magma association, and in a more advanced stage in the phonolite dykes described in Chapters 4 and 5. The latter group compares chemically with dyke rocks in which agpaitic properties have been reported from other areas (Azambre and Giron 1966, Bordet et al. 1955), and it may be that such magmas represent a stage in the evolution of the agpaitic rocks. The full extent of agpaitic character as described above may only be developed when such magmas are present in a large magma chamber in which volatile localisation and other such specialised processes thought to contribute to the agpaitic trend can occur (Sørensen 1969, Vlasov et al. 1966).

It is significant that augite syenite, rather than a more silica-undersaturated liquid, is regarded as parental to the Ilímaussaq agpaites (Ferguson 1970). Similarly there is evidence

(Chapter 4) that the Grønnedal-Íka peralkaline phonolites (phonolitic trachytes) have evolved largely by feldspar fractionation from an intermediate parent which was only marginally undersaturated with regard to silica. If these conclusions apply to the Xenolithic Porphyritic Syenite magma type, it seems that its association with the early syenite liquids is only indirect. Sørensen (1969) supposes that the upward migration of volatile and possibly felsic components in such a liquid has played an essential part in determining the trend towards agpaitic character. Such processes may by analogy have influenced the nature of the hydrous peralkaline rocks of the Grønnedal-Íka complex. It is quite possible that the Xenolithic Porphyritic Syenite association represents the final pegmatitic residuum of basic or intermediate magma at depth, and that the extreme build-up of volatile pressures during this process accounts for its evidently violent emplacement.

The carbonatite, the last major intrusive event in the complex before the mafic dykes, represents another volatile-controlled intrusion. Emeleus (1964) observed that in general carbonatites are not usually associated with nepheline syenite but with feldspar-poor and feldspar-free alkaline rocks (see, for instance, King 1965). In the present case, the carbonatite may be genetically unrelated to the syenites, its appearance in the complex being determined by the evident crustal weakness in the locality as a result of the faulting in the area (Chapter 1), but little can be said on this point until the chemistry of the carbonatite body has been studied.

The appearance of silica-saturated and marginally oversaturated trachyte dykes late in the development of the complex may possibly

be linked with the emplacement of the later Kûngnât complex nearby (Upton 1960). It has been argued (Chapter 7) that the lamprophyres and trachytes may represent part of a trend from trachydolerite to alkali rhyolite, as seen in the Tugtutôq peninsula (Macdonald 1969) and in the Kûngnât complex (Upton et al. 1971). One may perhaps relate the saturated trachyte and allied activity to the voluminous basalt and dolerite intrusions (including Big Feldspar Dykes) which preceded it.

From the pattern of development described in these pages there are grounds for distinguishing very tentatively a trend of declining silica-undersaturation with time in the Grønnedal-Íka complex. Such a trend might be compared with the temporal sequence from Miocene nephelinite through to trachytes and rhyolites in the Pleistocene and Recent which has been distinguished by King (1970) in the East African provinces. In the present state of knowledge of phase relations in the Petrogeny's Residua and allied systems, this trend is hard to reconcile with fractional crystallisation acting alone on a common basaltic parent. The pattern may reflect the changing influence of liquid fractionation as described by Upton (1960) and Bridgwater and Harry (1968), but it is impossible to predict the effects of subtle changes in such a process. An alternative view is that the trend towards silica saturation reflects the overall change with time of the magma type predominating in this part of the province. Such a change, if established more widely, might be an indication of increasing geothermal gradient due to developments in the heat distribution in the mantle underlying the province, a process which may play

an important part in the evolution of continental alkaline provinces in general. This conclusion is based merely on the present study of the salic rocks of the Grønnedal-Íka complex, however, and until regional work on the basic magmatism is available there is no evidence that the pattern extends to all the rock types of which the Gardar province is composed.

APPENDICES

APPENDIX 1

Specimen Preparation

The rocks selected for analysis were split into pieces ranging from 2 to 5 cm. in size using a Cutrock Engineering hydraulic splitter. Every effort was made at this stage to obtain for analysis material free of weathering and foreign material; in particular the xenolith-bearing varieties of syenite were broken into smaller pieces to ensure that xenoliths were not included. Composite specimens (i.e. layered rocks, contact specimens) were carefully separated into their component parts. Small hand specimens were put aside for the preparation of polished thin sections, should these be required.

The selected fragments of each rock were scrubbed in clean water to remove lichen and superficial deposits, any remaining paint spots and weathered surfaces having first been removed using a diamond-impregnated wheel. The clean fragments were reduced to a coarse gravel by means of a Sturtevant 2"x6" Roll Jaw Crusher. In the case of the syenites, for which the sampling of large hand specimens was desirable (Wager and Brown, 1960), the gravel was quartered representatively to obtain a volume of each suitable for further processing. In some cases $\frac{1}{2}$, 1/8 or 1/16 fractions were taken, as appropriate. In the case of syenites and lamprophyres the remainder of the rock-gravel was preserved with a view to mineral separation.

The rock-gravel, amounting to 50-150 g., was reduced to fine powder using a Tema Laboratory Disc Mill model T-100 with a tungsten carbide Widia grinding barrel. A small but representative sample of powder for the determination of FeO was withdrawn after 30 secs.

grinding for the reason given below. The rest of the powder was ground for a further 3-4 minutes, depending upon the amount of material, this period being the minimum found to give a sufficiently fine product.

The susceptibility of igneous rocks, particularly those containing ferrous layer silicates, was examined by the writer in collaboration with J.G. Fitton during the course of the work reported in this thesis. The results, which were published in Geochimica et Cosmochimica Acta, are given in the following pages.

Geochimica et Cosmochimica Acta, 1970, Vol. 34, pp. 518 to 524. Pergamon Press. Printed in Northern Ireland

The oxidation of ferrous iron in rocks during mechanical grinding

J. G. FITTON and R. C. O. GILL
Department of Geology, University of Durham, Durham, England

(*Received* 3 *November* 1969; *accepted* 3 *December* 1969)

Abstract—Experiments are described which demonstrate considerable atmospheric oxidation of ferrous iron in hydrous igneous rocks during routine grinding in a disc mill prior to chemical analysis. The causes and implications of this oxidation are discussed.

INTRODUCTION

THE SUSCEPTIBILITY of ferrous iron in rocks and minerals to non-quantitative oxidation during analysis is well established, and has received much attention from analysts over many years. The diversity of techniques by which this tendency can be suppressed has been covered in a recent review by SCHAFER (1966). In contrast, awareness among authors of the effects of sample preparation on the apparent oxidation status seems to be limited, and on the rare occasions when mention is made the reference is usually to practices accepted before mechanical methods of sample reduction became widespread.

The effect of the various methods of sample preparation on ferrous iron content is twofold:

(i) Contamination can arise from particles of metallic iron derived from milling equipment. This has only recently been examined by RITCHIE (1968). Errors become significant when comparisons are made between different laboratories and various methods, but otherwise the effect is relatively trivial.

(ii) Atmospheric oxidation of ferrous iron is possible during milling, particularly in the last stages when the powder is fine and local temperatures are high. This can be far more severe with some rocks than is commonly accepted, and the evaluation of such errors is the primary object of this note.

It has long been the practice among reputable analysts to carry out determinations of the oxidation status of a rock only on a coarsely ground (but representative) batch of fragments set aside for the purpose. This precaution can be traced back to the observation by MAUZELIUS (1907) that significant oxidation of most rocks could be brought about by very fine milling. It is interesting to note that up to this time the use of extremely fine powders had been advocated by such authorities as HILLEBRAND and WASHINGTON in the interests of the rapid solution of the material. In later publications, however, both authors adopt the cautionary tone set by MAUZELIUS (HILLEBRAND, 1908; WASHINGTON, 1919), although their recommendations differ in detail.

From the accounts given by these authors, it is clear that significant oxidation occurred only after crushing or grinding for long periods, usually much greater than half an hour. It is important to recognise that these times are not directly comparable

with milling times in modern mechanical equipment. In view of the high efficiency of modern methods, and the demand for fine powder imposed by rapid instrumental methods of analysis, there are good grounds for a review of the situation.

Technique

The mill used in these experiments was a Tema Laboratory Disc Mill model T 100 with a tungsten carbide Widia grinding barrel. The barrel was sealed with a smooth rubber gasket. The conditions were those routinely used in these laboratories, except for the method of repeated sampling described below.

All experiments were carried out on 100·0 ± 0·5 g of rock chips (less than 1 cm in size) produced by a mechanical jaw crusher. Two sampling methods were adopted. The first consisted of grinding separate 100-g samples of the same rock continuously for three and six minutes respectively. The results of this method define the broken line of Fig. 1.

The continuous line of Fig. 1 and all the data of Fig. 2 were derived by the alternative method which was designed to allow effectively free access of air and frequent sampling. In this method, the grinding process was interrupted at the intervals shown in Fig. 2 to permit the abstraction of a representative sample of approximately 1 g. The time axis of the graphs records the grinding times exclusive of sampling intervals.

All the ferrous iron measurements were obtained by the oxidising-decomposition method of Wilson (1955). The water determinations were carried out by the Riley (1958) method. For this purpose, the sample extracted after three minutes of grinding was chosen to represent each specimen, and all such samples were dried for several hours at 110°C prior to water determination.

Results

Figure 1 shows the results of experiments carried out on one rock, No. 12 in Table 1. The continuous line is the outcome of grinding interrupted at the times shown to allow sampling and the admission of fresh air. The line therefore approximates closely to the oxidation pattern in an abundant excess of air. The point

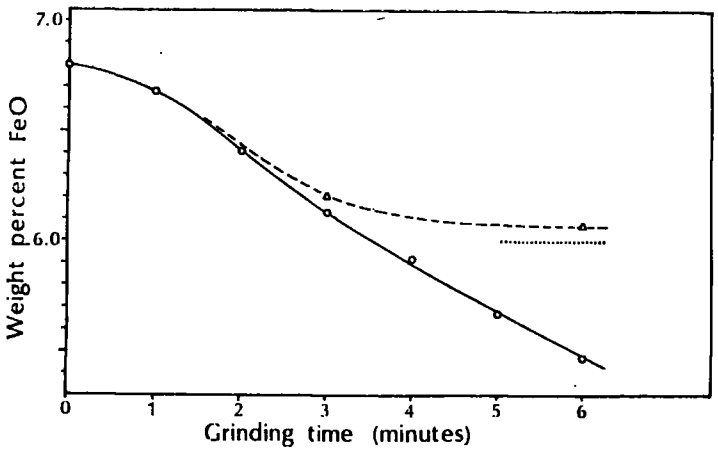

Fig. 1. The variation in FeO content with time of grinding for specimen No. 12. The unbroken line shows the result of repeated sampling as described in the text. The broken line represents experiments in which samples were ground continuously in the sealed mill for the times shown. The theoretical limit of oxidation under the latter conditions is shown by the dotted line.

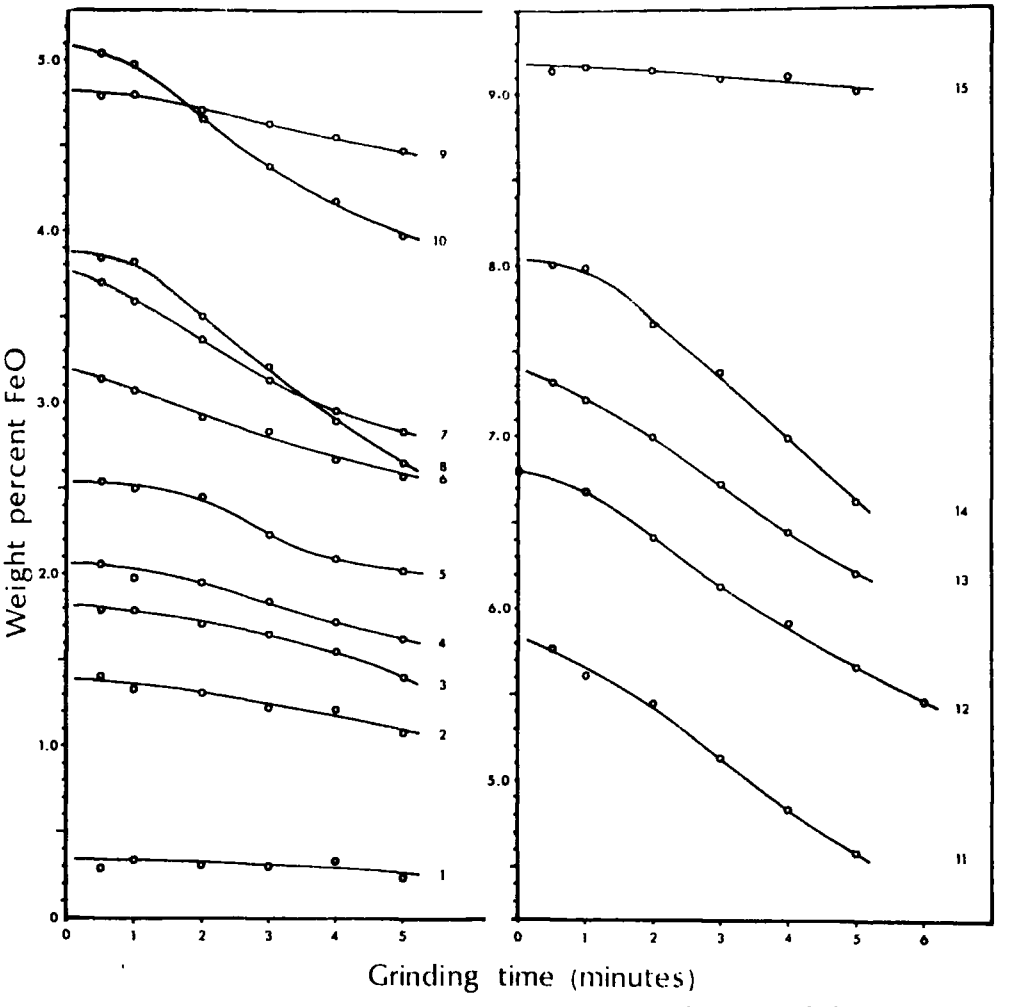

Fig. 2. "Loss curves" for the rocks described in the table. Open circles denote grinding with effectively free access of air (see text). The dark circle (rock No. 12 only) represents brief hand grinding under acetone.

appearing at zero grinding time was obtained from fragments ground briefly by hand under acetone in an agate pestle and mortar, and therefore represents the best possible estimate of the true FeO value.

Besides illustrating the degree of oxidation which can occur in circumstances which favour it, the curve has two features which are notable. The slight initial slope, which probably represents the rapid-breaking first phase of grinding during which little heat is generated, steepens into a region of maximum slope. This appears to be the upper part of a hyperbolic decay curve; the asymptotic character is more pronounced in other specimens studied.

The points shown by triangles identify two runs of continuous grinding for the times shown without admission of air beyond the amount present in the mill at the

Table 1

Specimen	Rock type	Locality	FeO-bearing mineral assemblage*	Initial % FeO (extrapolated)	% H_2O^+
1	Trachyte	S.W. Greenland	Bi	0·34	4·65
2	Granite	Aberdeen	Bi(–O)	1·39	0·70
3	Rhyodacite	Lake District	Chl–Am–O(–Gt)	1·82	1·55
4	Microsyenite	S.W. Greenland	Bi	2·06	0·80
5	Dacite tuff	Lake District	Chl–Am–O(–Gt)	2·54	1·60
6	Dacite tuff	Lake District	Chl–Am–O(–Gt)	3·20	1·95
7	Andesite tuff	Lake District	Chl–O	3·78	2·20
8	Dacite pitchstone	Lake District	Chl–O†	3·88	2·00
9	Eucrite	Ardnamurchan	Ol–Cpx–Bi	4·82	1·10
10	Andesite	Lake District	Chl–O	5·08	3·38
11	Foyaite	S.W. Greenland	Bi–Am	5·84	1·27
12	Basalt	Lake District	Chl–Cpx–O	6·80	2·90
13	Basalt tuff	Lake District	Chl–Cpx–O	7·40	3·80
14	Trachyte	S.W. Greenland	Bi–Chl–O	8·04	2·00
15	Olivine basalt	Iceland	Cpx–Ol–O	9·18	0·20

* Am = amphibole, Bi = biotite, Chl = chlorite, Cpx = clinopyroxene, Gt = garnet, O = opaque oxides, Ol = olivine.
Minerals arranged in order of abundance with minor phases in parenthesis.
† FeO is also present in the brown devitrified groundmass.

outset. Clearly the one-minute open circle also represents the result of an experiment of this type, and one can therefore draw through these three points a line (shown broken), comparable with the unbroken one, which describes the oxidation characteristic when the only air available is that defined by the volume of the milling vessel.

The divergence between the broken and unbroken curves demonstrates the limiting effect imposed by the quantity of oxygen available in the sealed milling vessel. A theoretical limit can be calculated from the known volume of the mill and this is represented by the dotted line in Fig. 1. The agreement with the declining rate of oxidation is obvious, and the oxidation is therefore undoubtedly atmospheric.

In the experiments described below, which provide the data for Fig. 2, the repeated admission of air to the mill when samples are being extracted is assumed to correspond, to all intents and purposes, to the ideal situation in which oxygen is freely available at all times. The data of Fig. 1 demonstrate that the assumption holds good for nearly all the curves. On the other hand, limitation of the oxidation in this manner can be significant at the continuous grinding times used in routine work with this equipment. This fact may find application as a means of correcting for ferrous iron loss when it is known to be large and long grinding times are used. A simple correction can be derived from the volume of the mill, the weight of rock used and the measured FeO content.

Figure 2 summarises the results of comparative experiments on fifteen rocks of widely varying composition, carried out with repeated admission of air. Comparison immediately shows a broad correlation between the amount of FeO lost and the initial ferrous iron content. This is difficult to evaluate because the loss curves are by no means linear and vary with a number of uncontrollable factors. Nevertheless some representation of susceptibility to oxidation has been attempted, and its relationship to the initial FeO content is shown in Fig. 3.

The function used is the area bounded by the loss curve in question, a horizontal line intercepting it at the five-minute stage, and the vertical axis. This area function has been found suitable on an empirical basis for the following reasons:

(i) The initial plateau present on some curves is given a low weighting in the final value. This is appropriate because it is regarded as a function only of rock hardness.

(ii) Cases of rapid but short-lived oxidation are distinguished from those in which oxidation begins late or proceeds slowly, but shows no sign of abating at five minutes. Taking simple differences in FeO values does not achieve this distinction.

(iii) Taking some slope function would only emphasise differences in the rate of reaction, which in itself is not the object of the present investigation.

Three distinct groups emerge from Fig. 3. Most of the rocks fall on a common trend running from No. 1 to No. 14. It is significant that all such rocks have chlorite or biotite as the principal ferrous iron-bearing phase. Accordingly they all contain significant amounts of combined water, but no correlation emerges beyond this qualitative one.

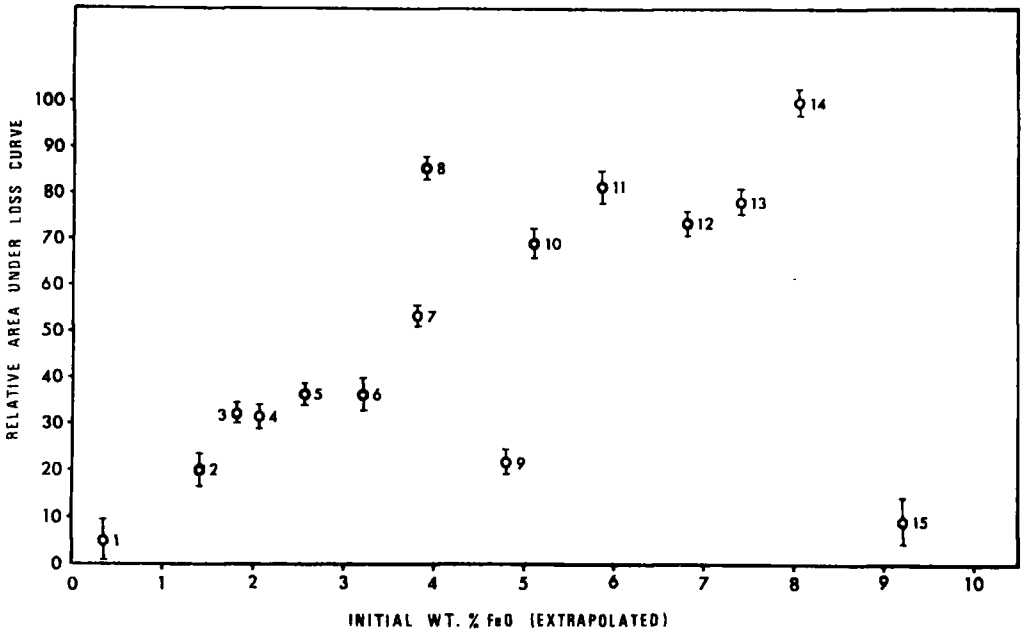

Fig. 3. Relative area under each loss curve, expressed as a percentage of the greatest (No. 14), plotted against initial weight percent FeO (extrapolated). Statistical uncertainty is shown by the vertical lines through the data points. The vertical extent is equal to twice the area of a hypothetical rectangle in Fig. 2 whose base is five minutes, and whose height is equal to the standard deviation of data points about the loss curve or the estimated analytical standard deviation, whichever is the larger.

Two rocks appear to have the power to resist oxidation on the scale shown by the main trend. This power is almost total in No. 15, an olivine basalt having no microscopically visible trace of any hydrous mineral phase. Specimen 9 is more readily oxidised but nevertheless stands apart from the main trend. In this rock, a eucrite, the ferrous iron resides mainly in fresh olivine and pyroxene, but minor biotite is also present. The intermediate position of this rock in Fig. 3 lends some weight to the influence of biotite (and, by analogy, chlorite) in determining susceptibility to oxidation.

Specimen 8, a porphyritic pitchstone containing a few small chlorite pseudomorphs after pyroxene, shows higher loss relative to initial FeO than any other rock in the experiment. In this rock, however, it is probable that a major part of the ferrous iron resides in the devitrified groundmass, conceivably in incipient chlorite. It is not unreasonable to ascribe the anomalous rate of oxidation to the extremely fine state of division of the groundmass iron-bearing phases.

The relationship between these three groups points to a pattern of oxidation strongly dependent on mineralogical constitution. This is supported by the forms of some of the loss curves which (Fig. 2, Nos. 5, 7, 10) show exponential decline towards asymptotes situated at fairly high levels of ferrous iron content. It is reasonable to suppose that such limits are determined by the proportion of minerals resistant to oxidation. It appears from the limited experiments described here that certain hydrous silicates are very susceptible to oxidation, while other minerals maintain considerable resistance to it.

Since the emphasis of this work is petrological, tests on individual minerals have not been attempted. It is nevertheless clear that a very large proportion of the ferrous iron in biotite and chlorite (and possibly some amphiboles) can become oxidised by the atmosphere during rock grinding. TZVETKOV and VALYASHIKHINA (1956) have observed oxidation in biotite with extended grinding which is brought about by structural water, but this is not the dominant mechanism for the effects described here. Simple surface oxidation is a much more likely explanation, since the potential for the generation of new surface area with grinding is clearly very great with the layer silicates. Such a model does, however, require that the sheets are reduced to an extraordinary degree of fineness in order to account for the amount of oxidation observed in these experiments. In fact a simple calculation shows that the average thickness of such sheets after a few minutes of grinding can be only one order of magnitude greater than the depth of penetration of oxidation. Very fine division of these minerals brought about by the abrasive effect of the hard silicates present can be expected in the rocks studied. Nevertheless some mechanism may exist, possibly involving exchange with hydroxyl ions, whereby oxidation can penetrate to considerable depths below the surface.

The evidence presented here clearly precludes the use of powders produced by routine disc-milling for ferrous oxide determination in a large number of cases. When ferrous oxide must be determined very accurately (for example, for the evaluation of oxidation ratios) it is essential that a sample of the rock be ground very carefully by hand, preferably in a non-oxidising medium such as acetone. During the course of these experiments it has been found that rock samples removed from the disc mill after only 30 sec of grinding are usually fine enough for complete

solution in cold hydrofluoric acid, although oxide minerals sometimes present a problem. Such samples show only slight oxidation (Fig. 2) and could well be used for routine ferrous oxide determinations on most rocks.

Acknowledgements—We are indebted to Dr. C. H. EMELEUS for providing some of the rocks used in this work, and we should like to thank Prof. G. M. BROWN for critically reading the manuscript.

REFERENCES

HILLEBRAND W. F. (1908) The influence of fine grinding on the water and ferrous-iron content of minerals and rocks. *J. Amer. Chem. Soc.* **30**, 1120–1131.

MAUZELIUS R. (1907) On the determination of ferrous iron in rock analysis. *Sverig. Geol. Unders. Arsbok.* **1**, 11 pp.

RILEY J. P. (1958) Simultaneous determination of water and carbon dioxide in rocks and minerals. *Analyst* **83**, 42–49.

RITCHIE J. A. (1968) Effect of metallic iron from grinding on ferrous iron determinations. *Geochim. Cosmochim. Acta* **32**, 1363–1366.

SCHAFER H. N. S. (1966) The determination of iron(II) oxide in silicate and refractory materials. Part I. A review. *Analyst* **91**, 755–762.

TZVETKOV A. I. and VALYASHIKHINA E. P. (1956) On the hydration and oxidation of micas. *Bull. Acad. Sci. URSS, Sér. Géol.* **5**, 74–83. (M.A. 13–396).

WASHINGTON H. S. (1919) *Manual of the Chemical Analysis of Rocks*, 3rd edition, pp. 183–184. John Wiley.

WILSON A. D. (1955) A new method for the determination of ferrous iron in rocks and minerals. *Bull. Geol. Surv. G.B.* **9**, 56–58.

APPENDIX 2

Correction for Mass-Absorption Differences in the Analysis of the Nepheline Syenites and Lamprophyres by X-ray Fluorescence Spectrometry

The X-ray fluorescence analytical procedure used in this Department is based on the use of rock-powder bricquettes, largely because of the saving in preparation time which this brings compared to fusion techniques. In most cases the analytical data are corrected for mass-absorption differences between standards and unknowns as described by Holland and Brindle (1966) and Reeves (1971). However, this correction procedure is open to criticism since, for reasons which are not entirely understood, convergence of the iterative calculation to produce realistic analyses depends to a considerable degree on normalisation of the analysis to total 100%. In addition, it is common for the relative proportions of elements to be in error to a similar degree. Tests have shown that such errors are insignificant for the phonolites and trachytes described in this work (Table A.1b), but the method is found to be inadequate when applied to the syenites and lamprophyres, among which the compositional variation is much greater. For these rocks, the analyses given have been obtained by direct comparison of the unknown with the uncorrected standard calibration, except in the case of SiO_2 where an empirical correction has been found to give the most satisfactory results. In this appendix the use of such methods is justified and some shortcomings of the Holland-Brindle method are discussed.

The matrix-correction scheme proposed by Holland and Brindle (1966) uses elemental mass-absorption coefficients calculated in the manner described by Heinrich (1966). Experimental determinations

of these coefficients are not available for many elements, but the calculated values given by Heinrich are widely regarded as acceptable, and considerable success has been achieved with electron microprobe procedures based on them (Sweatman and Long 1969). However, correction procedures in which the absorption constants are determined empirically from a wide range of standards are now more widely favoured in X-ray fluorescence spectrometry (Lucas-Tooth and Price 1961, Kodama et al. 1967, Norrish and Hutton 1969, Jenkins and de Vries 1970), although they are more often applied to fusion than to powder determination.

In the present study the need for inter-element corrections of this kind has been greatly reduced through the use of rocks of alkaline affinity as standards. The standards, which are listed at the end of this Appendix, range from alkali basalt through nepheline syenite to quartz syenite and are found to encompass the chemical variation in the analyses reported in Appendix 6 with an ample margin at each end of the range, except in the case of a very few extreme compositions. Inspection of the calibrations (counts versus weight percentage) for the major elements reveals that mass-absorption and enhancement effects are sufficiently minor to be ignored in every case except SiO_2 and Al_2O_3. With both of these elements there is found to be a dependence upon the percentage of total iron present, as is shown in Fig. A.1. That iron should be dominant in this respect is to be expected since it has the highest atomic number of the elements present in major quantities, and varies strongly in its concentration.

Correction is called for in the case of SiO_2 because of the pronounced divergence in the lower part of the calibration with

varying iron content, and because anomalous analysis totals are obtained with unknowns and standards of extreme (high or low) iron content when no correction is made. Thus 31878 with 14.20% Fe_2O_3 had a total of 102.5%, 27087 with 23.3% total Fe_2O_3 had a total of 107.5%, whereas 50272 with only 4.65% Fe_2O_3 had a total of 98.1% prior to correction. Reference to the SiO_2 calibration (Fig. A-1a) shows that standards with less than about 11% total iron oxide lie on an acceptable straight line, while the calibration line appears to suffer parallel displacement at successively higher iron contents outside this range. Correction has been carried out by placing the regression line through the specimens with less than 11% Fe_2O_3 and making a suitable correction to unknowns which do not fall within this range. Analysis totals are now found to be independent of iron content.

It will be observed that the normalised mass-absorption-corrected calibration (Fig. A.1c) appears not to be iron-dependent. This conclusion is false, however, since the concordance is brought about entirely by closure. The unnormalised calibration (Fig. A.1b) is of still poorer quality than the direct-comparison line. This dependence on closure to obtain satisfactory calibration is a characteristic failing of the Holland-Brindle method.

The uncorrected calibration for Al_2O_3, though revealing a small degree of iron-dependence, is regarded as satisfactory for present purposes. It will be seen from Fig. A.1 that the Holland-Brindle procedure severely overcorrects for this effect, giving poor results even after closure.

The Al_2O_3 contents of several lamprophyres determined by X-ray fluorescence have been confirmed by atomic absorption spectrophotometry, and those of a small sample of trachytes and phonolites by a colour-

FIGURE A,1

Calibrations for the determination of SiO_2 and Al_2O_3 in nepheline syenites and lamprophyres by X-ray fluorescence spectrometry, showing dependence on iron content.

a. SiO_2 - raw counts;

b. SiO_2 - corrected for mass absorption differences (Reeves 1971) but not normalised;

c. SiO_2 - corrected and normalised;

d. Al_2O_3 - raw counts;

e. Al_2O_3 - corrected not normalised;

f. Al_2O_3 - corrected and normalised.

Data points are ornamented to indicate the range of total iron content as follows:

Symbols	Fe_2O_3 range
△	6%
□	6-10%
◇	10-15%
○	15-17%
⚲	19%

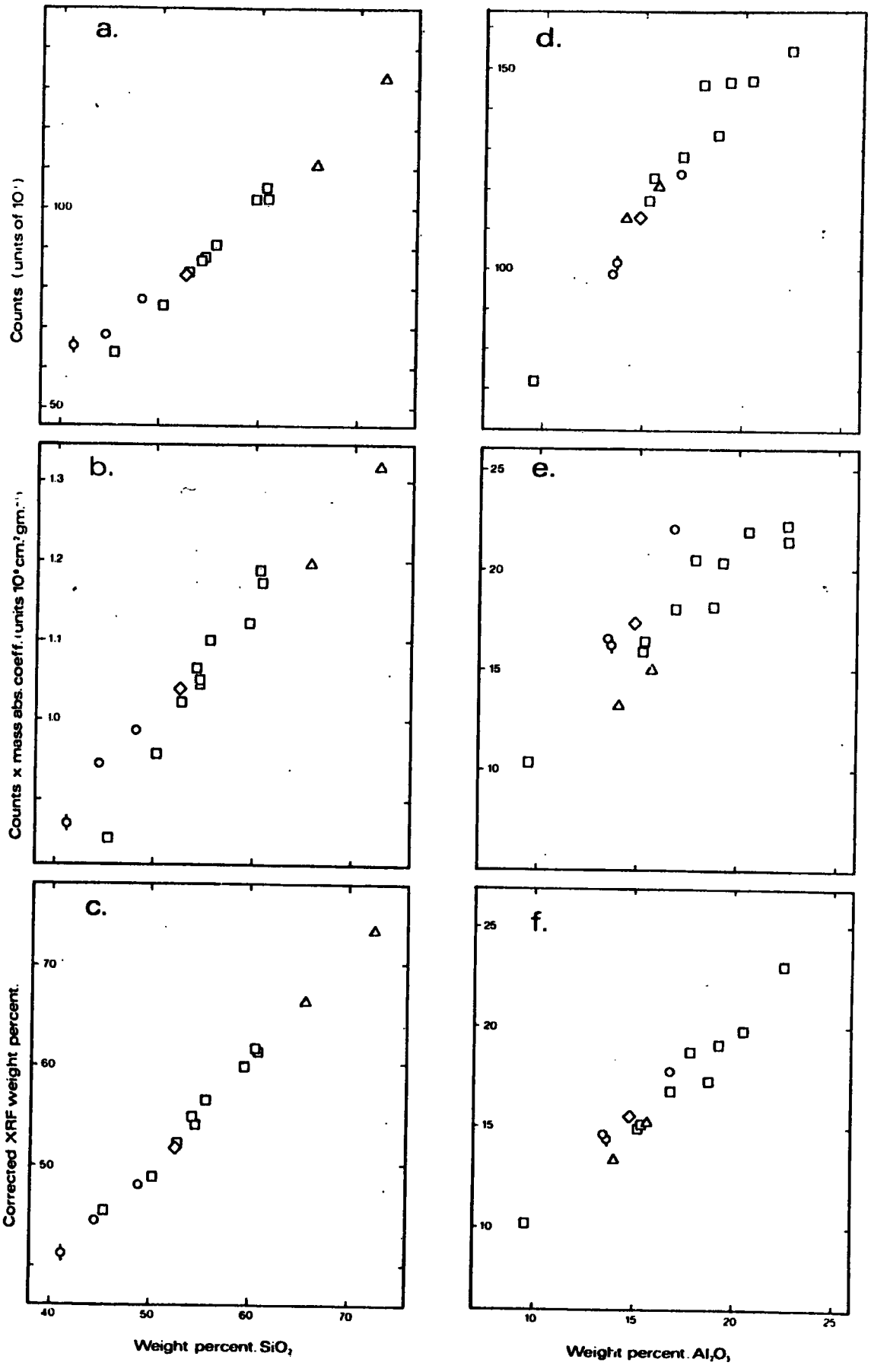
a.
b.
c.
d.
e.
f.
Counts (units of 10¹)
Counts x mass abs. coeff. (units 10⁴ cm²/gm.⁻¹)
Corrected XRF weight percent.
Weight percent. SiO₂
Weight percent. Al₂O₃

metric method.

A histogram of analysis totals for the unknowns (syenites and lamprophyres) is shown in Fig. A.2. Whilst there is significantly greater variation than would be acceptable from wet-chemical methods, and neither the mean nor the mode of the distribution coincides exactly with 100%, the results are regarded as satisfactory for the purposes considered in this thesis, particularly in view of the number of analyses presented.

Compatibility

The phonolites and trachytes on the one hand and the lamprophyres and syenites on the other have been analysed on separate occasions using the same suite of standards but different major-element correction procedures. Compatibility between the two sets of data has been assured by analysing a sample of phonolites on both occasions. The results are compared in Table A 1b, and show that the errors introduced by the Holland-Brindle method, discussed in this Appendix, prove to be insignificant for rocks with low iron content.

Table A.1a. Standards used for major element analyses of Grønnedal-Íka rocks

Standard	Type	Locality	Analysis Published
27099	Nepheline syenite	Grønnedal-Íka	Watt (1966, p.48)
27137	Nepheline syenite	Grønnedal-Íka	---- (----, p.46)
27159	Nepheline syenite	Grønnedal-Íka	---- (----, p.50)
27182	Mafic nepheline syenite	Grønnedal-Íka	---- (----, p.48)
30681	Nepheline syenite	Hviddal, Tugtutôq	---- (----, p.48)
30684	Syenogabbro	Hviddal, Tugtutôq	---- (----, p.62)
40452	Gabbro	Giant dyke Tugtutôq	---- (----, p.62)
40551	Gabbro	Krysddø syenogabbro, Tugtutôq	---- (----, p.54)
50216	Quartz syenite	Assorutit intrusion, Tugtutôq	---- (----, p.38)
50262	Quartz syenite	Ring-dyke, Tugtutôq	---- (----, p.38)
50345	Microsyenite	Unit 1, Tugtutôq	---- (----, p.38)
48004	Naujaite	Ilímaussaq	Ferguson (1964, p.56)
G-1	Granite	U.S.G.S.	Fleischer (1969)
W-1	Dolerite	U.S.G.S.	Fleischer (1969)
S-1	Syenite	C.A.A.S.	Sine et al. (1969)

Table A.1b. Comparison between major element analyses of three rocks obtained on two separate occasions. On the first occasion (A) the Holland-Brindle correction procedure was applied; the scheme described in this Appendix was followed in the second case (B).

	27058		27183		39792	
	A	B	A	B	A	B
SiO_2	54.94	53.72	53.75	53.98	54.39	53.86
TiO_2	0.04	0.06	0.52	0.66	0.00	0.02
ZrO_2	0.39	0.41	0.24	0.24	0.19	0.18
Al_2O_3	19.14	19.11	17.83	17.80	19.29	19.91
Fe_2O_3	4.64	5.51	3.83	4.16	3.28	4.03
FeO	0.25	0.25	3.60	3.60	1.70	1.70
MnO	0.32	0.28	0.26	0.23	0.27	0.24
MgO	0.17	0.05	0.55	0.62	0.16	0.00
CaO	0.63	0.89	2.55	2.39	2.03	1.99
Na_2O	11.05	11.23	7.70	7.41	8.95	9.14
K_2O	2.99	2.97	5.39	5.60	5.00	5.11
H_2O^+	4.80	4.80	2.84	2.84	4.18	4.18
P_2O_5	0.00	0.01	0.32	0.33	0.05	0.04
CO_2	0.64	0.64	0.47	0.47	0.50	0.50
Total	-	99.96	-	100.34	-	100.94

Fig. A.2

Frequency distribution of totals of analysis by correction of SiO_2 alone.

Unshaded column	nepheline syenites
Shaded column	lamprophyres

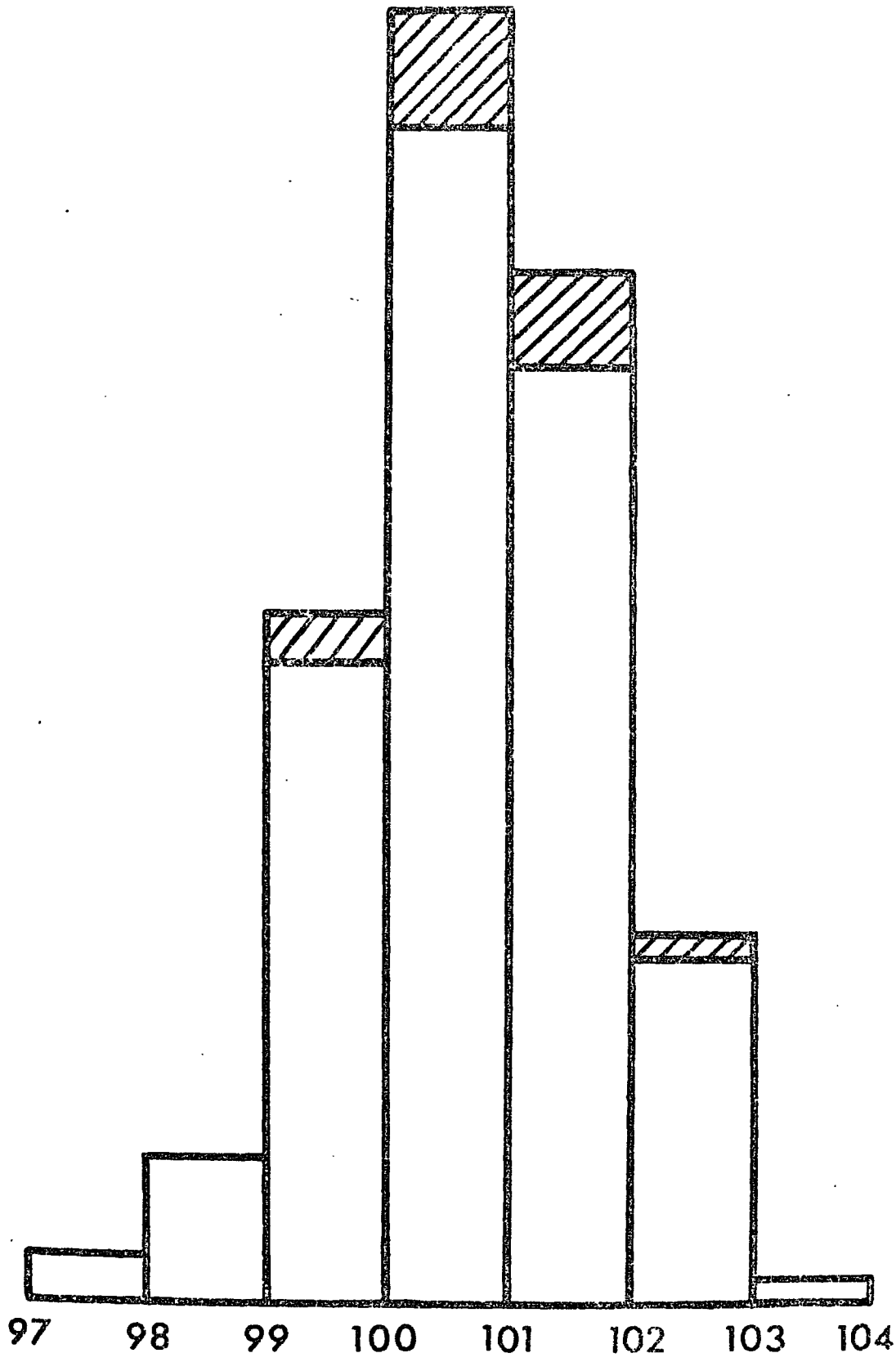
97
98
99
100
101
102
103
104

APPENDIX 3

A versatile computer programme for calculations associated with trace element determinations by X-ray fluorescence spectrometry

This programme carries out the calculations associated with routine trace element analysis by X-ray fluorescence spectrometry. The programme is designed to accept counts data as printed by a Philips PW 1212 automatic spectrometer, namely in blocks of four numbers per channel for any number of channels up to fifteen, but there should be little difficulty in modifying the read statements to accept data in other formats. In its present form the programme is written in PL-1 (IBM Programming Language 1).

For each element being determined, up to a total of fifteen, the analyst using the programme may choose between two alternative count-rate functions upon which to base his calibration. These are net peak intensity ($I_p - I_b$, in counts) and net peak counts divided by the background counts ($I_p/I_b - 1$, a dimensionless ratio). The latter function corresponds to the common practice of using scattered radiation as an internal standard. These two options may be varied freely from one element to another within one analytical programme.

The background-under-peak may be calculated from the raw data in one of three ways:

(a) it may be represented by a single satellite background reading;

(b) it may be calculated by linear interpolation from two satellite background readings* (not necessarily equidistant in two-theta from the peak position), or

*Intermediate background positions may be shared between consecutive peaks, in which case readings are supplied only once for each specimen.

(c) it may be calculated by polynomial (Newton-Gauss) interpolation from four equispaced background readings symmetrically disposed about the peak position in two-theta.

These three alternatives correspond respectively to situations in which the background is (a) level, (b) sloping linearly or (c) sloping non-linearly about the peak position. The third technique has been applied successfully to the analysis of trace amounts of copper using a LiF 200 crystal and a W target. In this case the Cu Kα peak is superimposed on the flank of a W characteristic line which produces a strongly concave background in the region of the analytical line.

Correction may be made for a blank/contamination reading and for K-beta interference from appropriate elements. The corrections are based on predetermined constants which are read before the main body of data.

The concentration of an element in p.p.m. or percent will be printed by the programme when the appropriate calibration data are supplied for that element. The concentration is calculated from the chosen corrected intensity function assuming a linear calibration. A quadratic or higher-order calibration curve may be substituted by a simple modification of the programme, but this practice is rarely necessary nor indeed advisable. Most trace element calibration curves have an extended linear portion which tails off at high concentrations, partly as a result of self-absorption. It is impossible to represent faithfully both the straight and curved portions of such a function using a single polynomial formula, and the writer believes that the simple numerical methods upon which the programme is based should be used only on the linear part of the calibration. Accordingly

three numbers are required by the programme for each element for which the concentrations are to be calculated. This need not necessarily be every element in the analytical programme. These numbers are the slope factor, as concentration units per intensity unit, the lower concentration for which the slope factor is applicable, and the upper limit, usually that at which the departure from linearity becomes unacceptable. A blank space is left in the concentration listing for every element-determination lying outside the appropriate limits; in such a case the concentration can be determined graphically.

Error messages are printed out when a number exceeds the number of digits allowed for it in the output format, or when dummy data has been substituted for counts in the input sequence. When the last data item has been processed, the programme prints a nominal detection limit for each element (that is, $3/(\bar{B}^{\frac{1}{2}})$ or $3x(\bar{B}^{\frac{1}{2}})$ depending on the intensity function used, where $\bar{B}$ is the mean background-under-peak in counts averaged over all the determinations processed. The number of analyses processed is also recorded.

Unless the calibration constants are known at the outset it is necessary to run the programme twice for a given set of data. In the first run the programme calculates the intensity functions upon which the calibration is based, the calibration constants being replaced by zeros with the result that the concentration listing is suppressed. The calculation is then repeated with calibration data supplied, when concentrations are printed out. It is useful to substitute the detection limit calculated in the first execution as the lower limit of applicability of the calibration supplied for the second run; in this way one avoids overlooking the sensitivity limit of the analytical method being used.

APPENDIX 4

A PROCEDURE FOR ELIMINATING INTERMITTENT ELECTRONIC INTERFERENCE FROM X-RAY FLUORESCENCE SPECTROMETRIC DATA

Introduction

The increasing load of electrical equipment on the power supplies to many research laboratories, and the crowded conditions within them, inevitably result in a high incidence of electrical disturbance detectable by sensitive electronic apparatus. X-ray fluorescence equipment is susceptible to interference of this kind, which may either be generated in the machine itself, for example by contaminated contacts, or be derived through the mains supply or electromagnetically from other sources. Cost factors and the intermittent nature of the disturbances often make it impracticable to track them down and achieve a complete cure immediately. In such cases the responsibility rests with the analyst to design procedures by which his results are effectively free of this interference.

This Appendix describes a procedure designed to overcome difficulties of this kind in routine X-ray fluorescence spectrometry, and gives details of the computer programme upon which the technique is based. The approach is extremely simple and the time taken in using it is only marginally greater than with conventional methods of counting. The method is discussed in terms of a fixed-time counting strategy, but is equally applicable to analyses using fixed counts.

The Method

In any intensity measurement of ionising radiation, the optimum counting time is determined by the theoretical precision required . Once this has been decided, it is conventional to count for one

period of time equal to this nominal counting time. Replicate analyses using the same counting interval are wasteful of machine and operator time, unless replication is to allow for specimen inhomogeneity in which case the repeats are carried out on separate specimen units. Where intermittent electronic interference has to be tolerated at a level which makes replication essential, the most efficient strategy is to use a shorter counting period which is repeated a fixed number of times such that the total counting time approximates to the calculated optimum counting time. Through the application of this procedure the analyst enjoys the benefit of replication while still making the most efficient use of machine time.

The procedure outlined below has been designed for use with a sequential multichannel XRF spectrometer, such as the Philips PW 1212. With this equipment, it is simpler to repeat complete cycles rather than individual counts as one would on a manual machine. The method is equally applicable to manual equipment, but the amount of operator participation is increased significantly (though not operator time). For such equipment, operators may prefer to re-design the procedure to suit their own requirements.

Suppose that an analyst has calculated that a counting time of 100 seconds is satisfactory for the determination of four elements A, B, C and D together with their backgrounds in a given series of samples, and that counting times of 10, 20, 40, 100 and 200 seconds are available with the equipment he is using. Conventional practice would be to switch to a counting time of 100 seconds, run through the sequence of measurements once and, if interference is anticipated, check the data by visual inspection. The alternative outlined here is to set the counting time to 40 seconds and to run through the

analytical cycle either two or three times.* On the Philips PW 1212 equipment this is achieved by the using the "recycle" facility. The effects of electrical disturbances are revealed as severe discrepancies between replicates, and self-consistent readings can be assumed to be free of interference. Visual inspection is replaced by computer scanning against criteria of acceptance which can be objectively defined. In the programme designed to do this, selfconsistent replicate counts are added together, thus preserving the fundamental relationship between the number of counts recorded and the theoretical precision. Data not meeting the predetermined standard of acceptance are clearly identified in the computer output, so that a repeat analysis can be carried out.

The Programme

The programme 'COMPARE', written in Programming Language 1 (PL-1), is available to carry out all the data handling requirements of the procedure outlined above. A flow chart of the programme is shown in Fig. A.3 and the data required are listed in the caption. The input procedure is designed for Philips PW 1212 data, and will require modification by users of other equipment.

Replicate determinations of the same variable are accepted by the programme if they agree with the first reading to within ten times the square-root of its value (in counts) in either direction. Consideration of the theory of counting statistics in radiation

---

*In the example chosen, it is not possible to subdivide the counting time exactly by 2 or 3. In choosing whether to use two cycles or three, there is therefore a compromise between the opposing demands of precision and machine time. In neither case are these demands affected greatly.

measurement shows that the above limits will encompass, with 99.99% confidence, the purely statistical variation about the first reading, taking it to be the mean of a large number of comparable determinations. Because the first reading differs from the mean, the actual confidence limit is lower, but will exceed 99.9%. With the counting rates considered usual in X-ray fluorescence spectrometry, even these apparently wide limits of acceptance permit rejection of quite small bursts of interference.

Accepted data are added together (giving the number of counts that would have been accumulated if the discrete counting intervals had been run continuously) and printed out. A blank is left in the output stream in place of readings outside the limits of acceptance. For these samples the separate readings, their sum and the value of $10x(\text{counts})^{\frac{1}{2}}$ are printed out at the side.

When all the data has been processed, a histogram of rejected readings as a function of channel number (PW 1212) is printed out. This provides a useful record of 2θ -dependent noise generated within the appartus, usually in the 2θ pulse-attenuator. The histogram also serves as a summary list of those specimens which need a repeat analysis and indicates for which elements this is necessary.

Application to Routine Analysis

The procedure has been used in the routine analysis of rock samples for major and trace elements, using a Philips PW 1212 spectrometer. Although extra earthed screening has been fitted to parts of this equipment to minimise aerial pick-up, quite severe spurious counting is still experienced at irregular intervals. Experience points to a number of separate sources of interference, some of it originating within the spectrometer itself. In addition, use of the

scheme has drawn attention to unsuspected intermittent errors in the printer and in the logic circuitry of the spectrometer. Only very stringent visual inspection would reveal errors of this kind.

The common belief that visual examination will bring to light nearly all instances of intermittent interference in a given set of data is founded on the assumption that the effects of individual surges in every case exceed the threshold at which they become "visible" in output. Moreover the threshold has to assume very large proportions in the peak intensities vary at all widely in the range of samples undergoing analysis. Even limited routine application of the proposed scheme has shown that by no means all instances are obvious to visual scanning; errors have quite frequently been recorded at less than 10% of the total counts. The method outlined above assumes only that errors begin at a level where acceptable random variation ceases. This level is determined by the analyst. Moreover the procedure reveals all significant disturbances no matter how much peak intensities may vary from one sample to another. In the circumstances which obtain in many analytical laboratories the amount of time spent in subdividing the predetermined counting time and repeating substandard analyses may be a small price to pay for the confidence that the analyst gains in his analyses.

FIGURE A.3 Caption

A simplified flow chart of the programme 'COMPARE' referred to in the text. The variables used are as follows:

TITLE: a character string describing the data (for user's reference).

MODE: the number of specimens per cycle (depending on whether a drift monitor is used).

REP: the number of times the analytical cycle is run through (2 or 3, depending on the factor by which the counting time is reduced).

N: the number of channels in use.

A: an array into which the counts data is fed.

P and SUM are integer variables. For simplicity, the input/output of specimen identifiers and the operation of optional punched card output have been omitted.

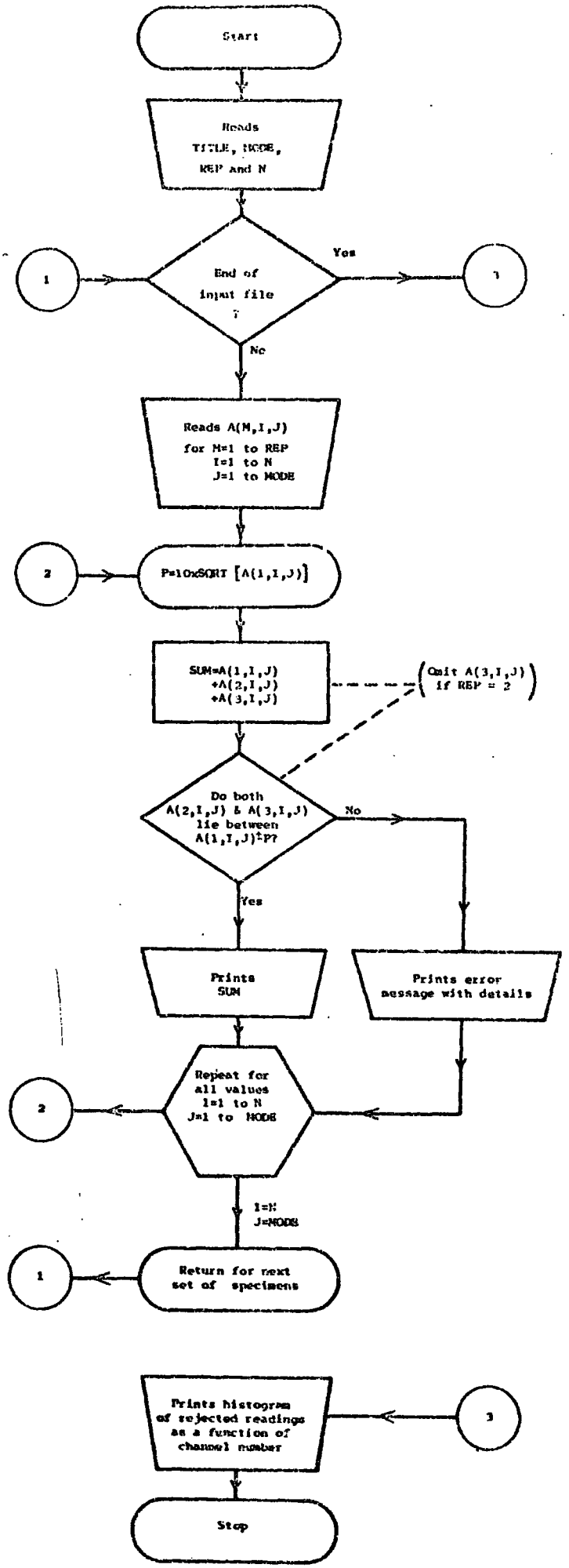
Start
Reads
TITLE, MODE,
REP and N
End of
input file
?
Yes
No
1
1
Reads A(M,I,J)
for M=1 to REP
I=1 to N
J=1 to MODE
2
P=10xSQRT [A(1,I,J)]
SUM=A(1,I,J)
+A(2,I,J)
+A(3,I,J)
Omit A(3,I,J)
if REP = 2
Do both
A(2,I,J) & A(3,I,J)
lie between
A(1,I,J)±P?
No
Yes
Prints
SUM
Prints error
message with details
Repeat for
all values
I=1 to N
J=1 to MODE
2
I=N
J=MODE
1
Return for next
set of specimens
Prints histogram
of rejected readings
as a function of
channel number
3
Stop

APPENDIX 5

ASPECTS OF FACTOR ANALYSIS RELEVANT TO THE APPLICATIONS DISCUSSED

Orthogonal and Oblique Solutions

Factor analysis is a technique for extracting the salient correlations existing in a given set of data, consisting of n observations (in the present application, chemical analyses) of v variables (element concentrations and other chemical or mineralogical parameters). R-mode factor analysis, the technique used in this work, consists of a series of matrix transformations carried out on the square matrix made up of the inter-variable correlation coefficients; this matrix is called the correlation matrix.* In geometric terms, the process may be regarded as the systematic analysis of the variance and covariance of the distribution of the data-points in v-dimensional concentration space. The factors (see Chapter 2) are represented geometrically by factor axes passing through the centroid of the point distribution. Factor analysis in these terms consists of rotating the axes to a configuration in which their relationship to the point distribution is optimised in one respect or another, and expressing each factor in terms of a linear combination of element loadings (see Chapter 2). Various solutions are obtained according to the criteria of rotation employed.

In the simplest solutions, the Principal Component and Principal Factor Solutions, the factor axes are orthogonal and the factor structure is rotated until each successive factor expresses the

---

*The alternative approach, Q-mode factor analysis, takes as its starting point the analogous matrix of inter-observation (inter-specimen) correlation coefficients.

maximum possible fraction of the total variance. The Varimax Solution (Kaiser,1958) is another orthogonal solution, but the criterion applied in this case is that the loadings on the factor axes should tend to unity or zero; in other words, the optimum solution is reached when the factor axes lie as close as possible to the major concentrations of data points in v-dimensional concentration space.

The Principal Factor Solution produces a representation of the point distribution which is often difficult to relate to physical reality (Cattell, 1965). Consequently its application in R-mode factor analysis is declining, although Le Maitre (1968) has illustrated its value as a position parameter for variation diagrams. The Varimax Solution, in recognising associations between variables, produces factors which are more readily equated with physical and chemical influences and is widely accepted as the most satisfactory orthogonal solution. If the factors are constrained to a mutually perpendicular relationship, however, there is no way in which any correlation which may exist between the physical controls can be made apparent. Consequently considerable progress has been made in recent years following the development of oblique solution methods of factor analysis. In these solutions, the orthogonality of factor axes is relaxed, and inter-factor correlation is taken into account. Oblique solutions reflect the inter-relationships among geochemical processes more accurately than orthogonal solutions (Spencer et al., 1967)

Of the various oblique solutions available, the Promax Solution (Hendrickson and White, 1964) is the simplest to compute, and this has been used for the patterns described in Chapters 2 and 5, and 6.

The aim is the achievement of maximum contrast in factor loadings in a similar manner to the Varimax Solution.

Choice of an Appropriate Promax Solution

The Promax approach to the oblique solution problem begins with the calculation of the Varimax solution described above. A series of solutions with progressively greater degrees of departure from orthogonality is calculated from the Varimax solution, each oblique solution being represented by a value of the integer k. It is assumed in the Promax approach that the object of rotation to the optimum oblique solution is to produce a factor pattern of higher contrast; that is to say, the high loadings in the Varimax solution should become higher in the oblique solution, while the small loadings are reduced. The controlled Promax rotation of the axes may be expressed, in simple terms, as raising the Varimax pattern to successively higher powers of the loadings, and allowing the axes of the oblique solution to rotate until there is a best-fit between the factor solution obtained and the Varimax-generated "ideal" pattern. The integer k is the power to which the Varimax pattern is raised.

The identification of the most appropriate of the available Promax solutions is given little attention by the authors responsible, Hendrickson and White (1964). In the present work, the "simple-structure" criterion has been applied in making this choice. As the factor axes are rotated the number of salient loadings* varies.

---

*A loading with an absolute value greater than 0.3 indicates that the factor concerned accounts for more than 10% of the variance of the variable to which the loading applies. Such a loading is referred to as "salient" or "significant". Variables whose loadings lie below this limit are regarded as making no significant contribution to the factor.

Intuitively, there is a high probability that the underlying physical influences which factor analysis is designed to identify each involve relatively few of the available variables (Cattell 1965a, p.207). If this hypothesis is correct, the best solution to take to represent a given situation is that in which the various factors each involve the smallest number of significant loadings. Thus, if one plots the number of loadings as a function of k for a given set of solutions, the point where the aggregate reaches a minimum and beyond which there is no further decline in the number of loadings indicates the preferred value of k. In practice, as shown by the example in Fig. A.4, the distribution is shallow and the minimum is ill-defined. In the absence of a more satisfactory criterion, the value k=3 has been found by this means to be most suitable for all the solutions discussed.

Representation of Solutions

The Promax pattern matrices of the several solutions discussed in Parts I and II of this thesis are tabulated, together with the inter-factor correlations and the factor scores, in Tables A.2 to A.6. Interpretation of the factor pattern is easier when the pattern matrix is shown diagrammatically. Therefore the solutions are shown in the main part of the thesis in the form of box-diagrams. These consist of a series of boxes representing the individual factors. Each box is divided into positive and negative fields, and the variable names are entered in the box in positions reflecting the relative magnitude of the loadings. Thus a variable with a strong positive loading, for example, appears at the extreme top of the positive field, whereas a weak negative loading is placed at the upper end of the negative field, near to the zero-line.

FIGURE A.4

Variation in the number of salient loadings with different factor-analytical solutions, using the Lower Series foyaites as an example. The solutions represented are the Principal Component Solution (PCS), the Varimax Solution (V) and the Promax Solution with k varying from 2 to 8 (P2, P3.....P8).

All factors except 1 and 5 have their minimum numbers of loadings at k=3 (P3).

Legend

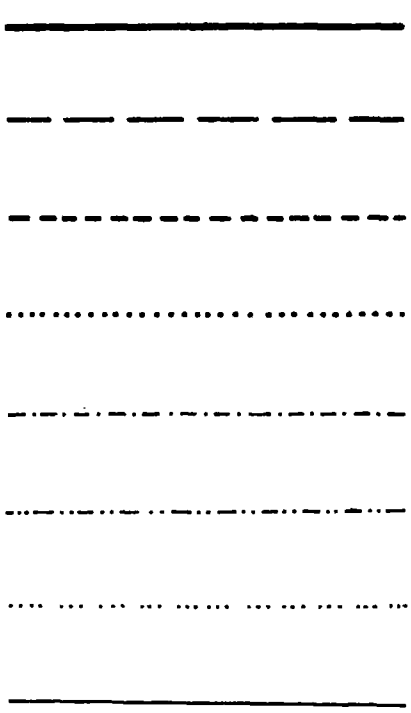

Factor 8

Factor 7

Factor 6

Factor 5

Factor 4

Factor 3

Factor 2

Factor 1

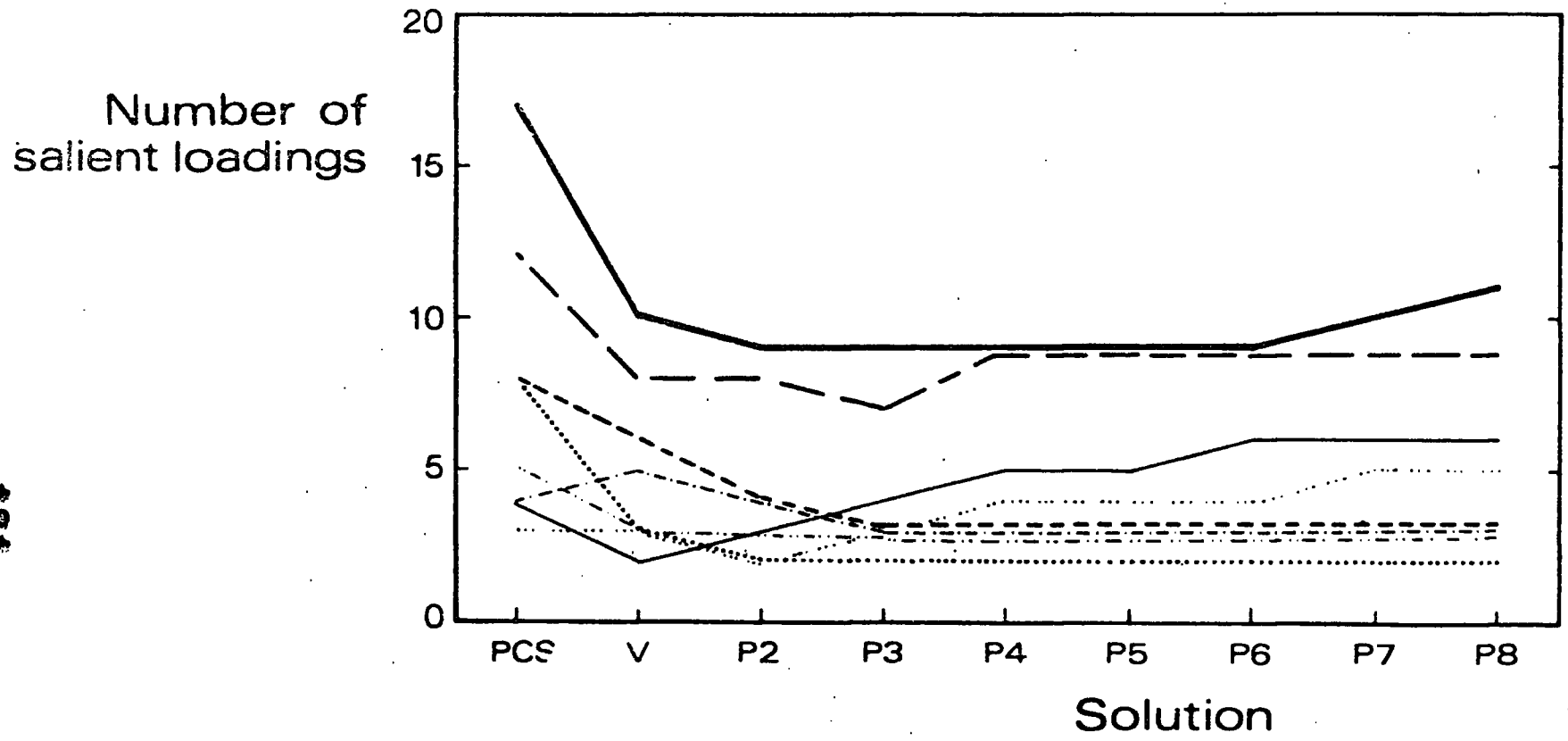
Number of
salient loadings
20
15
10
5
0
PCS
V
P2
P3
P4
P5
P6
P7
P8
Solution

Table A.2a. Promax oblique pattern matrix (k=3) for the Lower Series syenites excluding the feldspathic syenites of Group IV and the mafic syenite 27277.

	1	2	3	4	5	6	7	8
SiO_2	-0.050	0.025	-0.080	-0.010	0.173	0.211	0.922	-0.048
TiO_2	-0.191	-0.053	0.974	-0.019	-0.027	0.100	-0.019	-0.022
ZrO_2	0.367	0.031	-0.012	-0.168	0.106	-0.044	-0.084	1.056
Al_2O_3	0.033	-0.251	-0.005	-0.119	0.176	-0.057	-0.455	-0.689
Fe_2O_3	-0.031	-0.540	0.196	-0.137	0.095	0.005	-0.055	0.821
FeO	-0.065	0.496	0.249	-0.002	-0.061	-0.064	0.006	0.653
MnO	0.078	-0.044	-0.147	0.217	0.116	-0.129	-0.042	0.929
MgO	-0.259	-0.053	0.382	-0.015	-0.437	-0.097	-0.294	0.304
CaO	0.131	-0.198	-0.161	0.045	0.074	-0.064	-0.310	0.870
Na_2O	0.044	0.215	-0.074	0.048	0.003	-0.201	-0.840	-0.534
K_2O	0.089	-0.012	0.178	-0.020	0.264	0.228	0.769	-0.146
H_2O	-0.124	-0.931	0.038	0.142	-0.158	0.053	0.182	0.063
P_2O_5	0.213	0.079	0.484	0.175	0.113	0.048	-0.884	0.035
Rb	0.001	-0.037	0.166	0.117	0.109	-0.272	0.797	-0.239
Ba	0.070	0.006	0.066	0.134	-0.101	0.903	0.071	-0.196
Sr	0.068	-0.079	0.066	-0.024	-0.152	0.941	0.119	-0.136
Pb	0.762	0.130	-0.294	0.096	-0.281	0.185	-0.174	0.283
Zn	-0.167	-0.103	-0.013	0.144	-0.203	-0.293	0.168	0.574
La	-0.035	-0.143	-0.066	1.000	-0.004	0.068	-0.238	-0.078
Y	0.173	0.008	0.062	0.895	0.100	0.034	0.173	0.196
Nb	0.518	-0.055	0.113	0.020	-0.331	-0.462	0.563	-0.080
CO_2	0.329	-0.110	-0.008	-0.060	-1.135	0.168	-0.179	-0.120
% total variance	6	7	7	9	10	10	20	26

Table A.2b. Correlations between factors in the solution shown in Table A.2a.

	1	2	3	4	5	6	7	8
1	1.000							
2	0.129	1.000						
3	-0.016	0.056	1.000					
4	-0.046	-0.021	0.233	1.000				
5	0.302	-0.181	-0.217	-0.437	1.000			
6	0.110	-0.293	-0.288	-0.132	0.403	1.000		
7	-0.057	0.146	0.242	0.079	-0.010	0.000	1.000	
8	-0.303	-0.026	0.117	0.345	-0.463	-0.314	-0.199	1.000

Table A.2a. Factor Scores of the solution shown in Table A.2a.

	1	2	3	4	5	6	7	8
27090	1.257	0.148	-0.578	-0.879	1.520	0.164	0.627	-0.674
27092	-0.151	-1.422	-0.172	-0.473	0.425	2.006	0.520	0.775
27103	0.528	0.839	-0.016	-0.633	-0.202	-0.307	-1.412	-0.110
27118A	0.319	0.327	1.728	-0.057	0.491	2.234	-0.899	-0.440
27118B	0.809	0.011	-0.412	-2.142	-0.081	-1.026	-1.138	-0.597
27124	0.539	0.963	-0.961	-0.408	0.173	0.026	0.188	0.550
27126A	0.614	-0.223	0.733	-0.143	1.408	-0.213	1.188	-0.167
27126B	-0.986	-0.132	0.887	-0.007	1.704	-0.335	1.290	-0.488
27127	-2.660	0.447	1.372	-1.621	-0.755	-0.430	1.136	-1.387
27129	0.782	-0.180	-0.896	-1.560	2.019	0.929	0.439	-1.501
27130	-0.428	-1.023	-2.815	0.625	0.644	2.582	-0.772	-1.919
27159	-1.913	0.093	-0.499	0.685	-1.010	-1.556	-1.203	1.156
27202	-0.155	-0.588	0.373	0.539	-1.015	-0.127	0.488	1.518
27262	-1.804	0.646	-0.334	-0.025	-1.236	0.014	0.231	2.101
27267	-0.195	0.155	0.624	0.858	-0.852	-0.563	-1.309	1.037
27268	0.795	-0.260	0.368	0.866	0.320	-0.450	-1.176	-0.038
27272	1.572	-2.022	0.363	-0.307	-0.139	-0.322	-0.686	-0.995
39723	-0.393	-0.959	0.849	1.532	-1.024	-0.959	0.611	1.208
126703	0.528	-0.797	-0.439	0.598	-0.320	0.154	0.842	0.337
126704	-0.143	0.599	-0.157	0.424	0.989	-0.603	-1.556	0.436
126705	-0.385	-0.285	-1.356	-0.662	-0.447	0.014	-0.313	0.483
126713	1.249	0.347	1.660	2.366	-1.650	-0.531	1.432	-0.485
126714	0.219	3.316	-0.324	0.424	-0.961	-0.704	1.472	-0.799

Table A.3a. Promax oblique pattern matrix (k=3) for all upper series syenites excluding the coarse grained syenites and the sodalite-impregnated syenites 27234 and 27235.

	1	2	3	4	5
SiO_2	0.110	-0.152	0.013	0.048	-0.825
TiO_2	-0.135	0.413	0.388	0.130	0.610
ZrO_2	0.745	-0.045	0.024	-0.067	0.301
Al_2O_3	0.060	-0.056	-0.139	0.154	-0.892
Fe_2O_3	0.170	-0.266	0.194	0.050	0.884
FeO	-0.117	0.759	-0.131	-0.270	0.321
MnO	0.330	0.243	-0.017	-0.085	0.676
MgO	-0.142	0.277	0.014	0.078	0.821
CaO	0.130	0.010	-0.297	0.131	0.844
Na_2O	-0.174	-0.790	0.084	-0.407	0.088
K_2O	0.094	0.114	-0.077	0.221	-0.966
H_2O	-0.082	0.575	0.255	0.524	-0.147
P_2O_5	0.041	0.204	-0.512	0.187	0.512
CO_2	-0.121	-0.180	0.612	0.553	0.045
Rb	0.191	0.080	0.318	-0.159	-0.916
Ba	0.164	0.108	0.131	0.796	-0.202
Sr	-0.126	0.063	-0.093	0.755	0.284
Pb	0.689	0.026	0.074	0.037	-0.103
Zn	0.208	0.303	0.513	-0.121	0.473
La	0.306	0.004	-0.148	0.104	0.755
Y	0.397	-0.105	0.031	0.041	0.744
Nb	0.111	0.093	0.869	0.066	0.004
% of total variance	8	11	12	12	50

Table A.3b. Correlations between factors in the solution shown in Fig. A.3a.

	1	2	3	4	5
1.	1.000				
2.	0.088	1.000			
3.	0.060	0.172	1.000		
4.	0.078	-0.020	-0.234	1.000	
5.	0.393	0.407	-0.093	-0.109	1.000

Table A.3c. Factor scores of the solution shown in Table A.3a.

	1	2	3	4	5
27002	0.307	-0.033	0.947	-0.966	-0.214
27005	0.598	-1.977	0.762	-0.776	-0.123
27035	0.425	-0.412	0.651	-0.521	-0.396
27074	-2.134	-0.943	-0.694	2.494	-0.278
27077	-1.419	-0.037	1.795	-0.135	-0.486
27140	-1.626	-0.985	0.008	0.247	0.253
27141	-1.381	0.676	0.597	-0.631	-0.608
27142	-0.107	0.352	0.819	-0.977	0.033
27143	-3.378	-0.778	0.161	-0.247	-1.398
27154	-1.580	0.980	0.080	-1.521	-0.662
27157	-0.030	0.087	1.523	-0.643	-0.648
27158	-0.238	0.108	1.306	-0.683	-0.952
27181U	-0.323	-0.963	-1.297	1.198	-0.364
27185	0.054	-1.693	-1.459	0.555	-1.378
27194	0.709	-0.121	0.440	-0.041	-0.018
27205	0.661	-0.602	-0.953	0.075	-0.175
27207	1.245	-0.720	0.983	0.118	-0.413
27209	-0.003	0.051	0.834	-0.503	-0.659
27221	0.463	-0.878	0.310	1.908	-0.752
27227	0.559	-0.434	0.617	1.213	-0.430
27228*	-0.069	-0.817	0.376	-0.364	-0.711
39706A	-1.643	0.274	-0.506	-0.825	-0.513
39706B	-1.121	0.557	0.320	-1.245	-0.660
39736A	-2.610	-1.356	-1.075	-0.791	-1.371
39749	-0.084	0.955	0.759	-0.528	-0.489
39759	1.571	-1.670	0.374	-0.912	-0.373
58315	0.851	-1.272	0.294	0.015	-0.744
126710	0.146	-2.149	-1.233	-0.003	-1.124
126710	0.471	-0.228	-0.520	-0.542	-0.132
126727	1.578	0.711	1.229	-0.484	-0.593
27108	0.363	-0.978	-0.582	2.002	1.164
27165B	0.240	2.635	0.452	1.501	-0.635
27181L	0.250	0.497	-1.309	0.065	0.511
27182	0.276	0.373	-1.065	0.270	0.416
27186	0.070	1.685	0.153	1.765	-1.595
27192	1.175	0.492	-0.984	-0.980	0.875
27254	0.332	1.250	0.201	0.873	0.868
27261	0.280	0.265	-0.640	2.072	0.583
126711	1.383	0.115	0.911	0.665	0.907
27046	1.136	0.991	0.911	1.354	1.393
27107	0.251	0.118	-1.595	0.944	1.102
27179	-0.322	1.249	-1.028	-0.328	1.574
27181M	0.575	1.955	-0.063	-0.888	1.944
27193	0.260	0.741	2.407	-2.337	3.429
27259	0.149	0.448	-1.487	-0.488	1.324
39736B	1.103	-0.107	-2.809	-1.332	0.952
126708	0.587	1.588	-0.921	0.358	1.566

Table A.4a. Promax oblique pattern matrix (k=3) for the "felsic" syenites of the Upper Series omitting the sodalite-impregnated specimens 27234 and 27235.

	1	2	3	4	5	6	7
SiO_2	-0.777	0.210	0.165	0.136	0.181	-0.199	-0.106
TiO_2	-0.041	0.062	-0.103	0.072	0.092	0.991	-0.150
ZrO_2	0.150	0.112	-0.148	0.087	0.135	-0.267	0.934
Al_2O_3	0.332	-0.183	-0.185	0.431	0.079	-0.595	-0.360
Fe_2O_3	-0.069	0.209	-0.024	0.070	-0.374	0.083	0.822
FeO	0.061	-0.053	-0.162	-0.466	0.085	0.764	-0.260
MnO	0.006	-0.104	-0.059	-0.154	0.012	0.370	0.763
MgO	0.166	-0.069	0.032	0.053	0.070	0.977	-0.134
CaO	0.198	-0.321	-0.019	0.079	-0.398	0.034	0.637
Na_2O	0.802	0.134	0.335	-0.029	-0.020	-0.357	-0.102
K_2O	-0.740	-0.355	-0.085	0.105	0.000	-0.237	-0.193
H_2O	-0.039	0.129	-0.878	0.255	0.156	0.205	0.000
P_2O_5	0.006	-0.730	-0.046	0.072	-0.157	0.255	0.051
CO_2	0.193	0.796	-0.245	0.221	-0.105	0.219	0.062
Rb	-0.106	-0.043	-0.077	-0.385	0.806	-0.022	0.102
Ba	-0.104	0.178	-0.109	0.921	-0.061	-0.023	0.126
Sr	-0.199	-0.161	-0.475	0.649	-0.138	-0.146	-0.007
Pb	-0.030	0.021	-0.152	-0.181	0.248	-0.423	0.866
Zn	0.088	-0.058	-0.092	-0.035	0.612	0.619	0.255
La	-0.062	-0.222	0.451	0.172	0.018	0.167	0.668
Y	0.070	-0.063	0.332	0.182	0.265	0.031	0.719
Nb	-0.050	0.075	-0.071	0.172	0.744	0.508	0.022
% total variance	7	8	8	10	11	23	25

Table A.4b. Correlations between factors in the solution shown in Table A.5a.

	1	2	3	4	5	6	7
1.	1.000						
2.	-0.012	1.000					
3.	0.181	0.094	1.000				
4.	0.210	-0.075	0.068	1.000			
5.	-0.094	0.359	0.241	0.157	1.000		
6.	0.119	-0.082	-0.202	-0.125	-0.022	1.000	
7.	0.191	-0.050	0.124	0.162	0.017	0.379	1.000

Table A.4c. Factor scores of the solution shown in Table A.4a

	1	2	3	4	5	6	7
27002	-0.196	0.872	0.871	-0.606	0.208	1.096	0.848
27005	3.179	0.992	1.483	0.283	0.358	-0.507	0.833
27035	-0.292	0.951	0.590	-0.338	0.076	0.414	0.728
27074	0.100	-1.172	-1.205	2.846	-2.484	0.403	-0.765
27077	-0.595	2.010	0.443	0.637	1.028	1.075	-0.590
27140	2.960	-0.109	0.689	1.153	-1.269	1.067	-0.029
27141	-0.627	-0.470	-0.507	-0.864	0.249	0.980	-0.749
27142	0.786	0.801	-1.467	-1.824	-1.329	1.264	1.077
27143	-1.824	2.000	-0.006	-0.833	-0.490	-0.950	-2.617
27154	0.155	-1.915	-0.347	-0.930	0.819	0.559	-1.177
27157	0.356	1.224	0.059	-0.046	1.585	0.512	-0.257
27158	0.147	1.160	-0.135	-0.204	1.819	-0.107	-0.718
27181U	0.229	-0.517	-0.806	0.795	-2.258	-0.181	0.309
27185	-1.061	-0.154	-0.003	0.033	-0.526	-2.531	-0.621
27194	-0.444	-0.633	0.298	0.321	-0.167	1.133	1.329
27205	-0.172	-2.170	0.931	0.817	-0.525	0.170	0.939
27207	-0.793	-0.023	-0.133	0.393	0.700	0.028	1.233
27209	-0.097	0.278	-1.621	-0.951	0.423	-0.046	0.200
27221	-0.338	0.888	-2.242	1.174	0.423	-1.049	0.563
27227	0.099	-0.372	-0.417	1.964	0.774	0.249	0.541
27228*	1.265	-0.251	-0.120	0.199	0.755	-0.763	-0.238
39706A	-0.539	-1.715	-0.328	-0.924	-0.535	0.435	-0.602
39706B	-0.102	-1.249	-0.446	-1.434	0.594	0.328	-0.620
39736A	0.028	-0.218	0.696	-0.645	-0.381	-1.894	-2.480
39749	-1.109	0.139	-1.131	-1.005	0.074	1.156	0.485
39759	-0.517	0.426	2.926	0.168	0.945	-0.440	1.351
58315	-0.310	-0.022	1.071	0.896	0.939	-0.814	0.457
126710	-0.105	0.029	0.985	-0.088	-0.430	-2.272	-0.505
126710	-0.183	-0.780	-0.150	-0.984	-1.375	0.685	1.076

Table A.5a. Promax oblique pattern matrix (k=3) for the well-preserved phonolite dykes, omitting the potash-poor specimens 27058 and 27151.

	1	2	3	4	5	6
SiO_2	-0.047	0.273	0.376	0.421	0.327	0.434
Al_2O_3	0.136	0.298	0.122	-0.097	0.111	0.818
Fe_2O_3	-0.162	0.156	-0.907	0.169	-0.115	-0.110
FeO	-0.160	-0.019	0.638	-0.053	-0.096	-0.740
MgO	-0.163	-0.010	-0.138	-0.061	0.113	-0.926
CaO	-0.122	-0.057	-0.089	-0.045	-0.674	-0.445
Na_2O	0.120	-0.083	-0.029	0.014	0.574	0.552
K_2O	0.172	0.162	0.185	0.273	-0.684	-0.452
H_2O	-0.037	0.050	-0.056	-0.436	-0.200	0.839
CO_2	-0.042	-0.909	0.188	0.326	0.076	-0.159
TiO_2	-0.070	-0.093	0.054	-0.132	0.154	-0.895
MnO	0.053	-0.350	-0.214	0.875	0.280	-0.133
P_2O_5	-0.882	0.105	0.055	-0.188	0.004	-0.195
Ba	-0.092	0.082	0.015	-0.072	-0.020	-0.931
Nb	-0.185	-0.201	0.287	-0.093	0.438	0.649
Zr	0.042	0.016	-0.095	0.031	0.952	0.069
Y	-0.012	0.165	-0.016	-0.944	0.399	-0.149
Sr	-0.450	0.372	0.108	-0.052	-0.421	-0.280
Rb	0.824	0.314	0.254	-0.164	-0.028	0.140
Th	0.064	0.374	-0.544	-0.197	0.812	-0.230
Pb	-0.144	-0.242	0.176	-0.048	0.880	0.061
Zn	-0.237	0.180	0.121	0.074	0.592	0.594
La	-0.098	-0.103	-0.089	-0.321	-0.930	0.435
Cl	0.299	-0.252	0.350	-0.348	0.614	-0.283
% total variance	5	6	8	11	17	45

Table A.5b. Correlations between factors in the solution shown in Table A.5a.

	1	2	3	4	5	6
1.	1.000	-0.165	-0.056	-0.176	0.319	0.311
2.	-0.165	1.000	0.156	0.172	-0.154	-0.015
3.	-0.056	0.156	1.000	0.166	0.192	0.202
4.	-0.176	0.172	0.166	1.000	-0.024	-0.125
5.	0.319	-0.145	0.192	-0.024	1.000	0.305
6.	0.311	-0.015	0.202	-0.125	0.305	1.000

Table A.5c. Factor scores for the solution shown in Table A.5a.

	1	2	3	4	5	6
17007	1.038	-0.214	0.798	-0.518	0.837	0.712
27183	-0.500	0.278	0.373	0.420	-0.882	-2.364
39691	2.934	-0.903	-0.638	0.128	0.761	0.516
39731A	-0.191	-0.472	-1.012	-0.643	-0.377	-1.995
39731B	-1.347	-0.277	-0.504	0.410	0.226	-0.571
39751	-0.639	0.560	-0.032	2.492	1.237	-0.021
39762	0.205	0.463	1.512	-0.511	0.949	0.481
39794	-0.175	-1.036	0.185	-1.286	1.285	0.915
31821	-0.305	-1.480	-1.946	-1.205	-0.718	0.345
39730	0.044	0.614	-0.768	0.987	-1.167	0.604
39735A	-0.142	2.667	-0.590	-0.935	-0.890	0.285
39779	-0.150	0.381	1.144	-0.068	0.635	0.766
39792	-0.771	-0.581	1.478	0.729	-1.895	0.329

Table A.6a. Promax oblique pattern matrix (k=3) for the well-preserved and altered phonolites taken rogether. The potash-poor specimens 27058 and 27151 and a galena-bearing altered specimen 31818A have been omitted.

	1	2	3	4	5	6	7
SiO_2	0.071	-0.176	-0.116	0.007	-0.148	-0.221	0.972
Al_2O_3	-0.373	-0.098	-0.299	0.046	-0.126	-0.794	0.065
Fe_2O_3	-0.041	0.900	0.022	-0.126	-0.131	0.161	0.231
FeO	-0.004	-0.626	-0.049	-0.213	0.125	0.508	0.185
MgO	0.025	0.012	0.031	-0.189	-0.228	0.919	-0.038
CaO	0.199	0.041	0.756	-0.120	0.220	0.129	-0.276
Na_2O	-0.058	0.025	0.010	0.074	-0.021	-0.103	-0.943
K_2O	0.048	-0.042	-0.091	-0.008	0.141	0.117	0.917
H_2O	-0.168	0.003	0.019	-0.027	0.131	-0.046	-0.941
CO_2	0.994	-0.047	-0.057	0.120	0.113	0.082	0.248
TiO_2	0.129	-0.063	0.040	0.006	-0.243	0.637	0.529
MnO	0.029	-0.287	-0.281	-0.005	0.047	0.279	-0.771
P_2O_5	-0.172	-0.010	0.071	-0.919	-0.041	0.003	0.209
Ba	0.074	-0.031	0.149	-0.104	-0.111	0.435	0.700
Nb	0.256	-0.166	0.204	-0.153	-0.148	-0.878	0.103
Zr	0.160	-0.102	0.069	-0.006	-0.765	-0.242	-0.087
Y	-0.214	0.016	0.892	0.074	-0.300	0.020	0.067
Sr	-0.342	-0.218	0.156	-0.590	0.300	0.265	0.020
Rb	-0.282	-0.358	0.205	0.769	-0.020	-0.099	0.262
Th	-0.267	0.270	0.042	0.065	-0.982	0.252	0.017
Pb	0.212	-0.111	0.209	-0.057	-0.263	-0.167	-0.631
Zn	-0.103	-0.057	0.084	-0.195	-0.087	-0.350	-0.783
La	-0.027	0.204	0.234	0.090	0.473	-0.205	0.739
Cl	0.048	-0.215	0.203	0.290	-0.049	0.201	-0.839
% total variance	6	7	7	9	10	16	35

Table A.6b. Correlations between factors in the solution shown in Table A.6a.

	1	2	3	4	5	6	7
1.	1.000						
2.	-0.193	1.000					
3.	0.249	-0.027	1.000				
4.	-0.141	0.071	-0.104	1.000			
5.	-0.254	0.205	-0.189	-0.220	1.000		
6.	-0.002	0.005	-0.025	0.422	0.222	1.000	
7.	-0.172	0.035	-0.004	0.000	0.048	0.254	1.000

Table A.6c. Factor scores for the solution shown in Table A.6a. The table has been subdivided according to degree of alteration.

		1	2	3	4	5	6	7
No alteration	27007	0.350	-0.724	0.235	1.294	-0.876	-1.128	-0.785
	27183	0.176	-0.320	-0.250	-1.201	0.760	2.448	-0.182
	39691	0.502	0.369	-0.266	3.229	-0.594	-0.638	-1.132
	39731A	0.040	0.280	0.578	-0.580	-0.144	2.289	-0.348
	39731B	0.663	0.420	-0.244	-1.426	-0.304	0.754	-0.773
	39751	1.116	0.297	-1.231	-0.967	-1.102	-0.433	-1.062
	39762	0.031	-1.468	0.717	0.202	-0.848	-1.123	-0.767
	39794	0.584	-0.426	0.602	-0.049	-0.995	-1.165	-1.250
Incipient alteration	31821	0.718	2.264	0.377	-0.246	0.466	-0.436	-0.693
	39730	-0.779	1.126	-0.874	0.257	1.310	-0.230	-0.399
	39735A	-3.507	0.900	0.463	-0.128	0.807	-0.087	-0.412
	39779	0.030	-1.317	0.268	-0.251	-0.684	-1.212	-0.800
	39792	0.424	-0.614	-0.590	-0.798	3.400	-0.267	-0.441
Severe alteration	31822	0.053	1.196	0.442	-0.330	-0.312	-0.453	1.673
	31825	-0.000	1.252	1.473	0.694	-0.141	-0.384	1.582
	39689	0.437	-0.650	0.485	-0.295	0.031	0.430	0.699
	39781A	-1.835	0.243	-3.407	1.111	0.123	-0.095	1.498
	39783	0.117	-1.729	-0.309	-0.204	-0.460	0.875	1.187
	39798	0.448	-0.264	0.840	0.208	0.112	0.776	1.407
	39800	0.432	-0.836	0.690	-0.520	-0.549	0.082	1.001

APPENDIX 6 ANALYTICAL DATA

TABLE A.7

Major element analyses of nepheline syenites, phonolites, lamprophyres and trachytes from the Grønnedal-Íka alkaline complex, South Greenland, together with means, standard deviations ("S.D.") and minimum and maximum values. Analyses of specimen numbers marked with an asterisk were carried out in the laboratories of the Greenland Geological Survey in Copenhagen (Watt 1966, Borgen 1967). In the case of the well preserved phonolites and the lamprophyres, the symbol "+" is used to indicate alteration (of nepheline to gieseckite/cancrinite, and of feromagnesian minerals to chlorite respectively).

Syenites

A. Coarse-Grained Brown Syenite
B. Foyaites of the Lower Series
C. Granular Syenites
D. Feldspathic syenites from the gneiss raft
E. Upper Series syenites
F. Coarse-Grained Syenite
G. Xenolithic Porphyritic Syenite
H. Syenite Dykes

Dykes

I. Relatively fresh phonolites
J. Altered phonolites
K. Lamprophyres
L. Trachytes

A. COARSE-GRAINED BROWN SYENITE

	27123	27273	31896	MEAN	S.D.	MIN.	MAX.
SIO2	54.74	56.53	50.58	53.95	3.05	50.58	56.53
TIO2	0.11	0.16	0.10	0.12	0.03	0.10	0.16
ZRO2	0.15	0.07	0.07	0.10	0.05	0.07	0.15
AL2O3	23.80	21.35	27.86	24.34	3.29	21.35	27.86
FE2O3	3.60	5.44	1.58	3.54	1.93	1.58	5.44
FEO	2.61	1.97	1.91	2.16	0.39	1.91	2.61
MNO	0.15	0.16	0.09	0.13	0.04	0.09	0.16
MGO	0.31	0.17	0.08	0.19	0.12	0.08	0.31
CAO	0.38	0.35	0.66	0.46	0.17	0.35	0.66
NA2O	4.52	4.96	8.67	6.05	2.28	4.52	8.67
K2O	5.91	6.20	5.03	5.71	0.61	5.03	6.20
H2O+	1.81	1.61	4.26	2.56	1.48	1.61	4.26
P2O5	0.03	0.04	0.05	0.04	0.01	0.03	0.05
CO2	0.00	0.68	0.64	0.44	0.38	0.00	0.68
S	0.01	0.01	0.01	0.01	0.00	0.01	0.01
TOTAL	98.13	99.70	101.59	0.00	0.00	0.00	0.00

B. FOYAITE OF THE LOWER SERIES. GROUP I

	27103	27118A	27130	27159*	27267	27268	27272	27277A	27277M	126704	MEAN	S.D.	MIN.
SIO2	50.14	52.50	53.57	50.33	50.11	51.68	51.65	48.75	44.36	49.99	50.31	2.52	44.36
TIO2	0.12	0.30	0.06	0.15	0.14	0.13	0.14	0.17	0.24	0.12	0.16	0.07	0.06
ZRO2	0.09	0.10	0.04	0.14	0.12	0.11	0.08	0.13	0.19	0.11	0.11	0.04	0.04
AL2O3	22.33	22.18	24.21	20.49	20.03	22.23	23.05	20.46	16.61	22.00	21.36	2.10	16.61
FE2O3	3.38	3.38	2.45	4.13	4.40	3.77	4.49	5.09	7.59	3.96	4.26	1.38	2.45
FEO	2.98	2.43	0.75	3.57	4.53	2.50	0.81	5.15	8.08	3.37	3.42	2.16	0.75
MNO	0.20	0.14	0.12	0.31	0.28	0.21	0.14	0.34	0.50	0.25	0.25	0.12	0.12
MGO	0.32	0.32	0.12	0.63	0.55	0.35	0.22	0.68	1.08	0.31	0.46	0.28	0.12
CAO	2.41	1.29	1.10	3.87	3.72	2.12	1.72	4.33	6.49	2.89	2.99	1.65	1.10
NA2O	10.78	9.89	10.39	9.48	8.82	9.99	9.38	9.65	7.88	10.28	9.65	0.84	7.88
K2O	4.93	6.51	5.71	4.72	4.64	5.11	5.63	4.05	3.55	4.95	4.98	0.84	3.55
H2O+	0.72	1.05	1.60	1.23	1.25	1.25	1.63	1.14	0.80	0.84	1.15	0.31	0.72
P2O5	0.21	0.20	0.05	0.08	0.33	0.25	0.19	0.11	0.14	0.22	0.18	0.08	0.05
CO2	0.78	0.62	0.50	0.65	0.93	0.50	1.39	0.86	0.64	0.27	0.71	0.30	0.27
S	0.01	0.01	0.01	0.05	0.01	0.01	0.01	0.01	0.01	0.01	0.01	0.01	0.01
TOTAL	99.40	100.92	100.68	99.83	99.86	100.21	100.53	100.92	98.16	99.57	0.00	0.00	0.00

B. FOYAITE OF THE LOWER SERIES. GROUP I

	MAX.
SIO2	53.57
TIO2	0.30
ZRO2	0.19
AL2O3	24.21
FE2O3	7.59
FEO	8.08
MNO	0.50
MGO	1.08
CAO	6.49
NA2O	10.78
K2O	6.51
H2O+	1.63
P2O5	0.33
CO2	1.39
S	0.05
TOTAL	0.00

B. FOYAITE OF THE LOWER SERIES. GROUP II

	27124	27129	126703	126705	MEAN	S.D.	MIN.	MAX.
SIO2	54.00	55.78	55.79	53.03	54.65	1.37	53.03	55.79
TIO2	0.09	0.11	0.10	0.08	0.09	0.01	0.08	0.11
ZRO2	0.13	0.06	0.12	0.13	0.11	0.03	0.06	0.13
AL2O3	19.81	22.73	20.97	21.14	21.16	1.20	19.81	22.73
FE2O3	3.55	2.67	3.77	3.87	3.46	0.55	2.67	3.87
FEO	3.15	1.43	2.43	2.53	2.38	0.71	1.43	3.15
MNO	0.24	0.11	0.23	0.23	0.20	0.06	0.11	0.24
MGO	0.22	0.09	0.31	0.30	0.23	0.10	0.09	0.31
CAO	2.62	1.14	2.18	2.57	2.13	0.69	1.14	2.62
NA2O	8.54	9.04	7.21	9.02	8.45	0.86	7.21	9.04
K2O	5.88	6.57	6.54	5.59	6.14	0.49	5.59	6.57
H2O+	0.82	1.21	1.81	1.39	1.31	0.41	0.82	1.81
P2O5	0.06	0.05	0.05	0.06	0.05	0.01	0.05	0.06
CO2	0.57	0.17	0.75	0.89	0.59	0.31	0.17	0.89
S	0.01	0.01	0.01	0.01	0.01	0.00	0.01	0.01
TOTAL	99.69	101.17	102.27	100.84	0.00	0.00	0.00	0.00

B. FOYAITE OF THE LOWER SERIES. GROUP III

	27090	27092	27126A	27127	27202	27262	27274	39723	126713	126714	MEAN	S.D.	MIN.
SIO2	55.44	55.58	56.19	55.84	53.84	53.09	54.54	52.59	54.65	56.29	54.80	1.30	52.59
TIO2	0.10	0.13	0.18	0.24	0.18	0.13	0.16	0.20	0.22	0.11	0.16	0.05	0.10
ZRO2	0.10	0.10	0.08	0.04	0.15	0.15	0.12	0.14	0.06	0.07	0.10	0.04	0.04
AL203	22.13	21.15	20.88	21.70	18.57	17.26	19.95	19.23	19.62	19.35	19.98	1.50	17.26
FE203	3.15	5.49	4.02	2.92	5.34	5.27	5.22	5.40	2.71	1.82	4.13	1.38	1.82
FEO	1.65	2.11	2.29	2.55	4.34	5.00	2.95	3.30	3.49	3.64	3.13	1.04	1.65
MNO	0.16	0.24	0.19	0.09	0.32	0.34	0.27	0.29	0.19	0.14	0.22	0.08	0.09
MGO	0.13	0.28	0.24	0.45	0.40	0.51	0.33	0.44	0.37	0.21	0.34	0.12	0.13
CAO	1.37	2.69	1.41	0.54	3.21	3.96	2.45	2.55	1.32	0.62	2.01	1.13	0.54
NA2O	8.17	5.66	7.38	7.93	7.24	7.02	6.84	7.25	7.56	8.16	7.32	0.74	5.66
K2O	6.76	6.13	7.02	6.34	5.54	5.35	6.03	5.80	6.56	6.29	6.18	0.53	5.35
H2O+	0.90	1.76	1.25	1.18	1.96	1.15	1.10	1.98	1.55	0.39	1.32	0.50	0.39
P2O5	0.06	0.07	0.05	0.04	0.05	0.06	0.05	0.06	0.08	0.04	0.06	0.01	0.04
CO2	0.26	0.45	0.14	0.53	0.83	0.72	0.96	0.78	1.65	0.74	0.71	0.42	0.14
S	0.01	0.01	0.01	0.01	0.01	0.01	0.01	0.01	0.01	0.02	0.01	0.00	0.01
TOTAL	100.39	101.85	101.33	100.40	101.98	100.02	100.98	100.02	100.04	97.89	0.00	0.00	0.00

B. FOYAITE OF THE LOWER SERIES. GROUP III

	MAX.
SIO2	56.29
TIO2	0.24
ZRO2	0.15
AL2O3	22.13
FE2O3	5.49
FEO	5.00
MNO	0.34
MGO	0.51
CAO	3.96
NA2O	8.17
K2O	7.02
H2O+	1.98
P2O5	0.08
CO2	1.65
S	0.02
TOTAL	0.00

B. FOYAITE OF THE LOWER SERIES. GROUP IV

	27088	27133	27136	27137*	27168	27170	126706	MEAN	S.D.	MIN.	MAX.
SIO2	56.13	60.80	62.71	55.60	58.86	55.34	58.32	58.25	2.79	55.34	62.71
TIO2	0.30	0.08	0.11	0.33	0.22	0.36	0.32	0.25	0.11	0.08	0.36
ZRO2	0.02	0.01	0.02	0.01	0.11	0.06	0.03	0.04	0.04	0.01	0.11
AL2O3	20.98	21.83	20.79	18.79	20.06	19.88	19.92	20.32	0.97	18.79	21.83
FE2O3	4.69	1.93	1.72	2.06	0.76	6.48	3.09	2.96	1.99	0.76	6.48
FEO	2.14	1.23	1.47	6.27	3.75	2.50	3.93	3.04	1.76	1.23	6.27
MNO	0.17	0.04	0.06	0.20	0.05	0.14	0.18	0.12	0.07	0.04	0.20
MGO	0.31	0.03	0.02	0.49	0.29	0.52	0.48	0.31	0.21	0.02	0.52
CAO	0.65	0.44	0.43	0.10	0.01	0.02	0.55	0.31	0.27	0.01	0.65
NA2O	5.93	7.34	6.22	5.67	6.68	5.49	4.60	5.99	0.88	4.60	7.34
K2O	7.78	7.45	8.31	8.15	7.56	7.13	8.16	7.79	0.44	7.13	8.31
H2O+	1.10	0.49	0.34	1.23	1.36	1.40	1.69	1.09	0.50	0.34	1.69
P2O5	0.04	0.04	0.04	0.00	0.01	0.01	0.05	0.03	0.02	0.00	0.05
CO2	0.36	0.36	0.55	0.30	0.62	0.29	0.23	0.39	0.14	0.23	0.62
S	0.01	0.01	0.01	0.05	0.01	0.01	0.01	0.02	0.02	0.01	0.05
TOTAL	100.61	102.08	102.80	99.25	100.35	99.63	101.56	0.00	0.00	0.00	0.00

C. GRANULAR SYENITE. GS-1

	27093	27095	27C96	27122	27263	27270	27271	39725	126707	MEAN	S.D.	MIN.	MAX.
SIO2	49.79	47.94	51.94	52.95	52.71	51.78	51.70	49.82	54.70	51.48	2.02	47.94	54.70
TIO2	0.12	0.15	0.23	0.36	0.12	0.26	0.11	0.17	0.11	0.18	0.09	0.11	0.36
ZRO2	0.12	0.09	0.06	0.07	0.08	0.03	0.18	0.15	0.08	0.10	0.05	0.03	0.18
AL2O3	18.20	22.27	23.27	21.10	21.96	21.74	20.59	20.75	20.01	21.10	1.47	18.20	23.27
FE2O3	4.74	4.00	3.84	2.97	4.07	2.56	5.79	5.88	3.54	4.15	1.14	2.56	5.88
FEO	4.45	3.16	2.20	3.69	2.62	3.63	3.94	3.70	3.17	3.40	0.69	2.20	4.45
MNO	0.34	0.24	0.19	0.21	0.21	0.28	0.37	0.32	0.25	0.27	0.06	0.19	0.37
MGO	0.61	0.49	0.30	0.56	0.38	0.45	0.65	0.56	0.44	0.49	0.11	0.30	0.65
CAO	7.00	2.48	1.27	1.96	1.83	1.47	4.17	3.68	2.96	2.98	1.80	1.27	7.00
NA2O	7.18	12.16	9.51	7.22	8.76	8.38	7.94	9.20	7.10	8.61	1.60	7.10	12.16
K2O	4.72	4.11	6.11	7.05	5.31	6.48	4.21	4.42	6.39	5.42	1.11	4.11	7.05
H2O+	1.56	1.52	1.58	0.86	1.59	1.02	1.43	1.40	1.52	1.39	0.26	0.86	1.59
P2O5	2.04	0.08	0.19	0.30	0.22	0.22	0.05	0.39	0.12	0.40	0.62	0.05	2.04
CO2	0.46	1.47	0.13	0.38	0.53	0.34	0.82	1.04	1.12	0.70	0.44	0.13	1.47
S	0.01	0.01	0.01	0.01	0.01	0.01	0.01	0.01	0.01	0.01	0.00	0.01	0.01
TOTAL	101.34	100.17	100.83	99.69	100.39	98.65	101.96	101.49	101.52	0.00	0.00	0.00	0.00

C. GRANULAR SYENITE. GS-2

	27099*	27100	31898	126701	MEAN	S.D.	MIN.	MAX.
SIO2	54.57	55.07	49.93	54.10	53.42	2.36	49.93	55.07
TIO2	0.44	0.41	0.17	0.46	0.37	0.13	0.17	0.46
ZRO2	0.15	0.23	0.28	0.19	0.21	0.06	0.15	0.28
AL2O3	16.94	18.36	17.16	18.45	17.73	0.79	16.94	18.45
FE2O3	6.22	7.84	9.38	6.49	7.48	1.45	6.22	9.38
FEO	1.98	0.74	5.13	1.41	2.31	1.94	0.74	5.13
MNO	0.26	0.28	0.45	0.23	0.30	0.10	0.23	0.45
MGO	0.80	0.28	0.57	0.71	0.59	0.23	0.28	0.80
CAO	2.58	1.28	4.81	2.56	2.81	1.47	1.28	4.81
NA2O	7.48	8.19	7.27	8.20	7.78	0.48	7.27	8.20
K2O	4.90	5.61	4.10	4.98	4.90	0.62	4.10	5.61
H2O+	2.12	2.62	1.60	2.14	2.12	0.42	1.60	2.62
P2O5	0.22	0.09	0.08	0.17	0.14	0.07	0.08	0.22
CO2	0.85	0.46	0.46	0.48	0.56	0.19	0.46	0.85
S	0.05	0.01	0.01	0.01	0.02	0.02	0.01	0.05
TOTAL	99.56	101.47	101.40	100.58	0.00	0.00	0.00	0.00

D. FELDSPATHIC SYENITES FROM THE GNEISS RAFT

	27085	27087	MEAN	S.D.	MIN.	MAX.
SIO2	65.22	47.63	56.43	12.44	47.63	65.22
TIO2	0.03	0.97	0.50	0.66	0.03	0.97
ZRO2	0.02	0.12	0.07	0.07	0.02	0.12
AL2O3	19.79	14.03	16.91	4.07	14.03	19.79
FE2O3	1.82	16.57	9.19	10.43	1.82	16.57
FEO	0.21	7.88	4.04	5.42	0.21	7.88
MNO	0.04	0.40	0.22	0.25	0.04	0.40
MGO	0.00	0.19	0.09	0.13	0.00	0.19
CAO	0.46	1.75	1.10	0.91	0.46	1.75
NA2O	7.17	5.68	6.42	1.05	5.68	7.17
K2O	5.98	4.61	5.29	0.97	4.61	5.98
H2O+	0.01	0.02	0.01	0.01	0.01	0.02
P2O5	0.06	0.05	0.05	0.01	0.05	0.06
CO2	0.03	0.02	0.02	0.01	0.02	0.03
S	0.01	0.01	0.01	0.00	0.01	0.01
TOTAL	100.85	99.93	0.00	0.00	0.00	0.00

E. UPPER SERIES. 'FELSIC SYENITES'

	27002	27005	27035	27074	27077	27140	27141	27142	27143	27154	27157	27158	27181U
SIO2	54.56	51.37	55.01	52.36	55.88	51.40	54.27	51.58	57.72	54.42	54.47	54.80	54.39
TIO2	0.31	0.16	0.30	0.27	0.34	0.24	0.37	0.34	0.19	0.26	0.34	0.24	0.23
ZRO2	0.10	0.13	0.10	0.04	0.06	0.07	0.02	0.11	0.01	0.05	0.09	0.08	0.09
AL2O3	19.55	22.88	20.44	23.24	21.11	21.45	20.30	19.45	21.75	21.50	21.27	21.34	22.56
FE2O3	4.18	4.92	4.13	4.45	3.43	3.55	2.99	5.95	2.62	1.77	2.95	2.18	4.11
FEO	3.26	1.48	2.54	1.54	2.77	2.63	4.12	4.54	2.15	4.53	2.88	2.87	1.50
MNO	0.23	0.18	0.19	0.13	0.17	0.18	0.16	0.26	0.08	0.18	0.16	0.13	0.19
MGO	0.62	0.31	0.35	0.40	0.57	0.66	0.57	0.50	0.18	0.49	0.60	0.39	0.39
CAO	1.66	1.82	1.54	2.51	0.63	2.28	0.84	2.27	0.42	1.30	0.64	0.56	1.85
NA2O	8.43	11.45	8.41	7.85	7.80	10.68	7.81	8.26	7.95	8.29	8.64	8.56	8.19
K2O	5.87	4.80	5.99	7.05	5.93	4.75	6.34	5.52	6.73	6.43	5.75	5.90	5.83
H2O+	0.93	0.59	1.01	1.48	1.18	1.01	1.08	1.46	1.02	1.13	1.05	1.28	1.49
P2O5	0.06	0.07	0.07	0.25	0.04	0.22	0.22	0.07	0.04	0.21	0.06	0.05	0.25
CO2	0.50	0.85	0.61	0.52	1.06	0.77	0.41	0.60	0.65	0.17	0.65	0.54	0.49
S	0.01	0.01	0.01	0.01	0.01	0.01	0.01	0.01	0.01	0.01	0.01	0.01	0.01
TOTAL	100.27	101.02	100.70	102.10	100.98	99.90	99.51	100.92	101.52	100.74	99.56	98.93	101.57

E. UPPER SERIES. 'FELSIC SYENITES'

	27185	27194	27205	27207	27209	27221	27227	27228	27234	27235	39705	39706A	39706B
SIO2	56.17	54.05	54.26	55.35	54.49	55.18	54.83	52.72	52.93	52.62	53.90	53.53	53.11
TIO2	0.08	0.32	0.22	0.18	0.22	0.14	0.27	0.21	0.19	0.21	0.19	0.24	0.26
ZRO2	0.07	0.11	0.08	0.16	0.11	0.14	0.10	0.07	0.06	0.04	0.08	0.04	0.02
AL2O3	22.55	20.37	21.54	21.01	21.53	22.20	22.35	23.39	22.78	21.90	21.95	21.49	21.12
FE2O3	2.53	5.46	4.79	5.09	4.44	4.25	3.68	3.28	1.92	2.34	4.35	3.46	2.93
FEO	1.18	2.57	1.82	1.56	2.38	1.44	1.71	1.54	1.65	1.71	1.87	2.88	4.11
MNO	0.11	0.26	0.20	0.24	0.18	0.17	0.18	0.14	0.10	0.11	0.17	0.16	0.16
MGO	0.08	0.50	0.44	0.25	0.34	0.22	0.42	0.30	0.17	0.20	0.28	0.48	0.34
CAO	1.07	2.05	2.24	1.69	1.23	1.38	1.64	1.21	0.85	0.95	1.80	1.41	1.00
NA2O	8.59	7.65	8.23	7.71	7.86	8.06	8.17	9.44	11.55	11.37	8.50	7.46	7.94
K2O	7.08	6.17	6.17	6.49	6.06	6.10	6.13	6.12	5.25	5.32	6.08	6.75	6.28
H2O+	0.92	0.88	0.80	1.00	1.76	2.52	1.46	1.15	1.37	1.49	0.94	1.17	0.95
P2O5	0.09	0.20	0.24	0.18	0.13	0.04	0.17	0.09	0.04	0.05	0.22	0.23	0.19
CO2	0.31	0.43	0.12	0.62	0.52	0.65	0.54	0.41	1.24	1.73	0.14	0.23	0.27
S	0.01	0.01	0.01	0.01	0.01	0.01	0.01	0.01	0.01	0.01	0.01	0.01	0.01
TOTAL	100.84	101.03	101.16	101.54	101.26	102.50	101.66	100.08	100.11	100.05	100.48	99.54	98.69

E. UPPER SERIES. 'FELSIC SYENITES'

	39736A	39749	39759	58315	126710	126710	126727	MEAN	S.D.	MIN.	MAX.
SIO2	55.53	55.14	55.82	55.60	54.89	53.28	55.30	54.27	1.45	51.37	57.72
TIO2	0.10	0.32	0.14	0.18	0.09	0.23	0.49	0.24	0.09	0.08	0.49
ZRO2	0.02	0.07	0.13	0.10	0.08	0.13	0.17	0.08	0.04	0.01	0.17
AL2O3	23.35	20.05	20.19	21.95	23.09	19.95	21.70	21.55	1.10	19.45	23.39
FE2O3	2.08	3.88	4.59	4.30	2.85	5.10	5.86	3.77	1.14	1.77	5.95
FEO	1.49	4.00	1.22	0.99	1.11	3.04	2.18	2.34	1.03	0.99	4.54
MNO	0.09	0.23	0.20	0.16	0.12	0.25	0.26	0.17	0.05	0.08	0.26
MGO	0.20	0.54	0.27	0.24	0.13	0.50	0.21	0.37	0.16	0.08	0.66
CAO	0.77	1.32	1.54	1.23	1.00	2.32	0.98	1.39	0.57	0.42	2.51
NA2O	9.58	6.90	8.98	8.59	9.27	7.84	5.91	8.54	1.24	5.91	11.55
K2O	6.42	6.15	6.04	6.03	6.70	6.10	6.11	6.07	0.53	4.75	7.08
H2O+	0.62	1.85	0.44	0.95	0.47	0.73	2.04	1.16	0.45	0.44	2.52
P2O5	0.06	0.15	0.06	0.10	0.09	0.22	0.04	0.13	0.08	0.04	0.25
CO2	0.19	0.52	0.31	0.24	0.42	0.35	0.26	0.52	0.33	0.12	1.73
S	0.01	0.01	0.01	0.01	0.01	0.01	0.01	0.01	0.00	0.01	0.01
TOTAL	100.51	101.13	99.94	100.67	100.32	100.05	101.52	0.00	0.00	0.00	0.00

E. UPPER SERIES. 'LESS MAFIC SYENITES'

	27108	27165B	27181L	27182*	27186	27192	27254	27261	126711	MEAN	S.D.	MIN.	MAX.
SIO2	51.37	53.70	52.30	52.80	52.26	51.08	51.32	52.74	52.61	52.24	0.85	51.08	53.70
TIO2	0.35	0.40	0.37	0.25	0.15	0.33	0.73	0.27	0.27	0.35	0.16	0.15	0.73
ZRO2	0.08	0.08	0.14	0.11	0.05	0.14	0.10	0.08	0.20	0.11	0.05	0.05	0.20
AL203	18.09	18.90	19.90	17.92	27.25	18.23	17.62	19.08	18.13	19.46	3.01	17.62	27.25
FE203	7.59	1.90	6.17	4.60	1.41	4.59	5.15	5.51	8.59	5.06	2.35	1.41	8.59
FEO	1.49	6.73	3.81	3.55	3.69	5.04	5.27	2.60	2.72	3.88	1.59	1.49	6.73
MNO	0.28	0.19	0.33	0.25	0.17	0.33	0.28	0.27	0.40	0.28	0.07	0.17	0.40
MGO	1.26	0.98	0.84	0.79	0.14	0.80	1.23	1.06	0.65	0.86	0.34	0.14	1.26
CAO	6.25	1.22	3.82	4.32	0.92	4.63	4.35	5.08	3.85	3.83	1.73	0.92	6.25
NA2O	6.40	3.40	7.10	6.98	3.80	7.90	6.28	5.45	6.09	5.93	1.50	3.40	7.90
K2O	5.19	6.71	4.92	5.62	7.89	5.23	5.09	5.52	5.23	5.71	0.97	4.92	7.89
H2O+	0.99	2.40	1.60	1.36	2.46	0.62	1.65	1.96	1.55	1.62	0.60	0.62	2.46
P2O5	1.25	0.07	0.45	0.60	0.06	0.86	1.11	1.03	0.57	0.67	0.43	0.06	1.25
CO2	1.41	0.68	0.19	0.30	0.65	0.08	0.44	0.95	0.95	0.63	0.43	0.08	1.41
S	0.01	0.01	0.01	0.03	0.01	0.01	0.01	0.01	0.01	0.01	0.01	0.01	0.03
TOTAL	102.01	97.37	101.95	99.48	100.91	99.87	100.63	101.61	101.82	0.00	0.00	0.00	0.00

E. UPPER SERIES. 'MAFIC SYENITES'

	27046	27107	27179	27181M	27193	27259	39736B	126708	MEAN	S.D.	MIN.	MAX.
SIO2	50.77	50.91	49.40	42.79	43.56	49.38	52.08	48.10	48.38	3.43	42.79	52.08
TIO2	0.84	0.35	0.45	0.91	0.88	0.27	0.12	0.46	0.53	0.30	0.12	0.91
ZRO2	0.13	0.08	0.15	0.23	0.22	0.11	0.20	0.13	0.16	0.05	0.08	0.23
AL2O3	15.38	17.80	15.84	14.64	8.63	17.27	16.88	17.08	15.44	2.95	8.63	17.80
FE2O3	7.18	4.33	6.20	13.02	14.63	4.39	4.75	7.76	7.78	3.96	4.33	14.63
FEO	4.66	4.36	6.31	6.84	9.50	6.28	5.59	5.99	6.19	1.58	4.36	9.50
MNO	0.38	0.27	0.41	0.56	0.75	0.35	0.35	0.41	0.43	0.15	0.27	0.75
MGO	1.69	1.21	1.28	1.68	2.21	1.18	0.97	1.32	1.44	0.40	0.97	2.21
CAO	6.02	6.70	7.09	5.96	8.82	7.02	6.68	8.23	7.06	1.00	5.96	8.82
NA2O	5.94	6.34	6.61	5.36	7.57	7.57	7.73	4.60	6.46	1.14	4.60	7.73
K2O	5.17	5.03	4.01	3.57	2.04	3.88	4.20	3.89	3.97	0.96	2.04	5.17
H2O+	1.13	0.70	1.88	1.64	0.78	1.03	0.40	1.70	1.16	0.53	0.40	1.88
P2O5	1.60	1.66	1.18	0.88	0.04	1.49	1.10	1.56	1.19	0.54	0.04	1.66
CO2	0.98	0.35	0.15	0.15	0.36	0.28	0.06	0.24	0.32	0.29	0.06	0.98
S	0.01	0.01	0.01	0.01	0.01	0.01	0.01	0.01	0.01	0.00	0.01	0.01
TOTAL	101.88	100.10	100.97	98.24	100.00	100.51	101.12	101.48	0.00	0.00	0.00	0.00

F. COARSE-GRAINED SYENITE

	27065	27067	27114	27280	27285	27287	126721	MEAN	S.D.	MIN.	MAX.
SIO2	49.74	50.71	51.89	48.26	48.93	50.58	49.26	49.91	1.24	48.26	51.89
TIO2	0.12	0.31	0.28	0.42	0.22	0.16	0.33	0.26	0.10	0.12	0.42
ZRO2	0.07	0.06	0.09	0.08	0.08	0.12	0.10	0.09	0.02	0.06	0.12
AL2O3	20.33	20.90	20.30	16.24	23.61	23.56	21.15	20.87	2.48	16.24	23.61
FE2O3	3.59	5.36	4.38	5.04	3.30	2.36	4.68	4.10	1.06	2.36	5.36
FEO	2.83	1.30	3.10	4.03	1.64	1.65	2.46	2.43	0.97	1.30	4.03
MNO	0.36	0.25	0.24	0.39	0.15	0.15	0.24	0.25	0.09	0.15	0.39
MGO	0.64	0.57	0.92	1.45	0.26	0.40	0.91	0.74	0.40	0.26	1.45
CAO	4.36	3.62	4.64	6.42	1.54	1.90	3.40	3.70	1.67	1.54	6.42
NA2O	10.31	9.00	7.11	7.05	14.70	11.45	9.16	9.83	2.67	7.05	14.70
K2O	5.21	5.17	5.15	5.02	2.03	5.69	5.22	4.78	1.23	2.03	5.69
H2O+	1.97	1.14	0.71	1.03	1.66	2.24	0.90	1.38	0.58	0.71	2.24
P2O5	0.15	0.64	0.87	1.26	0.08	0.22	0.78	0.57	0.44	0.08	1.26
CO2	1.97	2.18	1.25	2.11	1.50	1.78	0.82	1.66	0.50	0.82	2.18
S	0.01	0.01	0.01	0.01	0.01	0.01	0.01	0.01	0.00	0.01	0.01
TOTAL	101.66	101.22	100.94	98.81	99.71	102.27	99.42	0.00	0.00	0.00	0.00

G. XENOLITHIC PORPHYRITIC SYENITE

	27189	31841	31846	31854	58314	58316	58317	58320	MEAN	S.D.	MIN.	MAX.
SIO2	52.71	54.02	52.83	51.46	55.76	54.19	52.61	53.28	53.36	1.30	51.46	55.76
TIO2	0.20	0.19	0.19	0.41	0.19	0.29	0.23	0.23	0.24	0.08	0.19	0.41
ZRO2	0.23	0.22	0.20	0.16	0.16	0.15	0.21	0.19	0.19	0.03	0.15	0.23
AL2O3	18.30	19.39	18.91	18.94	19.87	20.96	20.58	19.64	19.57	0.89	18.30	20.96
FE2O3	8.14	6.39	7.13	6.15	5.88	4.25	6.64	6.09	6.33	1.11	4.25	8.14
FEO	0.66	1.26	0.40	2.09	2.71	1.61	1.59	1.54	1.48	0.74	0.40	2.71
MNO	0.28	0.30	0.28	0.30	0.20	0.18	0.25	0.27	0.26	0.04	0.18	0.30
MGO	0.30	0.53	0.43	0.76	0.35	0.59	0.38	0.44	0.47	0.15	0.30	0.76
CAO	4.04	4.32	3.48	3.06	2.31	2.27	3.12	2.65	3.16	0.76	2.27	4.32
NA2O	8.22	6.95	9.83	9.97	7.55	8.97	8.51	8.56	8.57	1.04	6.95	9.97
K2O	4.42	5.29	4.85	4.74	5.27	5.24	4.87	5.19	4.98	0.31	4.42	5.29
H2O+	1.51	1.88	1.20	1.93	1.54	1.89	1.99	1.64	1.70	0.27	1.20	1.99
P2O5	0.40	0.46	0.23	0.24	0.07	0.14	0.32	0.30	0.27	0.13	0.07	0.46
CO2	2.58	2.44	2.45	2.51	0.92	0.32	1.16	0.97	1.67	0.92	0.32	2.58
S	0.01	0.01	0.01	0.01	0.01	0.01	0.01	0.01	0.01	0.00	0.01	0.01
TOTAL	102.00	103.65	102.42	102.73	102.79	101.06	102.47	101.00	0.00	0.00	0.00	0.00

H. SYENITE AND MICROSYENITE DYKES - GROUP 1

	27119	27128	27178	27200	39711	126712	MEAN	S.D.	MIN.	MAX.
SIO2	53.37	54.45	53.52	53.54	53.94	54.53	53.89	0.51	53.37	54.53
TIO2	0.20	0.16	0.17	0.25	0.26	0.20	0.21	0.04	0.16	0.26
ZRO2	0.02	0.01	0.04	0.07	0.04	0.02	0.03	0.02	0.01	0.07
AL203	22.02	23.79	23.56	20.27	22.55	22.52	22.45	1.26	20.27	23.79
FE203	1.46	2.76	3.67	4.07	6.11	3.04	3.52	1.55	1.46	6.11
FEO	4.37	2.49	1.32	3.50	1.60	1.90	2.53	1.19	1.32	4.37
MNO	0.13	0.14	0.12	0.22	0.22	0.12	0.16	0.05	0.12	0.22
MGO	0.36	0.31	0.26	0.45	0.41	0.29	0.35	0.07	0.26	0.45
CAO	1.52	1.47	1.09	1.40	1.48	1.16	1.35	0.18	1.09	1.52
NA2O	8.22	7.88	8.99	8.91	7.14	8.08	8.20	0.69	7.14	8.99
K2O	7.16	6.28	6.20	6.26	6.20	6.75	6.47	0.40	6.20	7.16
H2O+	0.61	1.28	0.78	0.70	1.23	1.14	0.96	0.29	0.61	1.28
P2O5	0.20	0.18	0.18	0.18	0.23	0.14	0.18	0.03	0.14	0.23
CO2	0.34	0.61	0.09	0.25	0.19	0.16	0.27	0.19	0.09	0.61
S	0.01	0.01	0.01	0.01	0.01	0.01	0.01	0.00	0.01	0.01
TOTAL	99.99	101.82	100.00	100.08	101.61	100.06	0.00	0.00	0.00	0.00

H. SYENITE AND MICROSYENITE DYKES - GROUP 2

	27086	27173	27275	39710	MEAN	S.D.	MIN.	MAX.
SIO2	54.97	53.59	55.58	51.02	53.79	2.03	51.02	55.58
TIO2	0.33	0.24	0.16	0.16	0.22	0.08	0.16	0.33
ZRO2	0.02	0.02	0.08	0.35	0.12	0.16	0.02	0.35
AL2O3	20.68	22.02	20.87	20.18	20.94	0.78	20.18	22.02
FE2O3	2.74	3.40	4.51	6.86	4.38	1.81	2.74	6.86
FEO	3.94	2.71	3.03	3.60	3.32	0.55	2.71	3.94
MNO	0.16	0.14	0.18	0.25	0.18	0.05	0.14	0.25
MGO	0.49	0.39	0.28	0.26	0.35	0.11	0.26	0.49
CAO	1.58	1.36	2.00	2.60	1.88	0.55	1.36	2.60
NA2O	7.94	7.90	8.58	10.66	8.77	1.30	7.90	10.66
K2O	5.82	6.61	4.92	4.29	5.41	1.02	4.29	6.61
H2O+	0.50	0.74	0.86	0.15	0.56	0.31	0.15	0.86
P2O5	0.22	0.20	0.05	0.01	0.12	0.11	0.01	0.22
CO2	0.15	0.31	0.16	0.17	0.20	0.08	0.15	0.31
S	0.01	0.01	0.01	0.01	0.01	0.00	0.01	0.01
TOTAL	99.55	99.64	101.27	100.57	0.00	0.00	0.00	0.00

H. SYENITE AND MICROSYENITE DYKES - GROUP 3

	31803	39740	39753A	39753B	MEAN	S.D.	MIN.	MAX.
SIO2	54.99	56.27	54.95	54.44	55.16	0.78	54.44	56.27
TIO2	0.15	0.17	0.36	0.35	0.26	0.11	0.15	0.36
ZRO2	0.21	0.16	0.05	0.04	0.11	0.08	0.04	0.21
AL2O3	18.96	18.85	20.88	21.64	20.08	1.40	18.85	21.64
FE2O3	7.15	5.95	3.32	2.76	4.79	2.10	2.76	7.15
FEO	1.30	2.60	3.90	3.25	2.76	1.11	1.30	3.90
MNO	0.27	0.29	0.19	0.17	0.23	0.06	0.17	0.29
MGO	0.34	0.33	0.49	0.54	0.42	0.11	0.33	0.54
CAO	0.98	1.06	1.31	1.44	1.20	0.21	0.98	1.44
NA2O	8.75	7.75	6.97	8.00	7.87	0.73	6.97	8.75
K2O	5.76	5.60	7.15	6.87	6.34	0.78	5.60	7.15
H2O+	0.62	0.80	0.89	0.42	0.68	0.21	0.42	0.89
P2O5	0.09	0.10	0.21	0.23	0.16	0.07	0.09	0.23
CO2	0.44	0.07	0.24	0.00	0.19	0.20	0.00	0.44
S	0.00	0.01	0.01	0.01	0.01	0.00	0.00	0.01
TOTAL	100.01	100.01	100.92	100.16	0.00	0.00	0.00	0.00

H. SYENITE AND MICROSYENITE DYKES - GROUP 4

	27068	27082	27156	39742	39777	58318	126715	MEAN	S.D.	MIN.	MAX.
SIO2	52.48	55.04	54.26	54.02	53.96	50.12	52.55	53.20	1.65	50.12	55.04
TIO2	0.28	0.30	0.24	0.24	0.40	0.12	0.37	0.28	0.09	0.12	0.40
ZRO2	0.04	0.10	0.14	0.07	0.06	0.07	0.15	0.09	0.04	0.04	0.15
AL2O3	21.99	22.15	19.37	20.28	21.04	19.10	19.48	20.49	1.26	19.10	22.15
FE2O3	3.52	4.05	4.33	4.70	2.71	4.86	6.17	4.33	1.09	2.71	6.17
FEO	1.79	2.13	4.25	3.45	1.98	1.88	1.38	2.41	1.04	1.38	4.25
MNO	0.14	0.21	0.25	0.22	0.11	0.38	0.23	0.22	0.09	0.11	0.38
MGO	0.43	0.27	0.38	0.45	0.53	0.83	0.53	0.49	0.18	0.27	0.83
CAO	2.35	1.25	1.90	1.82	2.32	5.45	2.84	2.56	1.37	1.25	5.45
NA2O	8.03	8.15	7.97	7.42	7.95	9.02	7.91	8.06	0.48	7.42	9.02
K2O	7.70	6.26	6.04	6.53	6.09	5.61	5.41	6.23	0.75	5.41	7.70
H2O+	1.01	0.49	0.60	1.20	2.32	1.90	3.11	1.52	0.96	0.49	3.11
P2O5	0.33	0.12	0.08	0.23	0.25	0.28	0.24	0.22	0.09	0.08	0.33
CO2	0.99	0.22	0.52	0.21	1.47	2.77	2.27	1.21	1.01	0.21	2.77
S	0.01	0.01	0.01	0.01	0.01	0.01	0.02	0.01	0.00	0.01	0.02
TOTAL	101.09	100.75	100.34	100.85	101.20	102.40	102.66	0.00	0.00	0.00	0.00

H. SYENITE AND MICROSYENITE DYKES - GROUP 5

	39770	39771	MEAN	S.D.	MIN.	MAX.
SIO2	53.75	54.49	54.12	0.52	53.75	54.49
TIO2	0.41	0.24	0.32	0.12	0.24	0.41
ZRO2	0.02	0.11	0.06	0.06	0.02	0.11
AL2O3	20.79	21.36	21.07	0.40	20.79	21.36
FE2O3	2.15	5.43	3.79	2.32	2.15	5.43
FEO	3.85	2.25	3.05	1.13	2.25	3.85
MNO	0.14	0.23	0.18	0.06	0.14	0.23
MGO	0.67	0.42	0.54	0.18	0.42	0.67
CAO	1.39	1.54	1.46	0.11	1.39	1.54
NA2O	7.77	8.04	7.90	0.19	7.77	8.04
K2O	6.60	5.73	6.16	0.62	5.73	6.60
H2O+	0.92	0.70	0.81	0.16	0.70	0.92
P2O5	0.21	0.22	0.21	0.01	0.21	0.22
CO2	0.75	0.19	0.47	0.40	0.19	0.75
S	0.01	0.01	0.01	0.00	0.01	0.01
TOTAL	99.43	100.96	0.00	0.00	0.00	0.00

I. WELL PRESERVED PHONOLITE DYKES.

	27007	27058	27151	27183	31821+	39691	39730+	39731A	39731B	39735+	39751	39762	39779+
SIO2	55.25	54.94	55.79	53.75	53.30	54.03	54.64	53.06	54.16	54.18	55.54	55.21	54.95
TIO2	0.00	0.04	0.02	0.52	0.01	0.00	0.00	0.48	0.24	0.00	0.04	0.00	0.00
ZRO2	0.43	0.39	0.54	0.24	0.32	0.50	0.23	0.33	0.36	0.28	0.56	0.47	0.50
AL2O3	20.39	19.14	19.49	17.83	19.12	19.74	19.76	18.04	18.87	20.09	19.35	20.19	20.06
FE2O3	3.10	4.64	3.39	3.83	5.22	3.79	4.44	4.88	4.70	4.81	4.38	2.81	2.89
FEO	0.34	0.25	0.20	3.60	0.04	0.10	0.20	2.40	1.10	0.25	0.25	0.50	0.60
MNO	0.25	0.32	0.26	0.26	0.23	0.32	0.31	0.30	0.32	0.19	0.39	0.23	0.27
MGO	0.12	0.17	0.16	0.55	0.18	0.15	0.15	0.71	0.36	0.19	0.21	0.15	0.15
CAO	0.49	0.63	0.46	2.55	1.67	0.62	1.24	2.23	1.47	1.35	0.58	0.65	0.66
NA2O	10.66	11.05	13.88	7.70	9.44	12.07	9.61	8.48	9.59	9.39	10.85	11.06	10.69
K2O	4.15	2.99	1.44	5.39	4.42	4.19	4.66	4.63	4.30	4.62	4.40	4.29	4.34
H2O+	4.55	4.80	3.56	2.84	4.38	4.13	4.57	3.54	3.98	4.63	3.13	4.09	4.65
P2O5	0.00	0.00	0.00	0.32	0.04	0.00	0.04	0.34	0.15	0.04	0.04	0.04	0.04
CO2	0.23	0.64	0.76	0.47	1.63	0.32	0.16	0.43	0.31	0.00	0.27	0.24	0.16

I. WELL PRESERVED PHONOLITE DYKES.

	39792+	39794	MEAN	S.D.	MIN.	MAX.
SIO2	54.39	54.15	54.49	0.80	53.06	55.79
TIO2	0.00	0.01	0.09	0.18	0.00	0.52
ZRO2	0.19	0.47	0.39	0.12	0.19	0.56
AL2O3	19.29	19.80	19.41	0.74	17.83	20.39
FE2O3	3.28	3.15	3.95	0.81	2.81	5.22
FEO	1.70	0.30	0.79	1.02	0.04	3.60
MNO	0.27	0.25	0.28	0.05	0.19	0.39
MGO	0.16	0.16	0.24	0.17	0.12	0.71
CAO	2.03	0.42	1.14	0.71	0.42	2.55
NA2O	8.95	12.80	10.41	1.65	7.70	13.88
K2O	5.00	3.48	4.15	0.94	1.44	5.39
H2O+	4.18	4.72	4.12	0.60	2.84	4.80
P2O5	0.05	0.04	0.08	0.11	0.00	0.34
CO2	0.50	0.19	0.42	0.39	0.00	1.63

J. SEVERELY ALTERED PHONOLITE-LIKE DYKES.

	31818A	31822	31825	39689	39781	39783	39798	39800	MEAN	S.D.	MIN.	MAX.
SIO2	57.86	58.67	60.02	57.06	60.56	60.13	60.71	60.61	59.45	1.41	57.06	60.71
TIO2	0.09	0.00	0.07	0.06	0.00	0.15	0.15	0.07	0.07	0.06	0.00	0.15
ZRO2	0.36	0.39	0.35	0.36	0.26	0.42	0.32	0.42	0.36	0.05	0.26	0.42
AL2O3	17.92	19.81	19.30	19.10	20.95	19.18	18.22	19.25	19.22	0.93	17.92	20.95
FE2O3	6.06	5.64	5.33	3.59	4.41	2.60	4.49	4.07	4.52	1.14	2.60	6.06
FEO	0.03	0.51	0.18	0.70	0.60	2.30	1.50	1.00	0.85	0.74	0.03	2.30
MNO	0.31	0.03	0.00	0.23	0.13	0.13	0.18	0.20	0.15	0.10	0.00	0.31
MGO	0.17	0.23	0.16	0.23	0.17	0.35	0.27	0.24	0.23	0.06	0.16	0.35
CAO	3.29	2.13	1.38	1.36	0.00	1.16	1.20	0.90	1.43	0.96	0.00	3.29
NA2O	5.53	5.01	5.55	4.82	5.42	5.45	5.65	5.51	5.37	0.29	4.82	5.65
K2O	5.64	6.18	6.03	5.87	6.25	5.88	5.91	5.86	5.95	0.20	5.64	6.25
H2O+	0.73	1.01	1.09	2.80	1.27	1.27	0.58	1.07	1.23	0.68	0.58	2.80
P2O5	0.11	0.06	0.04	0.04	0.00	0.10	0.04	0.04	0.05	0.04	0.00	0.11
CO2	1.89	0.26	0.51	3.73	0.00	0.82	0.79	0.78	1.10	1.20	0.00	3.73

K. LAMPROPHYRIC DYKES.

	27015	27030	270490	27109	27139	27148	27172	31865	31870	31878	39717Q	39734	MEAN
SIO2	46.15	46.67	42.67	48.60	48.28	47.66	50.59	47.83	47.46	45.09	45.91	45.57	46.87
TIO2	2.84	3.87	2.91	2.21	2.54	2.56	1.68	2.74	2.80	3.49	2.91	2.35	2.74
ZRO2	0.06	0.05	0.24	0.06	0.07	0.06	0.07	0.06	0.06	0.04	0.05	0.05	0.07
AL2O3	14.75	13.80	14.80	15.05	14.70	14.80	15.90	14.50	14.90	13.30	13.10	14.20	14.48
FE2O3	3.75	3.38	3.40	2.90	3.43	3.47	3.90	2.93	3.58	3.05	4.74	5.10	3.64
FEO	9.81	9.42	7.60	8.53	9.05	9.78	6.60	9.65	9.74	9.64	9.92	8.04	8.98
MNO	0.21	0.16	0.31	0.21	0.20	0.17	0.23	0.18	0.21	0.17	0.23	0.20	0.21
MGO	4.81	8.00	7.63	3.50	4.19	4.08	1.89	5.10	4.52	9.83	5.45	3.53	5.21
CAO	6.07	6.93	7.06	6.32	5.35	5.14	5.61	6.67	6.27	6.97	9.23	6.53	6.51
NA2O	4.06	3.21	2.60	4.44	4.12	4.06	5.03	3.39	4.20	2.59	4.34	4.39	3.87
K2O	2.26	2.81	5.31	3.62	3.39	2.42	2.87	2.96	2.31	2.80	0.89	2.65	2.86
H2O+	1.99	1.29	1.92	1.35	1.02	1.98	1.93	1.67	1.70	2.08	1.72	2.06	1.73
P2O5	1.82	0.58	0.15	1.40	1.72	1.79	0.86	1.72	1.81	0.58	0.48	1.33	1.19
CO2	1.48	1.15	4.87	2.73	2.43	2.64	2.78	2.74	1.49	1.95	0.74	4.04	2.42
S	0.01	0.01	0.01	0.01	0.01	0.01	0.01	0.01	0.01	0.02	0.02	0.01	0.01
TOTAL	100.07	101.33	101.48	100.93	100.50	100.62	99.95	102.15	101.06	101.60	99.73	100.05	0.00

K. LAMPROPHYRIC DYKES.

	S.D.	MIN.	MAX.
SIO2	2.02	42.67	50.59
TIO2	0.57	1.68	3.87
ZRO2	0.05	0.04	0.24
AL2O3	0.78	13.10	15.90
FE2O3	0.68	2.90	5.10
FEO	1.07	6.60	9.92
MNO	0.04	0.16	0.31
MGO	2.23	1.89	9.83.
CAO	1.06	5.14	9.23
NA2O	0.76	2.59	5.03
K2O	1.03	0.89	5.31
H2O+	0.34	1.02	2.08
P2O5	0.62	0.15	1.82
CO2	1.18	0.74	4.87
S	0.00	0.01	0.02
TOTAL	0.00	0.00	0.00

L. BIOTITE TRACHYTES.

	27036	27081	39750	39755	39756	39775	39797	39799	MEAN	S.D.	MIN.	MAX.
SIO2	58.93	57.60	57.04	58.66	57.67	58.99	56.85	57.75	57.94	0.83	56.85	58.99
TIO2	0.84	0.57	0.78	0.70	0.67	0.66	0.51	0.56	0.66	0.11	0.51	0.84
ZRO2	0.09	0.13	0.11	0.10	0.10	0.10	0.11	0.11	0.11	0.01	0.09	0.13
AL2O3	17.20	17.16	16.73	17.02	16.95	17.43	17.01	17.35	17.11	0.23	16.73	17.43
FE2O3	3.50	2.99	4.60	3.95	3.31	3.40	3.88	3.54	3.65	0.49	2.99	4.60
FEO	3.94	4.80	4.20	4.00	3.80	3.85	4.10	4.70	4.17	0.38	3.80	4.80
MNO	0.19	0.21	0.18	0.19	0.17	0.20	0.24	0.23	0.20	0.02	0.17	0.24
MGO	0.25	0.47	0.63	0.58	0.52	0.60	0.60	0.60	0.53	0.12	0.25	0.63
CAO	2.00	2.28	2.07	2.25	2.55	2.54	2.64	1.63	2.24	0.34	1.63	2.64
NA2O	5.74	6.54	5.17	5.53	6.11	5.68	5.57	5.58	5.74	0.41	5.17	6.54
K2O	4.89	4.98	5.29	5.54	5.80	4.97	4.78	5.48	5.22	0.37	4.78	5.80
H2O+	1.12	1.19	1.67	1.10	1.12	1.04	1.52	1.24	1.25	0.22	1.04	1.67
P2O5	0.23	0.13	0.17	0.16	0.16	0.16	0.19	0.20	0.17	0.03	0.13	0.23
CO2	0.88	1.15	1.24	0.10	0.94	0.15	1.77	0.89	0.89	0.55	0.10	1.77
S	0.01	0.01	0.01	0.01	0.01	0.01	0.01	0.01	0.01	0.00	0.01	0.01

L. BIOTITE-RIEBECKITE TRACHYTES.

	27037	31848	39733	39752	39754	39790	39795	MEAN	S.D.	MIN.	MAX.
SIO2	62.92	62.11	60.95	62.28	62.71	55.52	62.79	61.33	2.65	55.52	62.92
TIO2	0.36	0.36	0.54	0.34	0.10	1.35	0.08	0.45	0.43	0.08	1.35
ZRO2	0.18	0.20	0.16	0.18	0.18	0.09	0.20	0.17	0.04	0.09	0.20
AL2O3	15.80	15.85	14.94	15.84	15.74	14.19	16.07	15.49	0.68	14.19	16.07
FE2O3	4.88	5.80	5.77	4.29	4.40	5.72	4.28	5.02	0.72	4.28	5.80
FEO	2.20	1.33	2.70	2.35	2.70	4.80	2.35	2.63	1.06	1.33	4.80
MNO	0.15	0.16	0.17	0.15	0.18	0.19	0.18	0.17	0.02	0.15	0.19
MGO	0.39	0.31	0.23	0.30	0.34	1.16	0.30	0.43	0.32	0.23	1.16
CAO	0.75	0.82	1.35	1.14	0.80	3.61	1.01	1.35	1.02	0.75	3.61
NA2O	5.96	6.69	6.17	6.21	6.19	5.76	6.16	6.16	0.28	5.76	6.69
K2O	5.36	4.78	5.40	5.54	5.38	4.00	5.28	5.11	0.54	4.00	5.54
H2O+	0.83	0.87	0.88	1.02	0.75	1.04	0.78	0.88	0.11	0.75	1.04
P2O5	0.09	0.07	0.09	0.08	0.10	0.52	0.08	0.15	0.16	0.07	0.52
CO2	0.13	0.66	0.65	0.28	0.15	1.91	0.16	0.56	0.64	0.13	1.91
S	0.01	0.01	0.01	0.01	0.01	0.01	0.01	0.01	0.00	0.01	0.01

APPENDIX 6 (continued)

TABLE A.8

Trace element analyses of nepheline syenites, phonolites, lamprophyres, and trachytes from the Grønnedal-Ika complex, together with means, standard deviations ("S.D.") and minimum and maximum values. The table is subdivided in the same manner as Table A.6. Concentrations lower than the nominal detection limit (listed below) are indicated by a dash. Phonolites in which there is partial alteration of nepheline are indicated "+", as are those lamprophyres in which significant amounts of chlorite are present.

Detection limits (see Appendix 3):

Rb	3 p.p.m.
Ba	6
Sr	3
Pb	9
Zn	4
La	4
Y	3
Th	10
Nb	3

A. COARSE-GRAINED BROWN SYENITE

	27123	27273	31896	MEAN	S.D.	MIN.	MAX.
RB PPM	220	188	152	187	34	152	220
BA PPM	456	297	93	282	182	93	456
SR PPM	122	118	248	163	74	118	248
PB PPM	28	23	10	20	9	10	28
ZN PPM	149	228	83	153	73	83	228
LA PPM	46	46	26	39	12	26	46
Y PPM	31	23	12	22	10	12	31
TH PPM	10	-	13	10	-	-	13
NB PPM	193	116	99	136	50	99	193

B. FOYAITE OF THE LOWER SERIES. GROUP I

	27103	27118A	27130	27159	27267	27268	27272	27277A	27277M	126704	MEAN	S.D.	MIN.
RB PPM	154	140	145	134	161	146	188	102	95	166	143	28	95
BA PPM	93	285	444	23	85	104	106	51	28	82	130	132	23
SR PPM	263	615	664	175	208	206	270	136	110	163	281	196	110
PB PPM	17	11	16	-	11	13	13	25	21	14	15	-	-
ZN PPM	130	104	84	214	158	127	129	168	240	140	149	48	84
LA PPM	27	39	62	49	52	53	37	36	40	43	44	10	27
Y PPM	17	22	20	24	24	28	19	20	26	23	22	3	17
TH PPM	-	12	-	19	-	11	-	-	-	-	-	-	-
NB PPM	98	102	47	69	99	118	135	122	165	60	102	36	47

B. FOYAITE OF THE LOWER SERIES. GROUP I

	MAX.
RB PPM	188
BA PPM	444
SR PPM	664
PB PPM	25
ZN PPM	240
LA PPM	62
Y PPM	28
TH PPM	19
NB PPM	165

B. FOYAITE OF THE LOWER SERIES. GROUP II

	27124	27129	126703	126705	MEAN	S.D.	MIN.	MAX.
RB PPM	193	220	184	174	193	20	174	220
BA PPM	104	131	115	107	114	12	104	131
SR PPM	238	406	311	239	299	79	238	406
PB PPM	25	15	10	10	15	-	10	25
ZN PPM	130	82	149	157	130	34	82	157
LA PPM	27	20	41	28	29	9	20	41
Y PPM	21	13	31	17	21	8	13	31
TH PPM	-	-	-	-	-	-	-	-
NB PPM	98	76	153	77	101	36	76	153

B. FOYAITE OF THE LOWER SERIES. GROUP III

	27090	27092	27126A	27127	27202	27262	27274	39723	126713	126714	MEAN	S.D.	MIN.
RB PPM	210	179	256	265	178	172	204	237	313	238	225	45	172
BA PPM	118	175	93	108	102	113	102	81	125	82	110	27	81
SR PPM	274	726	260	244	255	217	431	200	293	246	315	158	200
PB PPM	12	12	19	-	18	-	18	10	43	14	15	11	-
ZN PPM	111	136	137	126	186	241	167	260	148	147	166	49	111
LA PPM	25	31	30	17	41	31	37	63	63	33	37	15	17
Y PPM	18	21	22	11	27	20	25	33	48	24	25	10	11
TH PPM	-	-	-	-	-	-	-	11	18	13	-	-	-
NB PPM	118	76	129	100	138	82	110	139	248	187	133	52	76

B. FOYAITE OF THE LOWER SERIES. GROUP III

	MAX.
RB PPM	313
BA PPM	175
SR PPM	726
PB PPM	43
ZN PPM	260
LA PPM	63
Y PPM	48
TH PPM	18
NB PPM	248

B. FOYAITE OF THE LOWER SERIES. GROUP IV

	27088	27133	27136	27137	27168	27170	126706	MEAN	S.D.	MIN.	MAX.
RB PPM	309	203	252	359	257	311	273	281	51	203	359
BA PPM	81	142	106	108	101	55	84	97	27	55	142
SR PPM	247	386	338	221	227	176	227	260	74	176	386
PB PPM	-	-	15	-	9	10	-	-	-	-	15
ZN PPM	149	40	100	254	142	257	183	161	79	40	257
LA PPM	27	13	17	15	10	17	51	22	14	10	51
Y PPM	18	7	14	11	3	12	26	13	7	3	26
TH PPM	-	-	-	-	-	-	-	-	-	-	-
NB PPM	103	42	50	148	97	191	148	111	55	42	191

C. GRANULAR SYENITE. GS-1

	27093	27095	27096	27122	27263	27270	27271	39725	126707	MEAN	S.D.	MIN.	MAX.
RB PPM	110	137	195	139	152	199	97	152	178	151	35	97	199
BA PPM	41	37	173	184	56	180	47	50	131	100	66	37	184
SR PPM	224	145	396	469	265	403	486	194	353	326	123	145	486
PB PPM	13	15	9	17	-	12	18	-	26	12	-	-	26
ZN PPM	163	162	171	145	135	114	192	196	108	154	31	108	196
LA PPM	257	41	31	56	58	42	54	58	32	70	71	31	257
Y PPM	85	24	24	27	24	18	27	30	19	31	21	18	85
TH PPM	-	-	-	-	-	-	-	-	-	-	-	-	-
NB PPM	60	134	153	89	150	75	153	145	75	115	39	60	153

C. GRANULAR SYENITE. GS-2

	27099	27100	31898	126701	MEAN	S.D.	MIN.	MAX.
RB PPM	214	273	128	214	207	60	128	273
BA PPM	489	188	80	494	313	211	80	494
SR PPM	799	453	212	1310	694	476	212	1310
PB PPM	12	60	29	23	31	21	12	60
ZN PPM	293	266	213	244	254	34	213	293
LA PPM	136	102	38	168	111	56	38	168
Y PPM	70	76	23	135	76	46	23	135
TH PPM	24	17	-	60	25	25	-	60
NB PPM	364	514	117	406	350	168	117	514

D. FELDSPATHIC SYENITES FROM THE GNEISS RAFT

	27085	27087	MEAN	S.D.	MIN.	MAX.
RB PPM	145	118	132	19	118	145
BA PPM	247	216	232	22	216	247
SR PPM	220	195	208	18	195	220
PB PPM	13	21	17	-	13	21
ZN PPM	25	402	214	267	25	402
LA PPM	22	132	77	78	22	132
Y PPM	12	38	25	18	12	38
TH PPM	-	18	-	13	-	18
NB PPM	13	69	41	40	13	69

E. UPPER SERIES. 'FELSIC SYENITES'

	27002	27005	27035	27074	27077	27140	27141	27142	27143	27154	27157	27158	27181U
RB PPM	217	201	210	116	225	153	227	177	195	221	246	238	140
BA PPM	182	181	193	758	235	266	146	104	126	91	240	220	275
SR PPM	165	150	187	1080	298	354	310	213	284	259	221	212	481
PB PPM	11	22	20	-	-	-	14	23	-	-	23	15	11
ZN PPM	162	140	144	86	195	137	150	162	75	178	189	162	72
LA PPM	47	45	43	24	30	40	23	24	10	20	26	24	39
Y PPM	25	32	27	11	19	25	13	16	8	15	17	16	15
TH PPM	11	-	-	11	-	-	-	-	-	-	13	-	-
NB PPM	135	110	95	85	192	70	132	99	72	135	173	187	31

E. UPPER SERIES. 'FELSIC SYENITES'

	27185	27194	27205	27207	27209	27221	27227	27228	27234	27235	39706A	39706B	39736A
RB PPM	184	207	178	210	234	226	204	216	198	191	228	243	197
BA PPM	253	236	243	199	123	369	552	184	237	314	83	83	133
SR PPM	396	366	485	347	246	1535	568	219	337	527	289	292	269
PB PPM	15	14	22	26	9	22	23	17	12	20	–	14	–
ZN PPM	68	199	136	182	150	131	173	130	110	175	116	158	73
LA PPM	25	56	68	39	18	25	38	28	31	26	35	29	14
Y PPM	15	28	30	25	15	20	27	21	17	15	16	15	6
TH PPM	–	–	–	–	–	–	12	–	17	–	–	–	–
NB PPM	37	113	69	249	140	87	146	101	89	114	70	131	50

E. UPPER SERIES. 'FELSIC SYENITES'

	39749	39759	58315	126710	126710	126727	MEAN	S.D.	MIN.	MAX.
RB PPM	232	219	221	193	192	250	206	30	116	250
BA PPM	167	172	331	192	164	224	227	135	83	758
SR PPM	205	189	224	314	287	178	359	276	150	1535
PB PPM	12	34	19	19	16	33	15	10	-	34
ZN PPM	164	151	105	73	141	165	139	39	68	199
LA PPM	37	77	39	26	35	52	34	15	10	77
Y PPM	15	50	27	17	18	33	20	9	6	50
TH PPM	-	13	19	-	-	13	-	-	-	19
NB PPM	122	138	162	37	53	166	112	50	31	249

E. UPPER SERIES. 'LESS MAFIC SYENITES'

	27108	27165B	27181L	27182	27186	27192	27254	27261	126711	MEAN	S.D.	MIN.	MAX.
RB PPM	109	154	123	144	256	133	165	137	131	150	43	109	256
BA PPM	299	1561	191	216	488	153	383	308	158	418	443	153	1561
SR PPM	648	306	358	386	992	385	573	894	484	559	244	306	992
PB PPM	21	23	11	-	12	17	12	21	19	16	-	-	23
ZN PPM	127	179	114	160	134	199	203	130	242	165	43	114	242
LA PPM	191	36	59	94	23	162	115	102	132	102	56	23	191
Y PPM	64	18	24	29	15	58	48	40	57	39	18	15	64
TH PPM	-	-	-	-	-	-	-	-	-	-	-	-	-
NB PPM	66	111	37	44	170	112	126	76	252	111	68	37	252

E. UPPER SERIES. 'MAFIC SYENITES'

	27046	27107	27179	27181M	27193	27259	39736B	126708	MEAN	S.D.	MIN.	MAX.
RB PPM	170	103	113	117	77	90	106	107	110	27	77	170
BA PPM	545	283	158	132	66	126	141	138	199	153	66	545
SR PPM	722	647	372	317	314	294	307	633	451	183	294	722
PB PPM	38	12	–	29	10	14	10	14	16	12	–	38
ZN PPM	317	121	196	217	519	146	142	204	233	131	121	519
LA PPM	203	213	205	82	222	141	107	152	166	53	82	222
Y PPM	68	66	67	31	139	55	48	62	67	32	31	139
TH PPM	16	–	–	–	–	–	–	–	–	–	–	16
NB PPM	175	59	56	88	301	47	25	73	103	92	25	301

F. COARSE-GRAINED SYENITE

	27065	27067	27114	27280	27285	27287	126721	MEAN	S.D.	MIN.	MAX.
RB PPM	129	116	124	120	91	153	141	125	20	91	153
BA PPM	676	279	284	301	145	368	254	330	167	145	676
SR PPM	1150	569	599	583	324	707	407	620	266	324	1150
PB PPM	21	22	13	26	14	16	13	18	-	13	26
ZN PPM	198	164	129	209	101	45	174	146	58	45	209
LA PPM	85	91	88	102	51	53	67	77	20	51	102
Y PPM	23	46	46	53	26	29	31	36	12	23	53
TH PPM	-	-	-	-	13	13	10	-	-	-	13
NB PPM	104	131	83	117	100	96	147	111	22	83	147

G. XENOLITHIC PORPHYRITIC SYENITE

	27189	31841	31846	31854	58314	58316	58317	58320	MEAN	S.D.	MIN.	MAX.
RB PPM	130	152	159	143	184	167	148	140	153	17	130	184
BA PPM	436	520	466	344	416	677	787	709	544	160	344	787
SR PPM	798	858	740	540	1190	1520	833	760	905	307	540	1520
PB PPM	28	34	29	23	29	14	29	66	32	15	14	66
ZN PPM	171	177	179	208	169	139	190	212	181	23	139	212
LA PPM	47	86	78	61	74	42	35	42	58	19	35	86
Y PPM	22	43	38	33	30	20	24	31	30	8	20	43
TH PPM	17	30	13	13	10	-	11	17	14	-	-	30
NB PPM	333	403	273	247	169	75	176	251	241	102	75	403

H. SYENITE AND MICROSYENITE DYKES - GROUP 1

	27119	27128	27178	27200	39711	126712	MEAN	S.D.	MIN.	MAX.
RB PPM	145	199	196	193	201	227	194	27	145	227
BA PPM	84	274	118	209	304	132	187	90	84	304
SR PPM	384	745	346	532	558	387	492	151	346	745
PB PPM	10	-	19	-	12	-	-	-	-	19
ZN PPM	83	67	92	197	168	81	115	54	67	197
LA PPM	28	20	19	43	24	20	26	9	19	43
Y PPM	16	9	12	17	12	8	12	4	8	17
TH PPM	-	-	-	-	18	-	-	-	-	18
NB PPM	71	23	65	79	87	45	62	24	23	87

H. SYENITE AND MICROSYENITE DYKES - GROUP 2

	27086	27173	27275	39710	MEAN	S.D.	MIN.	MAX.
RB PPM	163	203	178	175	180	17	163	203
BA PPM	239	104	243	161	187	67	104	243
SR PPM	582	310	485	171	387	183	171	582
PB PPM	10	-	17	41	17	17	-	41
ZN PPM	108	99	93	132	108	17	93	132
LA PPM	44	25	17	11	24	14	11	44
Y PPM	16	15	10	11	13	-	10	16
TH PPM	-	-	-	-	-	-	-	-
NB PPM	73	61	69	124	82	29	61	124

H. SYENITE AND MICROSYENITE DYKES - GROUP 3

	31803	39740	39753A	39753B	MEAN	S.D.	MIN.	MAX.
RB PPM	201	210	171	142	181	31	142	210
BA PPM	79	57	115	130	95	33	57	130
SR PPM	250	223	378	357	302	77	223	378
PB PPM	16	-	14	-	-	-	-	16
ZN PPM	259	322	170	122	218	89	122	322
LA PPM	150	95	18	50	78	57	18	150
Y PPM	69	26	7	21	31	27	7	69
TH PPM	-	-	-	10	-	-	-	10
NB PPM	329	377	153	84	236	140	84	377

H. SYENITE AND MICROSYENITE DYKES - GROUP 4

	27068	27082	27156	39742	39777	58318	126715	MEAN	S.D.	MIN.	MAX.
RB PPM	130	166	174	219	184	142	107	160	37	107	219
BA PPM	890	529	173	146	416	827	1044	575	355	146	1044
SR PPM	1190	1052	352	330	1183	1360	1670	1020	503	330	1670
PB PPM	17	23	15	-	17	37	-	16	13	-	37
ZN PPM	122	136	135	127	98	196	284	157	63	98	284
LA PPM	29	28	31	46	16	101	57	44	28	16	101
Y PPM	19	18	14	18	12	26	33	20	7	12	33
TH PPM	11	-	-	-	-	10	-	-	-	-	11
NB PPM	99	262	121	62	169	293	198	172	85	62	293

H. SYENITE AND MICROSYENITE DYKES - GROUP 5

	39770	39771	MEAN	S.D.	MIN.	MAX.
RB PPM	214	197	206	12	197	214
BA PPM	222	143	183	56	143	222
SR PPM	302	308	305	4	302	308
PB PPM	13	19	16	-	13	19
ZN PPM	107	208	158	71	107	208
LA PPM	33	28	31	-	28	33
Y PPM	15	14	15	-	14	15
TH PPM	-	-	-	-	-	-
NB PPM	70	70	70	-	70	70

I. WELL PRESERVED PHONOLITE DYKES.

	27007	27058	27151	27183	31821+	39691	39730+	39731A	39731B	39735+	39751	39762	39779+
RB PPM	393	141	295	262	252	482	365	317	238	360	263	414	370
BA PPM	25	63	37	503	58	32	41	325	80	70	75	76	26
SR PPM	26	122	31	1100	137	15	226	310	330	1000	144	141	248
PB PPM	46	50	61	26	36	49	21	30	36	25	47	52	48
ZN PPM	515	564	610	353	406	513	468	356	575	500	568	615	590
LA PPM	100	68	178	100	194	96	173	112	110	159	58	101	103
Y PPM	118	45	151	76	109	86	63	126	83	118	55	121	101
TH PPM	50	45	54	10	33	50	15	50	30	23	47	39	47
NB PPM	573	467	495	300	465	525	374	300	430	370	486	576	629

I. WELL PRESERVED PHONOLITE DYKES.

	39792+	39794	MEAN	S.D.	MIN.	MAX.
RB PPM	288	312	317	84	141	482
BA PPM	55	37	100	133	25	503
SR PPM	600	45	298	341	15	1100
PB PPM	29	49	40	12	21	61
ZN PPM	446	600	512	89	353	615
LA PPM	197	100	123	45	58	197
Y PPM	57	132	96	32	45	151
TH PPM	-	40	36	17	-	54
NB PPM	440	597	468	102	300	629

J. ALTERED PHONOLITE DYKES.

	27217	39782	39791	31818A	31822	31825	39689	39781	39783	39798	39800	MEAN	S.D.
RB PPM	230	262	388	375	334	400	360	399	355	377	357	349	55
BA PPM	100	15	158	472	310	566	735	192	344	428	784	373	252
SR PPM	330	28	762	11000	82	96	520	87	262	249	510	1266	3236
PB PPM	22	40	54	200	16	26	36	14	14	25	48	45	53
ZN PPM	428	434	433	375	281	313	386	267	231	242	447	349	84
LA PPM	184	125	296	371	193	272	188	222	110	280	210	223	77
Y PPM	80	101	114	140	119	135	102	49	93	118	111	106	26
TH PPM	40	44	30	-	25	50	30	43	32	32	30	32	13
NB PPM	400	483	514	450	531	460	446	360	398	473	494	455	52

J. ALTERED PHONOLITE DYKES.

	MIN.	MAX.
RB PPM	230	400
BA PPM	15	784
SR PPM	28	11000
PB PPM	14	200
ZN PPM	231	447
LA PPM	110	371
Y PPM	49	140
TH PPM	–	50
NB PPM	360	531

K. LAMPROPHYRE DYKES.

	27015	27030+	27049Q	27109+	27139	27148+	27172+	31865+	31870	31878	39717Q	39734+	MEAN
RB PPM	60	79	181	106	98	50	82	76	62	90	29	63	81
BA PPM	1356	1009	1036	2045	1750	1550	1135	1578	1322	1901	384	1570	1386
SR PPM	880	659	1460	1105	890	696	122	1050	935	821	567	976	847
PB PPM	30	21	32	22	24	20	-	36	24	39	11	-	23
ZN PPM	184	146	385	182	192	197	152	182	170	141	166	178	190
LA PPM	73	36	100	68	82	79	68	69	69	39	63	66	68
Y PPM	40	21	65	35	45	40	26	35	39	21	51	24	37
TH PPM	-	-	25	10	-	11	10	-	-	-	-	10	-
NB PPM	82	71	334	98	92	87	95	77	80	58	72	85	103

K. LAMPROPHYRE DYKES.

	S.D.	MIN.	MAX.
RB PPM	38	29	181
BA PPM	454	384	2045
SR PPM	327	122	1460
PB PPM	11	-	39
ZN PPM	64	141	385
LA PPM	17	36	100
Y PPM	13	21	65
TH PPM	-	-	25
NB PPM	74	58	334

L. BIOTITE TRACHYTE DYKES.

	27036	27081	39750	39755	39756	39775	39797	39799	MEAN	S.D.	MIN.	MAX.
RB PPM	92	144	94	131	184	78	99	103	116	35	78	184
BA PPM	1580	667	945	960	1005	1940	1150	1220	1183	403	667	1940
SR PPM	250	144	285	242	214	1590	276	146	393	486	144	1590
PB PPM	-	28	-	10	-	19	13	14	13	-	-	28
ZN PPM	191	215	223	202	188	169	228	224	205	21	169	228
LA PPM	82	97	82	83	88	89	106	100	91	9	82	106
Y PPM	43	61	39	39	40	38	43	44	43	7	38	61
TH PPM	14	14	24	16	15	10	15	20	16	-	10	24
NB PPM	131	182	149	154	146	148	166	168	156	16	131	182

L. BIOTITE-RIEBECKITE TRACHYTE DYKES.

	27037	31848	39733	39752	39754	39790	39795	MEAN	S.D.	MIN.	MAX.
RB PPM	202	95	178	175	215	133	190	170	42	95	215
BA PPM	132	670	199	225	145	2120	189	526	727	132	2120
SR PPM	63	78	23	55	30	331	138	103	108	23	331
PB PPM	23	21	24	23	25	17	29	23	-	17	29
ZN PPM	248	190	223	223	237	196	260	225	26	190	260
LA PPM	180	140	110	125	138	168	141	143	24	110	180
Y PPM	53	47	69	53	50	35	55	52	10	35	69
TH PPM	25	36	21	24	13	10	29	23	-	10	36
NB PPM	195	186	121	192	190	93	206	169	44	93	206

APPENDIX 6

TABLE A.9

C.I.P.W. norms and other petrochemical functions for nepheline syenites, phonolites, lamprophyres and trachytes from the Grønnedal-Ika complex, South Greenland. The norm and Differentiation Index (Thornton and Tuttle 1960) are given in weight percentage; the other functions are calculated from cation molecular percent.

Specimen numbers analysed in the laboratories of the Greenland Geological Survey are marked by an asterisk. The table is subdivided in the same manner as Table A.6.

A. COARSE-GRAINED BROWN SYENITE

NORMCAL .. R.C.O.GILL

SUMMARY NORM TABLE

	27123	27273	31896
QUARTZ	3.8	3.1	0.0
CORUNDUM	9.7	6.1	7.3
ZIRCON	0.2	0.1	0.1
ORTHOCLASE	36.3	37.6	30.7
ALBITE	39.7	43.1	28.5
ANORTHITE	1.8	1.5	3.0
NEPHELINE	0.0	0.0	25.6
HYPERSTHENE	2.8	0.4	0.0
OLIVINE	0.0	0.0	1.9
MAGNETITE	5.4	6.6	2.4
HEMATITE	0.0	1.0	0.0
ILMENITE	0.2	0.3	0.2
APATITE	0.1	0.1	0.1
WATER	1.8	1.6	4.3
DIFF. INDEX	79.8	83.8	84.9
NA/(NA+K)	0.54	0.55	0.72
(NA+K)/AL	0.58	0.70	0.71
F3/(F2+F3)	0.55	0.71	0.43

B. FOYAITE OF THE LOWER SERIES. GROUP I

NORMCAL .. R.C.O.GILL

SUMMARY NORM TABLE

	27103	27118A	27130	27159*	27267	27268	27272	27277A	27277M	126704
ZIRCON	0.1	0.1	0.1	0.2	0.2	0.2	0.1	0.2	0.3	0.2
ORTHOCLASE	29.8	38.8	34.2	28.5	28.1	30.7	34.1	24.2	21.7	29.7
ALBITE	11.0	9.8	21.5	15.3	18.5	20.7	20.3	13.9	5.7	13.0
ANORTHITE	0.0	0.0	2.6	0.0	1.4	0.7	4.3	0.6	0.0	0.0
NEPHELINE	42.4	37.2	36.7	35.5	31.4	35.3	33.1	37.2	33.7	40.0
ACMITE	3.4	5.2	0.0	1.0	0.0	0.0	0.0	0.0	0.9	1.2
DIOPSIDE	9.1	4.4	0.7	10.7	12.6	5.1	1.2	14.3	24.2	8.4
WOLLASTONITE	0.1	0.0	0.7	2.7	0.3	1.0	0.7	1.6	1.8	1.4
OLIVINE	0.0	1.1	0.0	0.0	0.0	0.0	0.0	0.0	0.0	0.0
MAGNETITE	3.3	2.3	2.7	5.6	6.5	5.6	2.7	7.5	10.9	5.2
HEMATITE	0.0	0.0	0.6	0.0	0.0	0.0	2.7	0.0	0.0	0.0
ILMENITE	0.2	0.6	0.1	0.3	0.3	0.3	0.3	0.3	0.5	0.2
APATITE	0.5	0.5	0.1	0.2	0.8	0.6	0.5	0.3	0.3	0.5
WATER	0.7	1.0	1.6	1.2	1.3	1.3	1.6	1.1	0.8	0.8
DIFF. INDEX	83.2	85.8	92.4	79.3	77.9	86.7	87.5	75.3	61.1	82.8
NA/(NA+K)	0.77	0.70	0.73	0.75	0.74	0.75	0.72	0.78	0.77	0.76
(NA+K)/AL	1.03	1.05	0.96	1.01	0.98	0.99	0.93	0.99	1.01	1.01
F3/(F2+F3)	0.51	0.56	0.75	0.51	0.47	0.58	0.83	0.47	0.46	0.51

B. FOYAITE OF THE LOWER SERIES. GROUP II

NORMCAL .. R.C.O.GILL

SUMMARY NORM TABLE

	27124	27129	126703	126705
ZIRCON	0.2	0.1	0.2	0.2
ORTHOCLASE	35.4	38.9	38.8	33.5
ALBITE	20.7	24.4	26.5	22.2
ANORTHITE	0.0	2.0	5.6	0.7
NEPHELINE	26.9	29.3	18.8	29.9
ACMITE	2.8	0.0	0.0	0.0
DIOPSIDE	8.7	1.3	4.2	5.0
WOLLASTONITE	1.2	0.7	0.0	2.5
OLIVINE	0.0	0.0	0.2	0.0
MAGNETITE	3.8	3.9	5.5	5.7
ILMENITE	0.2	0.2	0.2	0.2
APATITE	0.1	0.1	0.1	0.1
WATER	0.8	1.2	1.8	1.4
DIFF. INDEX	83.0	91.6	84.1	85.6
NA/(NA+K)	0.69	0.68	0.63	0.71
(NA+K)/AL	1.03	0.97	0.90	0.99
F3/(F2+F3)	0.50	0.63	0.58	0.58

B. FOYAITE OF THE LOWER SERIES. GROUP III

NORMCAL .. R.C.O.GILL

SUMMARY NORM TABLE

	27090	27092	27126A	27127	27202	27262	27274	39723	126713	126714
CORUNDUM	0.0	0.5	0.0	0.9	0.0	0.0	0.0	0.0	0.0	0.0
ZIRCON	0.1	0.1	0.1	0.1	0.2	0.2	0.2	0.2	0.1	0.1
ORTHOCLASE	40.3	36.4	41.5	38.0	33.0	32.2	36.0	35.2	40.0	38.4
ALBITE	24.3	33.5	26.4	31.7	27.3	25.5	29.1	25.9	26.3	28.9
ANORTHITE	3.8	12.9	3.1	2.4	1.8	0.0	6.0	2.9	0.2	0.0
NEPHELINE	24.6	7.9	19.6	19.7	18.7	18.7	15.9	20.2	21.6	20.5
ACMITE	0.0	0.0	0.0	0.0	0.0	0.4	0.0	0.0	0.0	4.1
DIOPSIDE	1.8	0.0	3.0	0.0	9.5	13.0	4.3	5.9	5.2	2.6
WOLLASTONITE	0.2	0.0	0.0	0.0	1.2	1.9	0.3	1.1	0.0	0.0
OLIVINE	0.0	0.5	0.0	2.4	0.0	0.0	0.0	0.0	1.9	4.5
MAGNETITE	4.6	7.2	5.8	4.3	7.8	7.6	7.7	8.1	4.1	0.7
HEMATITE	0.0	0.5	0.0	0.0	0.0	0.0	0.0	0.0	0.0	0.0
ILMENITE	0.2	0.2	0.3	0.5	0.3	0.3	0.3	0.4	0.4	0.2
APATITE	0.1	0.2	0.1	0.1	0.1	0.1	0.1	0.1	0.2	0.1
WATER	0.9	1.8	1.3	1.2	2.0	1.1	1.1	2.0	1.5	0.4
DIFF. INDEX	89.1	77.8	87.5	89.3	79.0	76.5	81.1	81.3	87.9	87.8
NA/(NA+K)	0.65	0.58	0.62	0.66	0.67	0.67	0.63	0.66	0.64	0.66
(NA+K)/AL	0.94	0.75	0.95	0.92	0.96	1.00	0.89	0.95	1.00	1.05
F3/(F2+F3)	0.63	0.70	0.61	0.51	0.53	0.49	0.61	0.60	0.41	0.31

B. FOYAITE OF THE LOWER SERIES. GROUP IV

NORMCAL .. R.C.O.GILL

SUMMARY NORM TABLE

	27088	27133	27136	27137*	27168	27170	126706
CORUNDUM	1.7	1.0	0.9	0.5	0.9	3.2	2.6
ZIRCON	0.0	0.0	0.0	0.0	0.2	0.1	0.0
ORTHOCLASE	46.4	43.5	48.2	49.3	45.4	43.0	48.4
ALBITE	29.3	36.8	38.0	23.8	34.0	37.8	34.5
ANORTHITE	3.0	1.9	1.8	0.5	0.0	0.0	2.4
NEPHELINE	11.5	13.3	7.4	13.7	12.7	5.2	2.5
OLIVINE	0.5	0.5	1.0	8.5	5.2	0.9	4.3
MAGNETITE	6.6	2.8	2.4	3.1	1.1	7.6	4.5
HEMATITE	0.2	0.0	0.0	0.0	0.0	1.4	0.0
ILMENITE	0.6	0.2	0.2	0.6	0.4	0.7	0.6
APATITE	0.1	0.1	0.1	0.0	0.0	0.0	0.1
CALCITE	0.0	0.0	0.0	0.0	-0.0	0.0	0.0
WATER	1.1	0.5	0.3	1.2	1.4	1.4	1.7
DIFF. INDEX	87.2	93.6	93.6	86.8	92.2	86.1	85.4
NA/(NA+K)	0.54	0.60	0.53	0.51	0.57	0.54	0.46
(NA+K)/AL	0.87	0.92	0.92	0.97	0.96	0.84	0.82
F3/(F2+F3)	0.66	0.59	0.51	0.23	0.15	0.70	0.41

C. GRANULAR SYENITE. GS-1

NORMCAL .. R.C.O.GILL

SUMMARY NORM TABLE

	27093	27095	27096	27122	27263	27270	27271	39725	126707
ZIRCON	0.2	0.1	0.1	0.1	0.1	0.0	0.3	0.2	0.1
ORTHOCLASE	28.1	25.0	36.4	42.3	31.9	39.4	25.0	26.4	38.2
ALBITE	20.5	1.3	17.0	16.8	26.0	16.0	25.5	20.4	23.2
ANORTHITE	3.5	0.0	2.8	4.4	5.0	2.6	8.1	2.3	3.9
NEPHELINE	22.0	50.4	34.8	24.5	26.8	30.8	22.7	31.5	20.4
ACMITE	0.0	10.2	0.0	0.0	0.0	0.0	0.0	0.0	0.0
DIOPSIDE	12.2	10.5	1.9	3.0	2.3	2.9	9.1	7.3	8.4
WOLLASTONITE	1.6	0.0	0.0	0.0	0.0	0.0	0.6	2.0	0.1
OLIVINE	0.0	1.1	0.5	3.1	1.1	3.3	0.0	0.0	0.0
MAGNETITE	6.9	0.9	5.6	4.4	6.0	3.8	8.4	8.6	5.2
ILMENITE	0.2	0.3	0.4	0.7	0.2	0.5	0.2	0.3	0.2
APATITE	4.9	0.2	0.5	0.7	0.5	0.5	0.1	0.9	0.3
WATER	1.6	1.5	1.6	0.9	1.6	1.0	1.4	1.4	1.5
DIFF. INDEX	70.5	76.7	88.2	83.6	84.7	86.2	73.1	78.3	81.7
NA/(NA+K)	0.70	0.82	0.70	0.61	0.71	0.66	0.74	0.76	0.63
(NA+K)/AL	0.93	1.10	0.96	0.92	0.92	0.96	0.86	0.96	0.93
F3/(F2+F3)	0.49	0.53	0.61	0.42	0.58	0.39	0.57	0.59	0.50

C. GRANULAR SYENITE. GS-2

NORMCAL .. R.C.O.GILL

SUMMARY NORM TABLE

	27099*	27100	31898	126701
ZIRCON	0.2	0.3	0.4	0.3
ORTHOCLASE	30.0	33.7	24.4	30.0
ALBITE	38.0	32.3	27.8	33.4
ANORTHITE	0.0	0.0	2.1	0.0
NEPHELINE	13.0	17.3	18.5	19.1
ACMITE	3.1	5.5	0.0	2.0
DIOPSIDE	4.5	1.5	7.3	3.9
WOLLASTONITE	2.5	1.6	5.3	2.9
MAGNETITE	6.2	2.1	13.7	4.0
HEMATITE	1.1	4.6	0.0	3.1
ILMENITE	0.9	0.8	0.3	0.9
APATITE	0.5	0.2	0.2	0.4
WATER	2.1	2.6	1.6	2.1
DIFF. INDEX	81.0	83.3	70.7	82.5
NA/(NA+K)	0.70	0.69	0.73	0.71
(NA+K)/AL	1.04	1.06	0.96	1.02
F3/(F2+F3)	0.74	0.91	0.62	0.81

D. FELDSPATHIC SYENITES FROM THE GNEISS RAFT

NORMCAL .. R.C.D.GILL

SUMMARY NORM TABLE

	27085	27087
CORUNDUM	0.8	0.0
ZIRCON	0.0	0.2
ORTHOCLASE	35.1	27.3
ALBITE	59.8	35.7
ANORTHITE	1.9	0.0
NEPHELINE	0.2	5.9
ACMITE	0.0	1.4
DIOPSIDE	0.0	1.6
WOLLASTONITE	0.0	2.7
MAGNETITE	0.7	23.4
HEMATITE	1.3	0.0
ILMENITE	0.1	1.8
APATITE	0.1	0.1
WATER	0.0	0.0
DIFF. INDEX	95.0	68.8
NA/(NA+K)	0.65	0.65
(NA+K)/AL	0.92	1.02
F3/(F2+F3)	0.89	0.65

E. UPPER SERIES. 'FELSIC SYENITES'

NORMCAL .. R.C.O.GILL

SUMMARY NORM TABLE

	27002	27005	27035	27074	27077	27140	27141	27142	27143	27154	27157	27158
CORUNDUM	0.0	0.0	0.0	0.0	0.8	0.0	0.0	0.0	0.7	0.0	0.0	0.0
ZIRCON	0.2	0.2	0.2	0.1	0.1	0.1	0.0	0.2	0.0	0.1	0.1	0.1
ORTHOCLASE	35.1	28.5	35.7	41.6	35.5	28.6	38.2	33.0	39.8	38.2	34.7	35.9
ALBITE	24.6	15.3	28.8	12.2	35.2	14.5	27.3	21.2	33.3	21.7	30.1	30.3
ANORTHITE	0.0	0.0	0.3	7.3	2.9	0.0	1.6	0.0	1.8	2.5	2.3	2.5
NEPHELINE	23.9	41.2	23.3	29.3	17.2	38.5	21.7	26.5	18.4	26.5	24.2	24.0
ACMITE	3.1	5.2	0.0	0.0	0.0	5.8	0.0	0.5	0.0	0.0	0.0	0.0
DIOPSIDE	6.7	2.1	4.0	2.1	0.0	8.5	1.0	9.4	0.0	2.3	0.4	0.1
WOLLASTONITE	0.0	2.5	0.9	0.3	0.0	0.0	0.0	0.0	0.0	0.0	0.0	0.0
OLIVINE	1.1	0.0	0.0	0.0	2.6	0.7	4.4	0.0	1.6	5.2	2.9	3.3
MAGNETITE	4.6	4.5	6.0	4.6	5.0	2.3	4.4	8.5	3.8	2.6	4.4	3.3
HEMATITE	0.0	0.0	0.0	1.3	0.0	0.0	0.0	0.0	0.0	0.0	0.0	0.0
ILMENITE	0.6	0.3	0.6	0.5	0.7	0.5	0.7	0.7	0.4	0.5	0.7	0.5
APATITE	0.1	0.2	0.2	0.6	0.1	0.5	0.5	0.2	0.1	0.5	0.1	0.1
WATER	0.9	0.6	1.0	1.5	1.2	1.0	1.1	1.5	1.0	1.1	1.0	1.3
DIFF. INDEX	83.6	85.0	87.8	83.2	87.8	81.6	87.3	80.7	91.6	86.4	89.0	90.2
NA/(NA+K)	0.69	0.78	0.68	0.63	0.67	0.77	0.65	0.69	0.64	0.66	0.70	0.69
(NA+K)/AL	1.03	1.05	0.99	0.88	0.91	1.06	0.97	1.01	0.94	0.96	0.96	0.96
F3/(F2+F3)	0.54	0.75	0.59	0.72	0.53	0.55	0.40	0.54	0.52	0.26	0.48	0.41

E. UPPER SERIES. 'FELSIC SYENITES'

NORMCAL .. R.C.O.GILL

SUMMARY NORM TABLE

	27181U	27185	27194	27205	27207	27209	27221	27227	27228	27234	27235	39705
CORUNDUM	0.0	0.0	0.0	0.0	0.0	0.1	0.0	0.0	0.0	0.0	0.0	0.0
ZIRCON	0.1	0.1	0.2	0.1	0.2	0.2	0.2	0.1	0.1	0.1	0.1	0.1
ORTHOCLASE	34.6	42.0	36.6	36.4	38.4	36.2	36.3	36.4	36.7	31.8	32.5	36.1
ALBITE	27.6	23.5	26.6	24.3	27.9	29.4	28.9	26.8	19.1	16.3	15.3	24.7
ANORTHITE	7.6	2.1	3.0	3.6	3.6	5.3	6.4	6.2	3.4	0.0	0.0	3.8
NEPHELINE	22.7	26.8	20.7	24.5	20.2	20.5	21.5	23.1	33.6	40.0	38.1	25.8
ACMITE	0.0	0.0	0.0	0.0	0.0	0.0	0.0	0.0	0.0	5.7	7.0	0.0
SOD METASIL	0.0	0.0	0.0	0.0	0.0	0.0	0.0	0.0	0.0	0.8	1.3	0.0
DIOPSIDE	0.0	0.7	3.0	2.4	1.3	0.0	0.2	0.6	1.6	3.5	3.9	1.5
WOLLASTONITE	0.0	0.8	0.9	1.2	0.8	0.0	0.0	0.0	0.0	0.0	0.0	0.7
OLIVINE	0.7	0.0	0.0	0.0	0.0	1.1	0.3	0.5	0.0	1.2	1.2	0.0
MAGNETITE	4.8	3.7	7.9	5.9	5.3	6.5	4.8	5.3	4.8	0.0	0.0	6.1
HEMATITE	0.8	0.0	0.0	0.7	1.4	0.0	1.0	0.0	0.0	0.0	0.0	0.2
ILMENITE	0.4	0.2	0.6	0.4	0.3	0.4	0.3	0.5	0.4	0.4	0.4	0.4
APATITE	0.6	0.2	0.5	0.6	0.4	0.3	0.1	0.4	0.2	0.1	0.1	0.5
WATER	1.5	0.9	0.9	0.8	1.0	1.8	2.5	1.5	1.1	1.4	1.5	0.9
DIFF. INDEX	84.9	92.3	83.9	85.1	86.6	86.0	86.7	86.2	89.4	88.2	86.0	86.7
NA/(NA+K)	0.68	0.65	0.65	0.67	0.64	0.66	0.67	0.67	0.70	0.77	0.76	0.68
(NA+K)/AL	0.88	0.97	0.95	0.94	0.94	0.91	0.89	0.90	0.95	1.08	1.12	0.94
F3/(F2+F3)	0.71	0.66	0.66	0.70	0.75	0.63	0.73	0.66	0.66	0.51	0.55	0.68

E. UPPER SERIES. 'FELSIC SYENITES'

NORMCAL .. R.C.O.GILL

SUMMARY NORM TABLE

	39706A	39706B	39736A	39749	39759	58315	126710	126710	126727
CORUNDUM	0.0	0.0	0.0	0.0	0.0	0.0	0.0	0.0	3.7
ZIRCON	0.1	0.0	0.0	0.1	0.2	0.1	0.1	0.2	0.3
ORTHOCLASE	40.6	38.1	38.1	36.8	36.0	35.8	39.8	36.4	36.4
ALBITE	22.2	24.0	23.4	31.9	26.2	29.7	21.4	23.9	40.1
ANORTHITE	5.3	3.5	1.8	5.6	0.0	3.5	1.6	1.2	4.6
NEPHELINE	22.8	24.4	31.4	14.7	24.1	23.5	31.2	23.4	5.6
ACMITE	0.0	0.0	0.0	0.0	5.1	0.0	0.0	0.0	0.0
DIOPSIDE	0.2	0.2	1.4	0.0	1.5	1.3	0.7	5.5	0.0
WOLLASTONITE	0.0	0.0	0.0	0.0	2.2	0.1	0.8	1.0	0.0
OLIVINE	2.6	4.5	0.6	4.1	0.0	0.0	0.0	0.0	0.4
MAGNETITE	5.1	4.4	3.0	5.7	4.1	3.2	3.7	7.5	6.5
HEMATITE	0.0	0.0	0.0	0.0	0.0	2.1	0.3	0.0	1.4
ILMENITE	0.5	0.5	0.2	0.6	0.3	0.3	0.2	0.4	0.9
APATITE	0.6	0.5	0.1	0.4	0.1	0.2	0.2	0.5	0.1
WATER	1.2	0.9	0.6	1.8	0.4	0.9	0.5	0.7	2.0
DIFF. INDEX	85.7	86.4	92.8	83.5	86.4	89.0	92.4	83.7	82.1
NA/(NA+K)	0.63	0.66	0.69	0.63	0.69	0.68	0.68	0.66	0.60
(NA+K)/AL	0.91	0.94	0.97	0.90	1.06	0.94	0.97	0.98	0.75
F3/(F2+F3)	0.52	0.39	0.56	0.47	0.77	0.80	0.70	0.60	0.71

E. UPPER SERIES. 'LESS MAFIC SYENITES'

NORMCAL .. R.C.O.GILL

SUMMARY NORM TABLE

	27108	27165B	27181L	27182*	27186	27192	27254	27261	126711
CORUNDUM	0.0	4.2	0.0	0.0	11.2	0.0	0.0	0.0	0.0
ZIRCON	0.1	0.1	0.2	0.2	0.1	0.2	0.2	0.1	0.3
ORTHOCLASE	30.8	42.1	29.0	34.0	47.7	31.2	30.5	33.0	31.1
ALBITE	24.3	30.5	27.3	25.1	25.6	16.7	27.6	28.6	32.8
ANORTHITE	5.3	5.9	7.9	1.0	4.3	0.0	4.9	11.4	6.7
NEPHELINE	16.3	0.0	17.7	19.1	3.9	26.3	14.3	9.8	10.3
ACMITE	0.0	0.0	0.0	0.0	0.0	1.9	0.0	0.0	0.0
DIOPSIDE	6.8	0.0	6.7	9.7	0.0	15.0	8.1	5.7	3.5
WOLLASTONITE	3.7	0.0	0.0	2.2	0.0	0.0	0.0	0.0	1.8
HYPERSTHENE	0.0	11.7	0.0	0.0	0.0	0.0	0.0	0.0	0.0
OLIVINE	0.0	1.5	0.5	0.0	4.7	0.3	2.9	0.2	0.0
MAGNETITE	4.7	2.9	8.9	6.8	2.1	5.7	7.6	8.1	9.4
HEMATITE	4.4	0.0	0.0	0.0	0.0	0.0	0.0	0.0	2.2
ILMENITE	0.7	0.8	0.7	0.5	0.3	0.6	1.4	0.5	0.5
APATITE	3.0	0.2	1.1	1.5	0.1	2.1	2.7	2.5	1.4
WATER	1.0	2.4	1.6	1.4	2.5	0.6	1.6	2.0	1.5
DIFF. INDEX	71.3	72.6	74.0	78.2	77.2	74.1	72.3	71.4	74.3
NA/(NA+K)	0.65	0.44	0.69	0.65	0.42	0.70	0.65	0.60	0.64
(NA+K)/AL	0.89	0.68	0.85	0.98	0.54	1.02	0.90	0.78	0.86
F3/(F2+F3)	0.82	0.20	0.59	0.54	0.26	0.45	0.47	0.66	0.74

E. UPPER SERIES. 'MAFIC SYENITES'

NORMCAL .. R.C.O.GILL

SUMMARY NORM TABLE

	27046	27107	27179	27181M	27193	27259	39736B	126708
ZIRCON	0.2	0.1	0.2	0.4	0.3	0.2	0.3	0.2
ORTHOCLASE	30.6	30.0	23.9	21.9	0.0	23.1	24.6	23.1
ALBITE	25.8	21.2	22.0	20.8	0.0	19.3	21.9	23.5
ANORTHITE	0.0	5.3	1.7	5.5	0.0	1.7	0.0	14.5
LEUCITE	0.0	0.0	0.0	0.0	9.2	0.0	0.0	0.0
NEPHELINE	13.3	17.9	18.7	14.2	17.3	24.5	22.3	8.5
ACMITE	0.0	0.0	0.0	0.0	26.5	0.0	1.7	0.0
DIOPSIDE	12.8	14.5	19.3	12.0	19.1	20.2	18.8	13.6
WOLLASTONITE	1.5	0.0	1.4	1.8	0.0	0.0	1.6	0.0
OLIVINE	0.0	0.1	0.0	0.0	12.5	0.6	0.0	0.8
CAL ORTHOSIL	0.0	0.0	0.0	0.0	6.1	0.0	0.0	0.0
MAGNETITE	10.4	6.3	9.1	19.6	7.3	6.4	6.0	11.3
ILMENITE	1.6	0.7	0.9	1.8	1.6	0.5	0.2	0.9
APATITE	3.8	4.0	2.8	2.2	0.1	3.6	2.6	3.7
WATER	1.1	0.7	1.9	1.6	0.8	1.0	0.4	1.7
DIFF. INDEX	69.7	69.0	64.6	56.9	26.5	66.9	68.8	55.0
NA/(NA+K)	0.64	0.66	0.71	0.70	0.85	0.75	0.74	0.64
(NA+K)/AL	1.00	0.89	0.96	0.87	1.70	0.96	1.02	0.69
F3/(F2+F3)	0.58	0.47	0.47	0.63	0.58	0.39	0.43	0.54

F. COARSE-GRAINED SYENITE

NORMCAL .. R.C.D.GILL

SUMMARY NORM TABLE

	27065	27067	27114	27280	27285	27287	126721
ZIRCON	0.1	0.1	0.1	0.1	0.1	0.2	0.2
ORTHOCLASE	27.3	31.2	30.7	31.0	12.4	34.2	31.6
ALBITE,	0.0	20.8	23.5	11.8	16.6	2.9	15.8
ANORTHITE	0.0	1.4	8.3	0.0	0.0	0.0	1.2
LEUCITE	3.3	0.0	0.0	0.0	0.0	0.0	0.0
NEPHELINE	41.9	30.9	20.2	25.1	52.8	47.8	34.4
ACMITE	10.5	0.0	0.0	3.7	9.9	6.6	0.0
SOD METASIL	0.0	0.0	0.0	0.0	0.8	0.0	0.0
DIOPSIDE	14.4	3.1	7.6	16.6	6.4	7.0	6.1
WOLLASTONITE	1.9	3.6	0.0	2.0	0.0	0.0	1.3
OLIVINE	0.0	0.0	0.5	0.0	0.3	0.3	0.0
MAGNETITE	0.1	4.2	6.4	5.8	0.0	0.2	6.9
HEMATITE	0.0	2.6	0.0	0.0	0.0	0.0	0.0
ILMENITE	0.2	0.6	0.5	0.8	0.4	0.3	0.6
APATITE	0.4	1.5	2.1	3.1	0.2	0.5	1.9
WATER	2.0	1.1	0.7	1.0	1.7	2.2	0.9
DIFF. INDEX	72.5	82.9	74.4	67.9	81.9	84.9	81.8
NA/(NA+K)	0.75	0.73	0.68	0.68	0.92	0.75	0.73
(NA+K)/AL	1.11	0.98	0.85	1.05	1.12	1.06	0.98
F3/(F2+F3)	0.53	0.79	0.56	0.53	0.64	0.56	0.63

G. XENOLITHIC PORPHYRITIC SYENITE

NORMCAL .. R.C.O.GILL

SUMMARY NORM TABLE

	27189	31841	31846	31854	58314	58316	58317	58320
ZIRCON	0.3	0.3	0.3	0.2	0.2	0.2	0.3	0.3
ORTHOCLASE	26.7	31.5	29.0	28.5	31.0	31.3	29.0	31.2
ALBITE	34.6	31.0	17.9	13.0	36.7	29.2	28.9	30.1
ANORTHITE	0.0	6.1	0.0	0.0	4.7	1.5	3.6	0.0
NEPHELINE	19.7	15.3	28.8	32.1	14.6	25.8	23.6	23.4
ACMITE	0.0	0.0	11.5	11.9	0.0	0.0	0.0	0.3
DIOPSIDE	1.6	2.9	2.3	8.0	2.2	3.2	2.1	2.4
WOLLASTONITE	6.5	3.6	5.4	1.8	1.4	2.0	3.0	3.5
MAGNETITE	2.5	4.5	1.7	3.1	8.5	5.0	5.3	5.3
HEMATITE	6.6	3.3	2.1	0.0	0.0	0.9	3.0	2.5
ILMENITE	0.4	0.4	0.4	0.8	0.4	0.6	0.4	0.4
APATITE	1.0	1.1	0.6	0.6	0.2	0.3	0.8	0.7
WATER	1.5	1.9	1.2	1.9	1.5	1.9	2.0	1.6
DIFF. INDEX	81.0	77.7	75.8	73.6	82.4	86.3	81.5	84.7
NA/(NA+K)	0.74	0.67	0.75	0.76	0.69	0.72	0.73	0.71
(NA+K)/AL	1.00	0.88	1.13	1.14	0.91	0.97	0.94	1.00
F3/(F2+F3)	0.92	0.82	0.94	0.73	0.66	0.70	0.79	0.78

H. SYENITE AND MICROSYENITE DYKES - GROUP 1

NORMCAL .. R.C.D.GILL

SUMMARY NORM TABLE

	27119	27128	27178	27200	39711	126712
CORUNDUM	0.0	1.8	0.5	0.0	1.9	0.1
ZIRCON	0.0	0.0	0.1	0.1	0.1	0.0
ORTHOCLASE	42.7	37.1	37.0	37.3	36.6	40.4
ALBITE	13.2	25.6	22.7	16.8	29.4	23.2
ANORTHITE	2.1	6.1	4.3	0.0	5.8	4.9
NEPHELINE	30.9	22.3	29.3	28.8	16.7	24.9
ACMITE	0.0	0.0	0.0	5.3	0.0	0.0
DIOPSIDE	3.7	0.0	0.0	5.0	0.0	0.0
OLIVINE	4.4	2.3	0.5	2.4	0.7	1.2
MAGNETITE	2.1	4.0	4.2	3.3	5.1	4.5
HEMATITE	0.0	0.0	0.8	0.0	2.6	0.0
ILMENITE	0.4	0.3	0.3	0.5	0.5	0.4
APATITE	0.5	0.4	0.4	0.4	0.5	0.3
WATER	0.6	1.3	0.8	0.7	1.2	1.1
DIFF. INDEX	86.8	85.0	88.9	83.0	82.7	88.5
NA/(NA+K)	0.64	0.66	0.69	0.68	0.64	0.65
(NA+K)/AL	0.97	0.83	0.91	1.06	0.82	0.91
F3/(F2+F3)	0.23	0.50	0.71	0.51	0.77	0.59

H. SYENITE AND MICROSYENITE DYKES - GROUP 2

NORMCAL .. R.C.O.GILL

SUMMARY NORM TABLE

	27086	27173	27275	39710
ZIRCON	0.0	0.0	0.1	0.5
ORTHOCLASE	34.8	39.6	29.0	25.3
ALBITE	29.5	21.9	34.6	14.2
ANORTHITE	3.6	5.2	3.9	0.0
NEPHELINE	20.8	24.9	20.5	35.5
ACMITE	0.0	0.0	0.0	9.0
DIOPSIDE	2.4	0.3	4.9	8.4
WOLLASTONITE	0.0	0.0	0.0	1.3
OLIVINE	3.6	2.2	0.1	0.0
MAGNETITE	4.0	5.0	6.5	5.4
ILMENITE	0.6	0.5	0.3	0.3
APATITE	0.5	0.5	0.1	0.0
WATER	0.5	0.7	0.9	0.1
DIFF. INDEX	85.1	86.4	84.1	75.0
NA/(NA+K)	0.67	0.64	0.73	0.79
(NA+K)/AL	0.94	0.92	0.93	1.10
F3/(F2+F3)	0.38	0.53	0.57	0.63

H. SYENITE AND MICROSYENITE DYKES - GROUP 3

NORMCAL .. R.C.O.GILL

SUMMARY NORM TABLE

	31803	39740	39753A	39753B
ZIRCON	0.3	0.2	0.1	0.1
ORTHOCLASE	34.4	33.4	42.3	40.7
ALBITE	27.5	40.0	23.1	20.3
ANORTHITE	0.0	0.1	4.6	2.9
NEPHELINE	20.9	14.2	19.5	25.7
ACMITE	7.6	0.0	0.0	0.0
DIOPSIDE	1.8	2.0	0.5	2.4
WOLLASTONITE	0.8	0.8	0.0	0.0
OLIVINE	0.0	0.0	3.9	2.7
MAGNETITE	4.7	8.7	4.8	4.0
HEMATITE	1.4	0.0	0.0	0.0
ILMENITE	0.3	0.3	0.7	0.7
APATITE	0.2	0.2	0.5	0.5
WATER	0.6	0.8	0.9	0.4
DIFF. INDEX	82.8	87.5	85.0	86.8
NA/(NA+K)	0.70	0.68	0.60	0.64
(NA+K)/AL	1.09	1.00	0.92	0.95
F3/(F2+F3)	0.83	0.67	0.43	0.43

H. SYENITE AND MICROSYENITE DYKES – GROUP 4

NORMCAL .. R.C.O.GILL

SUMMARY NORM TABLE

	27068	27082	27156	39742	39777	58318	126715
ZIRCON	0.1	0.1	0.2	0.1	0.1	0.1	0.2
ORTHOCLASE	45.9	37.0	36.0	38.8	36.9	33.9	32.9
ALBITE	9.7	27.5	24.3	24.1	24.7	2.8	28.2
ANORTHITE	1.2	5.4	0.0	2.8	3.8	0.0	1.7
NEPHELINE	31.9	22.5	22.9	21.2	24.0	35.6	22.0
ACMITE	0.0	0.0	1.3	0.0	0.0	8.4	0.0
DIOPSIDE	2.7	0.0	7.8	4.1	4.7	9.0	2.9
WOLLASTONITE	2.1	0.0	0.0	0.0	0.2	6.3	3.1
OLIVINE	0.0	0.8	1.2	1.1	0.0	0.0	0.0
MAGNETITE	5.2	5.9	5.7	6.9	4.0	3.0	4.2
HEMATITE	0.0	0.0	0.0	0.0	0.0	0.0	3.4
ILMENITE	0.5	0.6	0.5	0.5	0.8	0.2	0.7
APATITE	0.8	0.3	0.2	0.5	0.6	0.7	0.6
WATER	1.0	0.5	0.6	1.2	2.3	1.9	3.1
DIFF. INDEX	87.5	86.9	83.2	84.0	85.7	72.4	83.1
NA/(NA+K)	0.61	0.66	0.67	0.63	0.66	0.71	0.69
(NA+K)/AL	0.98	0.91	1.01	0.95	0.93	1.09	0.97
F3/(F2+F3)	0.64	0.63	0.48	0.55	0.55	0.70	0.80

H. SYENITE AND MICROSYENITE DYKES – GROUP 5

NORMCAL .. R.C.O.GILL

SUMMARY NORM TABLE

	39770	39771
ZIRCON	0.0	0.2
ORTHOCLASE	39.9	33.8
ALBITE	21.8	30.6
ANORTHITE	2.4	5.3
NEPHELINE	24.6	20.3
DIOPSIDE	2.8	0.7
OLIVINE	4.0	0.5
MAGNETITE	3.2	7.3
HEMATITE	0.0	0.4
ILMENITE	0.8	0.5
APATITE	0.5	0.5
WATER	0.9	0.7
DIFF. INDEX	86.3	84.7
NA/(NA+K)	0.64	0.68
(NA+K)/AL	0.96	0.91
F3/(F2+F3)	0.33	0.68

I. WELL PRESERVED PHONOLITE DYKES.

NORMCAL .. R.C.O.GILL

SUMMARY NORM TABLE

	27007	27058	27151	27183	31821+	39691	39730+	39731A	39731B	39735+	39751	39762
ZIRCON	0.7	0.6	0.8	0.4	0.5	0.8	0.4	0.5	0.6	0.4	0.9	0.7
ORTHOCLASE	25.8	18.7	8.9	33.0	27.8	25.9	28.9	28.5	26.6	28.6	26.9	26.5
ALBITE	35.7	42.1	48.2	28.4	33.7	26.4	35.0	32.0	34.3	36.7	29.6	32.2
NEPHELINE	27.2	24.1	26.1	19.3	24.2	30.0	24.1	20.5	22.8	24.2	26.0	27.8
ACMITE	7.8	10.9	10.3	3.1	5.8	11.5	5.2	4.4	7.4	1.7	13.1	8.5
SOD METASIL	0.0	0.0	3.4	0.0	0.0	2.8	0.0	0.0	0.0	0.0	0.6	1.1
DIOPSIDE	2.0	1.2	2.0	9.4	1.0	2.4	0.8	6.6	2.7	1.1	2.3	2.7
WOLLASTONITE	0.1	0.8	0.0	0.0	3.0	0.2	2.1	0.5	1.3	2.2	0.0	0.0
OLIVINE	0.0	0.0	0.2	0.5	0.0	0.0	0.0	0.0	0.0	0.0	0.4	0.3
MAGNETITE	0.8	1.7	0.0	4.2	0.9	0.0	1.7	5.2	3.4	1.5	0.0	0.0
HEMATITE	0.0	0.0	0.0	0.0	2.9	0.0	1.7	0.0	0.0	3.4	0.0	0.0
ILMENITE	0.0	0.1	0.0	1.0	0.0	0.0	0.0	1.0	0.5	0.0	0.1	0.0
APATITE	0.0	0.0	0.0	0.8	0.1	0.0	0.1	0.8	0.4	0.1	0.1	0.1
WATER	4.5	4.8	3.6	2.8	4.4	4.1	4.6	3.5	4.0	4.6	3.1	4.1
DIFF. INDEX	88.7	84.8	83.2	80.6	85.7	82.4	88.0	81.1	83.7	89.5	82.6	86.6
NA/(NA+K)	0.80	0.85	0.94	0.68	0.76	0.81	0.76	0.74	0.77	0.76	0.79	0.80
(NA+K)/AL	1.08	1.12	1.25	1.04	1.06	1.24	1.06	1.05	1.08	1.02	1.17	1.13
F3/(F2+F3)	0.89	0.94	0.94	0.49	0.99	0.97	0.95	0.65	0.79	0.95	0.94	0.83

I. WELL PRESERVED PHONOLITE DYKES.

NORMCAL .. R.C.O.GILL

SUMMARY NORM TABLE

	39779+	39792+	39794
ZIRCON	0.8	0.3	0.7
ORTHOCLASE	27.0	31.0	21.6
ALBITE	32.0	31.0	32.7
NEPHELINE	27.6	23.8	29.3
ACMITE	8.8	4.0	9.6
SOD METASIL	0.5	0.0	3.8
DIOPSIDE	2.7	4.9	1.6
WOLLASTONITE	0.0	1.9	0.0
OLIVINE	0.5	0.0	0.5
MAGNETITE	0.0	3.0	0.0
ILMENITE	0.0	0.0	0.0
APATITE	0.1	0.1	0.1
WATER	4.6	4.2	4.7
DIFF. INDEX	86.6	85.8	83.6
NA/(NA+K)	0.79	0.73	0.85
(NA+K)/AL	1.11	1.04	1.25
F3/(F2+F3)	0.81	0.63	0.90

J. SEVERELY ALTERED PHONOLITE-LIKE DYKES.

NORMCAL .. R.C.O.GILL

SUMMARY NORM TABLE

	31818A	31822	31825	39689	39781	39783	39798	39800
QUARTZ	0.0	1.0	1.4	3.5	4.8	2.1	2.2	3.8
CORUNDUM	0.0	1.2	1.2	2.6	5.3	2.0	0.4	2.3
ZIRCON	0.5	0.6	0.5	0.6	0.4	0.6	0.5	0.6
ORTHOCLASE	34.2	37.0	36.2	37.1	37.4	35.5	35.4	35.3
ALBITE	45.2	43.0	47.7	43.7	46.4	47.1	48.5	47.5
ANORTHITE	7.6	10.3	6.7	6.9	0.0	5.2	5.8	4.3
NEPHELINE	1.6	0.0	0.0	0.0	0.0	0.0	0.0	0.0
DIOPSIDE	0.9	0.0	0.0	0.0	0.0	0.0	0.0	0.0
WOLLASTONITE	3.0	0.0	0.0	0.0	0.0	0.0	0.0	0.0
HYPERSTHENE	0.0	0.6	0.4	0.6	0.4	3.0	0.7	0.6
MAGNETITE	0.9	1.8	0.4	3.0	2.4	3.9	5.1	3.7
HEMATITE	5.6	4.5	5.2	1.8	2.8	0.0	1.1	1.6
ILMENITE	0.2	0.0	0.1	0.1	0.0	0.3	0.3	0.1
APATITE	0.3	0.1	0.1	0.1	0.0	0.2	0.1	0.1
WATER	0.7	1.0	1.1	2.8	1.3	1.3	0.6	1.1
DIFF. INDEX	81.0	80.9	85.4	84.3	88.6	84.7	86.1	86.6
NA/(NA+K)	0.60	0.55	0.58	0.56	0.57	0.58	0.59	0.59
(NA+K)/AL	0.85	0.75	0.81	0.75	0.75	0.80	0.86	0.80
F3/(F2+F3)	0.99	0.91	0.96	0.82	0.87	0.50	0.73	0.79

K. LAMPROPHYRIC DYKES.

NORMCAL .. R.C.O.GILL

SUMMARY NORM TABLE

	27015	27030	27049Q	27109+	27139	27148+	27172+	31865+	31870	31878	39717Q	39734+
CORUNDUM	0.0	0.0	0.0	0.0	0.0	0.5	0.0	0.0	0.0	0.0	0.0	0.0
ZIRCON	0.1	0.1	0.4	0.1	0.1	0.1	0.1	0.1	0.1	0.1	0.1	0.1
ORTHOCLASE	13.8	16.8	20.9	22.1	20.6	14.9	17.8	17.9	13.9	17.0	5.4	16.7
ALBITE	35.5	22.6	0.0	29.0	35.2	35.8	42.1	29.3	36.3	18.0	27.9	31.9
ANORTHITE	15.9	15.1	13.8	10.8	11.9	14.4	12.9	16.0	15.3	16.8	14.0	11.9
LEUCITE	0.0	0.0	9.6	0.0	0.0	0.0	0.0	0.0	0.0	0.0	0.0	0.0
NEPHELINE	0.0	2.6	12.6	5.3	0.4	0.0	1.4	0.0	0.0	2.4	5.3	4.1
DIOPSIDE	2.5	12.7	17.8	10.1	3.1	0.0	8.7	5.3	3.6	11.9	24.4	10.9
HYPERSTHENE	1.1	0.0	0.0	0.0	0.0	12.7	0.0	6.4	1.9	0.0	0.0	0.0
OLIVINE	15.4	16.2	13.5	10.6	14.3	7.0	5.5	11.3	13.8	21.2	8.9	8.4
MAGNETITE	5.6	5.0	5.2	4.3	5.1	5.2	5.9	4.3	5.3	4.5	7.1	7.9
ILMENITE	5.6	7.4	5.8	4.3	5.0	5.1	3.3	5.3	5.4	6.8	5.7	4.7
APATITE	4.5	1.4	0.4	3.4	4.2	4.4	2.1	4.2	4.4	1.4	1.2	3.4
WATER	2.0	1.3	1.9	1.3	1.0	2.0	1.9	1.7	1.7	2.1	1.7	2.1
DIFF. INDEX	49.3	42.0	43.1	56.4	56.2	50.6	61.3	47.2	50.2	37.4	38.7	52.7
NA/(NA+K)	0.73	0.63	0.43	0.65	0.65	0.72	0.73	0.64	0.73	0.58	0.88	0.72
(NA+K)/AL	0.62	0.60	0.68	0.75	0.71	0.63	0.72	0.61	0.63	0.55	0.62	0.71
F3/(F2+F3)	0.26	0.24	0.29	0.23	0.25	0.24	0.35	0.21	0.25	0.22	0.30	0.36

L. BIOTITE TRACHYTES.

NORMCAL .. R.C.O.GILL

SUMMARY NORM TABLE

	27036	27081	39750	39755	39756	39775	39797	39799
QUARTZ	1.7	0.0	1.0	0.0	0.0	0.3	0.0	0.0
ZIRCON	0.1	0.2	0.2	0.2	0.2	0.2	0.2	0.2
ORTHOCLASE	29.5	30.1	32.2	33.2	35.0	29.8	29.3	33.1
ALBITE	49.7	45.6	45.1	47.4	41.2	48.8	48.8	47.8
ANORTHITE	6.9	2.8	7.0	5.3	1.7	7.5	7.6	6.3
NEPHELINE	0.0	5.9	0.0	0.0	6.3	0.0	0.0	0.3
DIOPSIDE	1.5	6.8	2.0	4.2	8.7	3.6	4.0	0.6
HYPERSTHENE	3.2	0.0	3.6	0.9	0.0	3.3	0.5	0.0
OLIVINE	0.0	2.7	0.0	1.3	0.3	0.0	2.3	5.0
MAGNETITE	5.2	4.4	6.9	5.8	4.9	5.0	5.8	5.3
ILMENITE	1.6	1.1	1.5	1.3	1.3	1.3	1.0	1.1
APATITE	0.6	0.3	0.4	0.4	0.4	0.4	0.5	0.5
WATER	1.1	1.2	1.7	1.1	1.1	1.0	1.5	1.2
DIFF. INDEX	80.9	81.6	78.3	80.6	82.5	78.8	78.1	81.2
NA/(NA+K)	0.64	0.67	0.60	0.60	0.62	0.63	0.64	0.61
(NA+K)/AL	0.86	0.94	0.85	0.89	0.96	0.84	0.84	0.87
F3/(F2+F3)	0.44	0.36	0.50	0.47	0.44	0.44	0.46	0.40

L. BIOTITE-RIEBECKITE TRACHYTES.

NORMCAL .. R.C.O.GILL

SUMMARY NORM TABLE

	27037	31848	39733	39752	39754	39790	39795
QUARTZ	6.3	4.0	3.5	3.3	4.3	0.6	4.7
ZIRCON	0.3	0.3	0.2	0.3	0.3	0.1	0.3
ORTHOCLASE	32.0	28.7	32.4	33.2	32.2	24.4	31.6
ALBITE	50.9	55.8	47.5	51.3	51.6	50.3	52.8
ANORTHITE	0.5	0.0	0.0	0.0	0.0	1.1	0.6
ACMITE	0.0	1.5	4.9	1.7	1.2	0.0	0.0
DIOPSIDE	2.0	1.7	3.1	3.5	2.8	10.7	3.3
WOLLASTONITE	0.0	0.6	1.0	0.4	0.0	0.3	0.0
HYPERSTHENE	0.0	0.0	0.0	0.0	1.3	0.0	0.1
MAGNETITE	6.6	3.8	6.1	5.4	5.8	8.6	6.3
HEMATITE	0.4	2.7	0.0	0.0	0.0	0.0	0.0
ILMENITE	0.7	0.7	1.0	0.7	0.2	2.6	0.2
APATITE	0.2	0.2	0.2	0.2	0.2	1.3	0.2
WATER	0.8	0.9	0.9	1.0	0.8	1.0	0.8
DIFF. INDEX	89.2	88.5	83.4	87.8	88.1	75.2	89.1
NA/(NA+K)	0.63	0.68	0.63	0.63	0.64	0.69	0.64
(NA+K)/AL	0.99	1.02	1.07	1.02	1.02	0.97	0.99
F3/(F2+F3)	0.67	0.80	0.66	0.62	0.59	0.52	0.67

REFERENCES

REFERENCES

ABBOTT, M.J. 1967: K and Rb in a continental alkaline igneous suite. Geochim. Cosmochim. Acta 31, 1035-1041.

ANDERMAN, G. and KEMP, J.W. 1958: Scattered X-rays as internal standards in X-ray emission spectroscopy. Anal. Chem. 30, 1306-1309.

AZAMBRE, B. and GIROD, M. 1966: Phonolites agpaitiques Bull. Soc. franç. Minér. Crist. 89, 514-520.

BAILEY, D.K. 1964: Crustal warping - a possible tectonic control of alkaline magmatism. J. Geophys. Res. 69, 1103-1111.

BAILEY, D.K. 1969: The stability of acmite in the presence of H_2O. Amer. J. Sci. (Schairer vol.) 267-A, 1-16.

BAILEY, D.K. and MACDONALD, R. 1969: Alkali feldspar fractionation trends and the derivation of peralkaline liquids. Amer. J. Sci. 267, 242-248.

BAILEY, D.K. and SCHAIRER, J.F. 1964: Feldspar-liquid equilibria in peralkaline liquids - the orthoclase effect. Amer. J. Sci. 262, 1198-1206.

BAILEY, D.K. and SCHAIRER, J.F. 1966: The system Na_2O-Al_2O_3-Fe_2O_3-SiO_2 at 1 atmosphere, and the petrogenesis of alkaline rocks. J. Petrol. 7, 114-170.

BAKER, B.H., WILLIAMS, L.A.J., MILLER, J.A. and FITCH, F.J. 1971: Sequence and geochronology of the Kenya rift volcanics. Tectonophysics 11, 191-215.

BAKER, P.E., GASS, I.G., HARRIS, P.G. and Le MAITRE, R.W. 1964: The volcanological report of the Royal Society Expedition to Tristan da Cunha 1962. Phil. Trans. Roy. Soc. A 256, 439-578.

BERTHELSEN, A. and NOE-NYGAARD, A. 1965: The Precambrian of Greenland In: RANKAMA, K. (editor) The Geologic Systems: The Precambrian vol.2, pp.113-262. New York, Interscience Publishers.

BORDET, P., FREULON, J.M. and LEFRANC, J.P. 1955: Phonolite à eudialyte du Jebel Fezzan. Bull. Soc. franç. Minér. Crist. 76, 425-431.

BORGEN, B.I. 1967: Analytical procedures used in the Geochemical Laboratory of the Survey. Rapp. Grønlands geol. Unders. nr. 10.

BRIDGWATER, D. 1965: Isotopic age determinations from South Greenland and their geological setting. Bull. Grønlands geol. Unders. 53. (Medd.Grønland 179 nr.4).

BRIDGWATER, D. and HARRY, W.T. 1968: Anorthosite xenoliths and plagioclase megacrysts in Precambrian intrusions of South Greenland. Bull. Grønlands geol. Unders. 77 (Medd. Grønland 185 nr.2).

CALLISEN, K. 1943: Igneous rocks of the Ivigtût region, Greenland. Part I. The nepheline syenites of the Grønne Dal-Îka area. Medd. Grønland 131 nr.8.

CARMICHAEL, I.S.E. 1963: The crystallisation of feldspar in volcanic acid rocks. Quart. J. Geol. Soc. London 119, 95-131.

CATTELL, R.B. 1965a: Factor analysis: an introduction to essentials. I. The purpose and underlying models. Biometrics 21, 190-215.

CATTELL, R.B. 1965b: Factor analysis: an introduction to essentials. II The role of factor analysis in research. Biometrics 21, 405-435.

CHAYES, F. 1963a: On the relative scarcity of intermediate members in the Oceanic Basalt-Trachyte Association. Carnegie Instn. Wash. Year Book 61, 121-123.

CHAYES, F. 1963b: Relative abundance of intermediate members of the oceanic basalt-trachyte association. J. Geophys. Res. 68, 1519-1534.

COOMBS, D.S. and WILKINSON, J.F.G. 1969: Lineages and fractionation trends in undersaturated volcanic rocks from the East Otago Volcanic Province (New Zealand) and related rocks. J. Petrol. 10, 440-501.

COX, K.G., GASS, I.G. and MALLICK, D.I.J. 1970: The peralkaline volcanic suite of Aden and Little Aden, South Arabia. J. Petrol. 11, 433-462.

CUNDARI, A. and Le MAITRE, R.W. 1970: On the petrogeny of the leucite-bearing rocks of the Roman and Birunga volcanic regions. J. Petrol. 11, 33-47.

CURRIE, K.L. 1971: A study of potash fenitisation around the Brent Crater, Ontario - a Paleozoic alkaline complex. Canadian J. Earth Sci. 8, 481-497.

DAVIES, O.L. (Editor) 1954: Statistical Methods in Research and Production. London, Oliver and Boyd. Second edition, xi + 292 pp.

DEER, W.A., HOWIE, R.A. and ZUSSMAN, J. 1963: Rock forming Minerals, volume 4: Framework Silicates. London, Longmans, Green and Co. Ltd., x + 435 pp.

ELDER, J.W. 1965: Physical processes in geothermal areas. In: W.H.K. Lee (editor): Terrestrial Heat Flow. Monog. Amer. geophys. Union 8, 211-

ELDER, J.W. 1966: Penetrative convection: its role in volcanism. Bull. Volc. 29, 327-343.

EMELEUS, C.H. 1964: The Grønnedal-Íka alkaline complex, South Greenland. Bull. Grønlands geol. Unders. 45 (Medd. Grønland 172 nr.3).

EMELEUS, C.H. and HARRY, W.T. 1970: The Igaliko nepheline syenite complex. General description. Bull. Grønlands geol. Unders. 85. (Medd. Grønland 186, nr.3).

ERNST, W.G. 1962: Synthesis, stability relations, and occurrence of riebeckite and riebeckite-arfvedsonite solid solutions. J. Geol. 70, 689-736.

EUGSTER, H.P. and YODER, H.S. 1955: The join muscovite-paragonite. Carnegie Instn. Wash. Year Book 54, 124-126.

FERGUSON, J. 1964: Geology of the Ilímaussaq alkaline intrusion, South Greenland. Bull. Grønlands geol. Unders.39. (Medd. Grønland 172, nr.4).

FERGUSON, J. 1970: The significance of the Kakortokite in the evolution of the Ilímaussaq intrusion, South Greenland. Bull. Grønland geol. Unders. 89 (Medd.Grønland 190, nr.1).

FITTON, J.G. and GILL, R.C.O. 1970: The oxidation of ferous iron during mechanical grinding. Geochim. Cosmochim. Acta 34, 518-523. (reproduced in Appendix 1 of this volume).

FLANAGAN, F.G. 1969: United States Geological Survey Standards - II First compilation of data for the new U.S.G.S. rocks. Geochim. Cosmochim. Acta 33, 81-120.

FLEISCHER, M. 1969: United States Geological Survey Standards - I Additional data on rocks G-1 and W-1, 1965-1967. Geochim. Cosmochim. Acta 33, 65-80.

GASS, I.G. 1970: Tectonic and magmatic evolution of the Afro-Arabian dome. In: Clifford, T.N. and Gass, I.G. (editors): African Magmatism and Tectonics. Edinburgh, Oliver and Boyd, pp. 285-300.

GILL, R.C.O. (in press): Chemistry of peralkaline phonolite dykes from the Grønnedal-Íka area, South Greenland. Contr. Mineral. Petrol. 34, 87-100, 1972.

HAMILTON, D.L. and MACKENZIE, W.S. 1965: Phase equilibrium studies in the system $NaAlSiO_4$ (nepheline)-$KAlSiO_4$ (kalsilite)-SiO_2-H_2O. Mineralog. Mag. 34, 214-231.

HAMILTON, D.L., BURNHAM, C.W. and OSBORN, E.F. 1964: The solubility of water and effects of water fugacity and water content on crystallisation in mafic magmas. J. Petrol. 5, 21-39.

HARRIS, P.G. 1967: Segregation processes in the upper mantle. In: S.K. Runcorn (editor): Mantles of the Earth and Terrestrial Planets. London, Interscience, pp.305-317.

HARRIS, P.G. 1969: Basalt type and African rift valley tectonism. Tectonophysics 8, 427-436.

HARRIS, P.G. 1970: Convection and magmatism with reference to the African Continent. In: Clifford, T.N. and Gass, I.G. (editors): African Magmatism and Tectonics. Edinburgh, Oliver and Boyd, pp. 419-437.

HARRIS, P.G., KENNEDY, W.Q. and SCARFE,C.M. 1970: Volcanism versus plutonism - the effect of chemical composition. In: G. Newall and N. Rast (editors): Mechanisms of Igneous Intrusion. Geol. Journal, Special Issue No.2, pp.187-200

HATCH, F.H., WELLS, A.K. and WELLS, M.K. 1961: Petrology of the Igneous Rocks. London, Murby and Co. Twelfth edition, 515pp.

HEIER, K.S. 1966: Some crystallo-chemical relations of nephelines and feldspars on Stjernoy, North Norway. J. Petrol. 7, 95-113.

HEIER, K.S. and ADAMS, J.A.S. 1964: Geochemistry of the alkali metals. Phys. Chem. Earth 5, 253-381.

HEINRICH, E.W. 1966: The Geology of Carbonatites. Chicago, Rand McNally and Co., xiii + 555 + lii pp.

HEINRICH, E.W. and MOORE, D.G. 1970: Metasomatic potash feldspar rocks associated with igneous alkalic complexes. Canad. Mineral. 10, 571-584.

HEINRICH, K.F.J. 1966: X-ray absorption uncertainty. In: McKinley, T.D., Heinrich, K.F.J. and Wittry, D.B. (editors): The Electron Microprobe. New York, Wiley & Sons, pp.296-377.

HENDRICKSON, A.E. and WHITE, P.O. 1964: Promax: a quick method for rotation to oblique simple structure. Brit. J. Statis. Psychol. 17, 65-70.

HOLLAND, J.G. and BRINDLE, D.W. 1966: A self-consistent mass absorption correction for silicate analysis by X-ray fluorescence. Spectrochim. Acta 22, 2083-2093.

HOLMES, A. and HARWOOD, H.F. 1937: The volcanic area of Bufumbira. Part II. Mem. geol. Surv. Uganda 3, 300pp.

JENKINS, R. and DE VRIES, J.L. 1970: Practical X-ray Spectrometry. MacMillan and Co., London. Second Edition, x + 190 pp.

KAISER, H.F. 1958: The Varimax criterion for analytical rotation in factor analysis. Psychometrika 23, 187-200.

KEMPE, D.R.C. and DEER, W.A. 1970: Geological Investigation in East Greenland. Part IX. The Mineralogy of the Kanderdlugssuaq alkaline intrusion, East Greenland. Medd. Grønland 190, nr.3.

KEMPE, D.R.C., DEER, W.A. and WAGER, L.R. 1970: Geological Investigations in East Greenland. Part VIII. The Petrology of the Kangerdlugssuaq alkaline intrusion, East Greenland. Medd. Grønland 190, nr.2.

KIM, K.T. and BURLEY, B.J. 1971a: Phase equilibria in the system $NaAlSi_3O_8$-$NaAlSiO_4$-H_2O with special emphasis on the stability of analcite. Canadian J. Earth Sci. 8, 311-337.

KIM, K.T. and BURLEY, B.J. 1971b: The solubility of water in melts in the system $NaAlSi_3O_8$-$NaAlSiO_4$-H_2O. Canadian J. Earth Sci. 8, 558-571.

KING, B.C. 1965: Petrogenesis of the alkaline igneous rock suites of the volcanic and intrusive centres of eastern Uganda. J. Petrol. 6, 67-100.

KING, B.C. 1970: Vulcanicity and rift tectonics in East Africa. In: Clifford, T.N. and Gass, I.G. (editors): African Magmatism and Tectonics. Edinburgh, Oliver and Boyd, pp.263-283.

KING, B.C. and SUTHERLAND, D.S. 1960: Alkaline rocks of eastern and southern Africa. Sci. Progr. 48, 298-321, 504-523, 709-720 (3 parts).

KODAMA, H., BRYDON, J.E. and STONE, B.C. 1967: X-ray spectrochemical analysis of silicates using synthetic standards with a correction for interelemental effects by a computer method. Geochim. Cosmochim. Acta 31, 649-659.

LE BAS, M.J. and MOHR, P.A. 1968: Feldspathoidal rocks from the Cainozoic volcanic province of Ethiopia. Geol. Rundsch. 58, 273-280.

Le MAITRE, R.W. 1962: Petrology of volcanic rocks, Gough Island, South Atlantic. Geol. Soc. Amer. Bull. 73, 1309-1340.

Le MAITRE, R.W. 1968: Chemical variation within and between rock series - a statistical approach. J. Petrol. 9, 220-252.

LIOU, J.G. 1971: Analcime equilibria. Lithos 4, 389-402.

LUCAS-TOOTH, H.J. and PRICE, B.J. 1961: A mathematical method for the investigation of inter-element effects in X-ray fluorescent analysis. Metallurgia 64, 149-152.

MACDONALD, R. 1969: The petrology of the alkaline dykes from the Tugtutôq area, South Greenland. Medd. dansk geol. Foren. 19, 257-282.

MACDONALD, R., BAILEY, D.K. and SUTHERLAND, D.S. 1970: Oversaturated peralkaline glassy trachytes from Kenya. J. Petrol. 11, 507-517.

McKIE, D. 1966: Fenitisation. In: Tuttle, O.F. and Gittins, J.(editors): Carbonatites. Interscience Publishers, New York, pp.261-294.

McKNOWN, J.S. and MALAIKA, J. 1950: Effects of particle shape on settling velocity at low Reynold's numbers. Amer. geophys. Union Trans. 31, 74-82.

METAIS, D. and CHAYES, F. 1963: Varieties of lamprophyre. Carnegie Instn. Wash Year Book 62, 156-157.

MILLHOLLEN, G.L. 1971: Melting of nepheline syenite with H_2O and H_2O+CO_2, and the effect of dilution of the aqueous phase on the beginning of melting. Amer. J. Sci. 270, 244-254.

MIYASHIRO, A. 1951: The ranges of chemical composition in nepheline and their petrogenetic significance. Geochim. Cosmochim. Acta 1, 278-283.

MOHR, P.A. 1971: Ethiopian rift and plateaus: some volcanic petrochemical differences. J. Geophys. Res. 76, 1967-1984.

MORSE, S.A. 1969: Syenites. Carnegie Instn. Wash. Year Book 67, 112-120.

NASH, W.P., CARMICHAEL, I.S.E. and JOHNSON, R.W. 1969: The mineralogy and petrology of Mount Syswa, Kenya. J. Petrol.10, 409-439.

NOBLE, D.C. 1970: Loss of sodium from crystallised comendite welded tuffs of the Miocene Grouse Canyon member of the Belted Range Tuff, Nevada. Geol. Soc. Amer. Bull 81, 2677-2688.

NOBLE, D.C. and HEDGE, C.E. 1970: Distribution of rubidium between sodic sanidine and natural silicic liquid. Contr. Mineral. Petrol.29, 234-241.

NORRISH, K. and HUTTON, J.T. 1969: An accurate X-ray spectrographic method for the analysis of a wide range of geological samples. Geochim. Cosmochim. Acta 33, 431-453.

O'HARA, M.J. and YODER ,H .S. Jr. 1967: Formation and fractionation of basic magmas at high pressures. Scott. J. Geol. 3, 67-117.

PETERS, Tj., LUTH, W.C. and TUTTLE, O.F. 1966: The melting of analcite solid solutions in the system $NaAlSiO_4$-$NaAlSi_3O_8$-H_2O. Amer. Mineral. 51, 736-753.

PIOTROWSKI, J.M. and EDGAR, A.D. 1970: Melting relations of undersaturated alkali rocks from South Greenland compared to those of Africa and Canada. Medd. Grønland 181, Nr.9.

PRESNALL, D.C. 1969: The geometrical analysis of partial fusion. Amer. J. Sci. 267, 1117-1194.

REEVES, M.J. 1971: Geochemistry and Mineralogy of British Carboniferous Seatearths from Northern Coalfields. Unpublished Ph.D. thesis, University of Durham.

REEVES, M.J. and SAADI, T.A.K. 1971: Factors controlling the deposition of some phosphate bearing strata from Jordan. Econ. Geol. 66, 451-465.

RILEY, J.P. 1958: Simultaneous determination of water and carbon dioxide in rocks and minerals. Analyst 83, 42-49.

SAGGERSON, E.P. 1970: The structural control and genesis of alkaline rocks in Central Kenya. Bull. Volc. 34, 38-76.

SAGGERSON, E.P. and WILLIAMS, L.A.J. 1964: Ngurumanite from southern Kenya and its bearing on the origin of rocks in the Tanganyika alkaline district. J. Petrol. 5, 40-81.

SAHA, P. 1961: The system $NaAlSiO_4$(nepheline)-$NaAlSi_3O_8$(albite)-H_2O. Amer. Mineral. 46, 859-884.

SCHAIRER, J.F. 1950: The alkali feldspar join the system $NaAlSiO_4$-$KAlSiO_4$-SiO_2. J. Geol. 58, 512-517.

SCHAIRER, J.F. and BOWEN, N.L. 1956: The system Na_2O-Al_2O_3-SiO_2. Amer. J. Sci. 254, 129-195.

SCHARBERT, H.G. 1966: The alkali feldspars from microsyenitic dykes of southern Greenland. Mineral. Mag. 35, 903-919.

SHAW, D.M. 1968: A review of K-Rb fractionation trends by covariance analysis. Geochim. Cosmochim. Acta 32, 573-601.

SINE, N.M., TAYLOR, W.O., WEBER, G.R. and LEWIS, C.L. 1969: Third report of analytical data for C.A.A.S. sulphide ore and syenite rock standards. Geochim. Cosmochim. Acta 33, 121-131.

SPENCER, D.W. 1966: Factor analysis. Ref.No. 66-39 Woods Hole Oceanographic Institution, unpublished manuscript.

SPENCER, D.W., DEGENS, E.T. and KULBICKI, G.L. 1968: Geochemical factors governing the distribution of elements in sedimentary rocks. In: L.H. Ahrens (editor): Origin and Distribution of the Elements. UNESCO, Paris.

STEWART, J.W. 1964: The earlier Gardar igneous rocks of the Ilimaussaq area, South Greenland. Unpublished Ph.D. thesis, University of Durham. 423pp.

STEWART, J.W. 1970: Precambrian alkaline ultramafic/carbonatite volcanism at Qagssiarssuk, South Greenland. Bull. Grønlands geol. Unders. 84 (Medd. Grønland 186, nr.4).

SUTHERLAND, D.S. 1965: Nomenclature of the potassic-feldspathic rocks associated with carbonatites. Geol. Soc. Amer. Bull. 76, 1409-1412.

SWEATMAN, T.R. and LONG, J.V.P. 1969: Quantitative electron-probe microanalysis of rock forming minerals. J. Petrol. 10, 332-379.

SØRENSEN, H. 1966: On the magmatic evolution of the alkaline igenous province of South Greenland. Rapp. Grønlands geol. Unders. nr.7.

SØRENSEN, H. 1969: Rhythmic igneous layering in peralkaline intrusions. An essay review on Ilímaussaq (Greenland) and Lovozero (Kola, U.S.S.R.). Lithos 2, 261-283.

TAYLOR, S.R. 1965: The application of trace element data to problems in petrology. Phys. Chem. Earth 6, 133-213.

THOMPSON, R.N. and MACKENZIE, W.S. 1967: Feldspar-liquid equilibria in peralkaline acid liquids: an experimental study. Amer. J. Sci. 265, 714-734.

THORNTON, C.P. and TUTTLE, O.F. 1960: Chemistry of igneous rocks. I. Differentiation Index. Amer. J. Sci. 258, 664-684.

TILLEY, C.E. and MUIR, I.D. 1964: Intermediate members of the oceanic basalt-trachyte association. Geol. Foren. Stockholm Forhand. 85, 434-443.

TURNER, F.J. and VERHOOGEN, J. 1960: Igneous and Metamorphic Petrology. New York, McGraw-Hill Book Co. Second edition, iv+694pp.

UPTON, B.G.J. 1960: The alkaline igneous complex of Kûngnât Fjeld, South Greenland. Bull. Grønlands geol. Unders. 27 (Medd. Grønland 123, nr.4).

UPTON, B.G.J. 1964a: The geology of Tugtutôq and neighbouring islands, South Greenland. Part II. Nordmarkitic syenites and related alkaline rocks. Bull. Grønlands geol. Unders. 44 (Medd. Grønland 169, nr.2).

UPTON, B.G.J. 1964b: The geology of Tugtutôq and neighbouring islands, South Greenland. Part IV. The nepheline syenites of the Hviddal Composite Dyke. Part of Bull. Grønlands geol. Unders. 48 (Medd. Grønland 169, nr.3).

UPTON, B.G.J. 1965: The petrology of a camptonite sill in South Greenaldn. Bull. Grønlands geol. Unders.50. (Medd. Grønland 169, nr.11).

UPTON, B.G.J. 1970: Basic rocks of the Gardar igneous province. Rapp. Grønlands geol. Unders. nr.28, 26-29.

UPTON, B.G.J. (in press): The Alkaline Province of South-West Greenland. In: Sørensen, H. (editor): Alkaline Rocks. Interscience.

UPTON, B.G.J., THOMAS, J.E. and MACDONALD, R. 1971: Chemical variation within three alkaline complexes in South Greenland. Lithos 4, 163-184.

VLASOV, K.A., KUZ'MENKO, M.Z. and ES'KOVA, E.M. 1966: The Lovozero Alkali Massif. Edinburgh, Oliver & Boyd, xvi+627pp. (Translated by D.G. Cry and K. Syers. Translation edited by S.I. Tomkeieff and M.H. Battey).

WAGER, L.R. and BROWN, G.M. 1960: Collection and preparation of material for analysis. In: Smales, A.A. and Wager, L.R. (editors): Methods in Geochemistry. New York, Interscience. pp.4-32.

WAGER, L.R. and BROWN, G.M. 1968: Layered Igneous Rocks. Edinburgh and London, Oliver and Boyd, xv+588pp.

WAGER, L.R. and DEER, W.A. 1939: Geological Investigation in East Greenland. Part III. Petrology of the Skaergaard Intrusion, Kangerdlugssuaq, East Greenland. Medd. Grønland 105, nr.4.

WALTON, B.J. 1965: Sanerutian appinitic rocks and Gardar dykes and diatremes north of Narssarssaq, South Greenland. Bull. Grønlands geol. Unders. 57 (Medd. Grønland 179,nr.9).

WARSHAW, C.M. and ROY, R. 1961: Classification and a scheme for the identification of layer silicates. Geol. Soc. Amer. Bull 72, 1455-1492.

WATT, W.S. 1966: Chemical analyses from the Gardar igneous province, South Greenland. Rapp. Grønlands geol. Unders. nr.6 .

WILLIAMS, L.A.J. 1969: Volcanic associations in the Gregory Rift Valley, East Africa. Nature 224, 61-64.

WILSON, A.D. 1955: A new method for the determination of ferrous iron in rocks and minerals. Bull. geol. Surv. Gt. Br. no.9, 56-58.

WOOLLEY, A.R. 1969: Some aspects of fenitisation with particular reference to Chilwa Island and Kangankunde, Malawi. Bull. Brit. Mus. nat. Hist.(Mineral.) 2, no.4, 191-219.

WRIGHT, J.B. 1965: Petrographic sub-provinces in the Tertiary to Recent volcanics of Kenya. Geol. Mag. 102, 541-557.

WRIGHT, J.B. 1966: Olivine nodules in a phonolite of the East Otago alkaline province, New Zealand. Nature 210, 519.

WRIGHT, J.B. 1969: Olivine nodules in trachyte from the Jos Plateau, Nigeria. Nature 223, 285-286.

WRIGHT, J.B. 1971: The phonolite-trachyte spectrum. Lithos 4, 1-5.

YODER, H.S. and TILLEY, C.E. 1962: Origin of basalt magmas: an experimental study of natural and synthetic rock systems. J. Petrol. 3, 342-532.

PLATES

Plates 1 and 2 are folded maps contained in the envelope inside the back cover.

PLATE 3

G.G.U. 27118 x 18, crossed polars.

A Lower Series foyaite of Group I (see text), showing small euhedral nepheline crystals enclosed in massive perthitic alkali feldspar.

PLATE 4

G.G.U. 31896 x 25, crossed polars.

A Coarse-Grained Brown Syenite having a poikilitic texture akin to those in the Group I foyaites. Severely altered nepheline crystals (in extinction) are enclosed by massive altered perthitic feldspar.

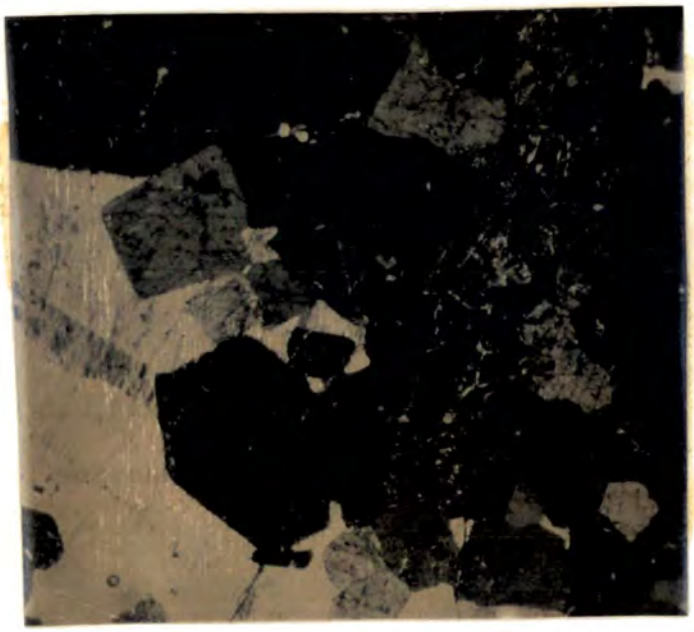

PLATE 5

G.G.U. 27136 x 18, crossed polars.

A well laminated pulaskite showing the pronounced feldspar lamination characteristic of Group IV.

PLATE 6

G.G.U. 27095 x 25, crossed polars.

A biotite-rich Granular Syenite (GS-1) showing a texture indicative of nepheline accumulation (c.f. Plate 3). A large crystal of cancrinite can be seen top right.

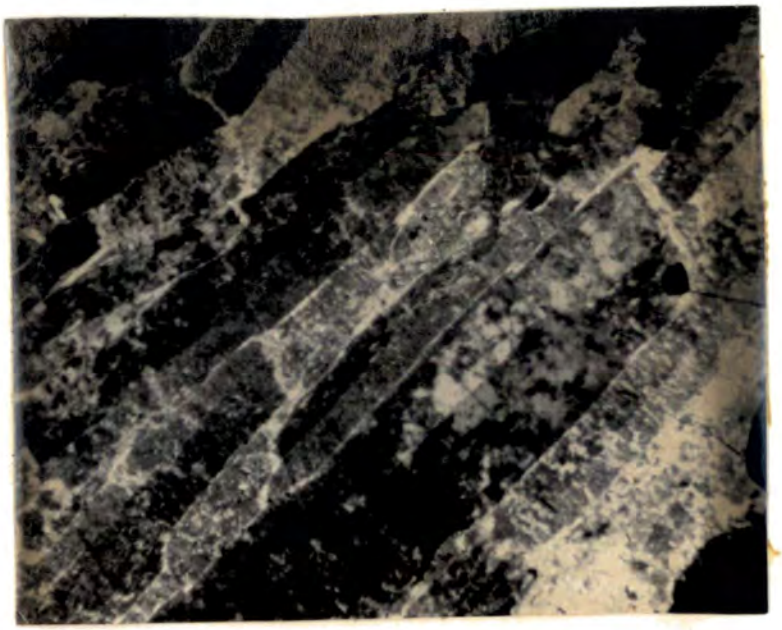

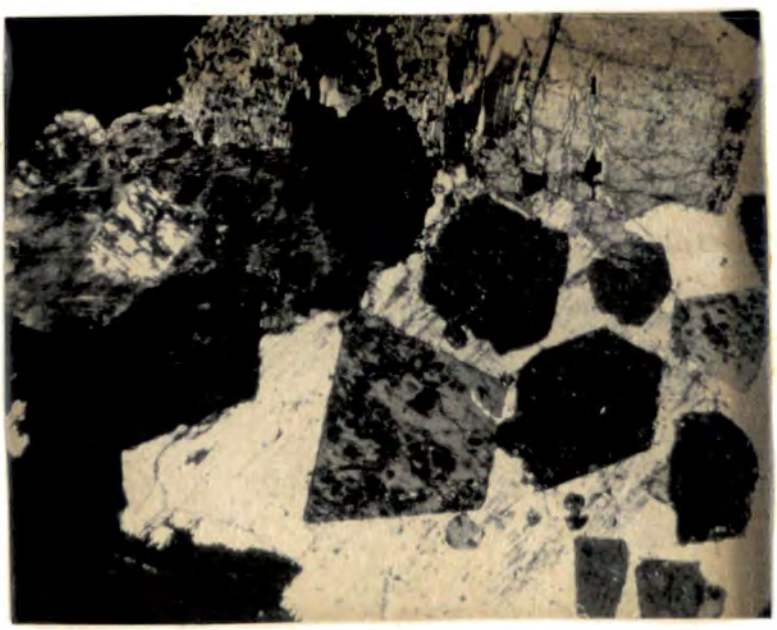

PLATE 7

G.G.U. 126721 x 18, crossed polars.

A Coarse-Grained Syenite with abundant euhedral nepheline enclosed by later feldspar and opaque material after original biotite.

PLATE 8

G.G.U. 27200 x 25, crossed polars.

A strongly porphyritic microsyenite dyke (Group 1), showing phenocrysts of nepheline (in extinction) and alkali feldspar set in a trachytic matrix of feldspar, nepheline, alkali pyroxene and biotite. An earlier, resorbed outline of the feldspar phenocryst is picked out by a dust zone (c.f. Nash et al. 1969, Plate 1c).

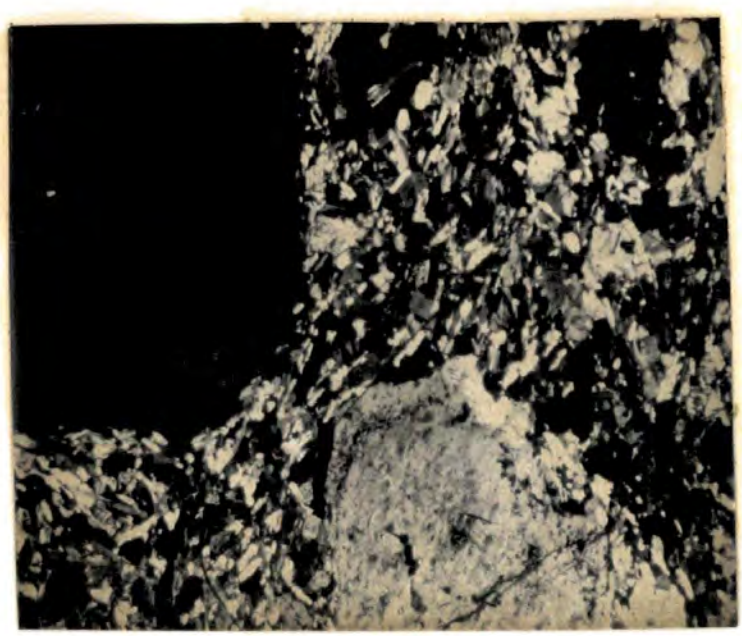

PLATE 9

G.G.U. 39770 x 18, crossed polars.

A porphyritic microsyenite dyke of Group 5. Phenocrysts of nepheline (cluster at centre), alkali pyroxene (lower centre), biotite (lower right) and feldspar (not shown) are set in a trachytic matrix resembling that of Group 1 (Plate 8).

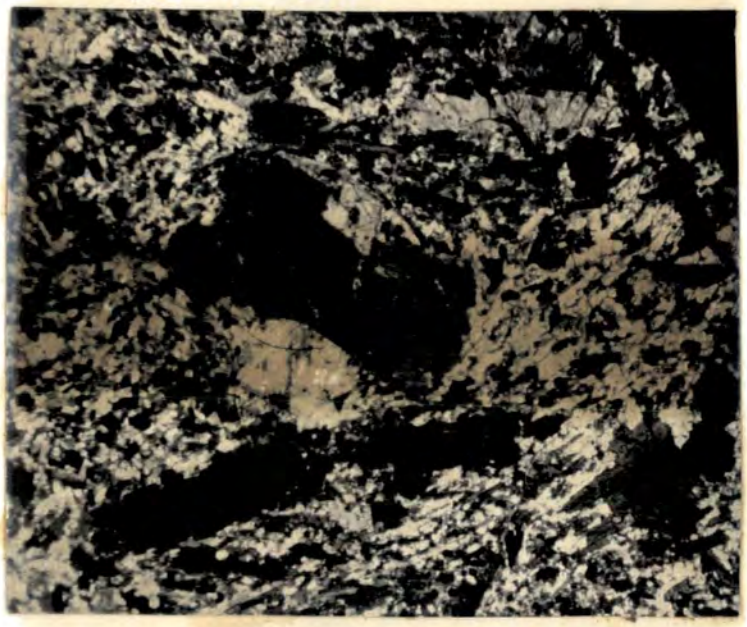

GRØNLANDS GEOLOGISKE UNDERSØGELSE
THE GEOLOGICAL SURVEY OF GREENLAND

PLATE 1

MEDD. OM GRØNL. BD. 172, NR. 3. (C. H. EMELEUS)

GEOLOGICAL MAP OF THE GRØNNEDAL - ÍKA COMPLEX, SOUTH GREENLAND

Scale 1 : 15 000

0.1 0 0.5 1km

Minor intrusions (post Igneous Complex)

- Trachyte, phonolite, etc.
- Porphyritic basalts
- Olivine dolerite etc.

(N.B. Many impersistent dykes are not shown)

Members of the Igneous Complex

- Carbonatite and breccia.
- Carbonate-impregnated rocks

Nepheline Syenites:

- Xenolithic porphyritic syenite
- Porphyritic microsyenite

Upper Series

- Coarse-grained syenite
- Foyaite and pulaskite
- Pyroxene-rich syenite

Lower Series

- Granular syenite
- Foyaite
- Coarse-grained brown syenite

Pre-Gardar

- Metasediments
- Gneiss

- Superficial deposits
- Faults and crush zones
- Geological boundaries, established
- ,, , inferred
- ,, , arbitrary
- 70 Strike and dip of igneous lamination
- Strike of vertical igneous lamination
- 30 Strike and dip of mineral layering

Heights in metres

Contour interval 100m

Road and Hut

Topography based on preliminary 1:20,000 maps prepared photogrammetrically from vertical aerial photographs by the Geodetic Institute, Copenhagen.

GRØNLANDS GEOLOGISKE UNDERSØGELSE
THE GEOLOGICAL SURVEY OF GREENLAND

A RECONSTRUCTION OF THE GRØNNEDAL - ÍKA COMPLEX

Scale 1 : 22000

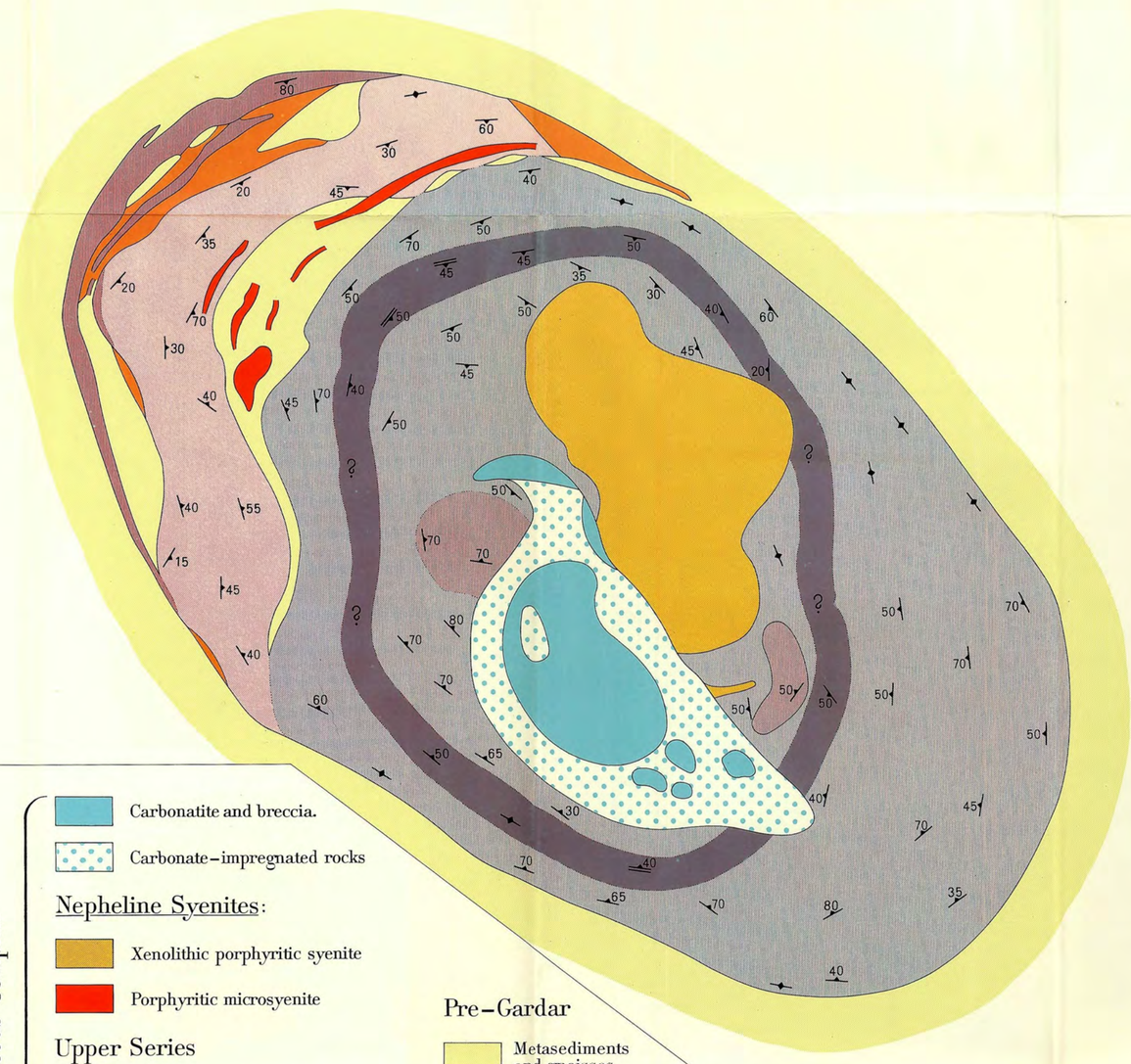

Members of the Igneous Complex

Carbonatite and breccia.

Carbonate-impregnated rocks

Nepheline Syenites:

Xenolithic porphyritic syenite

Porphyritic microsyenite

Upper Series

Coarse-grained syenite

Foyaite and pulaskite

Pyroxene-rich syenite

Lower Series

Granular syenite

Foyaite

Coarse-grained brown syenite

Pre-Gardar

Metasediments and gneisses

Geological boundaries

„ , arbitrary

70 Strike and dip of igneous lamination

Strike of vertical igneous lamination

30 Strike and dip of mineral layering

PLATE 2

Reproduceret ved Geodætisk Institut. København 1963